INVESTIGATION OF INJURY AND PHARMACOLOGICAL MODULATION OF BILIARY EPITHELIAL CELLS IN DUCTOPENIC DISEASE

Dr John G Brain

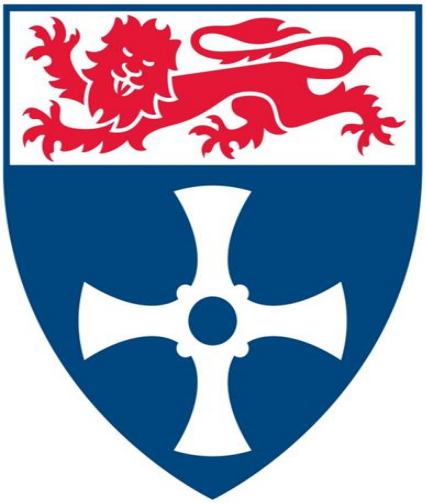

A thesis submitted in partial fulfilment of the requirements for the degree of

Doctor of Philosophy

Institute of Cellular Medicine

Newcastle University

September 2013

Acknowledgments

This thesis would not have come to pass but for the support of many individuals, it is inevitable that I will miss some of them, this is not deliberate and I apologise unreservedly.

In the lab, Helen Robertson (triple colour IHC), Trevor Booth (IF and analysis), Joe Willet, Chris Lamb and John Kirby all helped me to develop and mature as a bona fide Gilson wielding scientist. Alastair Burt, John Kirby and Dave Jones were all there to ensure I developed as an hypothesis testing, grant writing and analysing clinician scientist. Furthermore, all of them helped to a large degree in the setup of the fellowship and the following UK-PBC stratified medicine project of which I am proud to be a part of.

To the scientists and friends I made in Birmingham, Simon Afford and Liz Humphries, without whom this work would be far less complete.

There are also thanks to go to my family, but particularly my Wife, Helen, who managed to keep me sane during the whole project but particularly the write up period where she performed a stellar job of proof reading and correcting my appalling English.

List of Abbreviations

3-MA: 3-MethylAdenine

7-AAD: 7 Amino-Actinomycin D

ACR: Acute cellular rejection

ALD: Alcoholic liver disease

AMP: Adenosine mono-phosphate

AMPK: AMP activated protein kinase

ASH: Alcoholic steatohepaitis

AZA: Azathioprine

BEC: Biliary epithelial cells

BMP: Bone morphogenetic protein

BMT: Bone marrow transplant

cMet: Proto-oncogene, no abbreviation

CR: Chronic rejection

CsA: Cyclosporine A

Cvt pathway: caveolin mediated autophagy pathway

DAB 3, 3': Diaminobenzidine tetrahydochloride

DAPI: 2-(4-amidinophenyl)-1H -indole-6-carboxamidine

DBD: Donation after brain death

DCD: Donation after cardiac death

DEPC: Diethylpyrocarbonate

ECM: Extracellular matrix

EGF: Epidermal growth factor

ELISA: Enzyme-linked immunosorbent assay

EMT: Epithelial to mesenchymal transition

ERK: Extra-cellular signal regulated kinase

FAK: Focal adhesion kinase

FFPE: Formalin fixed paraffin embedded

FISH: Fluorescent in situ hybridisation

FITC: Fluorescein isothiocyanate

FSP-1: Fibroblast specific protein 1/S100A4

GAG: Glycosaminoglycan

GDF: Growth and differentiation factor

GR: Glucocorticoid receptor

GSK3β: Glycogen synthase kinase 3β

H_2O_2: Hydrogen peroxide

HCV: Hepatitis C virus

HGF: Hepatocyte growth factor

HGFR: Hepatocyte growth factor receptor

HLA: Human leukocyte antigen

HPF: High power field

HSC: Hepatic stellate cell

HSPG: Heparan sulphate proteoglycan

HOCl: Hypocholorous acid

IL-6: Interleukin-6

IRI: Ischaemia reperfusion injury

LAP: Latency associated peptide

LFT: Liver function test

MAPK: Mitogen activated protein kinase

MAPK: Mitogen-activated phospho-kinase

MCP-1: Monocyte chemoattractant protein

MET: Mesenchymal to epithelial transition

MF: Myofibroblast

MHC: Major histocompatibility complex

MMF: Mycophenolate mofetil

MMP: Metalloproteinase

MPO: Myeloperoxidase

MTT: 3-(4,5-dimethylthiazol-2-yl)-2,5-diphenyltetrazolium bromide

NAFLD: Non-alcoholic fatty liver disease

NFAT: Nuclear factor of activated T cells

NiDAB: Nickel 3,3' diaminobenzidine tetrahydochloride

NMR: Nuclear magnetic resonance

PAS: Phagophore assembly site

pERK: ERK phosphorylation

PARP: Poly-ADP ribose polyermase

PBC: Primary biliary cirrhosis

PBS: Phosphate buffered saline

PDC: Pyruvate dehydrogenase complex

PF: Portal fibroblast

PKB: Phospho-kinase B

PKC: Phospho-kinase C

PP2A: Protein phosphatase 2a

PSI: Plexin-semaphorin-integrin

PSC: Primary sclerosing cholangitis

qPCR: Real-time polymerase chain reaction

ROS: Reactive oxygen species

RT: Room temperature

SAHF: Senescence associated heterochromatin foci

SASP: Senescence associated secretory phenotype

SIRS: Systemic inflammatory response syndrome

SMA: Smooth muscle actin

SMAD: portmanteau of the genes: SMA (*Caenorhabditis elegans*) and mothers against decapentaplegic (MAD)

TBS: Tris-buffered saline

TIF: Telomere-dysfunction induced foci

TGF-β: Transforming growth factor beta

UUO: Unilateral ureteric obstruction

VBDS: Vanishing bile duct syndrome

VEGF: vascular endothelial growth factor

Abstract:

Senescence and its associated secretory phenotype have been investigated in several vanishing bile duct syndromes. The current study evaluated the presence of senescent biliary epithelial cells (BEC) in acute cellular rejection of human liver allografts to ascertain whether senescent cells contribute to human disease progression in liver transplantation. There was a significant correlation between senescent BEC and grade of rejection. Furthermore there was a significant correlation between grade of rejection and BEC undergoing epithelial to mesenchymal transition (EMT). There was never any overlap between senescence and EMT markers in BEC. Further investigation of the association between senescence and EMT in vitro using both primary and immortalised human BEC exposed to oxidative stress showed, for the first time, that TGF-b2 is part of the Senescence Associated Secretory Phenotype (SASP) in liver disease. Blockade of TGF-b signalling by inhibition of the TGFbR, prevented any of the oxidative stress-induced changes in BEC. Blockade of integrin aVb6 integrin also showed a variable ability to prevent TGF-b mediated changes in BEC. HGF and its mimetic, 1K1, were able to prevent oxidative stress induced EMT in BEC. Furthermore 1K1 showed a smaller induction of autophagy than HGF and was able to prevent up regulation of senescence markers.

The paradigm of oxidative stress-induced senescence leading to EMT was assessed in the current study, with identification of powerful therapeutic agents able to prevent these changes. This suggests that premature cellular ageing (senescence) in acute liver disease could be pharmacologically prevented from occurring. Inhibition of senescence prevents disease promotion by the effects of the SASP, blocking the progression to chronic disease; this may well apply to all organ systems.

1 Investigation of injury and pharmacological modulation of biliary epithelial cells in ductopenic disease

1.1 Anatomy of the Liver

1.1.1 Gross anatomy

The liver is the largest gland in the body, weighing around 1.5Kg in the average adult. It resides in the upper right quadrant of the abdomen enclosed mainly by the ribs. The liver is divided into two anatomical lobes (divided into left and right by the falciform ligament) and four physiological lobes (divided by the falciform ligament, IVC (*Cantlie's* line), *ligamentum venosum* and *ligamentum teres*) (Figure 1.1).

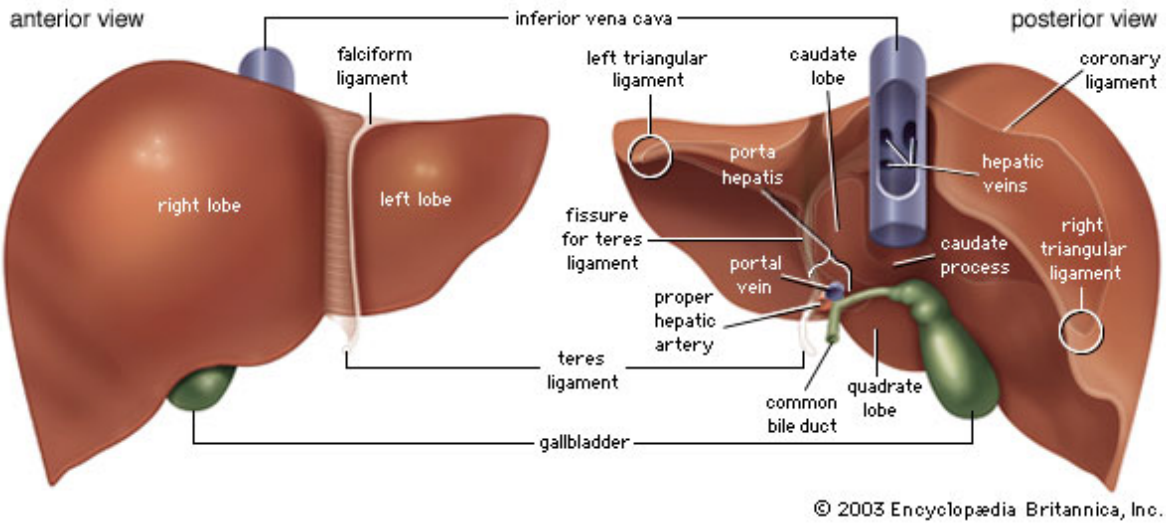

Fig. 1.1: Gross anatomy of the liver. The external features of the liver are labelled, with the two anatomical lobes noted on the left image and the remaining two physiological lobes (caudate and quadrate) noted on the right hand image. (Taken from the encyclopaedia Britannica(http://www.britannica.co.uk 2013))

It can also be divided into vascular segments, termed *Coinaud* segments (Figure 1.2), based upon the terminal branches of the hepatic artery. These eight or nine segments are important in liver surgery, where resections based upon this anatomy can minimise blood loss (Buechter, Zeppa et al. 1990, Brown 2008).

The liver is supplied with blood via the hepatic artery (a branch of the coeliac trunk) and the hepatic portal vein, which carries nutrient rich blood from the gut and is formed by a confluence of the superior and inferior mesenteric veins and the splenic vein. Bile is transported from the liver via the biliary tree, which emerges from the liver at the same point as the portal vein and hepatic artery. This point is known as the liver hilum or *porta hepatis*. Oxygenation of the liver occurs from both the hepatic artery and portal vein, with each supplying around half the oxygen but 25% and 75% (respectively) of the blood flow (Berzigotti, Reverter et al. 2013). Blood exits the liver from the hepatic veins into the inferior vena cava, and thence to the right side of the heart. The hepatic veins themselves are composed of central veins that drain the sinusoids (Kelly, Shiba et al. 2011).

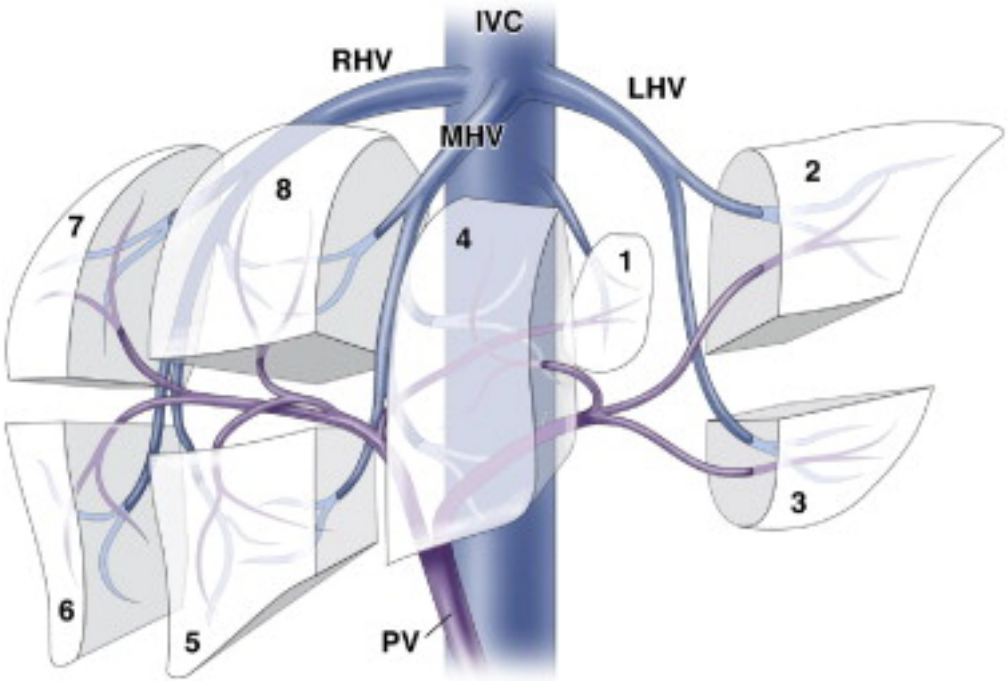

Figure 1.2: Vascular anatomy of the liver. The surgical Couinaud segments are shown as an exploded view, these are numbered accordingly. The venous branches are shown from each segment leading to the right hepatic vein (RHV), middle hepatic vein (MHV) and left hepatic vein (LHV). These all drain into the inferior vena cava (IVC). The venous supply to the liver via the portal vain (PV) is also shown. Image taken from (Brown 2008)

1.1.2 Biliary tree

The liver is composed of parenchymal cells known as hepatocytes, which make up 50-60% of the cell number but 80% of the cell mass (Bhogal, Hodson et al. 2011). Non-parenchymal cells, such as hepatic sinusoidal endothelial cells, Kupffer cells and hepatic stellate cells (HSC) make up between 5 and 10 % of liver mass (Shetty, Weston et al. 2011, Nagatsuma, Hano et al. 2013). 5% of liver mass is made up of biliary epithelial cells (BEC) also known as cholangiocytes (Bird, Lu et al. 2013). These are referred to as BEC from hereon in.

The biliary tree is defined by the presence of BEC and extends from the canals of Hering (small branches of ducts that link the hepatocytes and bile ducts) to the gallbladder. It is believed that progenitor cells of the liver (also known as oval or *ito* cells) become committed to a biliary lineage in the canals of Hering, and form bile duct radicles that become small terminal bile ducts – then these become intra-lobular ducts (Ijzer, Schotanus et al. 2010, Roskams, Katoonizadeh et al. 2010, Spee, Carpino et al. 2010). The next tier in the organisation of the biliary tree is the inter-lobular bile ducts, the hepatic ducts, common bile duct and thence to the gallbladder. The common hepatic duct also drains into the duodenum via the ampulla of vater. Once synthesised, bile is secreted into the ducts where it is modified and stored.

1.1.3 Micro anatomy

Micro-anatomically, the liver is composed of hepatocytes arranged in hexagonal lobules. At the centre of the lobule is a central vein and at each vertex of the hexagon there is a portal tract containing an arteriole from the hepatic artery, a branch of the portal vein and a bile duct radicle. Oxygenated blood and nutrient rich blood flow into this arrangement via the artery and portal vein. Deoxygenated blood, synthesised compounds and bile are excreted via the central vein and bile duct (Turanyi, Dezso et al. 2010). This arrangement means that hepatocytes around the portal tract have more access to nutrients and oxygen, whereas cells around the central veins have less oxygen and a higher concentration of breakdown products and waste. These cells are subdivided into three groups, (1) around the portal tracts, (3) around the central veins, with an intermediate type between the

two. This classical lobular arrangement is not readily seen in humans but is pronounced in pigs. The demonstration of areas by nutrient/oxygen abundance shown by Rappaport is a better physiological model, referred to as the acinus, which defines the positions of the cells relative to their blood supply (Figure 1.3) (Rappaport 1958, Ong, Jenner et al. 2009, Shih, Tseng et al. 2013).

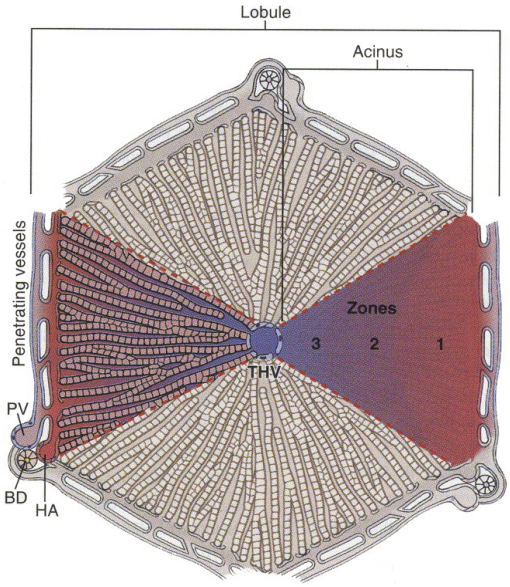

Figure 1.3 microanatomy of the liver. The classical hepatic lobule is shown, drained by a single vein. Also shown is the hepatic acinus as described by Rappaport, with the three zones of vascular supply noted. Image taken from (Isenberg and Wong 2006)

The liver has numerous physiological roles. These include glycogen storage and synthesis, glucose synthesis, production of triglycerides and cholesterol, synthesis of clotting factors, storage of vitamins such as A, B12 and D, drug metabolism, and bile synthesis. As yet, a synthetic liver or dialysis equivalent of the liver has proved impossible to produce.

Bile acids are synthesised by hepatocytes from cholesterol via the oxidative cytochrome P450 pathway. This leads to the production of two primary bile acids, cholic and chenodeoxycholic acid, which are secreted into bile ducts where they pass to the gallbladder for storage until required during digestion (Hofmann 2009). Once present in the gut lumen, these two primary bile acids can be dehydroxylated

by commensal bacteria into deoxycholic and lithocholic acid, the secondary bile acids. All four bile acids are then taken back up into the blood stream and reabsorbed by hepatocytes, a process known as enterohepatic recirculation (Heinen, Reuss et al. 2013). On passing through the hepatocytes a second time, the primary and secondary bile acids can be modified by conjugation with the amino acids glycine or taurine, potentially giving a total of eight tertiary bile acids (Modica, Gadaleta et al. 2010).

Bile enhances the digestion of fats and its main function is as a detergent / surfactant. The bile acids have both hydrophobic and hydrophilic surfaces, which aid the formation of micelles 14-35nm in size, with the hydrophobic surfaces of the bile acids forming the inner surface of the micelle membrane, in contact with fats (Hofmann 2009). The hydrophilic surfaces are located on the outer aspect of the membrane, in contact with the physiological fluids of the gut, lymphatics and blood stream. As bile is alkaline, it serves to neutralise stomach acid and act as an anti-microbial (Rizzo, Renga et al. 2005, Hohenester, Oude-Elferink et al. 2009, Gadaleta, van Mil et al. 2010). Ductopenic liver disease

Ductopenia derives from the Latin term duct, meaning a circumscribed channel carrying a fluid; “penia” derives from the Greek term for a lack / paucity of something. In the context of liver disease, the ducts referred to are the intrahepatic bile ducts. The medical definition of ductopenia is the presence of < 0.5 bile ducts per portal tract (when a liver portion comprised of > 6 portal tracts is assessed). Ductopenia is the characteristic feature of vanishing bile duct syndromes (VBDS) - the commonest VBDS being primary biliary cirrhosis (PBC); others include

ductopenic allograft rejection, primary sclerosing cholangitis (PSC), reactions to drug treatment, developmental abnormalities, neoplastic processes and graft versus host disease (GvHD) (Neuberger 1997, Sasaki, Ansari et al. 2000, Palmer, Kirby et al. 2002, Nakanuma and Harada 2011). The causes of VBDS most relevant to the current study are summarised below.

1.1.4 Primary Biliary Cirrhosis

PBC is an autoimmune disorder in which the cells of the immune system attack the small bile ducts of the liver, leading to their destruction and, eventually, loss with replacement by fibrosis. This process leads to cirrhosis of the liver and requires transplantation or results in death (Carbone, Bufton et al. 2013). Over 95% of patients with PBC develop anti-mitochondrial antibodies with the specific antigen targeted being either pyruvate dehydrogenase complex (PDC, which contains several of the antigens found in PBC) or other members of the 2-oxoacid dehydrogenase complex family (Mandai, Kanda et al. 2013, Sasaki, Miyakoshi et al. 2013). These proteins are fundamental parts of the respiratory complex in mitochondria found in all cells. Some PBC patients also have anti-nuclear antigens directed against the gp210 and Sp100 proteins (Palmer, Doshi et al. 2000).

In PBC, the transcytosis of antibodies through BEC may be relevant in that contact with cognate antigens is possible. However, the pathogenesis related to autoantibodies (and B- cell biology) in PBC is complex and is still not fully understood. There are current clinical trials in PBC aiming to deplete B-cells via the use of the biological agent Rituximab that specifically targets the mature B-cell marker CD20 (Neuberger 1997, Jones 2008).

B-cells are not the only potential effector cells present in PBC. The portal infiltrate in PBC contains large numbers of both CD4 and CD8 positive T-cells; a subset of which have been shown experimentally to be specific for self-PDC (Yeaman, Kirby et al. 2000). Macrophages are also found in PBC, where they have effector cell function alongside interaction with T-cells, and oxidative burst activity, which may well contribute to the oxidative stress seen in active disease (Harada and Nakanuma 2010). It is not known why the site of immune injury towards a ubiquitous antigen occurs in the BEC compartment of the liver, however not all of the features of PBC described are limited to the liver and can affect for example, the salivary glands or kidneys (Palmer, Doshi et al. 2000, Mandai, Kanda et al. 2013).

Patients with PBC have only one therapeutic option, to take ursodeoxycholic acid (UDCA or "Urso"). This is a modified bile acid and will prevent progression of disease in around 60-70% of patients (Carbone, Mells et al. 2013). For the remainder however, there is no response to treatment and there are no other therapeutic options. These patients experience progression of the disease, are forced to withdraw from the labour market, suffer intractable symptoms such as persistent pruritus and debilitating fatigue and ultimately require transplantation. This is a huge operative risk that gives rise to the possibility of all of the complications that go with that risk (Lee, Belanger et al. 2007, Hohenester, Oude-Elferink et al. 2009, Tanaka, Harada et al. 2011, Pells, Mells et al. 2013).

1.1.5 Transplant rejection

In a proportion of transplant recipients, the immunosuppressive balance is not met and they can suffer acute cellular rejection (ACR), where the lymphocytes that normally fight infection attack the liver (as discussed in section 1.2). The favoured sites for injury are the bile ducts and the portal veins. In order to quantify ACR, a consensus grading system, known as the Banff scheme, is used Banff working group (1997, Demetris, Adams et al. 2000, Demetris, Ruppert et al. 2002, Horoldt, Burattin et al. 2006). The Banff schema lists three component features: 1) portal immune infiltrate 2) bile duct injury, and 3) portal venous endothelial inflammation. The severity of each component (by proportion of biopsy affected) and the individual severity of the individual component are assessed. These components are then taken in aggregate to produce one overall grade: mild, moderate or severe rejection.

The Banff schema also includes inflammation of the central veins as a significant component, 'central perivenulitis'. AR may also present with isolated central perivenulitis (ICP) the features of which include hepatic vein inflammation, perivenular inflammation and some degree of perivenular hepatocyte loss. In order to diagnose severe rejection, features of perivenular inflammation and hepatocyte necrosis are required (Hubscher 2006, Neil and Hubscher 2010).

When ACR presents 'late', more than 3 months after engraftment, the histological features more often reflect ICP and less often include the portal component. Late ACR is also more often associated with features indicating chronic rejection (CR), including bile duct loss or perivenular fibrosis.

CR was classically described as graft failure within 12 months of engraftment with a constellation of features including bile duct loss and arterial lesions leading to obliteration of the medium and large arteries of the graft. CR is often divided into early and late. Early CR is recognised by the features of replicative senescence in bile ducts, a squamoid appearance, large cells with large nuclei and multi nucleation (Lunz, Contrucci et al. 2001). Centri lobular inflammation is also seen in early CR. Centri-lobular changes are also a feature of late CR and may include bilirubinostasis, hepatocyte ballooning and hepatocyte necrosis, potentially with confluent necrosis of zone 3. Late CR may include bile duct loss and associated portal fibrosis with a ductular reaction. Classically neither portal fibrosis nor ductular reactions are seen in CR (Demetris, Adeyi et al. 2006, Neil and Hubscher 2010).

The grade of ACR is linked to outcome, the more episodes of higher grade ACR a patient has, the more likely they are to experience chronic ductopenic rejection (CR) and graft failure. The mechanisms underlying progression from ACR to CR are not understood. There is some evidence that patients suffering a single episode of mild rejection that responds to treatment have a better outcome. It may be that this is important in establishing *prima facie* tolerance or in activating mechanisms that provide stable background for a tolerant state to exist (Wiesner and Fung , Hubscher 2006, Jiang, Lechler et al. 2006, Feng, Ekong et al. 2012, Miyagawa-Hayashino, Yoshizawa et al. 2012).

There is no known effective treatment for patients with CR and their prognosis is very poor.

1.1.6 Primary Sclerosing Cholangitis and Graft versus Host Disease

PSC and GvHD are the other main causes of VBDS. PSC is an autoimmune disorder similar to PBC, however extra-hepatic ducts, the bile ducts outside of the liver, are targeted, as well as the large ducts within the liver. The extra-hepatic ducts often show evidence of fibrosis with stricturing at multiple points. Bile flow disruption leads to similar clinical features to those observed in PBC; namely fatigue, jaundice, itching and eventually fibrosis, cirrhosis and transplantation or death (Burt 2011, Nakanuma and Harada 2011, Rupp, Mummelthei et al. 2013).

GvHD is an immune disorder seen in patients who have received a bone marrow transplant (BMT) (although there are caveats to this). BMT establishes a new immune system in the recipient, which does not have the benefit of the patient's central tolerance. Therefore, the immune system that has been transplanted may be primed to recognise the recipient's self-antigens as foreign and to attack them. The bile ducts are not the only site to be injured in GvHD; the skin and gastro-intestinal mucosa are easily accessible sites that show immune mediated injury. The effects of the immune system upon the bile ducts in GvHD are similar to the other VBDS (Burt 2011, Sagoo, Ratnasothy et al. 2012, Duarte, Greinix et al. 2013, Parkman 2013, Pidala, Sarwal et al. 2013).

1.2 Liver transplantation

Liver transplantation remains the only effective treatment for end stage liver disease. Thomas Starzl performed the first human liver transplant in 1963 in Colorado (Marchioro, Waddell et al. 1963, Starzl, Marchioro et al. 1963). There were several further procedures before any success, with one-year survival of 25%

being optimal during the 1970's. It was only once immunosuppression in the form of cyclosporine A was introduced by Sir Roy Calne in 1984 that outcomes improved and liver transplantation became considered as a standard treatment (Calne 1984, Calne 1984).

Liver transplantation is a complicated and technically challenging procedure and is performed only in specialist centres. Although it is possible to use live liver donors this is exceedingly rare. In paediatric transplantation, an adult left lobe can be resected and function as a whole liver for the recipient - the remaining right lobe will regenerate to the pre-operative size in the adult within around one month. This procedure has been performed in adults where the right lobe is resected and the donor is left with the smaller left lobe. These procedures remain rare however (Brown 2008).

Far more commonly, livers are donated from deceased patients. Causes of donor death include brain death, where the heart is still beating but the patient has been declared dead following neurological testing. This is known as DBD (donation after brain death) and is the most common form of donation; the donor remains relatively haemodynamically stable and so retrieval of organs can be undertaken relatively easily. It is also possible to utilise livers from patients that have undergone cardiac death – this is known as DCD (donation after cardiac death). In this situation, there is no functioning circulation and the organs may have been subject to extended periods of time without blood supply (ischaemia), restricting locations for organ harvest. Outcome data comparing DCD and DBD donors is difficult to interpret, with some studies suggesting an equivalent outcome and

other suggesting a superior outcome for DBD (Steen, Sjoberg et al. 2001, Bendorf, Kelly et al. 2013, Bradley, Pettigrew et al. 2013, Chang, Qu et al. 2013).

Once the patient has successfully received a liver they require intensive hospital care (duration variable) before being able to return home to a long period of convalescence. For the rest of their lives, transplant patients must take immunosuppressive medication, rendering them susceptible to infections and increasing the risk of diseases such as skin cancer, which can be fatal in and of themselves.

1.2.1 Allorecognition and rejection

Aside from the technical problems of transplanting a liver and the ever-present threat of infection, the most commonly incurred complication is rejection of the allograft (Starzl, Marchioro et al. 1963, Calne 1984, Cooper, Gregory et al. 1991). Rejection is usually an immune process and is dependent upon a number of things. The first is the influx of immune cells from the recipient, driven by the injury of the surgical insult and the ischaemia reperfusion of the organ. The second is the activation of the immune cells by the cytokines and adhesion molecules produced by the transplanted organ. The third is the ability of the immune cells to recognise tissue as either “self” or “non-self” which is dependent upon genetic region known as the major histocompatibility locus (Afzali, Lechler et al. 2007, Hoerter, Brzostek et al. 2013).

In humans the MHC locus is found on the short arm of chromosome 6 and is around 3.6Mb in length, encoding around 140 genes (Herskowitz, Tamura et al. 1989,

Lechler, Lombardi et al. 1990). This area is divided into three regions, I coding for peptide binding proteins and proteins involved in antigen presentation and processing. II coding for peptide binding proteins and proteins involved in antigen loading onto peptide binding proteins and III, coding for other immune related genes such as cytokines and the complement cascade (Bahr and Wilson 2012).

The immune system recognises cells and tissues as 'self' by recognising peptides bound to major histocompatibility antigen complexes (MHC) on cell surfaces. There are two classical types of MHC those coded for by region I of the MHC locus (and therefore referred to as Class I MHC) and those coded for by region II of the MHC locus (and therefore known as class II MHC) (Collins, Stephens et al. 2003, Lakkis and Lechler 2013).

In humans, MHC antigens are also known as Human Leukocyte Antigen (HLA). The two classes of MHC noted above have different tissue expression and slightly different functions. MHC class I are present on almost every cell in the body and are complexed to peptides that are produced by that particular cell. Therefore, the cells should be recognisable by the immune system as "self". If the cell is infected, for example with a virus, a proportion of class I MHC will be complexed to viral encoded peptides, the immune system is able (in most cases) to recognise these as "non-self" and to mount an immune response against the pathogen and the infected cells (Afzali, Lechler et al. 2007, Legoux, Gautreau et al. 2013).

Class II MHC are different to class I. They are restricted in expression to cells dubbed "Antigen Presenting Cells (APC)". The peptides complexed to these MHC

are not peptides produced by the cell expressing the MHC, but have been taken up by that cell, processed and complexed to the class II MHC. Therefore, the APC can take up peptides from invading pathogens, for example bacteria, which are then presented to T cells. The T cells are then able to recognise the MHC complexed to bacterial peptide as "non-self" and mount an adaptive immune response (Aichinger and Lechler 1995, Jin, Birlea et al. 2011).

Within any allograft, there is an organ containing cells with "non-self" HLA complexed to peptides (Lechler, Lombardi et al. 1990, Ali, Bolton et al. 2013, Lakkis and Lechler 2013). As a result, the immune system of the recipient can be activated by recognising peptide/HLA complexes from the donor. The recipient immune system is also able to take up donor peptides (largely HLA molecules) and recognise these in combination with self-HLA (Papassavas, Barnardo et al. 2002). Recently it has been shown that recipient cells are also able to take up and present whole MHC/peptide complexes from donor cells. This likely involves small vesicle transfer but may challenge the classical theories regarding CD4 and CD8 T cell stimulation in response to the allograft (discussed in more detail here: (Afzali, Lechler et al. 2007) These processes are referred to (respectively) as direct, indirect and semi-indirect allograft recognition and can lead to a large immune response to the graft – this is allograft rejection.

Rejection can be sub-divided into discrete types that can be recognised clinically, and the way each type responds is largely due to different immune responses (Yoshitomi, Koshiba et al. 2009, Hubscher 2012, Ali, Bolton et al. 2013)

Hyper-acute rejection can also occur and is due to a preformed antibody response to the graft. This situation may arise due to pre-sensitisation of the recipient, for example from a previous allograft, or from a memory response by the immune system to an entirely separate antigen. The recipient's immune system may have mounted an antibody response to a previous infection, and the combination of the microbial peptide plus HLA is very similar to a donor peptide complexed to a donor HLA. The effect of this is quite dramatic and can be observed in a short period of time (typically minutes) after the transplant has been re-perfused. Cellular injury due to a vigorous antibody mediated response involves direct cytotoxicity from effector cells, as well as complement activation. In such cases, the outcome for the graft, and therefore the patient, is poor (Uchiyama, Kayashima et al. 2012, Leventhal, Abecassis et al. 2013) As the liver plays a key role in phagocytosis and clearing of immune complexes, it is largely unaffected by hyper-acute rejection.

Anti-body mediated rejection (AMR) has received much interest of late as a potential cause of acute and possibly chronic rejection. This is a contentious area covered in more detail here (Hubscher 2012). It should be noted that the most frequent cause of AMR is mismatch of the ABO blood group. This phenomenon is well described in the blood transfusion sphere and has been described in liver allografts (Rostron, Carter et al. 2005). AMR is likely to feature more in the future as there is a current trend for ABO mismatched liver allografts, particularly in Japan (Neil and Hubscher 2010, Hubscher 2012).

Acute rejection typically occurs within 30 days after engraftment and is a T-cell mediated phenomenon, with the T-cells typically attacking the bile ducts and veins of the graft. The most common presentation of acute rejection is deranged liver function tests (LFTs), but pain and fever with accompanying jaundice all point to acute rejection too. The typical treatment for acute rejection is augmentation of the immune suppression regime (Shaked, Ghobrial et al. 2009, Miyagawa-Hayashino, Yoshizawa et al. 2012, Oetting, Jacobson et al. 2013). This is discussed further in section 1.2.1 (rejection) and Section 1.3 (immunosuppression).

Chronic rejection (CR) is by nature a much longer standing problem, and is also caused by a T-cell mediated immune response. It usually happens after a year or more of engraftment although it can occur earlier. Clinical features include jaundice, deranged LFTs, and the loss of the liver's synthetic functions. Histologically, the defining features are duct loss, ductopenia, and fibrosis of the graft (Demetris, Adeyi et al. 2006, Hubscher 2006, Oetting, Jacobson et al. 2013).

1.3 Immunosuppression

Immunological tolerance is defined as a state of indifference or non-reactivity to a substance that should normally elicit an immune response while maintaining normal immune responses to other substances (Billingham, Brent et al. 1955, Medawar 1956). This has been modified over the years to include the phrase "in the absence of immunosuppression". There has been a concerted effort to induce immunological tolerance to the allograft ever since the advent of transplantation in medicine. At the time of writing, no protocol has been established for any organ that allows reliable induction of a tolerant state. To maintain a state whereby a

patient does not mount an immune response to their allograft; drugs are required that dampen or prevent an immune response to the allograft.

The concept of '*prope*' tolerance has been developed indicating a state where transplant recipients receive 'minimal' immunosuppression (Ali, Bolton et al. 2013). This situation creates uncertainty regarding the exact definition of minimal.

'Operational' tolerance has been defined as stable or acceptable graft function in the absence of immunosuppression (Levitsky, Mathew et al. 2013). In the case of liver transplantation several centres have reported tolerance induction for graft recipients, either spontaneously or by a specific regimen, this may represent up to 60-80% of graft recipients (Feng, Ekong et al. 2012, Sagoo, Lombardi et al. 2012, Levitsky, Mathew et al. 2013, Safinia, Leech et al. 2013). These regimens are associated with chronic pathology, namely fibrosis, which is immune mediated (Yoshitomi, Koshiba et al. 2009). Thus the recipients are not tolerant to their grafts.

1.3.1 Definition

Immunosuppression is any act that supresses or reduces the efficiency of the immune system. This may be as a result of the effects of drugs (intentional or otherwise), surgery (e.g. splenectomy), radiation or due to immune compromisation e.g. due to HIV infection. An immunosuppressant is therefore any agent that supresses immune efficacy.

1.3.2 Types of immunosuppression

Immunosuppressive drugs can be sub-divided in terms of their effect on the immune system. One of the most widely known immunosuppressant drugs is

prednisolone (Trotter, Wachs et al. 2001). Prednisolone is a synthetic glucocorticoid/corticosteroid and acts upon nuclear glucocorticoid receptors (GR). GR activation has a number of effects, including the suppression of genre transcription genes including cytokines and cell adhesion molecules (Correale, Arias et al. 1998, Tripathi, Jafar et al. 2008, Matsuda, Koide et al. 2009, Jules- Elysee, Wilfred et al. 2012). The systemic adverse effects of steroids mean they are not used as a long-term treatment.

Azathioprine (AZA) was originally synthesised as a chemotherapy agent in 1957 and is a purine analogue. Metabolites of AZA (which is itself a pro-drug for 6-mercaptopurine) have various effects, the main effect being via the active metabolite methyl-thioinosine monophosphate (Mueller 2004). This blocks the enzyme amidophosphoribosyltransferase, which prevents synthesis of the purines adenine and guanine (Hoffmann, Rychlewski et al. 2001). As adenine and guanine are bases required for DNA synthesis, cells are thus unable to divide. Cells that are particularly affected are rapidly dividing cells without mechanisms for nucleotide salvage, for example lymphocytes (Mueller 2004).

Cyclosporine A (CsA) was isolated from a fungus in 1969 and found to have immunosuppressive activity in 1972 by Novartis (Drugge and Handschumacher 1988). The mechanism of action of CsA is by calcineurin inhibition and this gave rise to the class of drugs known as calcineurin inhibitors. CsA forms a complex with cyclophilin, which inhibits calcineurin by direct binding (Tocci and Sigal 1992). Under normal circumstances, activation or cross linking of the T-cell receptor leads to calcium flux within the cell; the rise in calcium acting via the calcium binding

protein calmodulin. Calmodulin activates calcineurin, which then de-phosphorylates the transcription factor nuclear factor of activated T cells (NFAT) (Billing, Giese et al. 2010, Dannewitz, Kruck et al. 2011, Wang, Tang Ch et al. 2013). NFAT activation results in transcription of interleukins and lymphokines, specifically IL-2 (Fig. 1.7). In the absence of IL-2, effector T cells are not produced as autocrine and paracrine IL-2 is a requirement for T-cell activation and maturation (Calne 1984).

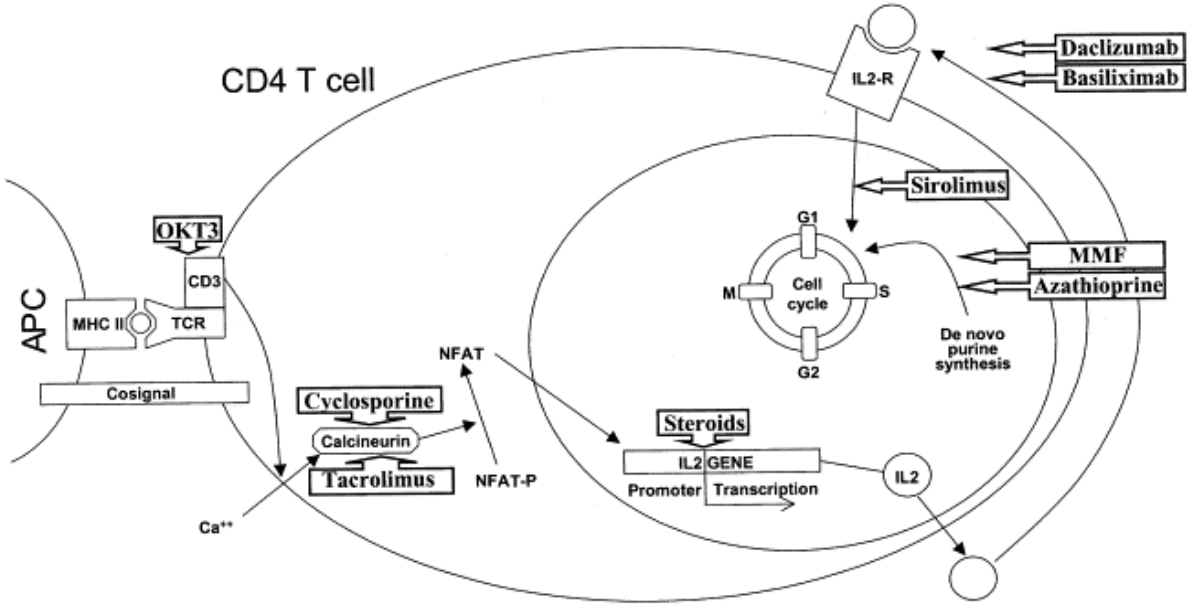

Figure 1.4: mechanism of action of immunosuppressive drugs. Shown to the left is a diagram indicating the site of action of the immunosuppressive drugs. Taken from (Mueller 2004)

Rapamycin (also known by the drug name Sirolimus) was discovered in 1975 by Brazilian researchers as a product from the bacteria *Streptomyces hygroscopicus* that was discovered in a soil sample from Easter Island ("Rapa-Nui"), giving rise to the name rapamycin (McKenna and Trotter 2012). It was first investigated as an anti-fungal agent before it was realised to have potent immunosuppressive

properties. It binds to the FK binding protein 12 (FK-BP12) complex that then binds the mTOR Complex 1 (mTORC1) preventing the action of mTOR (Khanna 2000, Saemann, Haidinger et al. 2009). By doing so, it prevents cells from responding to IL-2. This differs from calcineurin inhibitors that prevent synthesis/secretion of IL-2 rather than a response to IL-2.

Tacrolimus (FK506) is entirely different in structure and function to rapamycin. It was identified as a product of the bacteria *streptomyces tsukubaensis* from a fermentation broth of Japanese soil. Like rapamycin, it binds to FK-BP12, but rather than having an effect upon mTOR, the FK-12BP-tacrolimus complex inhibits calcineurin and acts in a similar manner to CsA (Tocci and Sigal 1992, Miyazaki, Fujikawa et al. 2007). Structurally, tacrolimus is a macrolide and was FDA approved in 1994 for use in organ transplantation (Fig. 1.4) (Kaminska, Gaweda-Walerych et al. 2004).

Mycophenolate mofetil (MMF) acts as a purine analogue and prevents the synthesis of guanine. It acts in a very similar manner to AZA, whereby it selectively targets dividing cells that do not have a nucleotide salvage process, namely T and B cells. MMF is available as a sodium salt to increase oral bioavailability (Neuberger, Mamelok et al. 2009, Rao, Haywood et al. 2013).

As noted in Figure 1.5, there are a number of agents that are used less frequently in transplantation, such as basiliximab or OKT3. Due to the rarity of their use (especially in liver transplantation) they are not discussed here.

1.3.3 Clinical use of immunosuppressive agents

All of the immunosuppressive agents listed above can and are used to prevent solid organ allograft rejection. Protocols for administration and specific drug use vary widely between the organ being transplanted and between individual centres. Each agent has its own profile of adverse reactions and interactions, which depend upon individual circumstances (Shaked, Ghobrial et al. 2009, Molinari, Berman et al. 2010). Broadly speaking, the protocols for immunosuppressive agents are divided into induction and maintenance regimes. The period of time immediately surrounding engraftment of the transplanted organ is when the majority of immune activation and response towards the graft occurs. For each MHC mismatch, there is a potential activation of up to 12% of the patient's immune repertoire (Suchin, Langmuir et al. 2001, van de Berg, Yong et al. 2012, Tay, Lu et al. 2013). When borne in mind that each organ can have numerous HLA mismatches and the normal response to a viral antigen activates around 0.01% of a patient's immune repertoire, the magnitude of the immune assault towards a graft can be appreciated.

Induction regimens often include high dose steroids combined with either tacrolimus or mycophenolate mofetil (MMF). Steroids are then tapered and stable doses of MMF or tacrolimus achieved. Often patients can be either placed on dual therapy, such as MMF and tacrolimus or with alternative combinations of a calcineurin inhibitor and a non-calcineurin inhibitor. Should any evidence of rejection occur, this is often treated with manipulation of the immunosuppression

such as increasing the dose of a maintenance agent or addition of short-term steroids (Wiesner and Fung , Levitsky, Mathew et al. 2013).

1.3.4 Duct sparing effects

It has been noted anecdotally that tacrolimus appears to spare the bile ducts in liver transplantation (Lunz et al 2001). As noted in section 1.2.1, the bile ducts are a key site of immune injury during the process of acute rejection. As a result, cholestatic effects due to this injury are often a feature of rejection episodes. In classic chronic allograft rejection of the liver, ductopenia is the main histological finding. However, patients treated with tacrolimus appear to have sparing of the bile ducts (Lerut, Mathys et al. 2008), though they still have evidence of rejection. This phenomenon has been described for some time, but no mechanistic studies have identified the biological reason behind this. Indeed, animal studies have shown exactly the reverse of the human data (Mohamed, Burt et al. 2001, Patsenker, Schneider et al. 2011).

1.4 Injury

1.4.1 Oxidative stress, reactive oxygen species, and other oxidative species

Oxidative stress is a cell injury process resulting from an imbalance in the redox (reduction / oxidation) state of an individual cell, tissue or organ. The balance is tipped in favour of the production of reactive oxygen species (ROS: free radicals and peroxides) as well as their resultant effects. ROS are highly reactive species containing at least one oxygen atom. ROS include molecules such as superoxide ($\bullet O_2^-$), which is formed by oxidative phosphorylation by mitochondria,

spontaneously forms hydrogen peroxide (H_2O_2) and can form hydroxyl radicals, both of which are more aggressive ROS (Kiani-Esfahani, Bahrami et al. 2013, Mracek, Holzerova et al. 2013, Orr, Ashok et al. 2013).

Cell injury due to oxidative stress is normally counterbalanced by antioxidants and cellular repair mechanisms, and oxidative stress may result from an increase in ROS or a decrease in antioxidant responses (Bhogal, Curbishley et al. 2010, Bhogal and Afford 2011, Orr, Ashok et al. 2013). The greater the reduction state of a species, the greater its reactivity, and the more lipid soluble a species, the more it can diffuse around the cell (Arnhold 2004). For instance, H_2O_2 is lipid soluble, and so can diffuse throughout cells and tissues. It has a two-electron reduction state, indicating two un-paired electrons. This indicates that H_2O_2 will give up two electrons readily and is therefore a more potent reducer than compounds with a one-electron reduction state, but less than those with a three electron reduction state (Kovacic and Pozos 2006, Aw 2012).

The hydroxyl radical (•OH) may be formed by the Fenton reaction or by decomposition of peroxynitrite. It is a highly reactive species that interacts with most cellular components. It has a three-electron reduction state. Peroxynitirite (ONOO-) is similar in activity to HOCl (hypocholorous acid) and both are highly reactive and lipid soluble. They will readily oxidise protein groups including methionine and amino groups. HOCl is formed by myeloperoxidase from H_2O_2.(Furtmuller, Arnhold et al. 2003, Mutze, Hebling et al. 2003, Panasenko, Spalteholz et al. 2003, Paiva and Bozza 2013)

Myeloperoxidase (MPO) is a haem-containing enzyme expressed by neutrophils and is an essential requirement for microbicidal activity. MPO can form a large number of oxidative species; each form can metabolise different substrates. In its native form, MPO binds H_2O_2 or superoxide, oxidising the haem iron ion to ferryl (Fe^{4+}) from ferric (Fe^{3+}) in the native state. This state of the enzyme is then able to react with Cl^- ions forming HOCl. Other states of the MPO enzyme exist and are able to participate in the formation of halides and peroxides. It follows that the presence of neutrophils during an inflammatory disorder indicates that a significant amount of oxidative damage can be produced (Arnhold, Furtmuller et al. 2003, Mutze, Hebling et al. 2003, Panasenko, Spalteholz et al. 2003, Arnhold 2004, Da Gama, Ribeiro-Gomes et al. 2004, Kovacic and Pozos 2006, Paiva and Bozza 2013).

MPO is not the only oxidative species that can cause oxidative stress during inflammation. Other immune cells can induce oxidative stress (for example via adhesion molecules, which can also form H_2O_2); senescent cells also have increased oxidative stress activity due to increased mitochondrial dysfunction. Ischaemia and the resultant oxidative injury can occur due to tissue injury (Weston and Adams , Arnhold 2004, Bhogal, Curbishley et al. 2010). Organ transplantation is a specific example of this.

1.4.2 Ischaemia reperfusion injury (IRI)

It is an inevitable consequence of the transplantation process that grafted organs are subjected to periods of ischaemia and then reperfusion. DBD organs have already undergone hypertensive crisis followed by a period of hypo-perfusion, which may or may not be partially corrected (Brain, Rostron et al. 2008, Rostron,

Avlonitis et al. 2008). Following this period of warm ischaemia, which can be extensive, the organs are flushed with ice-cold solution, removed and placed on ice for a variable period of time (this is the cold ischaemia time). Upon arrival at the implanting centre, further backbench preparation is performed before the organ is implanted, a process that can take a number of hours. Once the clamps are removed from the organ, blood can flow back into it, allowing reperfusion of the tissues (which also generates large amounts of ROS). DCD organs have had a much longer period of warm ischaemia and therefore tend to fare slightly worse than DBD organs (Steen, Sjoberg et al. 2001, Steen, Ingemansson et al. 2007, Lindstedt, Hlebowicz et al. 2011, Bendorf, Kelly et al. 2013, Snyder, Moore et al. 2013).

At a cellular level, ischaemia reduces the cell's energy production via oxidative phosphorylation. Anaerobic metabolism can continue for a period of time. Reduced energy production means reduced physiological processes, as these are energy dependent (Cooke, Evans et al. 2003, Droge 2003, Lunec, Holloway et al. 2003, Chapple and Matthews 2007, Okamura and Himmelfarb 2009). ATPases such as the cell membrane Ca^{2+}/K^{+} pump are unable to function effectively during periods of ischaemia, leading to a build-up of ion concentration gradients not normally found in homeostasis. Once reperfusion occurs, oxygen and calcium may flow back into the cells. This happens on a background of ATP depletion or absence, so the ATPases usually responsible for the maintenance of ion gradients do not function. Calcium therefore is able to influx into cells (this is also due to increased mitochondrial calcium uptake). The increased calcium levels may lead to swelling and rupture of organelles (mitochondria) and potentially the cells themselves -

ending in cell necrosis (Cooke, Evans et al. 2003, Droge 2003, Lunec, Holloway et al. 2003, Mutze, Hebling et al. 2003, Passos and von Zglinicki 2005, Hewitt, Jurk et al. 2012).

During reperfusion, the oxidation process can become de-coupled from phosphorylation, leading to inefficient or absent ATP production from the electron transport chain. This causes an increased number of free radicals to be produced, which in turn leads to further injury. The resultant changes in cellular pH can depress protein synthesis and enzyme function, as well as further inhibiting ATP production (Cooke, Evans et al. 2003, Kovacic and Pozos 2006, Ksiazek, Passos et al. 2008, Gorowiec 2009).

1.4.3 Effects of oxidative stress

Production of ROS leads to the oxidation of nucleotides, proteins and lipids. Lipid peroxidation (particularly of the polyunsaturated fatty acids required for membrane integrity) is the most serious of these sequelae, and if this happens to a significant degree, cells undergo apoptosis or necrosis (Ong, Jenner et al. 2009, Tojima, Kakizaki et al. 2011). DNA damage as a result of ROS results in formation of DNA adducts, of which there are numerous types (Cooke, Evans et al. 2003, Lunec, Holloway et al. 2003). These lesions are mutagenic and have been widely studied in the field of cancer research. If left unrepaired, such lesions may result in conformational changes in DNA, micro satellite instability, base or nucleotide switching - all of which can lead to cell death, senescence (section 1.8) or oncogenesis. Repair pathways do exist for the excision or repair of ROS generated

DNA adducts, however. Proteins altered by ROS are generally degraded rapidly by autophagy (section 1.9) (Rajawat, Hilioti et al. 2009)

1.5 TGF-β

One of the main fibrogenic and pro-epithelial to mesenchymal transition (EMT) factors is transforming growth factor-β (TGF-β). This belongs to a superfamily of cytokines including 42 individual members in several subfamilies: TGF-βs, Bone Morphogenetic Proteins (BMPs), Growth and Differentiation Factors (GDFs), Activins and inhibins (Massague 1990). The TGF-β subfamily consists of 5 members of which 3 (TGF-β1-3) are mammalian (Lawrence 1996). TGF-β4 and TGF-β5 were cloned from chickens and Xenopus laevis respectively (Hyytiainen, Penttinen et al. 2004). TGF- β has been described as the "master regulator" or "master switch" of fibrosis in many tissues and it has profound effects upon induction of fibrosis effector cells and the inhibition of epithelial cell function (Katsumoto, Violette et al. 2011)

TGF-β1 is the most commonly examined TGF-β isoform. Paradoxically, TGF-β1 was originally thought to be a growth-promoting factor. However, it has been shown to inhibit the proliferation of most cells and can lead to telomere independent senescence (Lunz, Contrucci et al. 2001). TGF-β1 can induce expression of extracellular matrix (ECM) proteins (including fibronectin and various collagens) and inhibit ECM-degrading enzymes (such as the metalloproteinases, MMPs (Flanders 2004). TGF-β also plays a role in cell adhesion and immunological responses via the regulation of integrin expression (Hyytiainen, Penttinen et al. 2004)

1.5.1 Latency Associated Peptide

When synthesised TGF-β molecules are almost ready for expulsion from the cell they are cleaved by furin like proteases producing the active 25-kDa TGF-β homodimer (formed of two 12.5 kDa TGF-β proteins) and a further 65-74-kDa homodimer from the N-terminal ends of the pro-TGF-β peptides and known as the latency associated peptide (LAP). The cleavage products associate non-covalently with each other, forming a hetero-tetramer (two TGF-β molecules and two LAP). The LAP facilitates exit of the TGF-β molecule from the cell and renders the TGF-β inactive (Khalil 1999).

Of the three human LAP's, TGF-β1 LAP (LAP-1) is the most well described. Binding of the LAP to TGF-β is dependent upon the cysteine residues within the LAP, as point mutated LAP with serines rather than cysteines at positions 223 and 225, TGF-β1 is excreted in an active form. The remaining cysteine forms a bond with the Latent TGF-β Binding Protein (LTBP-1). At the N-terminal, there are linked carbohydrates containing mannose-6-phosphate groups and these can interact with insulin like type II receptors upon the cell surface. When the TGF-β molecule is associated with the LAP alone it is referred to as the small latent complex (or SLC), when the SLC is bound to LTBP-1 it is referred to as the large latent complex (LLC), which is the only form of TGF-β that is secreted efficiently Depicted in Figure 1.5 (Ribeiro, Poczatek et al. 1999, Murphy-Ullrich and Poczatek 2000, Munger and Sheppard 2011).

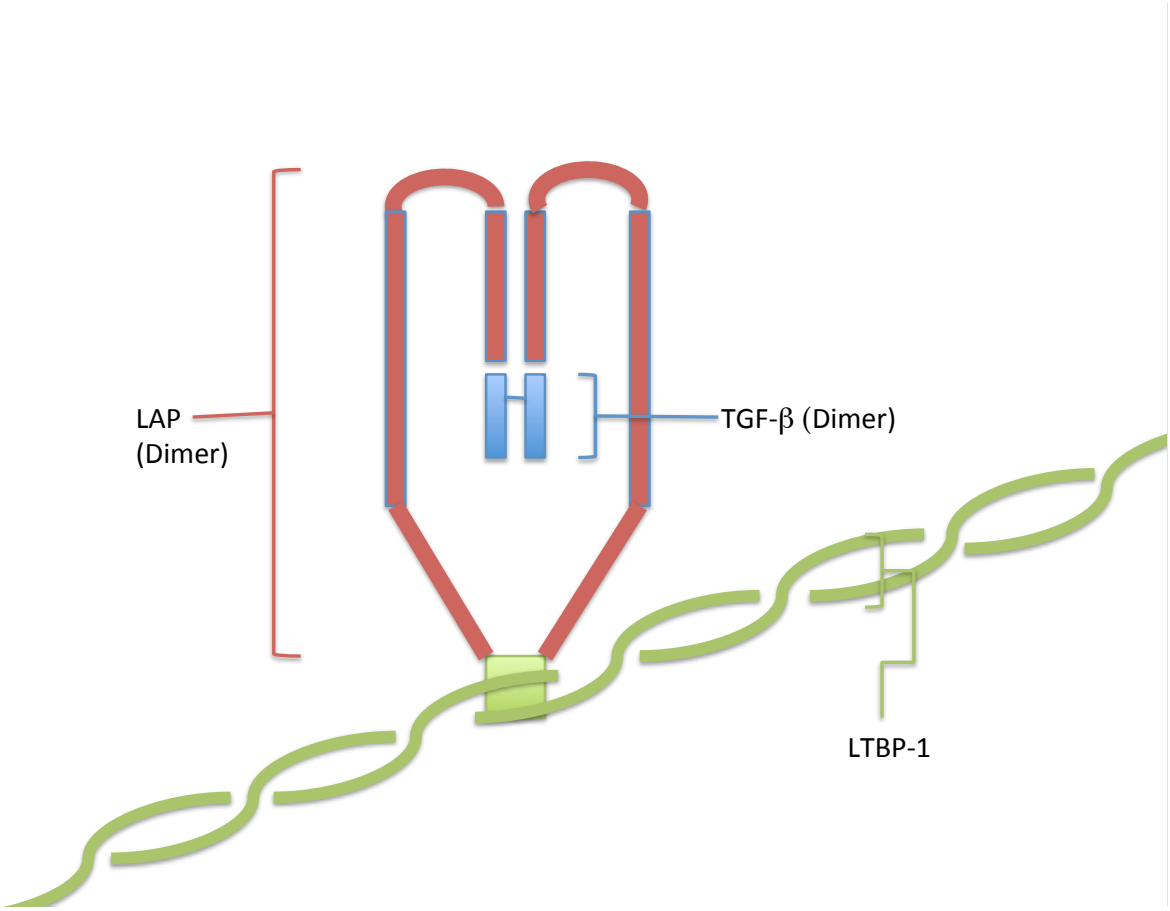

Figure 1.5: Latent TGF-β. Schematic representation of latent TGF-b, The TGF-b dimer is shown in blue, wrapped around this is the LAP dimer indicated in red. These molecules together are referred to as the small latent complex (SLC), which is a hetero-tetramer. Part of latent TGF-b binding protein (LTBP-1) is shown in green. When the SLC is complexed to LTBP-1 it is referred to as the large latent complex (LLC)

LAP's have been shown to contain sequences that may be involved in the regulation of TGF-β activity. One of these is the RGD motif (arginine-glycine-aspartic acid, the three amino acids that compose the region), which is recognised by many integrins and is present on fibronectin. It is known that the RGD motif is not present on LAP-2, but is present upon LAP-1 and LAP-3 (Humphries 2000, Williams, Kajander et al. 2004, Campbell and Humphries 2011, Sullivan, Kassel et al. 2011).

1.5.2 Signalling

The TGF-β receptors signal via serine/threonine kinase activity. The process is complex and requires three families of proteins. The first, the carrier protein β-glycan (a type III receptor), binds active TGF-β. This complex is then bound by two dimers, each composed of subunits of type I and type II TGF-β Receptors (TβR-1 and TβR-2) (Hanks, Holtzhausen et al. 2013, Li, Longobardi et al. 2013). There are seven TβR-1 and five TβR-2. However, only the alk-5 isoform of TβR-1 and the alk-1 isoform of TβR-2 are used in TGF-β1 signalling. The type 2 receptor is activated by ligand binding (Konkel and Chen 2011, Li and Zhou 2013). This leads to phosphorylation of the type 1 receptor in a regulatory segment upstream of the kinase domain. Phosphorylation blocks binding by the inhibitor Smad7 and allows binding of other members of the receptor regulated Smad (rSmad) family. Smad family proteins are differentially activated by TGF-β signalling. Neuropilin-1 has been shown to regulate R-Smad activity between either the Smad 1,5,8 and Smad 2/3 mediated pathways (Cao, Szabolcs et al. 2011). Activation leads to binding of various adaptor proteins and results in translocation of Smad complexes to the nucleus, where they regulate transcription of a number of potential targets. Smad 6 and Smad 7 have been utilised in a number of model systems to regulate TGF-β signalling (Lawrence 1996, Gorowiec 2009).

TGF-β Smad signalling is via the Smad 2 or 3, which are phosphorylated by the tyrosine kinase activity of the ALK-5 TGF-βR (Zode, Sethi et al. 2011). Once phosphorylated Smad 2 or 3 interacts with the common mediator Smad4, enabling nuclear trafficking and accumulation of the Smad 2/4 or 3/4 complex and

subsequent transcriptional regulation (Cao, Szabolcs et al. 2011, Masszi, Speight et al. 2011). As noted above, Smad 6 and Smad7 are inhibitory Smads, which compete for receptor phosphorylation with Smad 2 or 3 and are also able to recruit E3 ubiquitin ligase to the Smads or to the receptor complexes (Song, Wang et al. 2006, Cao, Szabolcs et al. 2011). This Smad dependent signalling is known as the canonical TGF-β signalling pathway.

Non-canonical signalling via TGF-β is not Smad dependent and may involve MAPK family members such as p38, JNK and ERK as well as Akt/PKB. All of these pathways are activated by the receptor tyrosine kinase activity of ALK-5 with co-dependency upon a PI3K (Zhang 2009). Appropriate assessment of signalling via TGF-β should therefore take into account both the canonical and non-canonical pathways as a number of potential signalling pathways may operate in parallel.

Previously, BEC have been shown to adopt a spindle cell appearance, very similar to myofibroblasts (MF), after application of active TGF-β1 in culture for 72 hours (Rygiel 2009). Further investigation revealed statistically significant decreases in ZO-1 and E-Cadherin expression and increase in αSMA expression, both characteristics of EMT. In the *in vitro* system used, (levels of TGF-β present in the medium were as low as to be insignificant (Rygiel 2009) indicating that this was entirely due to exogenous TGF-β).

1.5.3 Activity of TGF-β

TGF-β is known to exist in several inactive forms (Hyytiainen, Penttinen et al. 2004); these are described in section 1.5.1. Activation of latent TGF-β may be due to

expression of specific integrins (such as αVβ6) or other cell surface molecules (such as Thrombospondin (Lawrence 1996), allowing the associated TGF-β binding proteins that confer latency to be "peeled back" from the active TGF-β itself (Katsumoto, Violette et al. 2011).

TGF-β and *Wnt* (a family of growth factors) signalling have been shown to induce (the pro-EMT transcription factor) snail, (Meindl-Beinker and Dooley 2008). In turn, snail down regulates E-cadherin, triggering EMT. Snail is subsequently tagged by phosphorylation and ubiquitination for destruction by the proteasome complex (Thiery, Acloque et al. 2009). The phosphorylation event is mediated by glycogen synthase kinase 3β (GSK3β) and as such, can be inhibited by Axin-2 (part of the Wnt pathway). Work by the group of Diehl et al (Omenetti, Yang et al. 2007) implicated hedgehog signalling in EMT induction and fibrosis, showing that knockout mice deficient in hedgehog signalling demonstrate an exuberant fibrotic response following bile duct ligation (Omenetti, Yang et al. 2007). Hedgehog is known to up regulate transcription factors controlling senescence-associated genes such as the rodent isoforms of p16Ink4A and p19ARF (Fleig, Choi et al. 2007, Omenetti, Yang et al. 2007).

1.6 Integrins

Integrins are type 1 transmembrane spanning proteins that function as both cellular anchors and signal transducers. The existence of integrins was hypothesised as early as 1911, when it was noted that cells required "some form of support" to grow in culture (Harrison 1911). 102 years later, the functions and regulatory intricacies of integrin binding are still far from being completely understood.

Integrins are obligatory heterodimers, being composed of an α and a β chain (Wolfenson, Lavelin et al. 2013).

1.6.1 Integrin subunits

Mammals express 18 α subunits and 8 β subunits, forming up to a (currently described) 24 separate integrins. On average, α chains are 1000 amino acids in size; β chains are around 750. There are splice variants of some subunits, for example the β1 subunit has four potential splice variants (Mould, Symonds et al. 2003). Both α and β chains have C-terminal intracellular components, that are usually small in size. This is in contrast to the extracellular domains, which are usually much larger and can extend from the cell surface to distances over 20nm (Humphries 2000, Da Gama, Ribeiro-Gomes et al. 2004, Humphries 2004, Campbell and Humphries 2011, Geiger and Yamada 2011, Bridgewater, Norman et al. 2012).

1.6.1.1 α integrin subunits

The extracellular domains of the α subunit comprise a β propeller, a thigh and two calf domains. Half of all known α subunits also have an α-I domain inserted between the 2 and 3 blades of the β propeller. The I domain comprises seven alpha helices surrounding five β sheets. The thigh and calf domains resemble immunoglobulin β-folds. Sites between the β-propeller and thigh and the thigh and calf (knee or genu) offer extracellular flexibility (Kong, Li et al. 2013, Wolfenson, Lavelin et al. 2013).

1.6.1.2 β integrin subunits

The β subunits are more complex than the α chains and are composed of seven domains with various interconnections. There is a β-I domain, a plexin-semaphorin-integrin (PSI) domain, four epidermal growth factor (EGF) domains, which are cysteine rich, followed by a β tail domain. Both α and β subunits have membrane spanning helices (Campbell and Humphries 2011).

The N-terminal portions of both chains are specific for ligand binding. The regions and specificity of these regions can be inter-dependent upon the specific subunits involved. For example, certain α subunits contain the α-A domain similar to that found on von Willebrands factor, which is usually a collagen-binding domain. This is the case when α-A containing α subunit are bound to a β-1 subunit and the integrin binds to collagen sub-types in the ECM (Humphries, Byron et al. 2006, Askari, Buckley et al. 2009, Askari, Tynan et al. 2010, Bridgen, Gilchrist et al. 2013). If the α subunit is complexed with a β-2 subunit, it functions as a cell-cell interaction mediator. The RGD binding motif is a commonly found β subunit motif. This acidic domain functions as a cation binding site and is a specific for a number of proteins, notably fibronectin, but can also bind the RGD sequence in the LAP of TGF-β1 and 3 (Neurohr, Nishimura et al. 2006, Katsumoto, Violette et al. 2011)

1.6.2 Distribution and regulation of integrins

There is some exclusivity between certain subunits; as noted above, the specific subunits present in mammals would give 144 possible permutations (18 α and 8 β) before taking into account splice variants. However, only 24 integrins have been

described in mammals to date. Examples of exclusivity include the β6 and β8 subunits that will only associate with the αV subunit. The αVβ6 integrin is the only integrin that is restricted to epithelial cells. It appears that (in mouse models at least), only αVβ6 and αVβ8 integrins are relevant to TGF-β regulation in models of fibrosis and injury. Both integrins are present at minute concentrations, if at all, in sites such as the lung and skin, but are markedly up regulated in injury (Kim, Kugler et al. 2006, Neurohr, Nishimura et al. 2006, Katsumoto, Violette et al. 2011, Munger and Sheppard 2011, Henderson and Sheppard 2013). This injury specificity indicates that inhibitors of specific integrins rather than blanket TGF-β blockade could specifically target sites of interest (Katsumoto, Violette et al. 2011). The β propeller is the site of α and β binding and is cation dependent.

1.6.3 Activity of integrins

The structure of integrins is dynamically linked to their function and activity. Studies of integrin structure have been challenging due in part to the highly glycosylated nature of the chains. Integrins are synthesised in a folded or "bent" configuration and current evidence suggests that this is likely to be the active conformation of integrins once ligand binding has taken place. This can be seen in Figure 1.6, where the αXβ2 integrin is shown in ligand bound and unbound states.

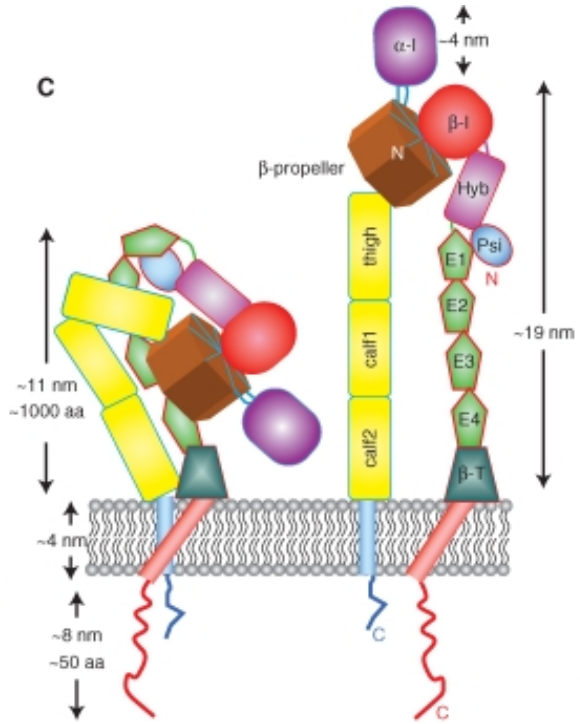

Figure. 1.6: structure of the αXβ2 integrin. The active or "bent" conformation of the integrin is shown on the left, with the extended form on the right. The sections of the integrin subunits are labelled, along with the functional names of the specific components, such as the calf and thigh. The difference in conformation between the two states is as described in the "switchblade" model (Taken from Campbell and Humphries 2011)

The conformational change displayed by integrins is the basis of their activity and signal transduction capabilities. Figure 1.6 demonstrates a significant change in morphology of the integrin, the so-called "switchblade" model. There is also an argument that smaller shifts in conformation can also be relevant to changes in integrin function, the "deadbolt" model (Humphries 2004). Core to both of these hypotheses is the concept that the conformational change in integrins is related to alteration of antibody recognition sites (Humphries 2004, Humphries, Byron et al. 2006, Askari, Buckley et al. 2009, Mould, Koper et al. 2009).

Integrins also have cation binding sites that may be relevant to activity via their effects upon structure. In a number of α-I containing integrins the binding sites MIDAS (metal ion dependent adhesion site, binds Mg^{2+} ions), ADMIDAS (adjacent to MIDAS, binds Ca^{2+} ion) and the SyMBS (synergistic metal ion binding site, binds Ca^{2+} ion) are present and have specific roles in determining integrin conformation. These three ions are essential, along with Mn^{2+}, for determining the active or open conformation of certain integrins. Mutations of these binding sites render the relevant integrins non-functional (Valdramidou, Humphries et al. 2008).

The cytoplasmic tails of integrin chains have not been reliably described by current technology, with crystallographic and nuclear magnetic resonance (NMR) structures varying widely between published studies. It is most likely that this indicates that the C-terminals have a large degree of flexibility, certainly under the isolated conditions of the reporting studies. The length and apparent flexibility of the cytoplasmic domains of integrin chains means they are able to simultaneously interact with a number of intracellular proteins (Askari, Buckley et al. 2009).

The cytoplasmic portions of integrins contain conserved NPXY motifs that interact with PTB domains on intracellular proteins, for example the integrin binding proteins talin and kindling. This interaction also appears to keep the α and β chains separate. Upon binding to ligands (most experimental data arises from the use of RGD peptides on RGD binding motif integrins), the cytoplasmic tail changes in conformation, exposing previously hidden or veiled binding sites (Watson, Humphries et al. 2007, Telci, Wang et al. 2008, Kong, Li et al. 2013).

Integrins function as adhesion points for cells. To do this, they form complexes such as the focal adhesion complexes and nascent adhesions (shown by light microscopy of migrating cells). In these foci, the C-terminals of the integrin subunits act as intermediates between the ECM and intracellular cytoskeleton. Adaptor proteins attaching to the C-terminals of integrins facilitate the interaction, with ligand binding of integrins (e.g. to an RGD motif on fibronectin), changing the conformation of the intracellular C-terminal of integrin and exposing the binding sites for adaptors such as talin. Adaptor proteins then mediate interaction with other signalling molecules and actin, meaning that anchor points for the cytoskeleton are established and signalling (e.g. via focal adhesion kinase) can occur, so called "outside in" signalling. It is also the case that binding of cytoskeletal proteins and adaptors to the C-terminal of integrins can cause a conformational change to the ligand binding N-terminal domains. The cell can therefore determine whether it wants to bind certain ligands by selective sampling, so called, "inside out" signalling (Mould and Humphries 2004, Askari, Buckley et al. 2009, Munger and Sheppard 2011).

Conformational change of the integrins is therefore a fundamental principle that dictates which ligands can be bound. This has been demonstrated in activation of latent TGF-β by $\alpha V\beta 6$ integrin in a Lysophosphatidic acid (LPA) dependent mechanism (Xu, Porte et al. 2009). This process appears to be dependent upon both the action of GTPases and also cytoskeletal traction (Giacomini, Travis et al. 2012) indicating that the process of activation is dictated by cell state and environment.

1.6.4 Blockade of integrin function

Blockade of integrin interaction is dependent upon sequence specific traits between the ligand and the ligand-binding domain. The most ubiquitous domains are the α-I domain and the RGD binding domain. Kraft (Kraft, Diefenbach et al. 1999) identified a non-RGD sequence specific for the binding of the RGD recognition motif on αVβ6, but not on other RGD binding ligands. This was shown to block the integrin αVβ6 specifically, rather than the non-specific RGD sequence peptides that had been used previously. Antibodies specific to αVβ6 have been successfully used to prevent biliary fibrosis after transplantation in a rodent model of liver transplantation, indicating that specific targeting of the αVβ6 integrin may be a therapeutic modality in other VBDS (Chen, Zhang et al. 2013). Indeed, a small molecule αVβ6 integrin has been used to block liver fibrosis in rodent models (Patsenker, Popov et al. 2008) whereas blockade of the αVβ3 integrin by the same group, lead to exacerbation of fibrosis in rodent models (Patsenker, Popov et al. 2009). This indicates that integrin blockade represents a targeted and specific therapeutic modality in fibrosis management.

1.7 Fibrosis

1.7.1 Definition

Tissue fibrosis is characterised by the accumulation of ECM deposited by MF. Liver fibrosis is one of the potential sequelae of chronic liver injury and may be seen as a consequence of inflammation, such as that seen in chronic infection (e.g. Hepatitis C), toxin mediated disease (e.g. alcoholic liver disease, ALD) and both allo- and

auto-immune disease (e.g. PBC and PSC) (Parola, Marra et al. 2008). End stage fibrosis is termed cirrhosis and is characterised by disruption of the architecture of the liver. End stage liver disease accounts for 4,000+ deaths per year in the UK alone; most estimates indicate this number will increase significantly in the next few years. As with other end stage organ failure, the only realistic option for many patients is transplantation. At present, only 600-700 orthotopic liver transplants are carried out each year in the UK. (www.UKTransplant.org.uk 2010), this is mainly due to a shortage of suitable donors.

1.7.2 Progression and reversal in liver disease

Fibrosis, and resultant cirrhosis, is a common end pathway for many forms of liver disease. There are various systems for scoring fibrosis found in liver biopsies and resections/explants, giving a numerical score that increases with increasing fibrosis. The loss of function of the liver is relatively preserved and can be maintained even in patients with established cirrhosis. The reduced physiological reserve associated with cirrhosis means that patients can decompensate very quickly from apparent minor stress such as an inter-current infection. Patients become rapidly jaundiced, blood clotting becomes prolonged and encephalopathy may result (Lo, Lefkowitch et al. 2008, Pells, Mells et al. 2013).

The numerical stage associated with fibrosis scoring indicates a progressive phenomenon, but this can also reverse, at least in early stages, when the injurious stimulus is removed. Whether cirrhosis can reverse and remodel to a near normal liver is uncertain, although evidence from biopsies and animal models would suggest this (McCrudden and Iredale 2000, Fallowfield, Kendall et al. 2006,

Henderson and Iredale 2007, Ramachandran and Iredale 2009, Iredale, Thompson et al. 2013). However in studies of explanted livers no evidence of complete reversal has been identified. It should be stated that remodelling of cirrhosis can occur, with the pattern of cirrhosis changing from micro nodular (being composed of nodules of less than 3mm in diameter) to a macro nodular cirrhosis (where the nodules are larger than 3mm in diameter) (Friedman 2008, Burt 2011).

1.7.3 Histological patterns of fibrosis

Key features of fibrosis in cirrhosis include the establishment of broad fibrous septa, linking portal tracts to each other and to central veins, and disturbance of the vascular architecture. Vascular disturbance may lead to increased portal pressure, resulting in features of portal hypertension (splenomegaly, varices etc.). This process is progressive, but over an uncertain timescale. There have been efforts to stage fibrosis progression with several different schemes. The two main fibrosis score schema used are the Ishak (Ishak, Baptista et al. 1995) and the METAVIR (Bedossa and Poynard 1996), which refer mainly to viral hepatitis but the fibrosis scoring has been used in various liver diseases. In the spectrum of non-alcoholic fatty liver disease (NAFLD) the Brunt (Brunt, Janney et al. 1999) and CRN (Kleiner, Brunt et al. 2005) schemes are used, though these contain necroinflammatory scores due to disease and the fibrosis scores are distillations of the METAVIR system. METAVIR uses a 4-point scale from 0, indicating no fibrosis to 4, indicating established fibrosis. The Ishak system expands this up to 6; again from 0 (indicating no fibrosis) to 6 (indicating established cirrhosis). Use of the METAVIR

system frequently leads to pathological staging of 3/4 from 4, an incomplete cirrhosis, this is an explicit stage in the use of the Ishak system (5 from 6).

Of key importance in the interpretation of these schemes is the fact that the number does not reflect a quantitative laboratory test (such as a biochemical parameter). The numbers generated should be used as a guide and in the context of clinic-pathological correlation. Resolution of fibrosis has been discussed elsewhere (section 1.7.2), no clinical scoring systems are yet available that take remodelling or reversal into account

1.7.4 Fibroblasts

MF are the cells responsible for laying down the ECM in fibrotic disease. These cells are intermediate in both form and function between fibroblasts and smooth muscle cells. αSMA is a cytoskeletal protein seen usually in relatively few cells, including vascular smooth muscle cells, and is associated with contractility and cellular locomotion (Guyot, Lepreux et al. 2006). This key feature confers the contractility seen in wound healing and MF are therefore characterised by αSMA expression. The precise origin of hepatic MF is uncertain and hepatic stellate cells (HSC) have been identified as strong potential candidates (Parola, Marra et al. 2008). HSC represent approximately 10% of cells in a normal/healthy liver and are present within the sinusoids in the space of Disse. During disease, HSC become activated and adopt a myofibroblastic phenotype; expressing αSMA and secreting type I collagen (Kent, Gay et al. 1976, Friedman, Roll et al. 1985).

However, HSC are not the only potential hepatic mediators of fibrosis; rodent models of cholestatic liver disease (Guyot, Lepreux et al. 2006, Beaussier, Wendum et al. 2007) demonstrated that portal fibroblasts (PF) may differentiate into MF; for instance, isolated rodent fibroblasts treated with TGF-β begin to express αSMA and develop a MF phenotype (Friedman 2008). This differentiation of HSC from PF was characterised by Desmin expression, HSC express desmin whereas PF do not (Kinnman, Francoz et al. 2003, Rygiel 2009). Studies from human liver also show that portal fibroblasts have the potential to generate significant numbers of myofibroblasts and that this may be disease dependant (Cassiman, Libbrecht et al. 2002, Libbrecht, Cassiman et al. 2002).

Further candidates for MF include bone marrow progenitors, as described by Forbes et al. (Forbes, Russo et al. 2004). This group demonstrated that, in a patient with liver fibrosis who had previously received a sex mis-matched bone marrow (BM) transplant, BM-derived progenitors constituted 12.4% of the hepatic MF. These data have also been verified in rodent models (Direkze, Forbes et al. 2003, Asawa, Saito et al. 2007). Perhaps most controversially, epithelial cells (including both hepatocytes and cholangiocytes) undergoing EMT have been suggested as the origin of some hepatic MF (Sicklick, Choi et al. 2006).

1.7.5 Epithelial to Mesenchymal Transition

EMT and the complimentary process, mesenchymal to epithelial transition (MET) are well recognised and are described during embryogenesis and oncogenesis (Zeisberg, Potenta et al. 2007). EMT is characterised by altered transcription and nuclear signalling with a phenotype shift characterised by the down regulation of

epithelial cell associated proteins and up regulation of mesenchymal cell-associated proteins (Lee, Dedhar et al. 2006). Characteristic changes include the loss of intracellular junctions such as tight and adherens junctions and desmosomes. These junctions are the defining feature of epithelia, allowing the maintenance of polarity and ordered 3D structure of both single and multiple layered sheets. Of the tight junctions, Zonula Occludens proteins (such as ZO-1) form the central role by interacting with claudins. This forms a scaffold and allows interactions with other proteins such as actins and catenins (Kirby, Robertson et al. 2008). ZO proteins also form links between tight and adherens junction proteins, such as E-Cadherin (Hartsock and Nelson 2008).

By contrast, mesenchymal cells are irregular, exhibiting spindle cell morphology with no uniformity in structure. A defining feature of mesenchymal cells is the capacity to migrate. These cells move individually, like invasive cancer cells, whereas epithelial cells migrate as a cohesive sheet (Lee, Dedhar et al. 2006).

A key function of adherens junctions is interaction between cadherins (containing extracellular domains involved in adhesion and signalling) and the actin cytoskeleton, which mediates motility and endocytosis. In particular, the interaction between E-cadherin and β-catenin is of interest. This interaction mediates signalling via the *Wnt* family of growth factors (Moon, Bowerman et al. 2002). Secreted *Wnt* proteins bind to one of the frizzled family seven-pass transmembrane receptors. This causes the axin and dishevelled proteins to associate, preventing GSK3β kinase activity. One of the key targets of GSK3β is β-catenin (Polakis 2000). Phosphorylation of β-catenin prolongs its action by

preventing E3 ubiquitin ligase-mediated proteosomal degradation. β-catenin has been shown to have a potential role in mediating EMT (Reya and Clevers 2005).

As a process, EMT has been shown to progress through a number of discrete, linked steps: disruption of adherens junctions, dissociation of tight junctions, loss of polarity, cytoskeletal remodelling and remodelling of the basement membrane. This paradigm holds for numerous models of EMT. However, there is emerging evidence that composition, degradation or modulation of the basement membrane may also initiate EMT (Ward, Forrest et al. 2005, Hosper, van den Berg et al. 2013). Type IV collagen and laminin comprise major amounts of the ECM in the healthy liver and have been shown to maintain epithelial characteristics via integrin signalling outside in. In the lung, for example, alveolar cells cultured on a collagen and laminin matrix are protected from EMT induced by activated TGF-β. Replacing the matrix with one composed of fibrin and fibronectin removes this protective effect (Kim, Kugler et al. 2006).

The origin of (myo) fibroblasts remains contentious, however there is evidence that epithelial cells may play a role in fibrogenesis. Following tissue injury, cells respond to stimuli present in the milieu of the organ. This may include factors such as TGF-β, that prompt epithelia to undergo EMT with adoption of a MF phenotype (Kalluri and Neilson 2003).

Iwano et al. (Iwano, Plieth et al. 2002) used the established unilateral ureteric obstruction (UUO) mouse model to investigate EMT in renal fibrosis. Transgenic

approaches to cell lineage tracing revealed that around 36% of fibroblasts in the UUO kidney originated via EMT of the tubular epithelium.

Humphreys et al (Humphreys, Lin et al. 2010) used a transgenic mouse model to label renal epithelial cells with green and red fluorescent protein. Following a UUO model the authors described no evidence of renal epithelial cell EMT. This is in direct contrast with the groups of Nielson, Zeisberg and Kalluri (Iwano, Plieth et al. 2002, Kalluri and Neilson 2003, Teng, Zeisberg et al. 2007, Zeisberg and Neilson 2011). These apparently divergent results from well respected groups caused wide spread disagreement amongst the scientific community, this was not restricted to renal disease.

In the area of liver fibrosis, a number of *in vitro* and *in vivo* models have demonstrated EMT of hepatocytes and cholangiocytes in the formation of fibrosis. Xia et al. (Xia, Dai et al. 2006) demonstrated that a cholangiocyte primary culture and a rodent bile duct ligation model both gave rise to fibroblasts by cholangiocyte EMT. The TGF-β induced EMT seen in culture was reinforced by the co-expression of CK19 and αSMA in cholangiocytes.

Kirby (Rygiel, Robertson et al. 2010) demonstrated evidence of EMT of cholangiocytes in human liver tissue from patients with chronic liver disease. Mesenchymal markers, and downstream effectors of TGFβ signalling (phospho-Smad2/3), were detected in cholangiocytes from fibrotic tissue (Robertson, Kirby et al. 2007, Rygiel, Robertson et al. 2008).

Hepatocyte EMT has also been investigated quite widely. Nitta et al (Nitta, Kim et al. 2008) used the CCL_4 hepatotoxicity model of liver fibrosis, demonstrating expression of ECM proteins such as vimentin and type I collagen in hepatocytes isolated from cirrhotic livers. This expression was also seen in TGF-β application to primary hepatocytes. Dooley et al (Dooley, Hamzavi et al. 2008) added the finding that EMT can be blocked in this model by induction of Smad7 expression.

Zeisberg et al. (Zeisberg, Yang et al. 2007) used transgenic mice to perform lineage tracing in hepatocytes from the CCL_4 induced fibrosis model. EMT was unequivocally demonstrated using AlbCre and R26RstoplacZ double transgenic mice. This engineering ensured LacZ was only transcribed in hepatocytes (as defined by albumin-positivity). Dual staining of (myo) fibroblasts for X-gal and FSP-1 (fibroblast specific protein 1/S100A4) revealed hepatocytes that appeared to have undergone an EMT (though not all hepatocytes or MF were double positive). Using a similar approach, but substituting GFP tagged collagen I for FSP-1, Taura et al. (Taura, Miura et al. 2010) demonstrated collagen I producing cells showed no evidence of hepatocyte lineage, i.e. there was no dual positivity for albumin and FSP-1. The same study also performed IHC for αSMA, FSP-1, desmin and vimentin. Having previously reported evidence of biliary EMT in patient samples (Diaz, Kim et al. 2008) Wells et al used a transgenic approach that showed no evidence of EMT in rodent BEC (Chu, Diaz et al. 2011), which appeared to confirm the work of Brenner et al (Scholten, Osterreicher et al. 2011) which also used transgenic mouse modelling to refute the idea of biliary EMT. It should be noted however that the

transgenic labelling had a maximum efficiency of between 40 and 60% as stated in the paper (Scholten, Osterreicher et al. 2011)

At around the same time, (Humphreys, Lin et al. 2010) applied a similar transgenic approach to the UUO model previously described. Results indicated that Pericytes form the MF population (within the kidney fibrosis due to UUO model). Extrapolation of this principle would imply that Pericytes or cells of Pericyte lineage would also form MF in hepatic fibrosis. The most obvious candidate hepatic cell population producing mature MFs would therefore be the HSC.

At the time of writing (September 2013) the apparent disparity in the literature between the "pro" and "anti" EMT investigators seemed to be reaching a resolution. Following an ambitiously titled article (Zeisberg and Duffield 2010) indicating a resolution of the EMT debate in renal disease, the concept of EMT in liver disease was debated at the Banff working group meeting in 2011 (Mengel, Sis et al. 2012). While the main topic of the meeting was antibody-mediated rejection, the existence of EMT was debated at some length (work from the current study was presented at the conference). In the follow up correspondence from the meeting it proved impossible for a consensus opinion to be reached (John Kirby personal communication).

Further evidence of EMT emerged in both renal (Xu-Dubois, Baugey et al. 2013) and liver (Brain, Robertson et al. 2013) disease during 2013, these studies used predominantly human material and Immunohistochemical techniques to define cells undergoing EMT. There was a further animal study from Kalluri et al (Lebleu,

Taduri et al. 2013) that can only be described as a seminal piece of work. This paper used a comprehensive suite of transgenic mouse experiments in the UUO model to comprehensively describe the origin of myofibroblasts. This is consistent with most of the published literature on the subject. This described epithelial cells as contributing around 5% of MF and endothelial cells 10% of MF along with 35% of MF deriving from bone marrow progenitors.

One of the major arguments of those seeking to abolish the concept of EMT in fibrosis has been that epithelial cells do not become true mesenchymal cells, do not produce collagen 1 and do not express αSMA (Scholten, Osterreicher et al. 2011). There has also been a desire to promote the pericyte as the main contender for MF production. In liver disease a large amount of work has focused upon the HSC as the predominant MF producing cells. These cells are of presumed pericyte lineage (Mallat and Lotersztajn 2013, Villalobos, Giles et al. 2013). A fundamental principle of work into HSC has been the use of αSMA to define activated HSC (Friedman 2008, Friedman 2008). There are no reliable markers to define HSC (Friedman 2008), as such, accepting that epithelial cells can express αSMA would cast a long shadow over a large amount of HSC research.

1.8 Senescence

1.8.1 Definition

Senescence is defined as the “irreversible condition in which a cell no longer has the ability to proliferate” (Erol). Senescent cells display a number of unique characteristics, including nuclear enlargement, loss of polarity, eosinopilic

cytoplasm, telomere shortening and an increase in expression of markers such as $p16^{INK4a}$, $p21^{WAF1/Cip1}$, γH2AX, senescence associated β galactosidase, and lipofuscin (Lawless, Wang et al. 2010, Lawless, Jurk et al. 2012).

1.8.2 Historical perspective

The classical description of senescence was by Hayflick (Hayflick and Moorhead 1961) in reference to cultured human cells. It was noted that these cells had a limited number of population doublings in culture after which they did not replicate further and entered what has been called replicative senescence. It was discovered that the end portions of the chromosomes within the cells, the telomeres, reduced in length with every round of DNA synthesis and that once the telomeres reached a certain length the cells entered replicative senescence, with the introduction of the Hayflick limit indicating the number of times a specific cell population will divide in culture (Evan and d'Adda di Fagagna 2009).

While measurement of telomeres in isolated cell populations is possible, there are other situations in which it is beneficial to measure cellular senescence, both *in vitro* and *in vivo*. Examples include measurement of senescence in animal models of ageing, as well as in disease models where premature ageing is a feature. There has therefore been a consistent push among investigators to find surrogate markers of senescence that can be applied robustly to indicate when cells are senescent.

1.8.3 Markers of senescence

While many markers of senescence have been proposed there are few that are robust in every situation or individually. Indeed, it is only relatively recently that

quantitative assessment of markers has been achieved (Lawless, Wang et al. 2010). Replicative senescence is not the only form of this process. Senescence can be induced by DNA damage responses, over-activity of oncogenes, and by external stressors such as cytokines. Each of these could potentially induce senescence, albeit by very different mechanisms.

DNA damage and related foci have been used as markers of senescence, indeed these are referred to as Senescence Associated Heterochromatin Foci (SAHF) and telomere-dysfunction induced foci (TIF). TIF have been described in rodent cells with activated telomerase, indicating a telomere independent senescence associated with these foci (Wang, Tsai et al. 2010). DNA damage activates a number of processes that are potentially senescence inducing and can therefore be used as surrogate markers. The histone H2AX is phosphorylated at Ser-139 by double stranded DNA breaks, becoming referred to as γH2AX. This histone is an important aspect of the DNA damage response, facilitating the formation of checkpoints and DNA repair elements such as 53BP1, NFBD-1 and Chk1 and2, directly leading to p53 and p21 up regulation. The marker p16 can also be up regulated via this pathway (Passos, von Zglinicki et al. 2006, Vicencio, Galluzzi et al. 2008, Evan and d'Adda di Fagagna 2009, Zhou, Han et al. 2009, Passos, Nelson et al. 2010).

Using a mathematical model of population doublings and cell senescence, Lawless (et al 2010) were able to quantify the presence of senescence markers alongside growth curve data using an *in silico* parameter inference and simulation modelling system. The inferences from this system were validated in mouse embryonic fibroblasts. Once allowances for biological variation were taken into account via

modelling the most reliable markers assessed in this experiment were β galactosidase, and a combination of the absence of the proliferation marker Ki67 and the presence of >5 DNA damage foci per nucleus. In combination in the same cell, positivity for the senescence marker γ H2AX and negativity for the proliferation marker Ki67 represented the gold standard for senescence estimation (Lawless, Wang et al. 2010).

Specific markers are related to up and down stream cellular processes within the cell, for example investigation of $p21^{WAF1/Cip1}$ has revealed that downstream signalling increases activation and expression of diverse molecules, including p38 and TGF-β2 (Passos, Nelson et al. 2010) Many of these form the senescence associated secretory phenotype (SASP). Cells exhibiting a senescent phenotype are known to generate more ROS and have more mitochondrial dysfunction. Passos, Nelson at al. showed that by knocking down $p21^{WAF1/Cip1}$, p38 and TGF-βR2 in an *in vitro* fibroblast culture system, the amount of mitochondrial ROS and DNA damage was significantly reduced (Passos, Nelson et al. 2010). This concurs with the existing evidence that TGF-β and p38 activation can induce both mitochondrial and NADPHoxidase-dependent ROS (Passos, Nelson et al. 2010).

1.8.4 Cell senescence in vanishing bile duct syndromes

The group of Nakanuma (Sasaki, Ikeda et al. 2005, Sasaki, Ikeda et al. 2008, Ikeda, Sasaki et al. 2009) have investigated senescence in cholangiocytes as a feature that may contribute to fibrosis and/or ductopenia in a number of liver diseases, namely PBC, PSC and non- alcoholic steato hepatitis (NASH). Cholangiocytes in human liver biopsies from patients with PBC were shown to up regulate the senescence marker

$p21^{WAF1/Cip1}$; this was replicated in culture by significant oxidative stress (Sasaki, Ikeda et al. 2008). In addition, Sasaki et al. (Sasaki, Miyakoshi et al. 2010) identified the ductular reaction in chronic liver diseases as harbouring increased numbers of senescent cholangiocytes. Using an *in vitro* model, primary and immortalised cells became senescent and exhibited altered protein expression following exposure to H_2O_2 as a surrogate form of oxidative stress (Katayanagi, Kono et al. 1998, Harada and Nakanuma 2006, Sasaki, Ikeda et al. 2008). Senescent cholangiocytes may acquire an SASP, which can be both pro-fibrogenic and pro-inflammatory (Sasaki, Ikeda et al. 2005, Sasaki, Ikeda et al. 2008, Passos, Nelson et al. 2010).

The findings of H_2O_2 exposure (200µM for 2 hours) to rodent BEC (Sasaki, Ikeda et al. 2005, Sasaki, Ikeda et al. 2008) showed that oxidative stress was sufficient to produce a significant increase in $p21^{WAF1/Cip1}$ expression. A peak in $p21^{WAF1/Cip1}$ expression was observed after 72 hours by Sasaki et al. (Sasaki, Ikeda et al. 2008, Sasaki, Ikeda et al. 2008). There followed a rapid fall in $p21^{WAF1/Cip1}$ expression (almost back to baseline). A statistically significant change of $p21^{WAF1/Cip1}$ expression was shown over the time course of the experiments. The definition of senescence given above would imply that an up regulation in $p21^{WAF1/Cip1}$ would be sustained, though the interpretation of senescence (and the concept of senescence versus deep senescence) is variable in the literature (Passos and von Zglinicki 2007, Passos, von Zglinicki et al. 2007).

It would appear from the work of Nakanuma, that the $p21^{WAF1/Cip1}$ mediated cycle of senescence followed by ROS inducing further senescence could be found within cholangiocytes exposed to a single insult by means of H_2O_2 mediated oxidative

stress. In human disease, one might expect that if oxidative stress is the cause of senescence, that this would be a chronic, rather than acute, exposure. This hypothesis does not fit with the principle that acute ischaemia reperfusion injury during transplantation sets up the described $p21^{WAF1/Cip1}$ senescence cascade leading to ductopenia and/or fibrosis. While the origin of oxidative stress in ALD disease is obvious (alcohol and its break down products) this is not the case for some other liver diseases. One hypothesis is that inflammation and infiltration of the portal tracts, a feature of both early PBC and acute transplant rejection (Demetris, Adams et al. 2000), sets up a significant immune response. As the respiratory burst is known to generate large amounts of superoxide (Chapple and Matthews 2007, Gorowiec 2009), it may be that the immune response itself is acting as an agent of oxidative stress.

1.8.5 Reversibility of senescence

Original descriptions of senescent cells focused entirely upon replicative senescence and the loss of telomeres. Studies in gametes showed that telomeres could be extended during reproduction, replacing the telomere repeats lost during replication. The enzyme telomerase was subsequently identified, and has the ability to render cells immortal. Indeed, telomerase has been identified as a pathogenic species within malignancies (Hewitt, Jurk et al. 2012).

Arguably, the fact there is one way of reversing senescence suggests there will be others, although this may depend upon the factor(s) that initiate the senescence. DNA damage, for example, is dependent upon signalling systems that identify the damage and either initiate repair, senescence or apoptosis. Mutations in the genes

controlling this process, such as p53, can therefore prevent the initiation of senescence. It is well described in the head and neck cancer literature that virus mutated p16 is associated with a significantly increased risk of developing squamous cell carcinoma. Mutated p16 accumulates in epithelial cells and can be detected by immunohistochemistry. This prevents the usual cell cycle checkpoints from operating and inducing either senescence or apoptosis and acts as a permissive event for the initiation of carcinogenesis (Ishikawa, Sasaki et al. 2004, Thirthagiri, Robinson et al. 2007, Zhou, Han et al. 2009).

It can therefore be deduced that senescence can potentially be reversed under many circumstances. However, few of these circumstances are non-pathogenic. Senescence induced by soluble factors such as cytokines can potentially be reversed under physiological circumstances.

1.8.6 Senescence Associated Secretory Phenotype

One key feature of senescent cells is their ability to secrete cytokines and other mediators, a secretome referred to as the aforementioned SASP. This process directly challenges the notion that senescent cells are biologically inert and that they can have significant and measurable impact upon the cytokine milieu and cell state in the local environment. The SASP has been referred to as the dark side of tumour suppression (Coppe, Desprez et al. 2011) by commentators interested in inducing cellular senescence as a means of preventing tumour progression.

Factors known to be secreted by senescent cells include: MCP-1, IL-6, IL-8, IL-1β, CCL-20 and vascular endothelial growth factor (VEGF) (Rodier, Coppe et al. 2009, Novakova, Hubackova et al. 2010, Coppe, Patil et al. 2011, Cao, Walker et al. 2013).

Nakanuma et al (Sasaki, Ikeda et al. 2008) have investigated the ability of senescent BEC to secrete certain factors; these investigations have centred on the production of pro-inflammatory cytokines such as MCP-1 and IL-6 along with their ability to induce activation and migration in other cell types. There has been no investigation of other aspects of the BEC SASP.

Passos (Passos, Nelson et al. 2010) performed an in depth analysis of $p21^{WAF1/Cip1}$-initiated and senescence-associated expression of proteins in a cultured fibroblast population. This identified a putative, complicated, signalling pathway that may induce up regulation of TGF-β2, TβR2 and TβR1 as well as GADD45, p38, Smad 3 and 7. However, the exact levels of mRNA and protein expression were not quantified, and it may be that the response of senescent cholangiocytes is to secrete TGF-β2, inducing other cells to undergo EMT.

1.9 Autophagy

1.9.1 Autophagy introduction and mechanisms

Autophagy ("self eating") is a fundamental cellular process that encompasses a number of terms. The work described here will focus on macroautophagy (hereafter referred to as autophagy); the concepts of microautophagy and chaperone mediated autophagy are outside the scope of this work and are reviewed elsewhere (Yang and Klionsky 2011). Autophagy was initially regarded as

a cellular waste disposal system following discoveries of membrane bound “dense bodies” containing cellular organelles that were subsequently shown to contain semi-digested mitochondria and lysosomal enzymes. More recently, autophagy has been shown to play a significant role in providing nutrients and energy in response to cellular stress. This has implications for all disease states where exposure to cellular stress and the adaptive response of the cell are of fundamental importance, the most obvious example being in cancer therapy, though developmental biology and neurodegeneration are two others in a long list (Shibata, Yoshimura et al. 2010, Yang and Klionsky 2011). Most mechanisms of autophagy have been investigated in yeast, nematode worms and fruit flies, leading to the identification of autophagy related genes, labelled Atg1-31.

1.9.2 Autophagy function at the cellular level

Autophagy is present at basal levels within any cell for turnover of proteins with long half-lives and for dealing with damaged or surplus organelles. Autophagy is also a key response to stress at a cellular level, be this nutrient deprivation, heat or oxidative stress. Insufficient autophagy is potentially also a source of stress and cell death (Komatsu, Wang et al. 2007) Autophagy can be activated by a number of mediators responsible for monitoring and maintaining homeostasis. One such candidate is mTOR, the target of rapamycin’s nutrient sensor. Blocking 5' adenosine monophosphate-activated protein kinase (AMPK) mTOR (for example with rapamycin) potentiates autophagy by removing mTOR inhibition of the development of the isolation membrane. The role of autophagy in liver diseases has been reviewed elsewhere (Rautou, Mansouri et al. 2011), but to summarise, many

liver diseases exhibit both direct and indirect modulation of autophagy. Nutrient deprivation is seen in many liver diseases and leads to increased mTOR activity and increased autophagy via AMPK and uncoordinated 51-like kinases (Ulk) -1 or 2. The same is true of ethanol, which has a direct stimulant affect on AMPK, leading to increased autophagy. At the level of vesicle fusion regulation and membrane formation, there are numerous points at which the process can be inhibited, be it by ethanol inhibition of isolation membrane formation or hepatitis C virus (HCV) mediated prevention of autophagosome to autolysosome maturation.

1.9.3 Formation of autophagy complexes

Autophagy occurs by the formation of a single or double membrane bound phagophore (produced at the phagophore assembly site or PAS), which then fuses with lysosomes to form the autolysosome. Investigation of this process has identified a number of autophagy specific genes with core groups of "molecular machinery" required for successful completion of the process (Figure 1.7). The class III PI3-K complex I is one of the key complexes required for the production of the isolation membrane, leading to formation of the autophagosome. Within this, the genes Atg14 (which is autophagy specific) and Vps34 (which is a class III PI3-Kinase specific for autophagy that has received a degree of attention due to its feasibility as a drug target) are of particular interest (Simonsen and Tooze 2009, Sasaki, Miyakoshi et al. 2010).

Autophagy induction is controlled largely by TORC1, one of the two complexes containing the mTOR protein. TORC1 regulates the induction of the Atg1 protein (mammalian homologues the uncoordinated 51-like kinases 1 and 2/Ulk-1 and -2),

which is essential for autophagy induction. Atg1 activity is dependent upon formation of a complex containing Atg13 and Atg17 (Chan, Kir et al. 2007). The exact substrate for Ulk-1 and -2 is unknown, though recently FIP200 was identified as an Ulk related protein that is required for autophagy induction (Hara, Takamura et al. 2008). While this complex is the initiating step in autophagy, it is also controlled upstream by various pathways such as the tuberous sclerosis complex (TSC-1 and -2) via Akt and class I PI3K. Insulin-like growth receptors may also feed into this pathway as part of the nutrient sensing system in mammalian cells.

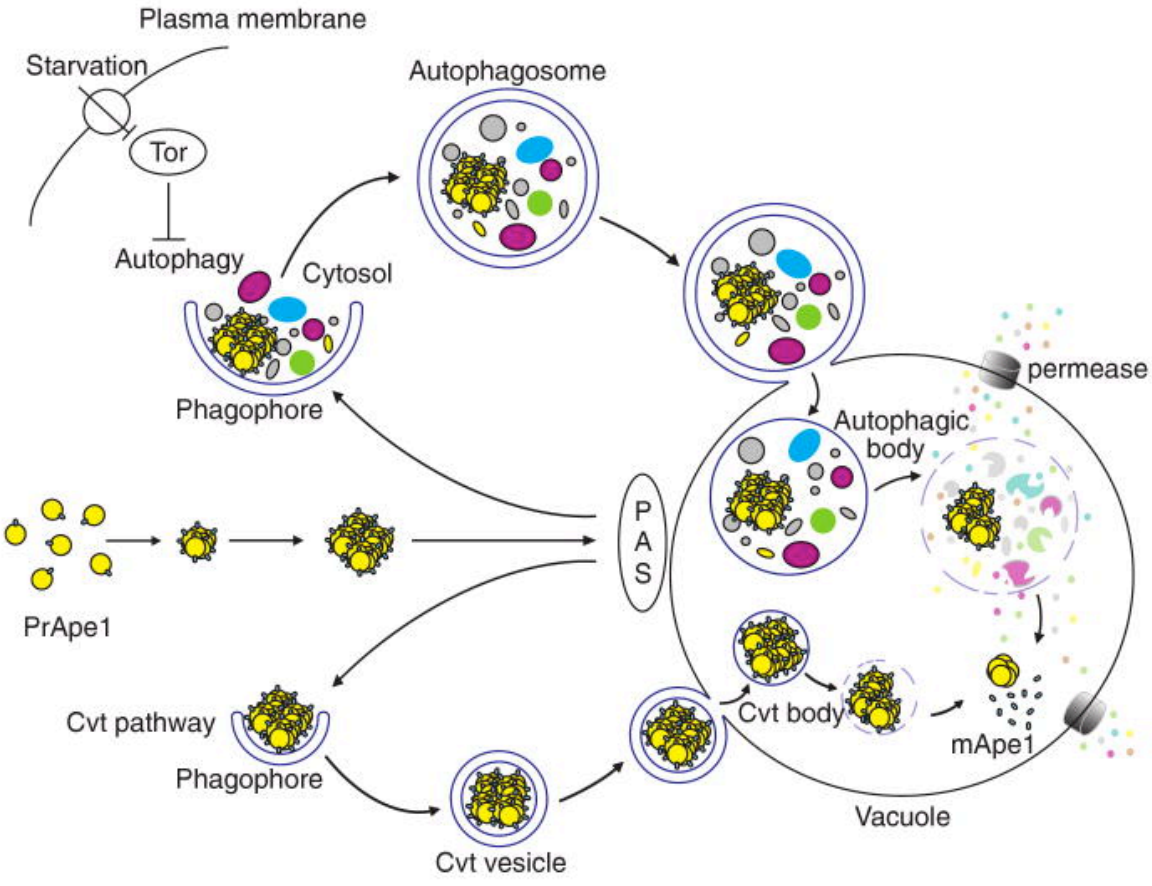

Figure 1.7: initiation and formation of the autophagosome. The process for initiation and extension of the phagophore is shown, with the double-layered membrane clearly shown. The caveolin mediated autophagy pathway (Cvt pathway) is also shown, note the similarities (the differences being the molecules targeted for breakdown). (Taken from Yang and Klionsky 2009)

Formation of the Class III PI3K complex is key to autophagy regulation. The class III PI3K in mammals is hVps34 and it is regulated by p150 (in yeast Vps15) and the regulator associated protein Beclin 1 (in yeast Vps30/Atg6). P150 is required for activity and membrane association of Vps34 via its serine/threonine kinase activity. The PI3K complex is recruited to the PAS and it is believed that the production of posphatidyl-inositol (3) phosphate recruits binding proteins to the PAS, initiating downstream signalling via phospho-kinase B (PKB) and possibly by feedback into mTOR. The pathways in mammals are much more complicated than their yeast homologues and the exact processes are not identical (Chan, Kir et al. 2007, Simonsen and Tooze 2009, Tooze, Jefferies et al. 2010).

A further complex involved in autophagy initiation is regulated in a similar manner to an E2 ubiquitin conjugation system. Atg10 activity leads to the formation of a complex containing Atg12, -5 and -16. This complex is a functionally essential part of the lipidation of membrane proteins, leading to the addition of membrane components and to extension and completion of the double layer membrane of the autophagosome. The Atg16 complex specifies the site of LC3 lipidation and addition to the membrane. (Klionsky and Emr 2000) (Shimada and Klionsky 2012) (Yorimitsu and Klionsky 2005)

In order to monitor autophagy within cells, identification of specific markers is required. To monitor the formation of the autophagosome, LC3 may be used. This is a microtubule-associated protein that is produced as a proform, LC3-I, and is present in the cytoplasm as a soluble monomer. Following activation of the autophagy system due to cellular stress, LC3-I is modified by Atg7 and Atg3 to LC3-II which is membrane bound, specifically to the autophagosomal membrane via the Atg16 complex. This can therefore be measured as a marker of autophagy with antibodies specific for LC3-II or fluorescent-tagged probes for live cell microscopy (Shibata, Yoshimura et al. 2010). In mammals, the LC3B protein is the functional homologue of the yeast LC3 protein. A diagram summarising the autophagosome assembly process including relevant complexes is shown in Figure 1.8.

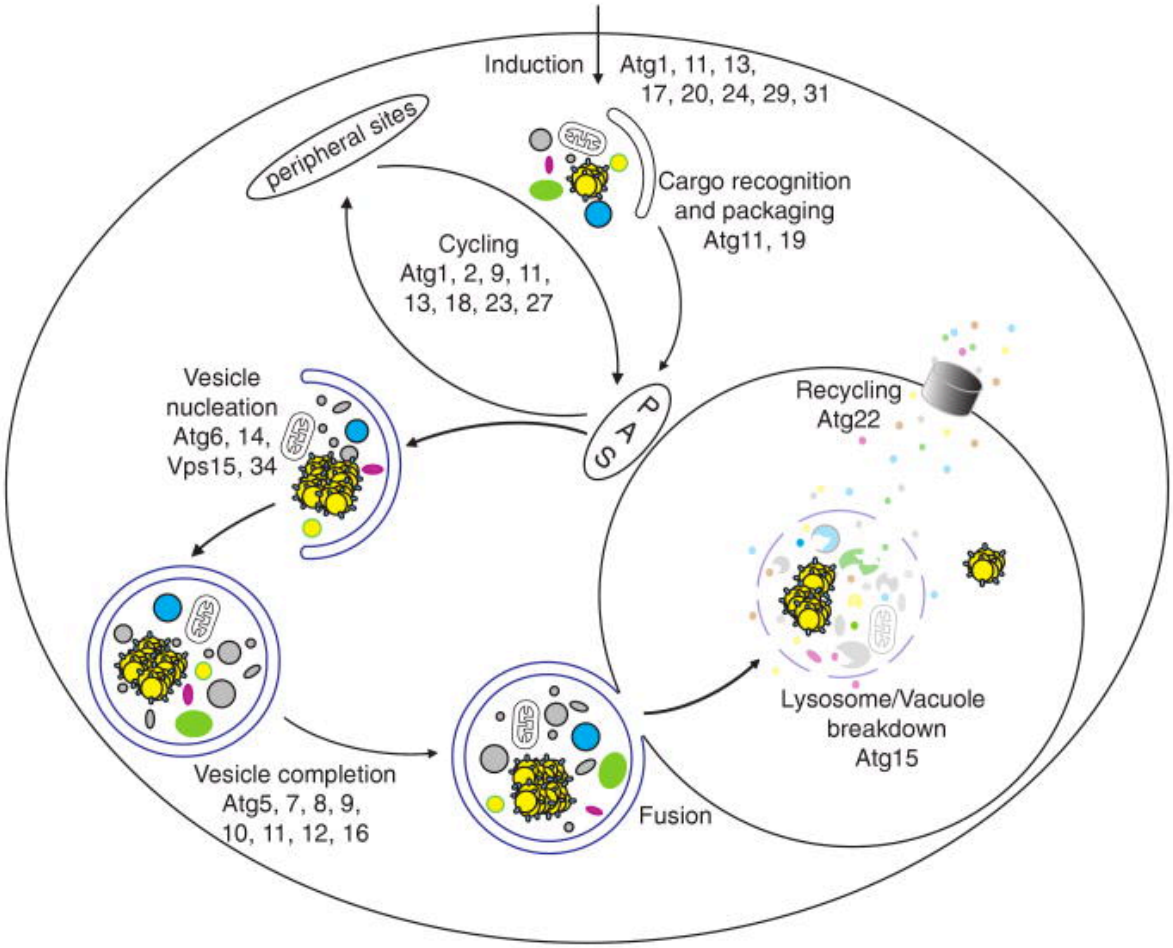

Figure 1.8: autophagosome cycling with Atg complexes shown. The specific Atg proteins are shown at various stages in the autophagosome flux, in particular note the specific nature of Atg14 and vps34 at the vesicle nucleation step. Both are early indicators of autophagy. LC3 is not shown. (Taken from Yang and Klionsky 2009)

1.9.4 Potential targets and inhibitors of autophagy

Autophagy appears to be a key feature of cells' ability to respond to oxidative stress. The cellular response also appears to be intimately entwined with senescence and other, well described cell stress responses such as poly-ADP ribose polymerase (PARP) and apoptosis. Autophagy is mediated largely by mTOR and Vps34 (Sasaki, Miyakoshi et al. 2010). It has been shown that blocking autophagy

reduces senescence and may inhibit bile duct injury. Inhibitors of mTOR (e.g. rapamycin) and PI3K inhibitors (wortmannin, LY294002) can reduce fibrosis in cell culture and animal models (Shegogue and Trojanowska 2004, Damiao, Bertocchi et al. 2007). Autophagy can also be induced by the inhibition of mTOR, potentiating senescence and reducing αSMA expression and collagen deposition in renal fibrosis (Damiao, Bertocchi et al. 2007). Rapamycin and LY294002 are able to reduce collagen I synthesis by in cultured fibroblasts (Shegogue and Trojanowska 2004).

1.10 Hepatocyte Growth Factor

Hepatocyte Growth Factor (HGF) has also been referred to as scatter factor, tumour cytotoxic factor and 3-D epithelial morphogen. It will be referred to as HGF throughout this work. HGF is a growth factor that was first described as a mitogen in rat partial hepatectomy experiments. It is one of the fundamental factors allowing the swift regeneration of the liver (for example, a rat with two-thirds hepatectomy can regenerate in less than a week) (Doignon, Julien et al. 2011).

1.10.1 Discovery of HGF

HGF was originally described and partially characterised in the early 1980's, with purification from human plasma in 1988 (Gohda, Tsubouchi et al. 1988). In 1989, HGF was cloned as cDNA (Nakamura, Nishizawa et al. 1989) and following that, in 1991, several groups identified that the separate entities HGF, scatter factor and tumour cytotoxic factor were in fact one and the same. Furthermore, the HGF receptor was identified as the product of the cMet oncogene in the same year (Nakamura, Sakai et al. 2011).

1.10.2 Structure of HGF

HGF is synthesised as a single protein which is cleaved twice, removing a signal peptide domain of 31 amino acids and then separating the remaining molecule into α and β chains linked by a di-sulphide bond (Gherardi, Hartmann et al. 1997). The α chain comprises an N terminal and four kringle domains linked by a disulphide bond (between two half-cysteine residues) to the β chain containing an inactive serine protease domain (Chirgadze, Hepple et al. 1998). The N terminal domain can be cleaved from full length HGF *in vivo* but this domain is important in receptor binding. Kringle domains are large loops stabilised by three internal disulphide bonds and are found in clotting cascade proteins such as plasminogen and urokinase like plasminogen activator. Kringle domains are believed to be important in binding of mediators and receptor docking (Machide, Hashigasako et al. 2006, Hashiguchi, Kobayashi et al. 2011).

1.10.3 cMet

HGF was discovered to bind to the product of the cMet gene, which is also known as HGF receptor or HGFR (Gherardi, Hartmann et al. 1997, Grzelakowska-Sztabert and Dudkowska 2011). cMet is a single pass tyrosine kinase receptor that is composed of extracellular structural domains including a SEMA domain (with homology to the semaphorins), a PSI domain and four IPT domains (described as a cysteine rich MRS domain) within the cell (Chirgadze, Hepple et al. 1998). The cMet receptor has a juxtamembrane domain which is followed by the intracellular tyrosine kinase (Gherardi, Hartmann et al. 1997, Chirgadze, Hepple et al. 1998). Upon HGF binding, cMet forms homodimers with the tyrosine kinase residues

trans-auto-phosphorylating each other, and inducing further phosphorylation of the juxtamembrane domain. This phosphorylation activity recruits intracellular signalling molecules, including subtypes of PI3K (via the p85 subunit), Grb2, Gab1, and PLCγ and Shp2. Gab1 activity is crucial - knockouts of Gab1 show a very similar phenotype to either HGF or C-Met knockout mice (Inagaki, Higashi et al. 2008, Grzelakowska-Sztabert and Dudkowska 2011, Nakamura, Sakai et al. 2011).

The SEMA domain of cMet forms a β-propeller of 7 domains, which resembles a funnel on crystallographic analysis. The kringle domains of HGF therefore interact with the β-propeller blades 2 and 3. The α chain can also bind to cMet, however the structural relationship has not been demonstrated (Nakamura, Sakai et al. 2011).

1.10.4 cMet downstream signalling pathways

Phosphorylation of Ser985 in the juxtamembrane domain of the cMet receptor regulates activity, being phosphorylated by phospho-kinase C (PKC) and de-phosphorylated by protein phosphatase 2A (Hashigasako, Machide et al. 2004). The scaffold proteins Gab1 and c-src (both contain src-homology domains) activate specific pathways including the mitogen-activated phospho-kinase (MAPK) pathway (extra cellular signal regulated kinase/ERK via RAS), STAT3 and Akt (PKB) (Lee, Jeong et al. 2012, Liu, Shi et al. 2012, Matsumura, Kubota et al. 2013). Further downstream of these events HGF/cMet is known to signal via β-catenin, NOTCH and focal adhesion kinase (FAK) (Dulak, Gubish et al. 2011) leading to the scattering and motility effects of HGF signalling.

Degradation of cMet is regulated by the E3 ubiquitinase Cbl. This binds to the phosphorylated Y1003 in the juxtamembrane domain leading to ubiquitination of the protein, endocytosis and transport to the endosome for degradation (Machide, Hashigasako et al. 2006, Dulak, Gubish et al. 2011, Nakamura, Sakai et al. 2011).

1.10.5 Biological variants of HGF

NK1 and NK2 are two widely described biological splice variants of HGF; they comprise the N-terminal and either the first or first two kringle domains respectively.

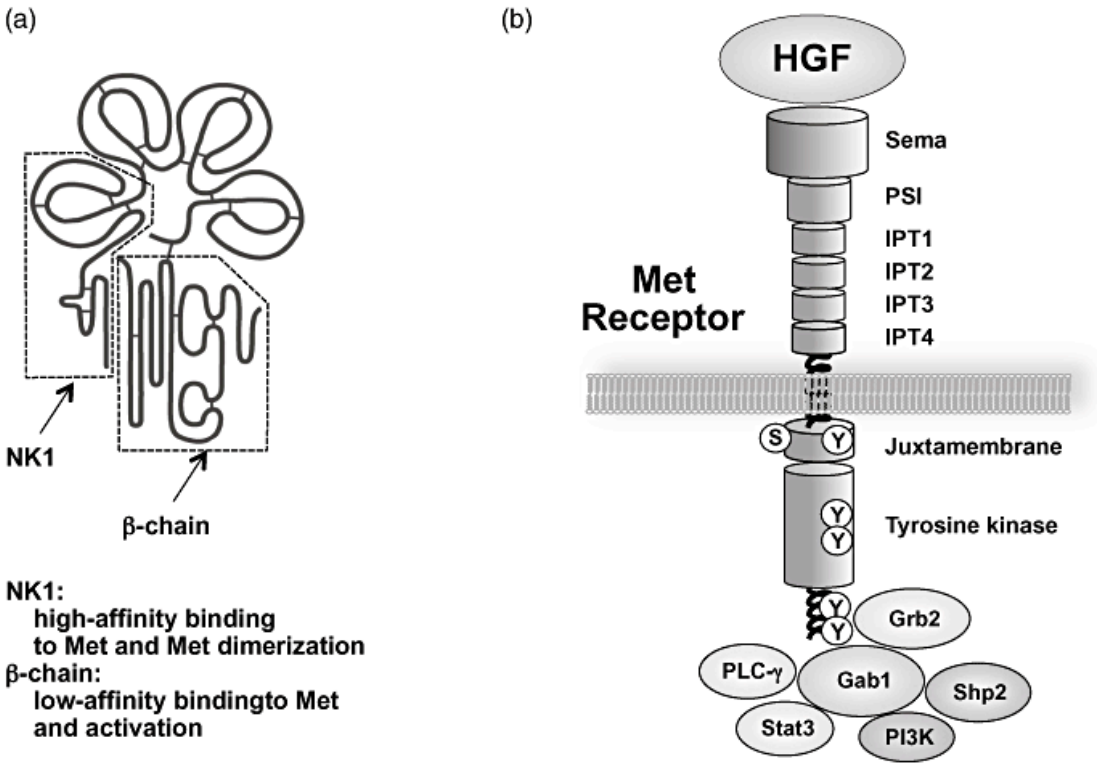

Figure 1.9: Structure of HGF and NK1. Panel (a) shows the full length HGF and the splice variant NK1 (dotted outline). Panel (b) shows a schematic representation of the structure of the cMet receptor. (Taken from Nakamura et al 2008)

An α chain variant, known as NK4, is also described in the literature. NK1 and NK2 were originally described as antagonists to cMet (Lokker, Presta et al. 1994, Youles, Holmes et al. 2008) however they were then discovered to be partial agonists of cMet, dependent upon the addition of heparan sulphate proteo-glycans (HSPG) (Schwall, Chang et al. 1996).

Extensive work has been conducted on protein engineering of the NK1 fragment as a receptor antagonist for potential therapeutic applications in cancer biology (Lietha, Chirgadze et al. 2001, Youles, Holmes et al. 2008).

Protein engineering approaches by Ross (Ross, Gherardi et al. 2012) targeted HSPG binding sites, of which there are two in HGF. The first, high affinity site, is in the N terminal and the second, lower affinity binding site, is found in the first kringle domain. By targeted reverse charge mutations to Lysine 132 and Arginine 134, the lower affinity HSPG binding site in the K1 region of NK1 had less affinity than the un-mutated form. The induction of DNA synthesis by 1K1 in primary hepatocytes was increased 17.3 fold in the presence of heparin, compared to a DNA synthesis increase of 10-fold with HGF in the presence of heparin (Ross, Gherardi et al. 2012).

1.10.6 Glycosaminoglycan (GAG)

Glycosaminoglycans (GAGs) are long un-branched polysaccharides made up as polymers of a hetero-disaccharide. GAGs are classified into four based on the disaccharide units they are composed of. GAGs are important in their own right, for example as heparin, which is used in clinical practice as an anticoagulant, and as a fundamental part of tissues such as cartilage or cornea. In some tissues, and on the

surface of most cells, GAGs are present as proteoglycans (PGs, e.g. Aggrecan, a component of cartilage) (Ali, Hardy et al. 2003).

As the name may imply, proteoglycans are composed of protein complexed to GAG's. GAGs may be produced in the Golgi and it is a this point that protein cores produced in the rough endoplasmic reticulum can be modified by glycosyltransferases, which add GAGs to proteins, one example is O-glycosylation, where GAG's are joined to oxygen molecules. Enzymes can add GAGs at various points, such as nitrogen groups or sulphate groups (N- or S- glycosylation) or component proteins and may specify which group on the particular moiety is bonded, such as 6-O (Mishra, Chandavarkar et al. 2013).

PG can also be further modified, for example by sulphation. This means that a large number of different branched molecules can be produced that are variably sulphated. Due to the charged nature of PG they are able to bind cations and water, this may include molecules such as cytokines (Johnson, Proudfoot et al. 2005, Wells, Power et al. 2006) or drugs (Chen, Repunte-Canonigo et al. 2013). The sulphation patterns of PG have been linked to disease states and may represent a means of targeting therapeutics (Willet, Pichitsiri et al. 2013). In reference to HGF/cMet binding, GAG presence is required for signalling, this can be removed by protein engineering (Ross, Gherardi et al. 2012).

1.11 Hypothesis

The hypothesis under test is that acute disease may lead to senescent epithelial cell production and that senescent epithelial cells are able to promote further disease injury leading to chronicity and fibrosis by altering the milieu interior.

1.12 Aims

The aims of this project are:

- To identify whether senescence contributes to the development of acute and chronic rejection in liver allografts
- To investigate the SASP elements that may promote fibrosis or epithelial cell loss of function
- To investigate the therapeutic potential of the compound 1K1 in treating VBDS

2 Materials and Methods

2.1 Ethics

Ethical approval was obtained from a local-regional ethics committee concerning the use of patient samples. Samples represented excess tissue that had been taken for diagnostic purposes; each sample was identified by means of a number allocated by the Cellular Pathology department. The diagnosis, grading and staging of disease (where appropriate) was supplied by ADB. No patient identifiable information was obtained, stored or used during the project. Approval reference REC 06/Q0905/150 Amendment 1 date of amendment 09/01/2007, by the Newcastle and North Tyneside Local Research Ethics Committee 1. In addition biopsies of alcoholic liver disease were used under ethical approval Ref: 10/H0903/32 provided by the Northern and Yorkshire REC, the chief investigator for this was Dr Steven Masson.

2.2 Cell culture

The Human H69 cholangiocyte cell line was created by Grubman (Grubman, Perrone et al. 1994) from human intrahepatic biliary epithelial cells, isolated from dissected portal tracts. Immortalisation was by SV40 large T antigen applied to the cells via retrovirus. This was followed by maintenance in co-culture with lethally (40Gy) irradiated NIH/3T3 fibroblasts. Selection was carried out with G418 antibiotic.

The H69 cells were cultured in 25cm^2 or 75cm^2 flasks in a mix of Dulbecco's Modified Eagle's medium and Nutrient Mixture F12 Ham (2:1) (Sigma) supplemented with:

24.3mg/l (1.8 x 10^{-4} M) adenine (Sigma)

1.345µg/l (2 x 10^{-9} M) triiodothyronine (Sigma)

1.0mg/l (5.5 x 10^{-6} M) epinephrine (Sigma)

ITS-X supplement (10mg/l insulin, 5.5g/l transferrin, 2.0g/l ethanolamine, 6.7µg/l sodium selenite) (Invitrogen)

362.46µg/l (1µM) hydrocortisone solution (Sigma)

10% Heat inactivated FCS (Sigma) and

PenStrep (100U/ml of penicillin and streptomycin) (Sigma)

2.3 Primary cell isolation and culture

Primary human cholangiocytes/biliary epithelial cells were isolated in Dr Simon Afford's laboratory at the University of Birmingham, from liver explant material obtained under appropriate ethical approval. These cells were cultured on coated flasks before either use in experiments in Birmingham or being frozen in liquid nitrogen and shipped, via the Birmingham Bio-Repository, to Newcastle upon Tyne for experiments there. Isolation and culture techniques were performed initially under supervision by Dr Elizabeth Humphreys.

2.3.1 Isolation of biliary epithelial cells

Fresh liver tissue from human explants was divided up into 30g sections. Each section was then diced finely in a sterile Petri dish in a class II containment hood. The material was then transferred to a sterile beaker containing collagenase 1A solution (100μg/ml) with incubation at 37°C for 30-45 mins dependent upon the disease state. Following digestion the mixture was passed through a coarse mesh with the final volume adjusted to 160ml with sterile PBS and decanted into 8 universals and centrifuged at 2000g, resuspended in sterile PBS and centrifuged at 2000g. Supernatants were decanted and cell pellets pooled in PBS to a total volume of 24mls. For density centrifugation, fresh percoll gradients were prepared. Within a 15ml flacon tube 3ml of 33% percoll was added, beneath this 3ml of 77% percoll was carefully layered, creating a clear interface. Upon the percoll gradients 3ml of cell suspension was layered before centrifugation at 2000g for 30mins at room temperature. After centrifugation the top layer was discarded and cells at the interface removed and pooled in sterile PBS with mixing to prevent further gradient formation. This mixture was then centrifuged at 2000g for 5 mins and the supernatant decanted. Cell pellets were resuspended in 10ml PBS with further centrifugation at 2000g for 5 mins. The resultant pellet was resuspended in 500μl RPMI containing 50μl Ep-CAM (final concentration 5μg/ml, HEA125 clone, Progen Biotechnik) with incubation at 37C for 30 mins with agitation. This suspension was then diluted to 10ml with sterile PBS and centrifuged at 2000g for 5 mins before being resuspended 500μl RPMI with 10μl Dynabeads (Dynal Biotech, M-280 sheep anti-mouse) with incubation at 4°C for 30 mins with agitation. This was then diluted

in 5ml of ice cold PBS and allowed to stand in a MACS separation magnet for 5 mins. With the tube still held in the magnet the supernatant was decanted and replaced by ice cold PBS 3 times to minimised fibroblast and macrophage contamination. The magnet was then removed and the cells added to 5ml of Epimed at 37°C and placed in a rat tail collagen coated T25.

Cells were cultured until 80-90% confluent and split at a maximum of 1:3. All experiments were conducted on cells at passage 3 or 4.

2.3.2 Composition of "Epimed" Primary biliary cell culture medium

Primary BEC were cultured in Epimed made fresh and stored for a maximum of 3 weeks. Epimed was formulated as follows:

90ml HAMS F12 (Sigma)

90ml DMEM (Sigma)

20ml Human Serum (TCS Biosciences)

0.02M penicillin/streptomycin (Sigma)

10μg/ml EGF (Peprotech)

24.8IU human insulin (Gibco)

200ng/ml hydrocortisone (Sigma)

100ng/ml Cholera toxin (Sigma)

2nM tri-ido-thyronine (Sigma)

10μg/ml HGF (Peprotech)

2.3.3 Production of Rat Tail Collagen

A suitable number (4-5) of mature rat-tails were thawed thoroughly and then blunt dissected with pliers, exposing the tendons. These tendons were dissected out and placed in sterile PBS. Once dissection was complete the tendons were transferred to 70% ethanol

and incubated at room temperature for 10 mins. The wet collagen was then removed from the ethanol, excess fluid drained and weighed. For every 1g of wet collagen, 100ml of 4% acetic acid was added to a sterile beaker. This was covered with foil and placed on a mechanical stirrer for 3 days at 4°C. The solution was then decanted into centrifuge tubes and centrifuged at 20,000g for 30 min at 4°C. The supernatant was then sieved through a fine mesh and stored at 4°C until required. Prior to plating, flasks or plates were coated with a thin layer of the collagen solution and allowed to dry overnight.

2.4 Antibodies

Antigen	Manufacturer	Catalogue No	Species	Immuno -Fluorescence	Western blot	IHC
CK19	DAKO	M0772	Mouse	1:100	N/A	1:1000
S100A4	DAKO	A5114	Rabbit	1:100	N/A	1:200
CD3	DAKO	M7254	Mouse	N/A	N/A	1:100
Ki-67	DAKO	IS626	Mouse	N/A	N/A	1:100
CD56/NCAM	ABCAM	Ab8077-1	Mouse	1:100	N/A	N/A
Fibronectin	Sigma	F0916	Mouse	1:100	1:5000	N/A
Fibronectin	Sigma	F3648	Rabbit	1:100	1:5000	N/A
αSMA	Sigma	A5228	Mouse	1:100	1:5000	N/A
Collagen 1A2	Santa Cruz	B2406	Rabbit	1:100	1:4000	N/A
Collagen 3A1	Santa Cruz	A2308	Rabbit	1:100	N/A	N/A

GFAP	DAKO	Z0344	Rabbit	1:100	N/A	N/A
MMP9	DAKO	A1050	Rabbit	1:100	N/A	N/A
Vimentin	DAKO	M7020	Mouse	1:100	1:4000	N/A
$p21^{WAF1/Cip}$	ABCAM	Ab7960	Rabbit	1:100	N/A	N/A
$p21^{WAF1/Cip}$	Santa Cruz	Sc-6246	Mouse	1:100	1:5000	1:50
EMA	Leica	NCL-EMA	Mouse	1:100	N/A	N/A
LC3B	Sigma	L7543	Rabbit	1:100	N/A	N/A
Atg14	Sigma	A6354	Rabbit	1:100	N/A	N/A
CD10	Leica	NCL-CD10-270	Mouse	1:100	N/A	N/A
P16	BD	550834	Mouse	1:50	N/A	N/A
Integrin β6	R&D	MAB4155	Mouse	1:50	N/A	N/A
Integrin β6	R&D	MAB41551	Mouse	1:50	N/A	N/A
CK7	DAKO	OV-TL 12/30	Mouse	1:100	N/A	N/A
ZO-1	Invitrogen	33-9100	Mouse	1:100	N/A	N/A
αSMA	DAKO	M0851	Mouse	1:100	N/A	N/A
E-Cadherin	DAKO	NCH-38	Mouse	1:50	N/A	N/A
E-Cadherin	BD	610405	Mouse	1:100	N/A	N/A
γH2AX	Cell signal	#9718P	Rabbit	1:50	N/A	N/A
αSMA	Sigma	A5228-200ul	Mouse	1:100	N/A	N/A

P21	ABCAM	Ab7960	Rabbit	1:100	N/A	N/A
pSMAD2/3	Santa Cruz	SC-11769-12	Rabbit	1:50	N/A	N/A
hTGF-β BP1	R&D	MAB388	Mouse	1:100	N/A	N/A

Table 2.1: List of primary antibodies used in the study

2.4.1 Immunofluorescence and densitometry

For immunofluorescence experiments, H69 cholangiocytes were seeded onto glass 8-chamber slides (Cultureslides, BD Falcon) at 40,000 cells per chamber with 250µl of culture medium. Cells were incubated for 24-72h until a 90-95% confluent monolayer was present. Cells were treated with Hydrogen peroxide at 50-200µM for 2 hours as a form of oxidative stress. The slides were then rinsed in PBS and fresh culture medium added. At pre-determined time-points (24, 48, 72, 96 and 120 hours) the cells were rinsed with PBS and fixed with 4% phosphate-buffered paraformaldehyde (30min at 22°C) before permeabilisation with 0.1% Triton X-100 in PBS (15min at 22°C). Blocking was performed by incubation (at 22°C) with 5% BSA in PBS for 90 minutes to minimize non-specific antibody binding.

Primary antibodies as noted in table 2 were titre optimised by using several different concentrations (1:200, 1:100, 1:50) during incubation with pre-optimised secondary antibodies. Assessment of the results determined the concentration used. Primary antibodies were added in 5% BSA for 48 hours at 4°C. For each time point and antigen a no-primary antibody treated preparation was used for a negative control. The cells were then washed for 5 minutes, 5 times with 0.1%

Tween-20 in PBS prior to addition of FITC- conjugated anti-mouse or anti-rabbit (DAKO, 1:100/1:160) secondary antibodies in 5% BSA (again for 48h at 4°C in the dark). Following further washing in PBS the slides were stained with DAPI in distilled water (at a final concentration of 1µg/ml) for 10min at 22°C. The slides were then washed in PBS and mounted in fluorescence mounting medium (Sigma). If immediate analysis was not performed, storage was in a humidified chamber at 4°C in the dark.

2.4.2 Laser Scanning Confocal Microscopy (LSCM)

Conventional light sources (e.g. tungsten filament bulb) emit light at a number of wavelengths. Each wavelength is then refracted by differing amounts at a given interface (such as the glass/air and air/glass interfaces in microscopy); therefore different wavelengths of light focus at different planes; a phenomenon known as chromatic aberration. In addition, as such light sources illuminate large areas of a specimen at a particular time; there is refraction of light from areas adjacent to the visualised area. This can then be picked up by the detector, resulting in an out of focus image; this phenomenon is known as spherical aberration. As such, laser (light amplification by the stimulation of emitted radiation) light represents a more ideal light source for microscopy, as it is concurrently both monochromatic and coherent, minimising chromatic aberration. Due to the brightness of laser light, it is also possible to use a small point source of light to illuminate the specimen, alleviating spherical aberration. Detectors used in confocal microscopy feature a pinhole aperture; further reducing refractive error.

In LSCM; a beam of generated laser light enters the scanning system and is reflected from a dichroic mirror through the objective. The beam is then focused onto a point of the specimen by the objective. Light is absorbed by specific chromagens in the specimen and emitted at a different (longer) wavelength. This light fluorescence returns through the objective (via the dichroic mirror and pinhole aperture). Only light focused in the objective (and therefore light that is emitted from the focal plane) passes through to the detector.

Photomultipliers are the most commonly used detectors in confocal microscopy. Photons incident upon the photosensitive surface within the photomultiplier generate an electrical charge. The photon energy is absorbed by the photocathode and is transferred to an electron. This is accelerated by dynodes (electron multipliers), which emit further electrons. Once the electrons reach the anode the circuit is completed and results in the generation of electrical energy. This is collected and converted into an image. CLSM uses scanning mirrors to rapidly move the laser beam across the specimen. Larger areas can then be visualised. In addition to visualisation of the XY plane, the mirrors also allow recording of successive focal planes, the XZ or YZ axes. These images, when taken together are referred to as a z series. Z series production allows a three dimensional image of the specimen to be produced.

This work utilised a Leica TCS SP2 UV laser-scanning confocal microscope (LSCM) to visualise emission spectra for two different dyes: FITC (green, excitation 488nm, emission 510-535nm) and DAPI (blue, excitation 345nm, emission 458nm). Representative z series were taken of each section/specimen and used for

densitometric and morphological analysis. Densitometry analysis was by ImageJ software. All experiments were conducted in triplicate or quadruplicate (REF MRes).

For each antigen and time point no less than 3, and usually 4, sections are stained with representative images obtained as a z stack. Controls are performed for each time point and each staining run and consist of a no primary antibody control and an isotype control for each of the isotypes used in any given run. A representative image of the controls is acquired.

2.4.3 Densitometry

Densitometry was used to quantify the amount of antigen expression seen in immunofluorescence images by dividing the mean channel fluorescence with the area sampled to give a mean brightness. In order to do this Velocity software was employed. However during the study this was replaced by open source software to allow easier analysis. All analysis in this study was performed on ImageJ software, mean pixel intensity was generated by splitting colour channels and identifying the threshold of staining for each colour, the whole field is then analysed. Mean pixel intensity data is then analysed by ANOVA (one or two way) using PRISM5 software (Graphpad).

2.5 Flow Cytometry/Fluorescence activated cell sorting

2.5.1 Flow Cytometry

What we now know as flow Cytometry was originally named pulse cytophotometry and developed for commercial use in 1968 at the University of Munster. This was

based around a Zeiss fluorescent microscope. At that time absorbance methods were much preferred by scientists, however, all haematology laboratories were utilising haemocytometers based upon the coulter principle by 1964. This had first been described in 1954 using goat erythrocytes, as a cell passes through an aperture between two solutions of saline at constant voltage it creates impedance, the larger the cell the larger the impedance and therefore the larger the voltage produced within a photovoltaic cell. Having optimised the width of the aperture in this system it was therefore possible to determine the size of cells within a diluted blood sample and therefore to infer the type of cells within a given sample. From the 1960's onward technology was further developed to include laser based sorting (developed at Stanford University in 1972 and coining the term Fluorescent Activated Cell Sorting (FACS) which is often used synonymously with flow Cytometry) and use of further dyes and ultimately, antibodies.

The basic characteristics of any modern flow cytometer are very similar; a sample is refined by the use of fluid dynamics until it is focused in an approximately single cell stream that passes through a series of lasers. The light refracted and reflected from these lasers is directed by use of dichroic mirrors and filters to photomultiplier tubes that serve as detectors. The fundamental characteristics of the cell population(s) under study are described by the forward and side scatter properties. Laser light incident upon the cells is refracted by the cell size by a small amount, forward scatter. Therefore the size of the measured forward scatter is proportional to the size of the cell. To prevent the direct laser light from activating the detector, a blocking bar is used; therefore the PMT can sit in line with the laser to measure

only the scattered light. Some of the light incident upon the cells is reflected from intracellular organelles and granules, this is scattered more so than by the cells size and is referred to as side scatter. The amount of light scattered is therefore proportional to the granularity of the cells. By plotting the forward and side scatter on the X and Y axes of a scatter plot, we can therefore show graphically distinct cell populations; for example those that are small and non-granular (erythrocytes), those that are small and granular (lymphocytes) and those that are large and granular (granulocytes) or not granular (monocytes).

While the characteristics of populations can be described in terms of forward and side scatter profiles, these are enhanced markedly by the addition of chromophores, either as dyes or conjugated to antibodies. Generically, the excitation of the fluorescent dye causes an increase in the energy of orbiting electron(s), which then return to their resting state potential by releasing energy as heat and light (strictly electromagnetic (EM) radiation). Therefore the emitted EM radiation is always of a lower energy and longer wavelength than the exciting energy. The difference between the excitation and emission energy is called the Stokes shift. The characteristics of the fluorescent dyes used can therefore be described in terms of their excitation and emission spectra. The flow cytometer used for all experiments was a Becton Dickinson FACSCanto II fitted with three lasers a 405nm, 488nm and 633nm. A diagram displaying the optics for emission spectra is included below (Figure 2.1)

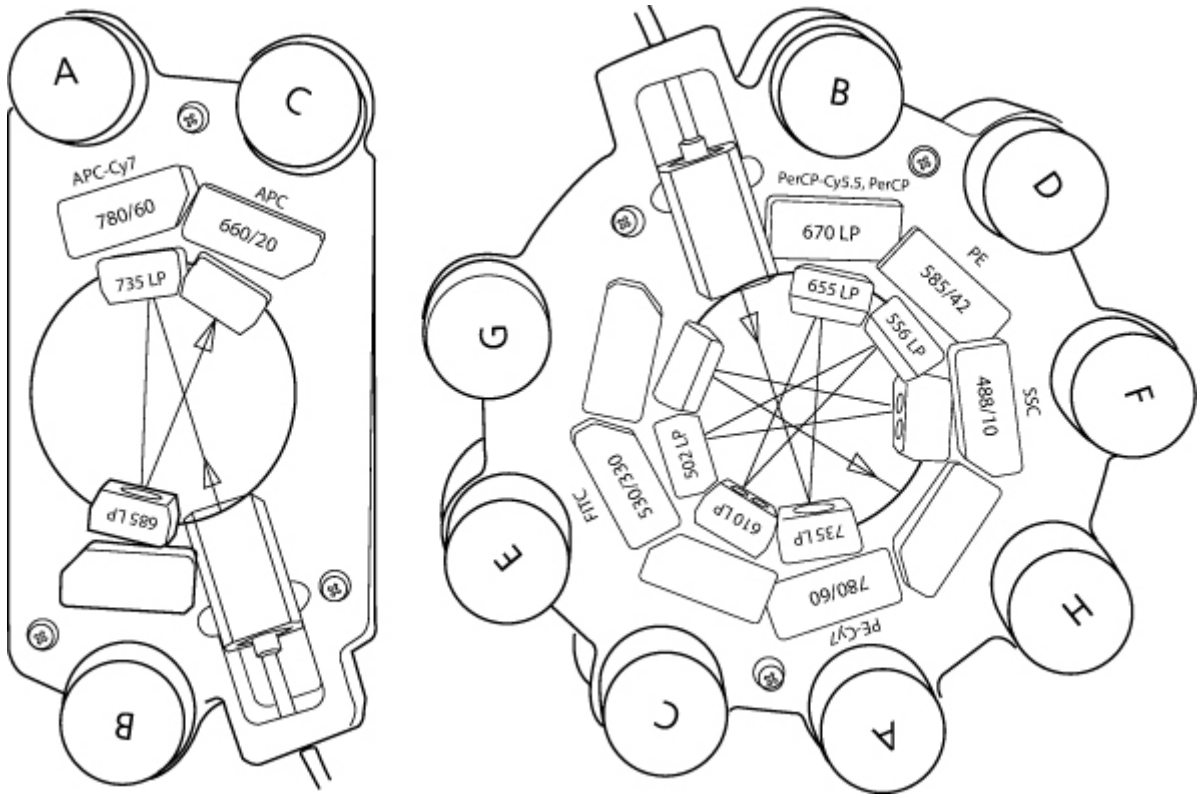

Figure 2.1: Diagram of FACSCanto II collection optics. As shown there is a separate laser path for the 633nm laser (left) whereas the 405 and 488nm lasers share a signal path (right). Reproduced from BD biosciences.

All of the fluorescent markers used in this study were dyes, with the exception of Annexin V; all were intracellular and are discussed below:

2.5.2 H_2DCFDA, 2, 7, Dichlorofluorescin-diacetate (DCF)

This soluble dye is used as a marker for Reactive Oxygen Species (ROS) and nitric oxide. In the stable form H_2DCFDA, the substance is not fluorescent, but is oxidized by reaction with horseradish peroxidase (HRP) compound I to form $DCF^{\bullet -}$ which is then oxidised by reaction with oxygen to form the fluorescent dye DCF. (Myhre et al 2003). DCF excites at 488nm and emits at 530nm

2.5.3 Monodansylcadaverine MDC

MDC is a soluble dye used as a marker of autophagic vacuole formation. It is preferentially incorporated into autophagic vacuoles as determined by sucrose gradient separation (Mazzanti et al 2009, Biederbick et al 1995). The specific process leading to MDC accumulation in autophagic vacuoles remains poorly understood but does depend upon rapid protein synthesis (Munafo and Colombo 2001) The optimum excitation for MDC is at 380nm (in the FACSCanto II the 405nm laser was used) and emits at 515nm (in the FACSCanto II the 510/10nm filter was used)

2.5.4 7 Amino-Actinomycin D (7-AAD)

7-AAD is viability dye that can be used in place of proprium iodide (PI) when spectral overlap with FITC or PE is undesirable. 7 AAD does not pass readily through intact cell membranes and therefore it is excluded from viable cells. 7 AAD has a strong affinity for DNA, particularly GC rich regions, leading to its use in a number of fluorescent applications. Once intercalated into DNA 7 AAD excites at 488nm (though optimal is 546nm) and is collected using a 670nm long pass filter (emission commences at 650nm and has a wide far red tail). The molecule therefore has a large Stokes shift, which is one of the characteristics that make it a potentially useful tool in multi-colour flow cytometry.

2.5.5 Annexin V

Annexin V (or a5) is a small molecule that binds to phosphatidylserine (PS) molecules with high affinity. This makes it useful in laboratories for identifying cells

undergoing apoptosis or platelet activation as both of these processes result in significant presence of PS residues on the outside of either cells or platelets. It should be remembered that while cells in early apoptosis display PS residues, they also retain membrane integrity and would therefore stain negative with a viability stain such as 7 AAD. Necrotic cells with lack of membrane integrity will stain positive for both 7 AAD and Annexin V as the PS residues on the internal membrane surface are not isolated from the external environment. In the assays within this project, Annexin V was used conjugated to Pacific Blue dye. This excites at 405nm (FACSCanto II has a 405nm laser) and emits at 455nm (FACSCanto II has a 450/50 filter).

Cells were stained initially in 6 well plates, giving 0.5-1.0x10^6 cells. Media was removed with a pipette and then washed with PBC before adding HBSS without calcium or magnesium. Removed media was centrifuged at 500g for 5 mins and the cell pellet added to the HBSS. At this point both MDC and 2,7 DCF were added at optimised concentrations and incubated for 30mins at 37°C. Supernatant was removed and centrifuged (500g for 5 mins) while the adherent cells were trypsinised (with trypsin EDTA) for 5 mins before addition of an equivalent volume of FCS. Cells were resuspended in 2 ml of Annexin V binding buffer in 12x75mm 5ml polystyrene tubes (BD). Annexin V and 7 AAD were added with incubation for 15 mins at 4°C. after washing in HBSS, cells were resuspended and then analysed by flow cytometry.

2.6 Protein lysate preparation

Initially lysates from H69 cultured in 75cm^2 flasks were produced by: rinsing with PBS and drainage followed by addition of 500µl lysis buffer (Phosphosafe, Calbiochem) and scraping the cells off with a cell scraper. The contents of the flasks were then pipetted into centrifuge tubes and then sonicated for 10 seconds; this was followed by centrifugation at 12,000g. Supernatant was aliquoted into fresh centrifuge tubes and frozen at -80°C. Supernatant Total protein concentration was estimated with a BCA protein assay kit (Pierce, USA). This allowed production of a standard curve for absorbance at 562nm. Extracts were then stored at -20°C. This method produced lysates with protein concentrations of 0.1-0.5 mg/ml making detection of antigens difficult as only a maximum of 2-3 µg per lane could be loaded during SDS-PAGE. This method was modified to utilise 100µl of lysis buffer consisting of Cell Lytic (Sigma), protease inhibitors (MiniComplete, Roche) and phosphatise inhibitors (Thermo Fisher scientific). Trypsin was employed to detach the cells from culture flasks, they were then washed in ice cold PBS and lysed on ice for 30 minutes, with vortexing at 10 minute intervals. This was followed by sonication and centrifugation as above. This modified method gave yields of 3-5mg/ml protein when compared with the standard curve of a Bradford protein assay (absorbance at 595nm). Following persistent low yields an alternative protocol was followed. Cells were washed with ice cold PBS and detached with a cell scraper. The resultant cells were pelleted by centrifugation at 400g for 5 mins and then resuspended in 100µl Phosphosafe™ (Novagen) cell lysis buffer and sonicated for 10 seconds at moderate intensity. No further centrifugation was

carried out. For use in SDS-PAGE; samples were thawed and supplemented with 10% β-mercaptoethanol and 4x sample buffer (12% Sodium Dodecyl sulphate, 60% v/v 20% glycerol, 30% v/v 0.0012% bromo-phenol blue,, 0.37M TRIS base (pH 6.8)). Samples were boiled (10 minutes), cooled, and added to SDS-PAGE gels.

2.7 SDS-Polyacrylamide electrophoresis and Western blotting

15µg of total protein lysate per well was separated by either 7.5% or 10% Sodium-dodecyl sulphate Polyacrylamide gel electrophoresis (SDS-PAGE). Separation was carried out using stable current, (40mA per gel). Separated proteins were transferred from the gel to Hybond-P PVDF membrane (Amersham Pharmacia Biotech, UK) overnight at 50mA. Non-specific antibody binding sites on the membrane were blocked with 5% skimmed milk in TBS for 90 minutes. Primary antibodies were diluted in 5% milk/TBS to optimal concentrations (see table 2). The membranes were incubated with these primary antibody solutions for 3 hours at 22°C and washed five times with PBST (PBS supplemented with 0.1% Tween-20). Membranes were then incubated with solutions of secondary antibodies conjugated with HRP (Horse Radish Peroxidase) for 1h at 22°C. After washing with PBST, the membrane was developed using Pierce Chemiluminescence kit (Pierce). Under darkroom conditions X-ray film was exposed to the membrane for between 5 seconds and 10 minutes depending on the signal intensity.

Following development, membranes were washed and stripped of antibodies by incubation with stripping buffer (ABCAM) at 22°C for 10 minutes. This was changed and a further incubation for 10 minutes in fresh buffer performed. Membranes

were repeatedly washed in PBST before re-blocking in 5% skimmed milk for 60 minutes and incubated overnight at 4°C with anti-α-tubulin antibody (1:5000) in 5% skimmed milk and TBS. Secondary antibody was anti-mouse HRP conjugated antibody (1:5000) (Sigma) with development as above. The intensity of α-tubulin was used to validate equal loading and compared with the PVDF membrane that was treated with copper solution to visualise total protein loading.

2.8 Immunohistochemical (IHC) triple staining of human liver biopsies

This technique was developed by Dr Helen Robertson. Significant assistance from her was provided in carrying out this aspect of the research project.

Paraffin embedded tissue sections were obtained anonymised, from the Cellular Pathology department of Newcastle Hospitals NHS Foundation Trust. These represented excess material from diagnostic procedures. Sections were de-waxed by incubation in xylene for 10 minutes and rehydrated by 1-minute washes in 100% and 95% ethanol. To reduce endogenous peroxide activity, sections were incubated in 0.2% hydrogen peroxide in methanol for 10 minutes at 22°C. Antigen retrieval was by pressure cooking (heat-induced antigen retrieval) for 1min in EDTA buffer pH 8 – 9. Several biotinylated antibodies were used; therefore endogenous biotin in the tissue was blocked using a biotin-avidin kit (Vector). Following washing in TBS, sections were incubated in 20% normal swine serum (in TBS) for 1 hour at 22°C; to reduce non-specific antibody binding. Primary antibody was then added (anti-$p21^{WAF1/Cip1}$ (Santa Cruz) 1:50; anti-CD3 (DAKO) 1:100) in 20% normal swine serum

at 4°C overnight in a humidified chamber. After washing in TBS, biotinylated goat anti-mouse IgG (Vector, 1:200) in 20% normal swine serum was added for 1 hour at 22°C. Sections were then washed in TBS and developed with the Vector ABC (peroxide) kit according to the manufacturer's instructions. The First stage was developed with Nickel 3,3' diaminobenzidine tetrahydochloride (NiDAB), giving a black colour. Following washing in TBS the samples were incubated with a mix of anti-Cytokeratin 19 (DAKO; 1:1000) and anti S100A4 (Santa Cruz/BD, 1:200) in 20% normal swine serum at 4°C overnight in a humidified chamber. A further wash with TBS followed by incubation with peroxide conjugated horse anti-mouse IgG (Vector; 1:100) in 20% normal swine serum for 1 hour at 22°C. This was then developed with 3, 3' diaminobenzidine tetrahydochloride (DAB) producing a brown colour where CK19 was detected. A further secondary antibody was added; biotinylated goat anti-rabbit IgG (Vector; 1:200) in 20% normal swine serum for 1 hour at 22°C. This was developed with the Vector ABC-AP kit according to the manufacturer's instructions. The final development was with Vector red in Tris-HCl buffer, pH 8.2-8.4, with 2.5% Levamisole for 10 min. This gave a red colour where the presence of S100A4 was seen. A light counter stain was added with Mayer's haematoxylin before washing in TBS, dehydration in an ethanol series (70%, 90%, 95% and 100%) and mounting with DPX.

This technique was used to evaluate the expression of CD3, Ki67 (MIB-1), γH2AX or $p21^{WAF1/Cip1}$ alongside S100A4 and CK19 in liver biopsies.

2.9 Enzyme-Linked Immunosorbent Assay (ELISA)

ELISA is a form of ligand binding assay and specifically is a technique whereby detection of proteins is achieved by antibodies bound to a 96 well plate. Once the specific antigen is bound a second antibody is used to bind to a second epitope on the same protein (though a single antibody can be used, this is less usual). The secondary antibody is conjugated with an enzyme that allows the detection of the amount of antigen present as a result of the enzyme linked reaction. The reaction product is usually measured by absorbance but various detection technologies are available.

The ELISA performed in this study were a novel format of commercially produced ELISA supplied by R&D systems Ltd. Rather than using a lysate or other produced analyte, the 96 well plate is coated in a similar manner to tissue culture flasks. Cells can therefore be grown in the analysis plate and subjected to experimental conditions. Once the reaction is to be terminated a detergent is used to lyse the cells in situ, the resultant proteins being bound to the surface of the plate. In order to quantify the proportion of phosphorylated to un-phosphorylated protein two separate primary antibodies are used, one specific for a phosphorylated form (or forms) of the target and one specific for the un-phosphorylated form, each of these are raised in different species, one in mouse and the other in rabbit. By using secondary antibodies specific for the species (either mouse or rabbit) and conjugated with different distinguishable fluorophores, quantitation of the relative proportions of phosphorylated protein can be made.

In this study four assays were used (phosphorylation sites in parenthesis):

C-Met (Y1234/Y1235) Catalogue KCB 2480

ERK 1 (T185/Y187) and ERK 2 (T202/Y204) KCB 1018

SMAD 3 (S423/S425)/Smad2 (S465/S467) Catalogue KCB 3226

AKT (S473) Catalogue KCB 887

In all assays the secondary antibodies were developed with the same proprietary reagents giving excitation/emission figures of 540/600nm (for the phosphor specific antibodies) and 360/450nm (for the non-phosphorylated proteins). The relative phosphorylation was calculated according to the manufacturers instructions, that of a fold change relative to the native protein level and therefore can correct for cell number discrepancies.

2.10 RealTime PCR

2.10.1 Polymerase Chain Reaction (PCR)

Polymerase Chain Reaction (PCR) is an amplification process that allows the generation of many copies of DNA from small amounts. As an example 25 successful cycles of PCR will increase the DNA copy number by over 1 million fold. The basis of the technique centres on a sequence of *in vitro* reactions first outlined in 1986 and resulting in the award of the Nobel Prize for chemistry in 1993. This first of three phases in a PCR reaction is heating (to around 95°C) as this allows the DNA double helix to denature into single strands. The second stage is precipitated by cooling to allow pre-designed primers to anneal to complementary sequences on the DNA strands. These primers are designed to be complementary to the

coding and non-coding strands of the gene of interest; meaning that the double stranded DNA eventually becomes two independent double stranded molecules. Once the primers have annealed the next step is a further heating step (to 70°C) that is required for DNA polymerase to attach and extend the newly forming DNA strand by addition of bases complementary to the strand it is attached to. One key feature of PCR is the thermal stability of the DNA polymerase; the polymerase used in all experiments was derived from the bacteria *Thermus Aquaticus*, referred to as *Taq*. This is stable to very high temperatures with an error rate of around 1 in 130,000. Due to the enzyme activity being optimal at high temperatures an initial 95°C phase is required; it is thus referred to as a "hot-start" enzyme.

2.10.2 RNA extraction via Trizol Reagent

H69 cells or primary BEC growing on plastic culture flasks where rinsed with PBS (sterile, 4°C) and detached using cell scrapers. The resulting suspension was centrifuged at 1000g for 5 min with removal of the supernatant. The remaining cell pellet was resuspended in 1ml Trizol reagent with incubation at RT for 5 min. Trizol is a mono-phasic solution composed of phenol and guanidine isothiocyanate, which maintains RNA integrity while also solubilising cell components. 200uL of chloroform was added to each tube with agitation for 20 sec. A further incubation of 5 min at RT was followed by centrifugation at 12000g for 15 mins, pre cooled to 4°C. The upper, aqueous phase containing the RNA was transferred to a fresh sterile microcentrifuge tube with 500ul of isopropyl alcohol with mechanical agitation and incubation at RT for 10 min with subsequent centrifugation at 12000g for 10 min pre cooled to 4°C. RNA quality was assessed using a NanoDrop spectrophotometer (NanoDrop ND-1000, Thermo Scientific, Wilmington, USA).

2.10.3 Quantification of RNA and DNA

The NanoDrop spectrophotometer (NanoDrop ND-1000, Thermo Scientific, Wilmington, USA) was used extensively in the quantification and purity assessment of RNA and DNA. This machine measures absorbance at three wavelengths; 260nm for nucleic acid content, 230nm and 280nm for organic solvents and protein content respectively. By calculating the ratios of the absorbance peaks it is possible to ascertain the relative purity of the sample. When calculating a 260/280 peak, a ratio of 1.8 indicates relative purity of DNA with 2.0 indicating the same for RNA. Samples with a 260/280 below 1.8 were discarded (figure 2.2).

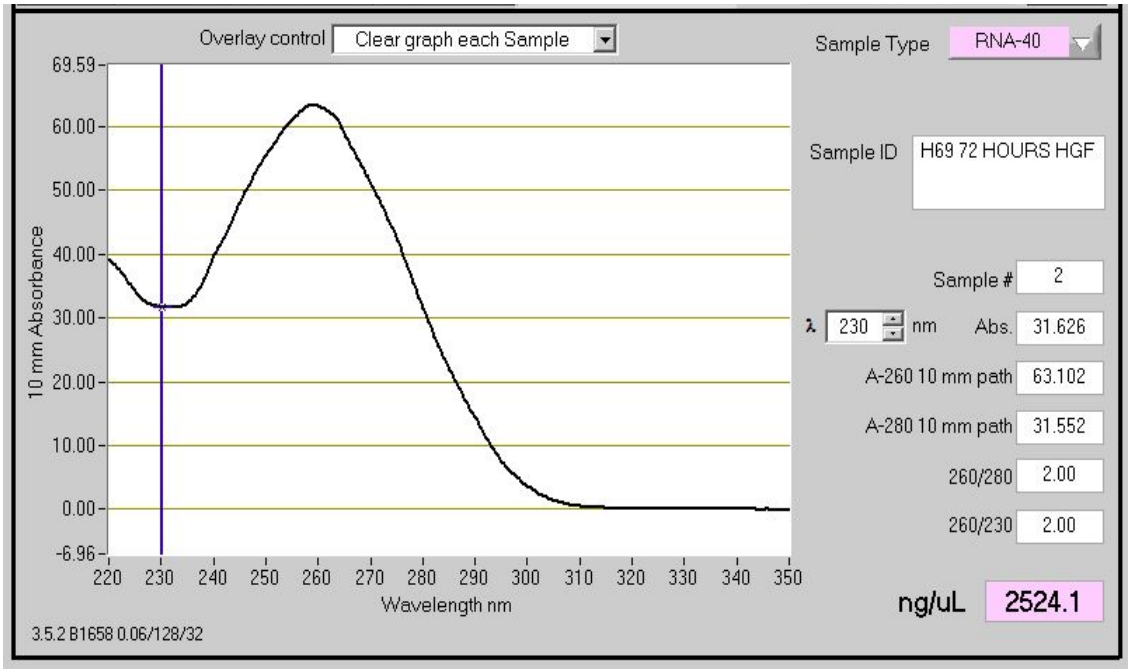

Figure 2.2: Output screen of NanoDrop spectrophotometer. Display shows a representative sample of RNA from H69 cells. Both the 260/280 and 260/230 ratios are 2.00.

2.10.4 Synthesis of cDNA from RNA

In order to amplify and analyse isolated RNA it must first be converted into DNA. To do so a reverse transcription is necessary and must be carried out under RNAse free conditions. The first step in the reaction is heating the RNA solution containing an oligo dT primer to anneal to the poly-A tail of the RNA strand. This occurs at 65°C,

after 5 mins this is allowed to cool for a further 10 mins. Components added at this stage were: 2µl affinityScript reverse transcriptase (RT) buffer (x10), 0.8µl dNTP mix (25mM each dNTP), 0.5µl RNase block ribonuclease inhibitor and 1µl and affinityScript multiple temperature reverse transcriptase (RT). Incubation was at 55°C for 60 mins with reaction termination by heating to 70°C for 15 mins. Reverse transcription occurred at a further 55°C, 60 min incubation step with termination by heating at 72°C for 15 mins.

2.10.5 Primer design

All primers used in this study were commercially produced; the discussion of primer design that follows is therefore to illustrate the principles involved. Primers are usually 15-30 base pairs in length, exhibiting a high degree of homology to the sequence to be amplified (the target sequence). One of the key characteristics governing primer utility is the melting temperature, this being the temperature at which a DNA duplex will dissociate into single strands. Primers are usually designed with a melting temperature (Tm) between 52 and 58°C, those primers with Tm above 65°C have a higher probability of secondary annealing. In order to predict the Tm a simple formula may be used; Tm = 4(G+C) + 2(A+T). From this it can be deduced that overall primer length as well as the ratio of bases influence the hypothetical Tm. The G/C content of the primer is kept as close to 50% of the sequence as possible. It follows that in replicating both strands of DNA both forward and reverse primers must be used. As a reaction can hold only one annealing temperature the Tm of both primers should be as closely matched as

possible. In practice the actual melting temperature is dependent upon other factors of the reaction, such as ion concentrations and solvents; therefore a melting curve of primers should be obtained to determine the actual Tm and reduced primer-dimer and mispriming artefact.

2.10.6 RealTime PCR (RQ-PCR)

RealTime PCR (RQ-PCR) uses fluorogenic probes to allow monitoring of the PCR reaction through all phases. There are three distinct phases during a PCR reaction exponential, linear and plateau, the first phase, exponential, occurs when exact doubling of the product/amplicon with each temperature cycle. The linear phase occurs after exponential, the reaction is slowing down and amplifies at a less specific rate as reagents are consumed. The plateau phase is the last and at this point the reaction has stopped and the products begin to degrade. While traditional PCR measures only during the plateau phase, with the product visualised as a band on agarose gel, RQ-PCR can measure all three phases and thus allow accurate quantitation by measurement in the exponential phase, when reaction kinetics are determined by the quantity of cDNA template, rather than the quantities of reagents as in the linear phase.

2.10.7 Applied Biosystems "TaqMan" RQ-PCR

Applied Biosystems TaqMan RQ-PCR system uses a fluorogenic probe to allow detection of a specific PCR amplicon during all PCR cycles. Each probe has a reporter high-energy dye (at the 5' end) and a low energy Quencher (at the 3'end). When

light of the correct wavelength is incident upon the probe the emission of the 5' reporter is absorbed by the quencher in a process termed FRET (Fluorescence Resonance Energy Transfer).

When the probe is utilised in a reaction it anneals to the sequence and is removed by the action of 5' nuclease Taq polymerase. Once the quencher and reporter are removed they are no longer in close proximity and can therefore emit light. As long as the probes are in abundance they will be incorporated at double the rate every cycle with a concurrent increase in fluorescence.

The TaqMan probes used here consist of an oligonucleotide containing FAM (6-carboxyfluorescein) or VIC (proprietary compound) as a Reporter dye at the 5'end, and a minor groove binder, with a non-fluorescent Quencher at the 3'end (in this study tetramethylrhodamine (TAMRA) was used). The minor groove binder acts as a probe melting temperature (Tm) enhancer. These probes are short, enhancing the Tm differential between matched and mismatched probes. A single mismatched probe is therefore more likely to be displaced by DNA polymerase than cleaved during amplification.

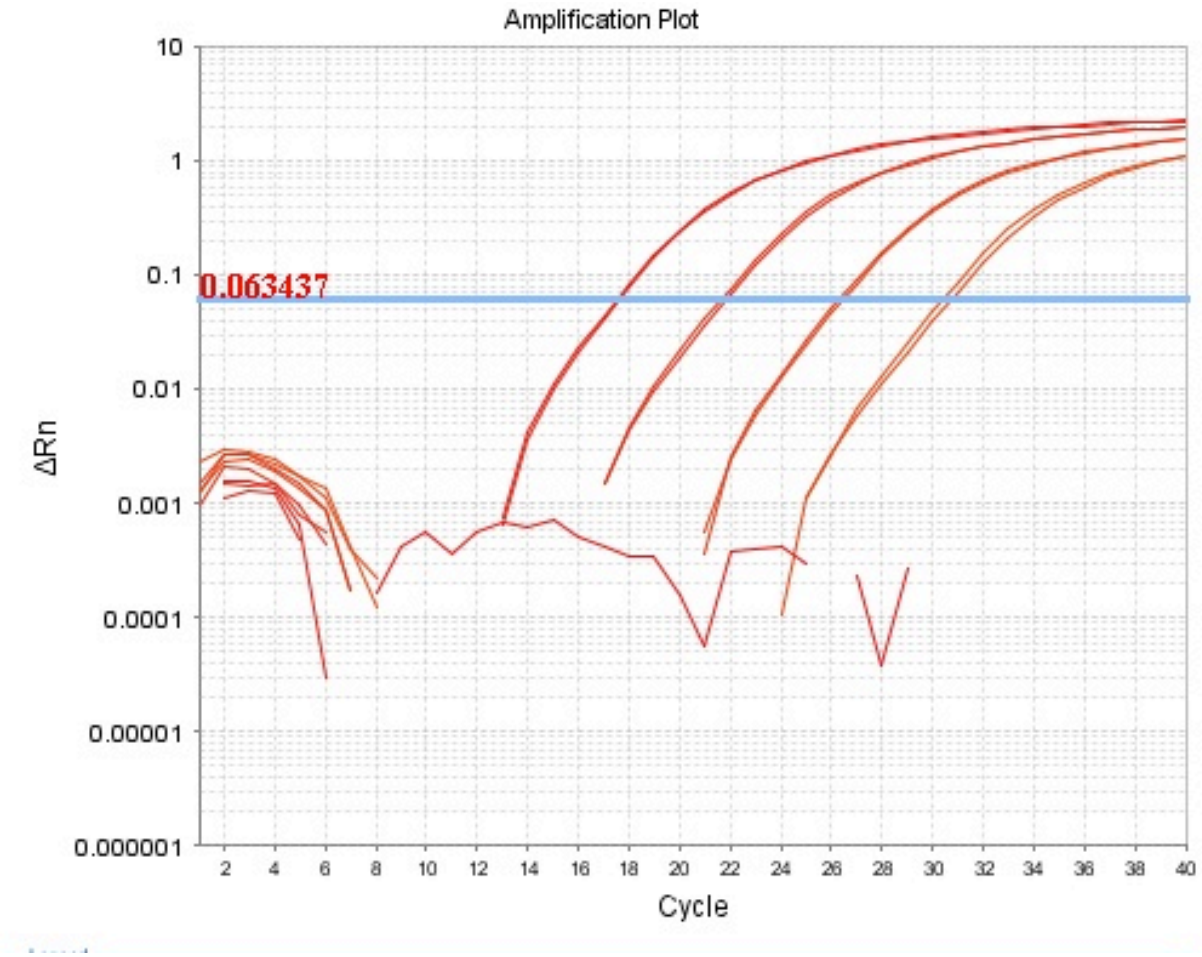

Figure 2.3 Sample amplification plot of RQ-PCR GAPDH primer. This is an actual amplification plot from an experiment run during this study. The samples shown are all amplifications of the GAPDH primer with the same cDNA neat and at dilutions of 1:10, 1:100 and 1:1000 in order to calculate the efficiency of the primers. The threshold is shown, this was routinely used at half way through the logarithmic phase of the reaction, as shown here.

2.10.8 RQ-PCR Reaction Ingredients

RQ-PCR experiments in this study utilised inventoried TaqMan Gene Expression Assays, for human:

TGFβ1 (Hs00998133_m1), GAPDH (Hs99999905_m1), TGFβ2 (Hs00234244_m1), TGFβ3 (Hs01086000_m1) and p21 (Hs99999142_m1)

The assays contain two gene-specific PCR primers; (forward and reverse, final concentration 900nM) and FAM labelled TaqMan probe (final concentration 250nM). The probes are designed to span exon junctions and therefore they do not detect genomic DNA.

The 20x assay mixture consisted of:

500 – 800ng of cDNA template

TaqMan Universal Master Mix (2X).

Mastermix contains AmpliTaq Gold (DNA Polymerase), AmpErase UNG, dNTPs and ROX

ROX dye provides an internal fluorescence reference for the reporter dye signal to be normalised against. This allows variations caused by changes in reaction concentration or volume to be compensated.

2.10.9 Quantification of RQ-PCR gene expression ($\Delta\Delta C_T$ method)

Prior to carrying out any experiments the efficiency of primers was assessed using serial dilutions. 1μl (neat) cDNA was diluted to 0.1μl (1:10) then again to 0.01μl (1:100) and so on until 0.001μl (1:1000). The ΔCt for each reaction varies relative to the template dilution. The gradient of linear regression determined is then utilised to calculate the amplification efficiency. This is done by calculating the gradient of the efficiency curve (as shown in figure 2.4) and using the formula efficiency of reaction = $10^{(-1/slope)}$-1x100. All primers used in this study had efficiencies of 97-

98%. As discussed above, numerous variables can affect the efficiency of a PCR reaction including amplicon length, primer quality and the cDNA template.

Data in this study was then analysed using the comparative CT method (ΔΔCT). The CT value is the cycle number at which an exponentially increasing fluorescence signal can be separated from background noise. This method relies on arithmetic formulas to compute relative quantification; alternatively the standard curve method may be used. ΔΔCT method calculates the expression of a target gene in relative to a reference control (endogenous control gene, in this case GAPDH). This endogenous control is chosen as it does not vary in expression between the calibrator (control template) and the target. The comparative CT method may be used only when efficiencies of PCR amplifications in gene of interest and reference/control are approximately equal. Validation is performed using the formula:

Comparative expression level = $2^{-\Delta\Delta CT}$

where:

ΔΔCT = ΔCT target - ΔCT reference

And must be conducted before further analysis is performed.

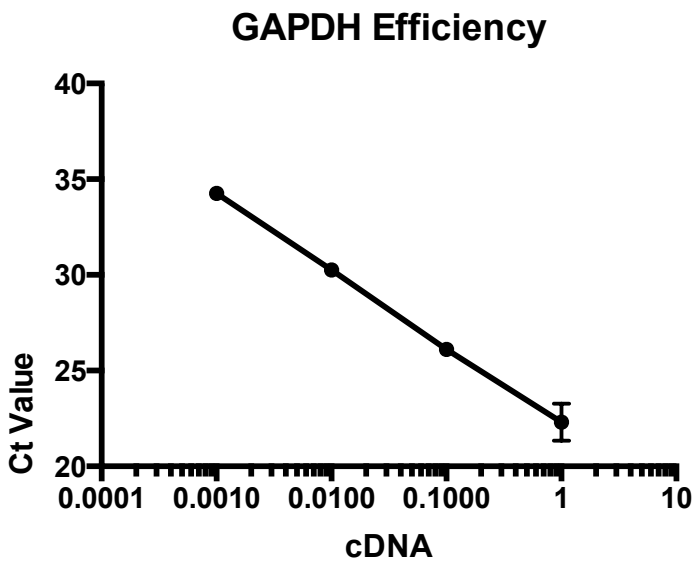

Figure 2.4 Efficiency curve of GAPDH primers in RQ-PCR. The Ct values of the primers are shown on the Y axis. The X axis shows the dilution of the cDNA, with 1 representing the undiluted cDNA, 0.1 the 1:10 dilution and so forth. The gradient of the line was determined by the change in y values divided by the change in x values for two specific points on the curve, this gave a result of -3.39 and an efficiency of 97.3%.

2.11 Histology and light microscopy

During the study many standard histology specimens were assessed in addition to the specific immune and tincture stains performed during the study. All histology was assessed using a Nikon Eclipse microscope with JVC camera attached for image capture onto a Lenovo PC.

3 Addressing The First Gap in Translation: Novel Studies in Human Liver Biopsies

3.1 Introduction

3.1.1 Rejection in orthotopic liver transplantation

With the advent of calcineurin inhibitor-based immunosuppression regimes such as cyclosporine, and the development of more novel agents such as mycophenolate mofetil (MMF), there has been a significant fall in the reported incidence of classical ductopenic rejection in liver allografts (Demetris, Adeyi et al. 2006, Hubscher 2006, http://www.britannica.co.uk 2013). Indeed, this diagnosis is now regarded as a rare entity. This does not mean however that immune-mediated liver injury does not occur in allografts. There has been an increasing recognition of chronic rejection in the absence of ductopenia (defined as predominantly centrilobular necroinflammation with or without fibrosis or portal changes with preservation of intralobular bile ducts), as well as recognition of acute and chronic antibody-mediated rejection (Bellamy, Herriot et al. 2007, Yoshitomi, Koshiba et al. 2009). Three questions therefore remain: how – and why – does the application of immunosuppression in transplant recipients influence duct loss, and whether this phenomenon is due to liver injury mediated by the immune system.

3.1.2 Senescence in liver disease

The senescence of BEC (BEC) is an established feature of chronic ductopenic rejection, with the characteristic morphology of senescent BEC described consistently in the literature (Demetris, Adams et al. 2000, Burt 2011, Hubscher

2011). BEC senescence has been studied in other ductopenic disorders, including primary biliary cirrhosis (PBC) and primary sclerosing cholangitis (PSC) (Sasaki, Ikeda et al. 2010, Sasaki, Miyakoshi et al. 2010). The primary cause of BEC senescence in these diseases remains unclear. Cases of senescence due to oncogene activation, toxins and replicative exhaustion have all been described (Evan and d'Adda di Fagagna 2009, Rajawat, Hilioti et al. 2009). Previous investigators of BEC senescence have used *in vitro* models of oxidative stress to induce the senescence markers p21 and p16, mapping these findings from culture to animal models and to immunohistochemistry in human biopsies (Sasaki, Miyakoshi et al. 2010).

Investigation of senescent cells in culture has revealed their potential to secrete pro-inflammatory cytokines and chemokines. This is known as the Senescence Associated Secretory Phenotype (SASP) (Sasaki, Ikeda et al. 2008) and has the potential to drive acute disease. The SASP, if present, could potentially therefore provide a pro-inflammatory driver of acute rejection.

3.1.3 Epithelial to mesenchymal transition in transplantation

The phenomenon of epithelial to mesenchymal transition (EMT) has been described in the context of embryogenesis for many years. EMT is fundamental to the establishment of mesenchymal cells (and of epithelia by the reverse process, mesenchymal to epithelial transition or MET) from a single pluripotent cell (Evan and d'Adda di Fagagna 2009, Thiery, Acloque et al. 2009). In more recent years, the potential for adult cells to undergo either EMT or MET has been investigated. These processes have been studied extensively in carcinogenesis with tumour type dependent processes being key to the establishment of both invasive malignancy

and metastasis (Coppe, Desprez et al. 2011). EMT has also been proposed as a mechanism of fibrosis in the spectra of benign disease (Sicklick, Choi et al. 2006). Our group was the first to look at transplanted tissue with investigation of EMT in renal allograft biopsies (Robertson, Ali et al. 2004). More recently, there has been opposition to the concept of EMT as a mechanism in fibrotic liver disease, with the publication of several murine models. Despite severe weaknesses in these data (discussed in section 1.7.5), they have been accepted by many as proof that EMT is not a significant contributor to fibrosis in liver disease (Taura, Miura et al. 2010, Chu, Diaz et al. 2011).

3.1.4 Oxidative stress in transplantation

Ischaemia reperfusion injury (IRI) is a well-defined event in transplantation and is linked to episodes of acute cellular rejection (ACR) though the evidence for IRI in the pathogenesis of AR is controversial. However: the durations of both warm and cold ischaemia are independent predictors of rejection episodes and are minimised as far as possible in the clinical arena (Lu 1996, Pirenne, Gunson et al. 1997, Schneeberger, Aydemir et al. 1997, Serrick, Giaid et al. 1997). Preservation solutions, such as University of Wisconsin solution, include mediators to reduce the impact and severity of reperfusion injury (Pirenne, Gunson et al. 1997).

Organ donors will have undergone the trauma of either brain or cardiac death; both are associated with hypo-perfusion and activation of the systemic inflammatory response syndrome (SIRS) (Brain, Rostron et al. 2008). Following this process, organs are perfused with ice-cold solution before being transported on ice for several hours and then re-warmed during the implantation procedure. While

normothermic perfusion systems are gaining popularity and can potentially negate most of the features associated with cold ischaemia, it will be some time before they are adopted wholesale into clinical practice. It is therefore clear that ischaemia and reperfusion will remain significant contributors to allograft outcome for the foreseeable future. While IRI clearly has the ability to induce cell damage leading to senescence (Erol , Sasaki, Ikeda et al. 2008) there are no references in the literature that investigate a possible correlation between acute rejection and senescent cells within the allograft.

3.1.5 Alcohol-mediated liver injury

In the context of liver disease, alcohol and its effects on the liver represent an entirely separate entity. Alcohol is a toxin and the predominant injury is to hepatocytes, preferentially those in zone 3 of the liver lobule. The toxic effects of alcohol on liver metabolism are extensive and are reviewed here (Burra, Senzolo et al. , MacSween and Burt 1986, Bellamy, DiMartini et al. 2001, Yip and Burt 2006). The pattern of injury is of interest as, despite the main injury being to the hepatocytes, there is frequently a ductular reaction and a regenerative response from the ductular precursor cells. It has been hypothesised that the biliary epithelium plays a key role in the determination of the liver's response to alcohol (Michalak, Rousselet et al. 2003).

The patterns of fibrosis seen in alcohol-mediated liver disease differ from those seen in biliary diseases. In biliary diseases, there is portal tract expansion followed by spur formation and bridging, eventually leading to cirrhosis. In alcohol and other toxin-mediated liver injury there is some portal tract expansion, with expansion

around the central veins, as well as peri-sinusoidal fibrosis, which looks rather like chicken wire upon collagen specific stains. Several patterns of fibrosis initiation in this situation have been described (Raynard, Balian et al. 2002, Bedossa and Paradis 2003, Michalak, Rousselet et al. 2003).

As a counterpoint to allograft injury, alcohol-mediated disease represents an entirely different condition, yet it retains the biliary epithelium as one of its potential key regulators and arguably site of injury.

3.1.6 An early stage of the same disease

It is well established that there is an association between severity and number of acute rejection episodes and development of chronic ductopenic rejection; however the mechanisms behind this association have not been described (Pirenne, Gunson et al. 1997, Shaked, Ghobrial et al. 2009). Indeed, liver allograft outcome data can be confusing, with some studies reporting better graft outcomes where patients have experienced mild rejection episodes, and some reporting a linear relationship between number and severity (measured by Banff grade) of rejection episodes and either chronic ductopenic rejection or graft failure (Horoldt, Burattin et al. 2006, Neuberger, Mamelok et al. 2009). As noted above, acute rejection has been linked to myofibroblast production by EMT (Robertson, Ali et al. 2004, Rygiel, Robertson et al. 2008). However, fibrosis is a feature of chronic, rather than acute, rejection. Potentially, this may point to a link between IRI, senescence, acute and chronic rejection.

3.1.7 Aims

The specific aims of this chapter are:

To identify whether senescent BEC are present in ACR in liver allografts

To identify whether there is evidence of EMT in ACR in human liver allografts

To determine whether there is a link between senescence and EMT in ACR

To establish whether senescence can be induced in primary human BEC by oxidative stress

To characterise the response of primary human BEC to oxidative stress

3.2 Specific materials and methods

3.2.1 Analysis of Triple Colour Immunohistochemistry

Samples comprised time 0 biopsy sections (n=9, tissue taken at the point of reperfusion of transplanted liver) that were used as control tissue and the ACR sections (n=25, biopsies of transplanted liver with mild, moderate or severe acute rejection). The sections were stained with either $p21^{WAF1/Cip1}$, CK19 and S100A4 antibodies or CD3, CK19 and S100A4 antibodies. Complete triple labelled sections were scanned using an Aperio slide scanner at x200 magnification and remotely accessed files were analyzed. Each biopsy was assessed by two observers (JGB and HR) and scored for number of portal tracts, number of interlobular bile ducts (excluding ductules and ductular reaction, except in ALD biopsies), maximum number of bile ducts per portal tract, number of $p21^{WAF1/Cip1}$ positive BEC, number of S100A4 BEC, number of dual stained BEC (S100A4 and $p21^{WAF1/Cip1}$) and number

of $p21^{WAF1/Cip1}$ and S100A4 BEC adjacent to one another. There was good agreement between the observers, any discrepancies were noted and a consensus opinion reached. As a number of immune cells stain positive for S100A4, there was a chance that infiltrating macrophages or T-cells could be mistaken for BEC. This was usually straightforward to assess morphologically. Serial CD3 stained sections allowed assessment of T-cell mediated EMT. In order to answer the queries raised by a reviewer for the journal American Journal of Transplantation, it was necessary to

Due to the presence of more than two groups of approximately normally distributed data, statistical analysis was by one-way ANOVA with significance defined as $p < 0.05$. Significant one-way ANOVA was followed by post-hoc T tests to further define exact differences.

3.3 Results

3.3.1 Markers of senescence, EMT and proliferation in allograft rejection

In order to determine whether senescent cells are present in ACR a group of 34 biopsies were identified. 9 were time zero biopsies showing no significant changes and were used as a control group. A further 25 were all histologically found to have ACR and were graded using the Banff scale of rejection: mild (n = 3), moderate (n = 3) and severe (n = 19). Sections from these biopsies were stained using triple colour immunohistochemistry (Section 3.2.1), initially for the markers CK19 (to delineate the BEC component), p21 (as a marker of senescence) and S100A4 (as a marker of EMT). These biopsies were scored independently by two blinded observers (JGB

and HR). It should be noted that the biopsies used for this study do not represent the incidence of ACR subtypes seen in clinical practice. The biopsies were chosen as a matter of expedience and in accordance with the existing ethics. There is often an attempt by hepatologists to minimise biopsy procedures (due to the associated morbidity and mortality), which may lead to skewing of the pathological subtypes seen in histology.

Results from the staining can be seen in Fig. 3.1, with positivity for CK19 and S100A4 or p21 in the BEC component. No BEC were found to be positive for both S100A4 and p21. Infiltrating cells, (particularly monocytes that were stained positive for S100A4 within the ducts) were identified morphologically and this evidence was consistently reproducible. Such cells were CK19 negative and so were not included in any cell counts. Examples are shown in Fig. 3.1. However, to assist in the identification of T-cells that may be S100A4+, sections were also triple stained for the T-cell marker CD3 (rather than p21) as well as CK19 and S100A4 (data not shown).

There was a correlation between Banff grade and the expression of p21 and S100A4 by BEC. A one-way ANOVA test showed this correlation to be significant ($p < 0.034$ and $p < 0.0068$ respectively) (Fig. 3.2). There was also a correlation between p21 and S100A4 expression, despite these factors not being expressed in the same cell. This was assessed by correlation and the Spearman correlation coefficient was found to be significant ($p < 0.0013$), results are shown in Fig 3.2, panel C. Interestingly, $S100A4^+$ and $p21^+$ BEC were never adjacent to one another.

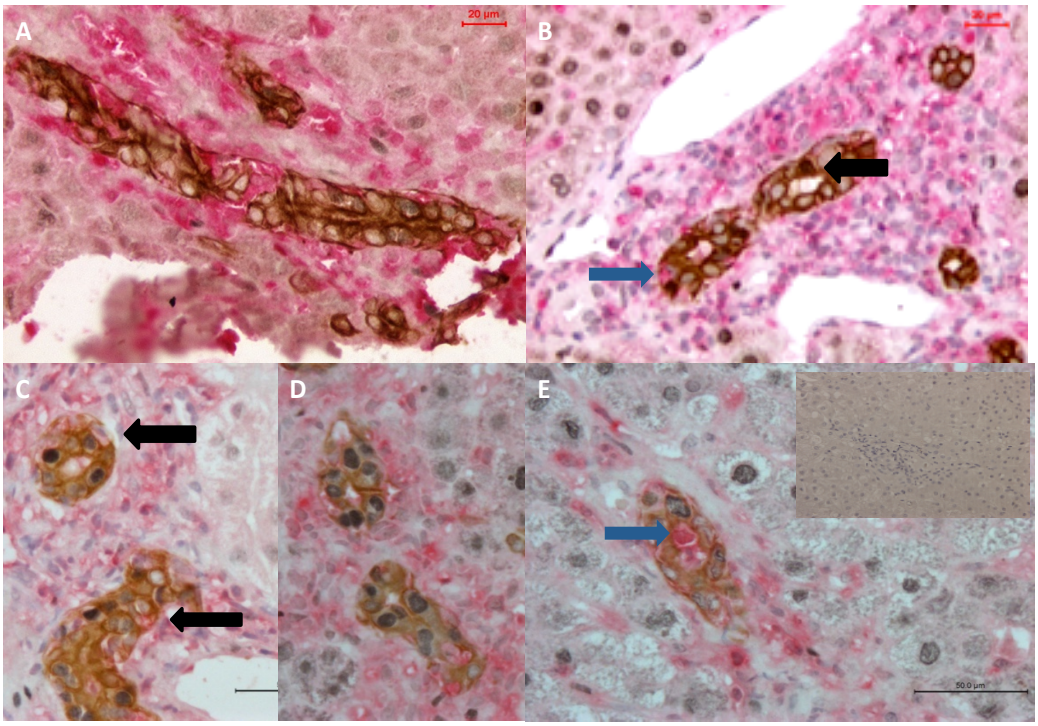

Figure. 3.1: Triple colour immunohistochemistry of human allograft liver ACR biopsies. Panel A is a time zero biopsy, demonstrating CK19 (brown) staining alongside S100A4 (red), which is limited to the infiltrating cells. Panel B shows a mild ACR biopsy in which p21 staining (black) is evident in a CK19 positive BEC (black arrow); a blue arrow denotes an S100A4^{+} BEC. Panels C and D demonstrate BEC positive for CK19 and either p21 or S100A4 (black arrows). Panel E shows an infiltrating S100A4^{+} cell (blue arrow), the inset shows a control sample with no primary antibody.

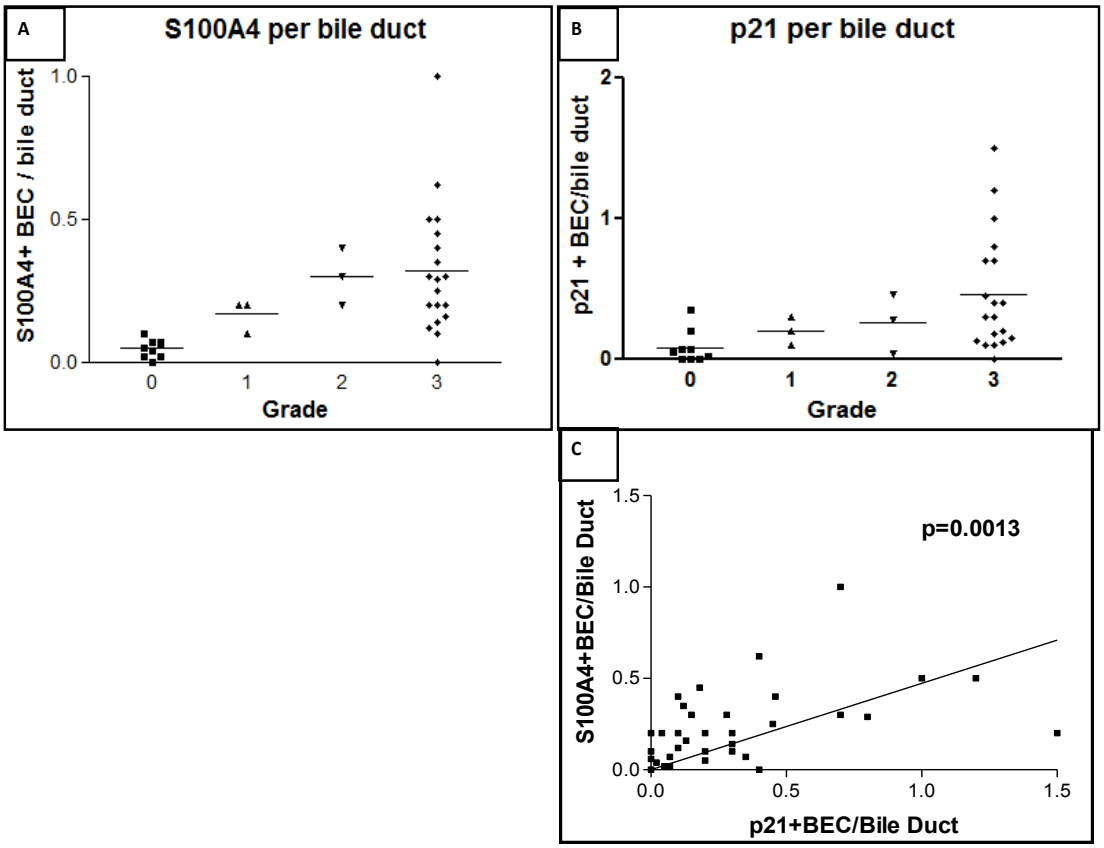

Figure 3.2: Number of BEC staining positive for S100A4 (panel A) or p21 (panel B) arranged by Banff grade. Grades are 0 = time zero controls, 1 = mild, 2 = moderate and 3 = severe rejection. S100A4$^+$ cells were associated with grade of rejection; this was shown by one-way ANOVA to be statistically significant ($p < 0.0068$). p21$^+$ BEC were positively correlated to Banff grade again shown by one-way ANOVA ($p < 0.034$). Panel C shows the correlation between p21 and S100A4$^+$ BEC, confirmed by the Spearman correlation coefficient significant ($p < 0.0013$).

As p21 on its own is not a specific marker of senescence, further characterisation of the potentially senescent cell population was required. Based on the work of Professor von Ziglickni's group (Lawless, Wang et al. 2010) staining was carried out for a number of different antigen combinations in human liver ACR biopsy material. The non-specific marker Ki67 (Ki67 is positive at all points of the replicative cycle, indicating all cells undergoing mitosis not just those at a specific stage) was used instead of p21 alongside S100A4 and CK19 – results are shown in Fig. 3.3, panels A-C. It was shown that Ki67 stained cells were frequently also positive for S100A4, indicating that a number of proliferating cells were also expressing S100A4 (van den Heuvel, de Jong et al. 2004). Large numbers of $S100A4^+$ cells were also negative for Ki67, indicating the presence of a compartment of cells that were $S100A4^+$ but not proliferating. $S100A4^+$ cells were also seen adjacent to $Ki67^+$ cells. This staining would indicate that a significant proportion of $p21^+$ BEC were also $Ki67^-$. As there were only a small number of biopsies (9-10 plus 5 time zero controls), statistical analysis was not deemed appropriate. However, an association was observed between increasing Banff grade and both $Ki67^+$ BEC and $Ki67^-$ BEC positive for either S100A4 or p21.

In order to validate the staining of the triple coloured immunohistochemistry, biopsies from patients with biliary strictures and obstruction (forms of biliary injury unrelated to intra-hepatic bile duct injury) were chosen as control samples, and stained for the same markers as primary BEC. Results are shown in Fig. 3.3 panels D-H and indicate that the staining performed on primary BEC was specific and reproducible.

As a marker of senescence, p21 is not the most specific, being also expressed in the G1/S transition and forming part of the cell cycle checkpoint. It does however have some interesting associations. In order to further clarify that the $Ki67^-$ / $p21^+$ BEC in the transplant biopsy series were indeed senescent, further staining was conducted. A dual stain for Ki67 and p21 was performed in further human liver ACR biopsies. This demonstrated that there was indeed a $Ki67^-$ / $p21^+$ compartment in BEC. The senescence marker γH2AX was also used, both singly and in a dual stain with Ki67. Results are shown in Fig. 3.4. Again, there was a paucity of biopsy material and so only 10 ACR biopsies and 5 controls were stained. There was an association between Banff grade and γH2AX staining (with a minimum of 5 foci per nucleus required for a cell to be defined as senescent). There was also an increase in $Ki67^-$, $\gamma H2AX^+$ BEC with increasing Banff grade.

Like p21, lipofuscin, another marker of senescence, is associated with senescence-induced oxidative stress. Lipofuscin is autofluorescent on FITC excitation at 488nm but has a separate emission peak from FITC, so un-de-paraffinised sections were mounted with water-based mountant and visualised using a confocal microscope with a 488nm laser. Lipofuscin granules were clearly visible on the sections (see Fig. 3.5). Granules were present largely in the biliary epithelium and vascular endothelium - elastic fibres were also present. The internal elastic lamina of a vessel can be clearly seen in panel C. These findings indicate cellular senescence due to oxidative stress within the tissues.

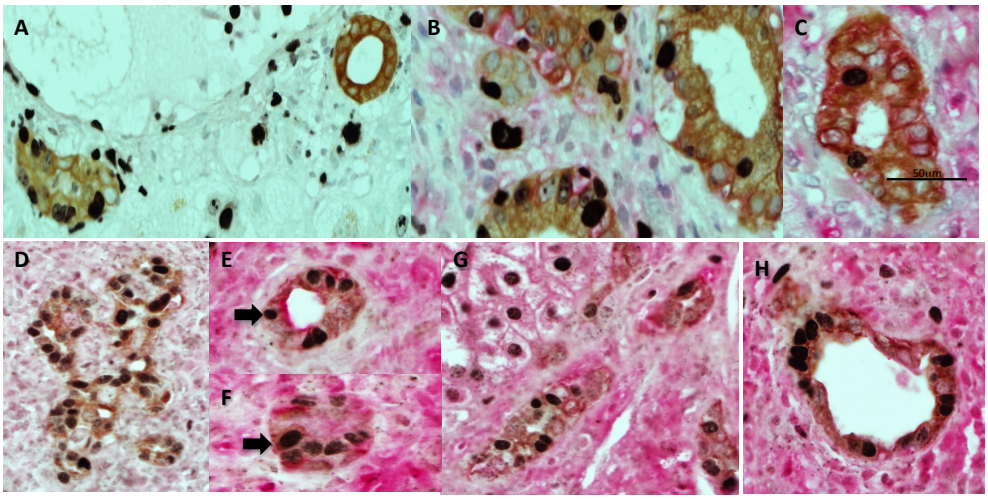

Figure 3.3: Triple colour immunohistochemistry of proliferation markers and control human transplant biopsies. Panels A-C represent transplant biopsies stained for Ki67 (black), S100A4 (red) and CK19 (brown). Panel A demonstrates mild rejection and $Ki67^+$ BEC are clearly seen in the absence of S100A4. Panel B shows $Ki67^+$ / $S100A4^+$ BEC in moderate rejection, with the spatial relationship between $S100A4^+$ or $Ki67^+$ BEC apparent. Panel C shows a field from a severe rejection biopsy, indicating the number of $S100A4^+$ BEC relative to $Ki67^+$ BEC. Panels D-H represent fields from human liver transplant recipients with biliary anastomosis obstruction or stricturing. These are stained with $p21^{WAF1/Cip}$ (black), S100A4 (red) and Ck19 (brown) as control material. Cells dual positive for Ki67 and S100A4 are indicated by black arrows. Staining for all antigens is abundantly apparent.

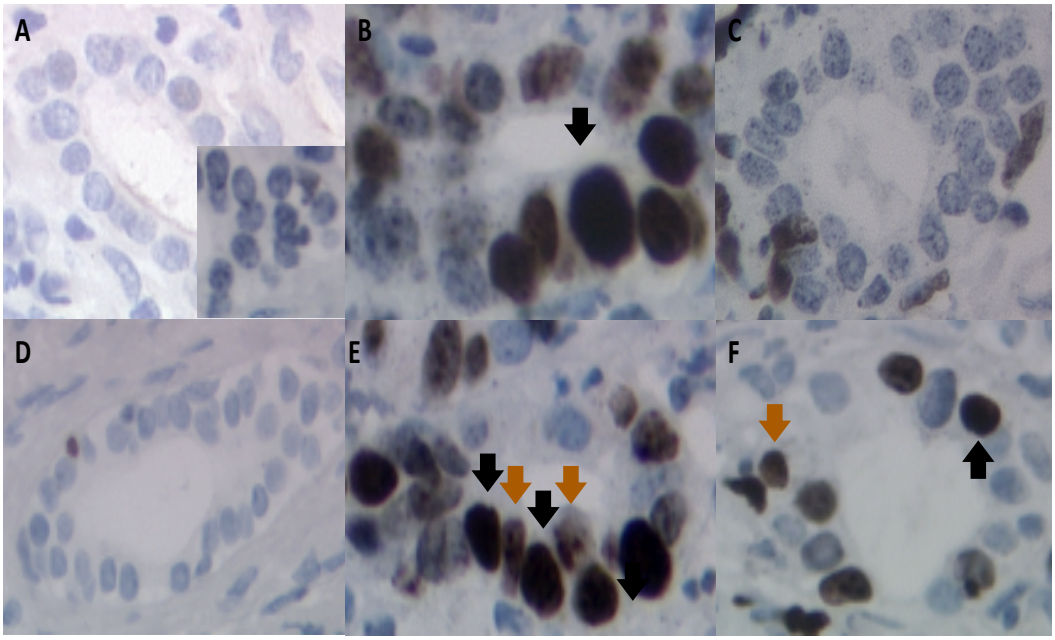

Figure 3.4. Immunohistochemistry of transplant acute rejection biopsies for markers of proliferation and senescence. Panels A – C show dual staining for Ki67 (brown) and γH2AX (black) Panel A shows ACR biopsy material - the main image is a negative control, the inset image is a biopsy single-stained for γH2AX and shows a characteristic, punctate nuclear staining pattern. Panel B is from a moderate ACR biopsy; $Ki67^-$ and $\gamma H2AX^+$ cells are seen. Panel C shows a severe ACR biopsy with a clear increase in the numbers of $Ki67^-$ and $\gamma H2AX^+$ cells. Panels D - F show dual stained Ki67 (brown, brown arrows) and $p21^{WAF1/Cip1}$ (black, black arrows). Panel D is from a mild ACR showing only Ki67 positivity, Panel E is moderate and panel F severe ACR.

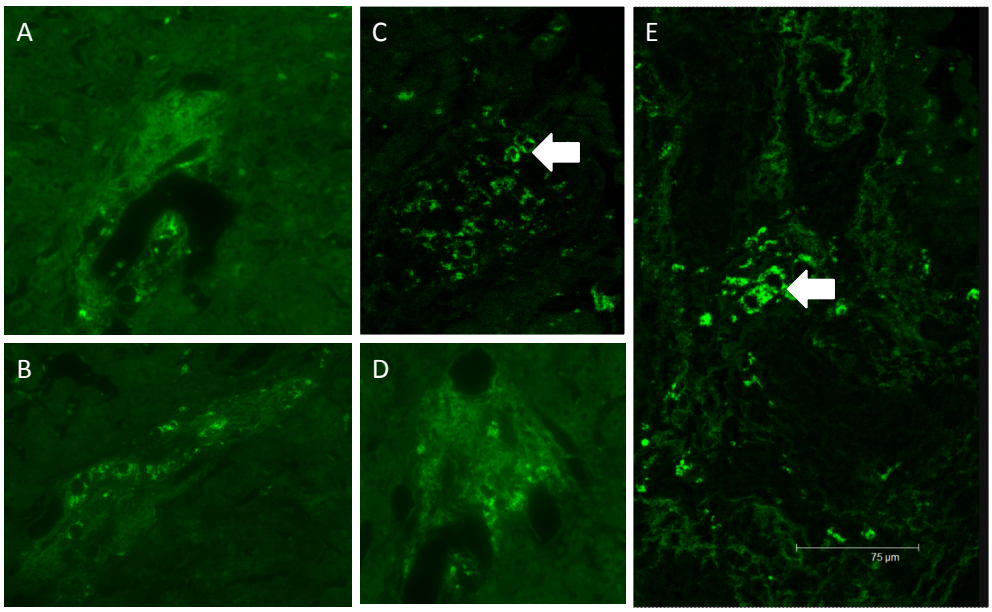

Figure 3.5: Lipofuscin expression in human liver biopsies with ACR. Elastic fibres are clearly visible, notably in the elastic lamina of the arteries. Bright lipofuscin inclusions are seen, mostly in BEC but also in hepatocytes adjacent to portal tracts. Panel(s) A-B show positivity in time zero/mild rejection, whereas panels C-E demonstrate lipofuscin positivity in moderate/severe rejection. Positive biliary cells are depicted with white arrows.

3.3.2 Markers of senescence and EMT in alcoholic liver disease

To provide a comparison to ACR in allografts, alcohol-mediated liver disease in native liver was also assessed by the same triple colour immunohistochemistry technique. The antigens examined were p21, S100A4 and CK19; the results are shown in Fig. 3.6. It is evident that there is more S100A4 positivity within both the epithelial and immune cell populations. Rather than using Banff grade, as this is not a system that translates to alcoholic liver disease (ALD) biopsies, biopsies were stratified by degree of fibrosis using the modified Newcastle fibrosis score, where 0 is no fibrosis and 6 is established cirrhosis. This score is based on the Ishak staging system but includes perivenular/pericellular fibrosis in stages 1-3 in addition to portal fibrosis and bridging. This means that the system can be used as a universal staging system.

Due to relatively small numbers of biopsies in some grades, analysis was performed on groups of stages 0-2, 3-4 and 5-6. The biopsies were all double reported by two blinded observers (JGB and HR). The results of scoring are shown in Fig. 3.7 and show a positive association between BEC p21 expression and fibrosis stage, shown as statistically significant in a one-way ANOVA ($p < 0.05$). There was no evidence of an association between fibrosis stage and BEC S100A4 expression.

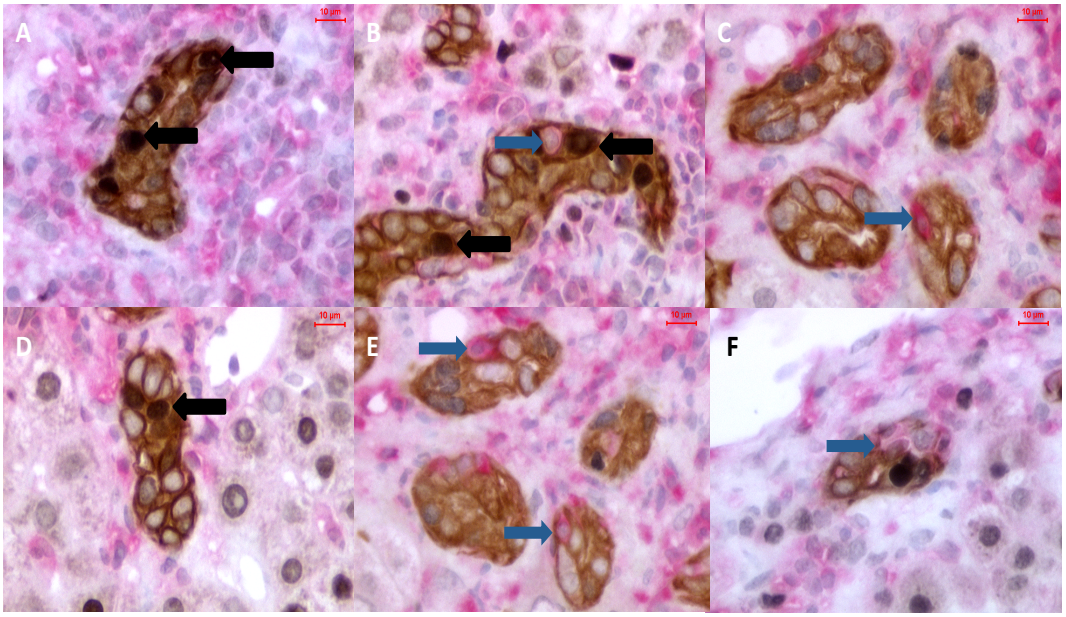

Figure 3.6: Triple colour immunohistochemistry of sections from ALD patients. These sections were selected according to stage of fibrosis, staining for p21 (black) in BEC (brown) was less common than in acute rejection biopsies. S100A4^{+} (red) BEC were more common. P21^{+} BEC are shown by black arrows (panels A, B and D), S100A4^{+} BEC are shown by blue arrows (panels B, C E and F). In all panels a pink/red staining can be seen in the background indicating the infiltrating immune cells. The staining above is seen in bile ductules, which is a different staining pattern to that observed in ACR where the bile ducts were stained positive.

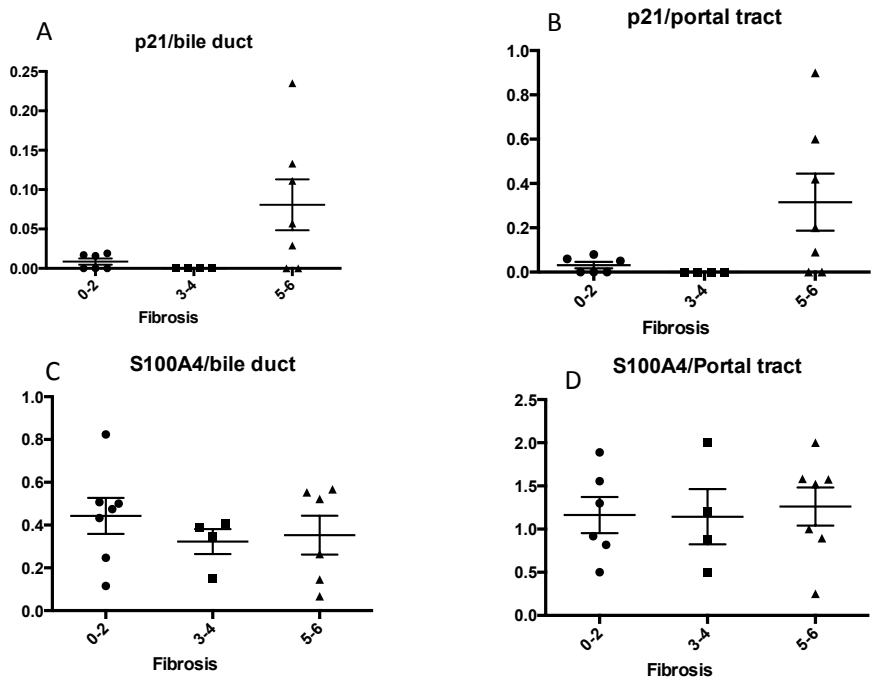

Figure 3.7: The association between fibrosis stage and BEC staining for either p21 (panels A and B) or S100A4 (Panels C and D). P21 staining was significantly associated with fibrosis stage, shown by a one-way ANOVA ($p < 0.05$). There was no association between S100A4 staining and fibrosis. Information is presented as positive cells per bile duct and also as positive cells per portal tract, this was to take account of the numerous positive ductules that were present in these cases that were excluded by using the method of examining only bile ducts.

3.3.3 Oxidative stress and senescence in primary human BEC

Models of senescence induced by oxidative stress have been described by Professor Nakanuma's group (Sasaki, Miyakoshi et al. 2010). In order to develop the observations made in human liver biopsy tissue in the current study, an attempt was made to recapitulate some of Nakanuma's work. In Nakanuma's work, the experiments had been largely carried out in rodent cells, either primary or immortalised. Using primary human BEC therefore would add significant value to the current study's observations. In collaboration with Dr Simon Afford from the University of Birmingham, primary human BEC were isolated as noted in section 3.2.3. These cells were all derived from explanted liver tissue with diagnoses of ALD, PBC or cryptogenic cirrhosis and had been frozen (passage 0 or 1) at -80 °C. In order to retain consistency and maximise efficiency, cells were expanded and used at either passage 3 or 4. It has been well established that primary human BEC retain their characteristics in culture until at least passage 5 (Leon, Kirby et al. 1995).

Due to the limited availability of primary BEC, a pragmatic approach was taken in developing the oxidative stress model. Based on the findings of Nakanuma (Sasaki, Miyakoshi et al. 2010) two concentrations (100μM and 200μM) of H_2O_2 were used to attempt senescence induction. Both concentrations were applied to BEC for 2 hours in the first instance, with removal of the H_2O_2 containing medium (EpiMed), washing in PBS and then replacement of fresh EpiMed medium with incubation for a further 24, 48 or 72 hours. Nakanuma reported a transient but significant up-regulation of p21 at 72 hours following H_2O_2 exposure, with a rapid down-regulation after this time. Expression of p21 in primary BEC is shown in Figure 3.8.

p21 was up regulated at all time points, with a marginal increase at 48 hours rather than 72, though staining at 72 hours was still present. Individual batches of cells gave different results, with some staining more diffusely positive. This made accurate interpretation difficult. All experiments were conducted in technical replicates and repeated three times.

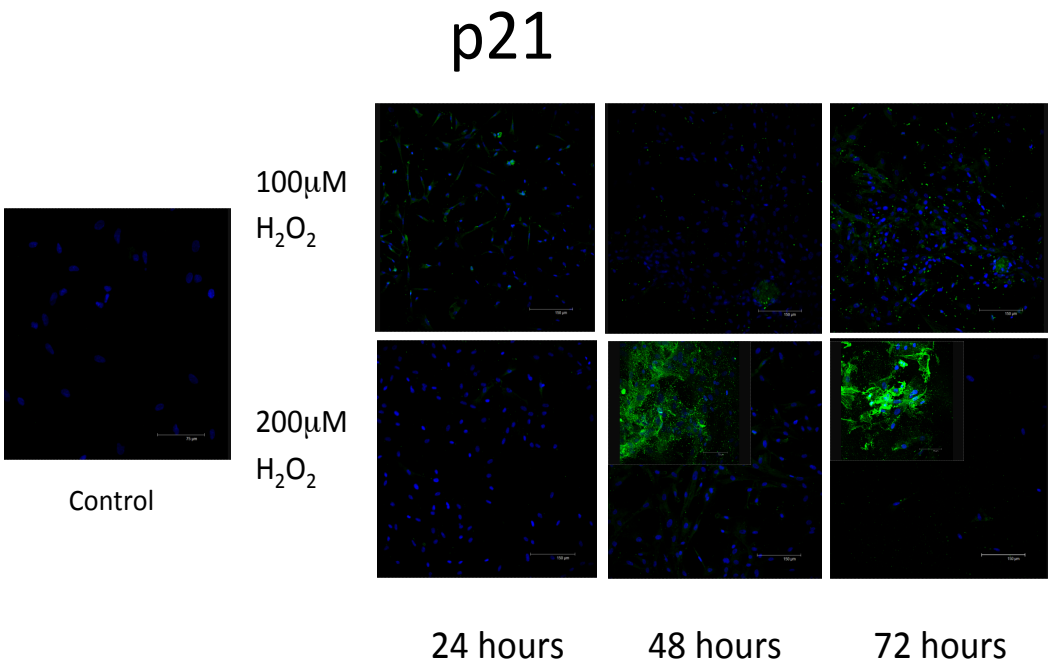

Figure. 3.8: p21 immunofluorescence staining in primary human BEC. The expression of p21 was low at baseline (control image) and did not increase in culture until the cells were over 90% confluent. Following exposure to H_2O_2 (100 or 200μM) for 2 hours and then incubation in fresh medium for 24, 48 or 72 hours the expression of p21 increased. The 100μM series shows a consistent up regulation at all time points, with more being seen at 48 rather than 72 hours. Staining of 200μM treated cells was more inconsistent with some cells showing nuclear up regulation (larger images) and some batches showing a more diffuse staining pattern (inset images). There was however an increase at 48 hours that was still present to a slightly lesser degree at 72 hours.

In addition to the expression of p21, a dramatic change in the morphology and phenotype of primary BEC was observed. A change akin to EMT was expected (based upon the findings in the ACR biopsy material). The epithelial antigens CK7, CK19 and E-Cadherin, and the mesenchymal antigens Vimentin, αSMA and S100A4 were all investigated. Results are shown in Figs. 3.9 – 3.13. There was a clear shift in antigen expression - from a largely epithelial pattern, to an intermediate or mesenchymal pattern. There was also a striking change in the morphology of the cells that can be seen most easily in Fig's 3.10 and 3.12, from a typical cobblestone epithelial type to a spindle cell (or biphasic) cell type, indicating a loss of epithelial cell function.

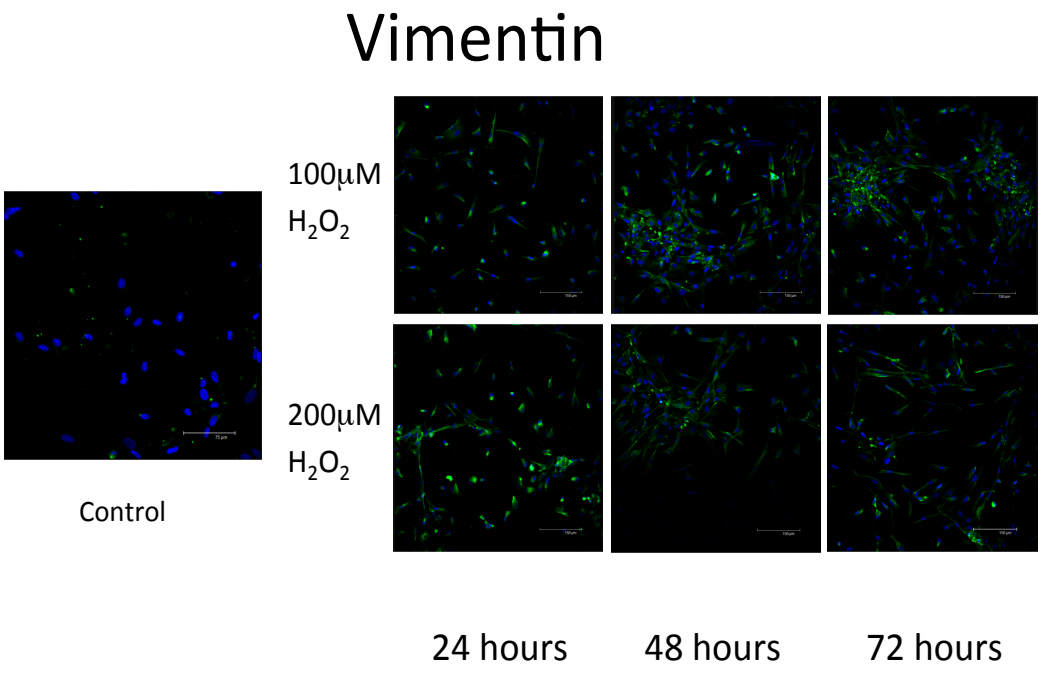

Figure 3.9 Expression of vimentin by primary human BEC (representative images from 3 separate experiments). Cells were used at passage 3 or 4 for all experiments; the control panel shows expression of Vimentin (green) at passage 3, nuclei are stained with DAPI (blue). Cells at passage 3 or 4 were then treated with H_2O_2 at 100 or 200μM for 2 hours with incubation in fresh medium (EpiMed) for a further 24, 48 or 72 hours. There is a clear increase in vimentin expression at all time points.

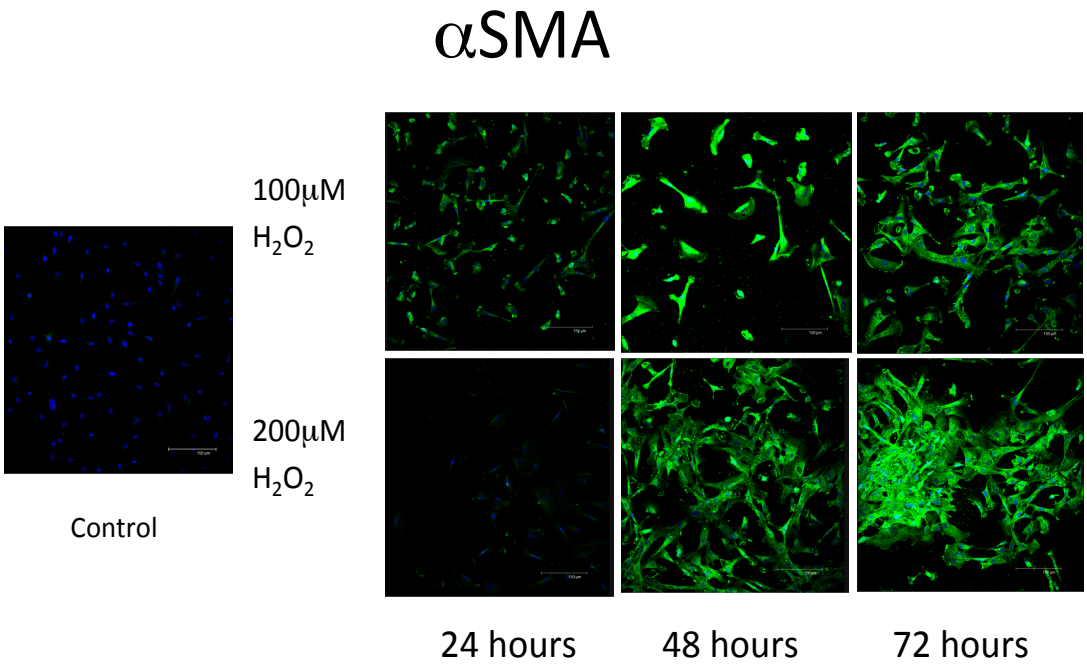

Figure 3.10 Expression of αSMA by primary human BEC (representative images from 3 separate experiments). Cells were used at passage 3 or 4 for all experiments; control shows expression of αSMA (green) at passage 3, nuclei are stained with DAPI (blue). Cells at passage 3 or 4 were then treated with H_2O_2 at 100 or 200μM for 2 hours, then incubated in fresh medium (EpiMed) for a further 24, 48 or 72 hours. There is a clear increase in αSMA expression specifically at 48 and 72 hours for both concentrations of H_2O_2.

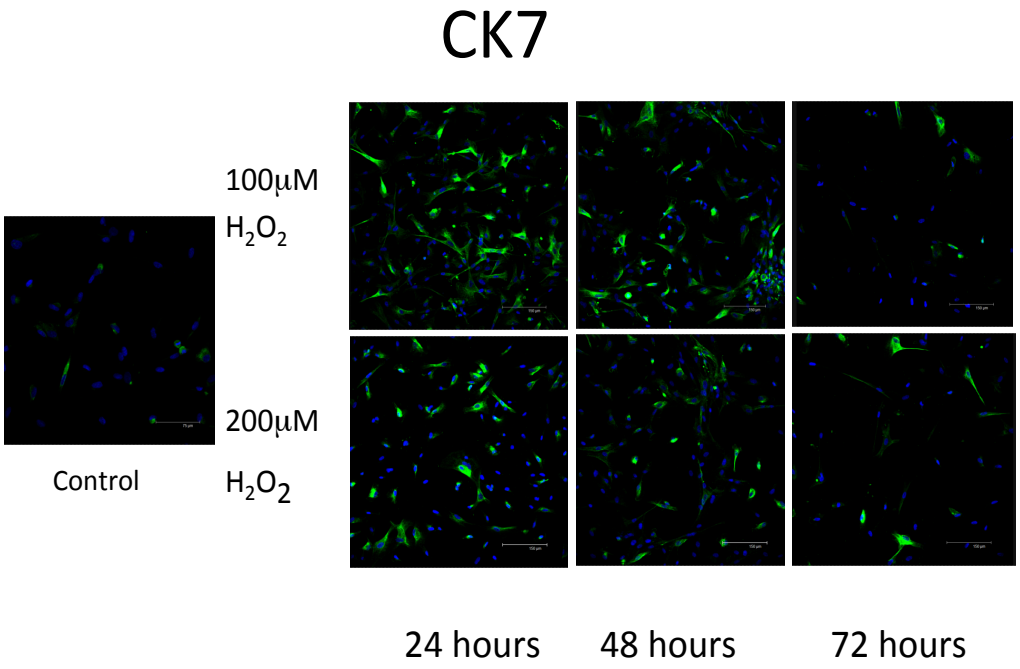

Figure 3.11 Expression of CK7 by primary human BEC (representative images from 3 separate experiments). Cells were used at passage 3 or 4 for all experiments; the control shows expression of CK7 (green) at passage 3, nuclei are stained with DAPI (blue). Cells at passage 3 or 4 were then treated with H_2O_2 at 100 / 200μM for 2 hours and incubated in fresh medium (EpiMed) for a further 24, 48 or 72 hours. There is a clear decrease in CK7 expression specifically at 48 and 72 hours for both concentrations of H_2O_2.

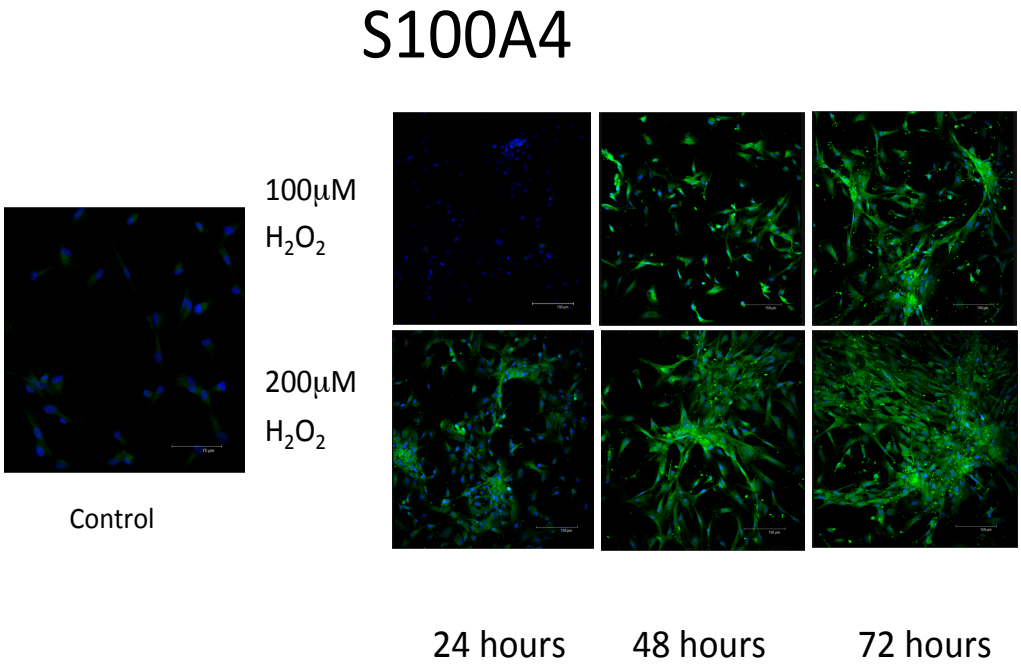

Figure 3.12 Expression of S100A4 by primary human BEC (representative images from 3 separate experiments). Cells were used at passage 3 or 4 for all experiments; the control shows expression of S100A4 (green) at passage 3, nuclei are stained with DAPI (blue). Cells at passage 3 or 4 were then treated with H_2O_2 at 100 / 200μM for 2 hours and incubated in fresh medium (EpiMed) for a further 24, 48 or 72 hours. There is a clear increase in S100A4 expression specifically at 48 and 72 hours for both concentrations of H_2O_2. A change in cell morphology can also be seen, shifting from cobblestoned at control to spindle or biphasic appearance at 48 and 72 hours.

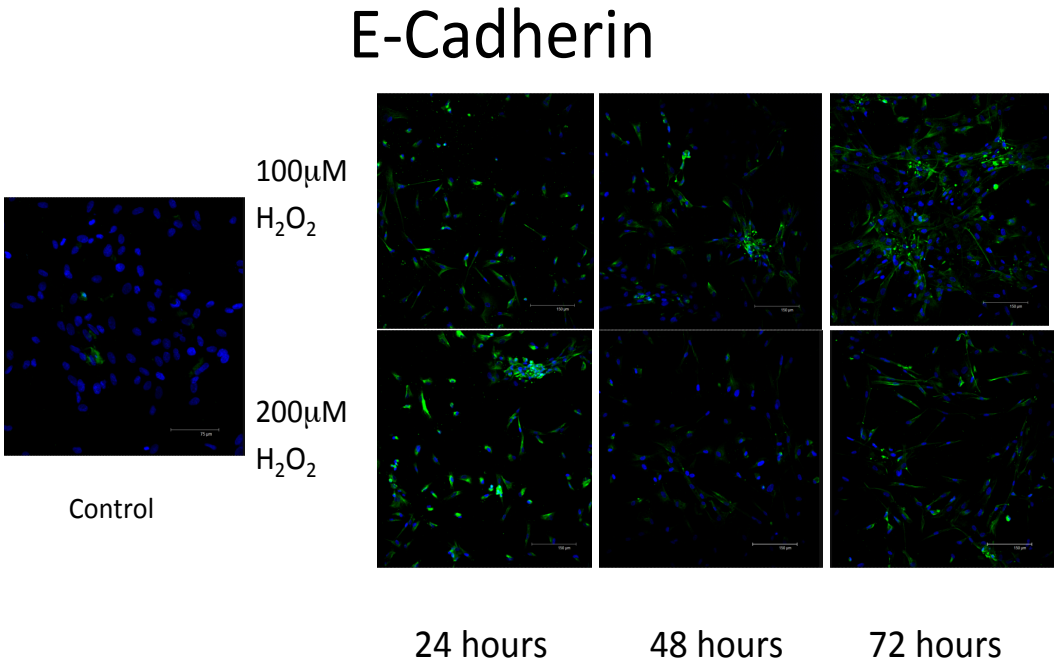

Figure 3.13 Expression of E-Cadherin by primary human BEC (representative images from 3 separate experiments). Cells were used at passage 3 or 4 for all experiments; the control shows expression of E-Cadherin (green) at passage 3, nuclei are stained with DAPI (blue). Cells at passage 3 or 4 were then treated with H_2O_2 at 100 or 200μM for 2 hours with incubation in fresh medium (EpiMed) for a further 24, 48 or 72 hours. There is a clear decrease in E-Cadherin expression specifically at 48 and 72 hours for both concentrations of H_2O_2.

3.3.4 Expression of p21 and TGF-β at mRNA level

As an apparent change in primary BEC protein expression had been observed, the decision was taken to investigate p21 mRNA expression and by doing so, to assess potential inducers of the observed EMT. Previous observers had noted an EMT in epithelial cells exposed to oxidative stress, however the factors influencing this process had not been described. To date, such an EMT had been induced *in vitro* (within the same timescale as that induced here by oxidative stress) by the addition of active TGF-β1. For this reason, it was decided that investigation of TGF-β isoform expression at mRNA level could be a useful method for identifying the cause of EMT following oxidative stress.

Previous data in this chapter have shown that protein expression of the studied antigen is maximal between 48 and 72 hours post H_2O_2 exposure. To allow for mRNA transcription and translation, primary BEC mRNA was obtained at baseline, 6, and 12 hours post H_2O_2 exposure. A sample amplification plot is shown in figure 3.15.

To maximise the potential of this approach, it was additionally conducted in immortalised BEC using a longer time scale, namely baseline, 4, 8, 12 and 24 hours after exposure. Results are shown in Figure 3.14 and show a clear up regulation of p21 at 48 and 72 hours. Interestingly, there was no change in TGF-β1 expression, there was however a marked change in TGF-β2 expression. The changes were seen in both primary and immortalised BEC, though a slight difference in the apparent kinetics of TGF-β subfamily expression was noted.

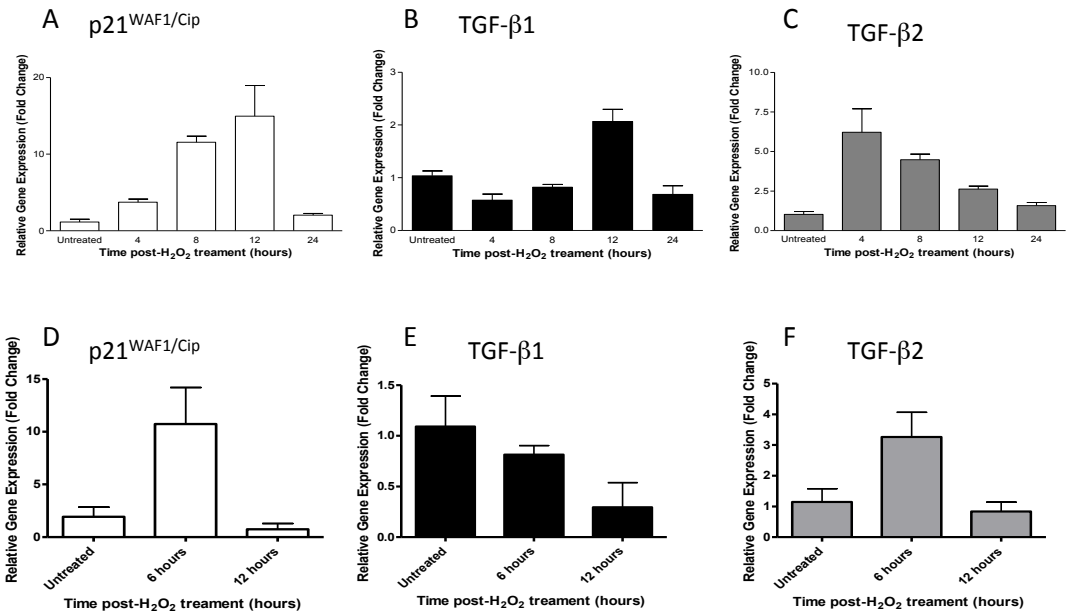

Figure 3.14: Real-time Polymerase Chain Reaction (qPCR) of immortalised and primary BEC. Graphs represent triplicate replicates of representative qPCR experiments. Panels A-C show mRNA expression in immortalised BEC post exposure to 200µM H_2O_2 at a number of time points. Panels D-F show mRNA expression in primary BEC post exposure to 200µM H_2O_2 at a number of time points. A one way ANOVA showed $p21^{WAF1/Cip}$ expression in immortalised BEC to be significant ($p < 0.001$) and in primary BEC ($p < 0.0285$), and showed TGF-β2 expression in immortalised BEC to be significant ($p < 0.001$) and in primary BEC ($p < 0.042$). Each experiment was repeated three times and results are representative.

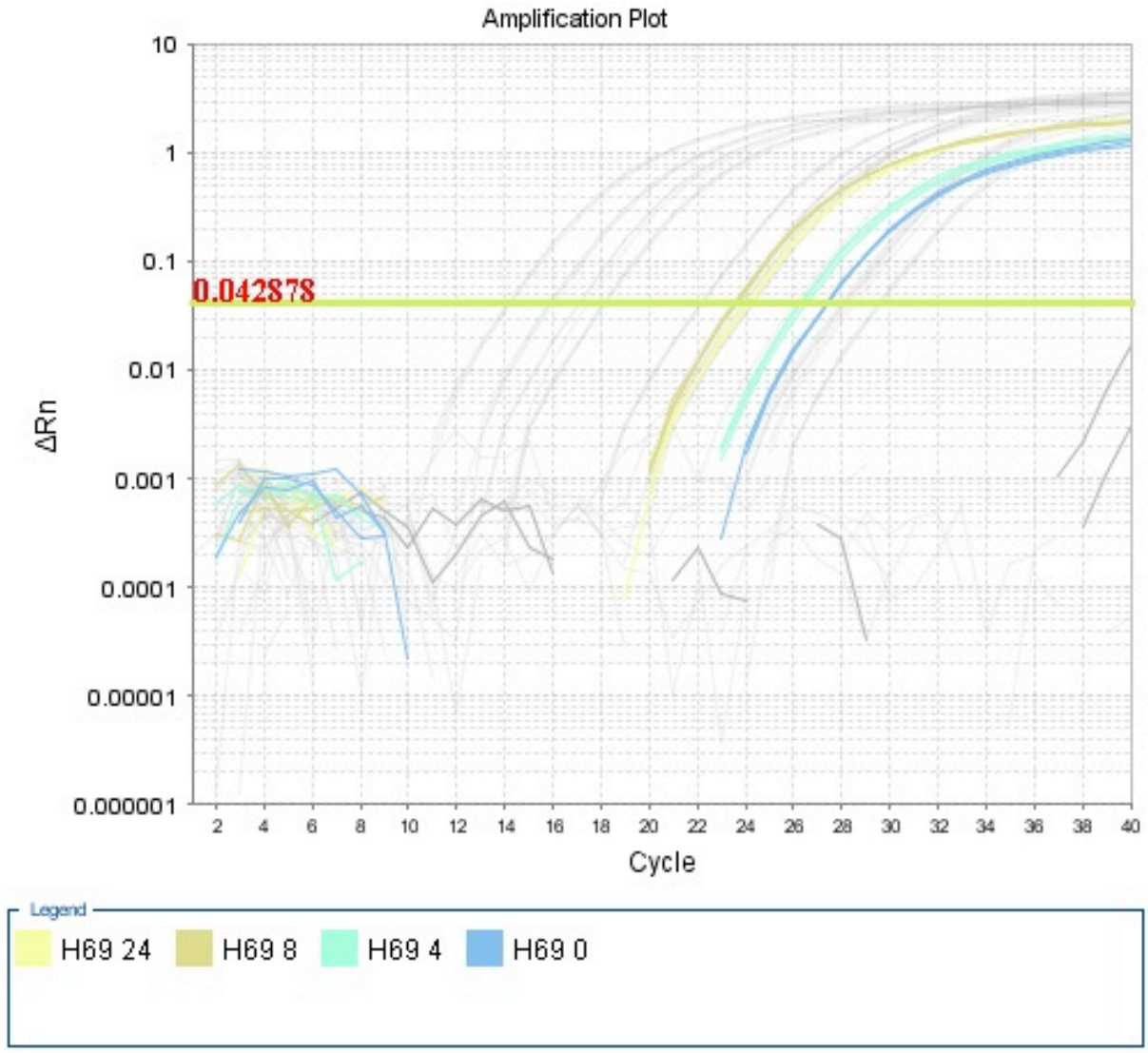

Figure 3.15 Amplification plot of immortalised BEC. A typical amplification plot from an RQ-PCR experiment is show with immortalised BEC labelled "H69". There is a shift towards lower Ct values (indicating earlier amplification and therefore more abundant cDNA) with increasing time following H_2O_2 exposure, with control labelled "H69 0" and 4, 8 and 24 hours post H_2O_2 exposure labelled "H69 4", "H69 8" and "H69 24".

3.4 Discussion

The first aim of this chapter – to identify the presence of senescent BEC in ACR of human liver allografts – was addressed by the use of triple colour immunohistochemistry. Results of the immunohistochemistry provided clear evidence of an association between a senescence marker in BEC and rejection grade that had not previously been described. Furthermore, the role of senescence in ACR was also demonstrated by the use of the Ki67 and γH2AX markers, in combination with and alongside p21 (Lawless, Wang et al. 2010). There were clear demonstrations of $Ki67^-$, $p21^+$ BEC associated with increasing Banff grade and $Ki67^-$ / $\gamma H2AX^+$ BEC associated with Banff grade. These findings allow the presence of early senescent BEC in ACR to be linked for the first time to the well-established phenomenon of morphologically senescent BEC in chronic ductopenic rejection. While this has not been previously described in the context of transplantation, there is a body of literature concerned with other vanishing bile duct syndromes (VBDS) (including PBC and PSC) that indicates a potential role for senescent BEC in the progression of disease (Sasaki, Ikeda et al. 2010, Chiba, Sasaki et al. 2011).

S100A4 expression was also studied in ACR biopsies; this has been used as a surrogate marker of EMT and has been extensively studied in cancer biology (Hemandas, Salto-Tellez et al. 2006, Saleem, Kweon et al. 2006, Ai, Lu et al. 2008, Sherbet 2009). As a cytoskeletal and calcium-binding protein, S100A4 confers motility to cells, thus indicating the presence of a mesenchymal phenotype. As well as being expressed as an early marker in EMT, S100A4 is also found in other motile cells, most notably macrophages and monocyte lineage cells (Dukhanina,

Lukyanova et al. 2008). In order to minimise the possibility of these cells being mistakenly counted, a separate stain was performed for T-cells, with infiltrating macrophages being excluded on the basis of morphology. Both p21 and S100A4 correlated strongly with Banff rejection grade (Fig. 3.2) in the biopsies, indicating the presence of BEC entering senescence, and an increase in EMT/cellular plasticity of BEC with increased rejection grade.

Surprisingly, no BEC stained positive for both p21 and S100A4 despite a statistically significant (Fig. 3.2) correlation between both markers. This could indicate a number of things, but most likely that p21 expressing cells, in this instance, were prevented from undergoing EMT. During staining for proliferation and senescence markers, in became evident that dividing ($Ki67^{+}$) BEC could express S100A4, even though these cells were fewer in number than Ki67- cells. There is a known association between Banff grade and proliferation of BEC (Kinnman, Francoz et al. 2003, van den Heuvel, de Jong et al. 2004), meaning it was necessary to demonstrate the presence of non-proliferating, $p21^{+}$ cells. It was also necessary to show whether non-proliferating cells were also capable of expressing S100A4. S100A4 has been described as a feature in the peri-biliary glands and has been described as a feature of proliferating BEC, in a study that observed abundant non-proliferating $S100A4^{+}$ BEC, indicating that S100A4 expression was indeed an indicator of mesenchymal phenotype (van den Heuvel, de Jong et al. 2004). No cells were shown to be positive for both S100A4 and p21, indicating that senescence and plasticity were separately linked to rejection grade. At the same time however this

indicated that the nature of the relationship between senescence and plasticity is not straightforward or step-wise.

ALD biopsies were stained and scored for p21 and S100A4 as a counterpoint to ACR. The contrast observed between these sections was very interesting. While there was a clear correlation between $p21^+$ BEC and fibrosis grade (Fig. 3.7), this was not seen between $S100A4^+$ BEC and fibrosis. This was not wholly unexpected. As described here previously (section 1.7), there are very different fibrosis patterns seen in VBDS (such as chronic allograft rejection) and toxic hepatocellular injury diseases (such as ALD). The effector cells in ALD are much more likely to be activated hepatic stellate cells (HSC), giving rise to peri-cellular and peri-venular fibrosis. This is in contrast to the predominantly portal fibrosis seen in biliary diseases where portal fibroblasts (and potentially myofibroblasts) derived from EMT/epithelial plasticity play a more significant role (Michalak, Rousselet et al. 2003). There is, however, a clear link between injury, fibrosis development and senescent BEC in both disease states, as well as and in other diseases as described by several authors (Lunz, Contrucci et al. 2001, Sasaki, Ikeda et al. 2005, Aravinthan, Scarpini et al. 2013). There were higher numbers of $S100A4^+$ BEC in the ALD series than in the ACR series. It may be that BEC plasticity in ALD is related to inflammation and/or disease activity, for example alcoholic steatohepatitis (ASH). Both ACR and ALD have inflammatory components and it may be that BEC plasticity is related to inflammation or to the presence of a local cytokine response.

Many factors contribute to the nature of liver injury in ALD, with a significant amount of toxic injury and oxidative stress that mostly occurs in hepatocytes

particularly in zone 3/perivenular areas. The timing and persistence of injury also differ, with transplant biopsies having a relatively short period of warm and then cold ischaemia, followed by reperfusion injury. ALD tends to have a more protracted course, with a variable amount and duration of injury, often over decades. Nevertheless, both forms of injury can ultimately lead to fibrosis.

The presence of senescent cells represents one part of a more complex picture. The well-described SASP has the potential to enhance the progression of disease due to its pro-inflammatory effects (Coppe, Desprez et al. 2011). Nakanuma et al (Harada and Nakanuma 2006, Sasaki, Ikeda et al. 2008) have shown the ability of senescent BEC to produce chemokines (e.g. monocyte chemoattractant protein, MCP-1) and cytokines (e.g. Interleukin-6, IL-6) and of these factors to induce the activation and migration of HSC. When using the same techniques as Nakanuma, it has been shown in the work described here that H_2O_2 exposure can induce transient p21 expression in BEC, and that these BEC undergo significant phenotypic and morphological changes. It was shown here that oxidative stress alone was able to induce an EMT-like phenomenon in primary human BEC. This was characterised by loss of key epithelial markers such as CK19 and CK7 and tight junction proteins such as E-Cadherin. There was also an up-regulation of mesenchymal markers such as S100A4, vimentin and αSMA. These findings indicate that while the injured cells would not be able to function as epithelial cells, they do at least have the ability to survive as mesenchymal cells.

There are significant limitations to these findings as they stand. Firstly, the correlation between senescent BEC and de-differentiating BEC in ACR biopsies was

only observational. This was aided partly by the development of an *in vitro* model using primary BEC, indicating that oxidative stress is able to induce not only senescence but also an EMT. The factors driving this EMT were not clear, neither was it possible to determine if the EMT was linked to senescence. In order to address these questions, expression of TGF-β family proteins in H_2O_2 treated cells was investigated. Alongside primary BEC, a cell line of immortalised normal human BEC was used and was exposed to H_2O_2 under the same conditions as the primary BEC. Interestingly, the expected rise in TGF-β1 was not seen, but rises in TGF-β2 and 3 were.

It has been shown in the senescence literature that there is a putative pathway linking p21 expression and the expression of TGF-β2 and TGF-β receptors (Passos, Nelson et al. 2010). This would be consistent with the hypothesis of senescent cells driving the EMT *in vitro*. In addition, similarities in mRNA expression provide initial validation for the use of a human cell line (rather than primary cells) as an *in vitro* model system. Assuming results were directly comparable, it was felt that a human cell line would have fewer limitations than primary cells. The primary cells used for these experiments were all obtained by digestion of explanted transplant tissue. In order to qualify, samples were taken from the liver of patients that had been suffering from end stage disease, and which was removed incurring significant ischaemia. Liver tissue was sliced and mechanically pulverised before being digested enzymatically and the final cells were extracted using magnetic beads. Due to the significant trauma and oxidative stress incurred during end stage liver disease and during the isolation process, these cells will vary considerably in their

phenotype, meaning that consistency can be a problem. Indeed, the most likely factor influencing these cells is the nature and extent of the primary disease that led to the transplant in the first place. There have been several studies looking at the effect of factors (such as chemotherapy) upon extracted primary cells (REF D Mann/Simon personal communication). Anecdotally, the type of response seen with such cells from different disease states differs markedly. A cell line-based *in vitro* system for assessing these phenomena is therefore warranted.

4 Translating to *in vitro*: studies of biliary injury in human cells and cell lines

4.1 Introduction

4.1.1 The merits of using a cell line model

The previous chapter demonstrates that observations from human biopsy material must be translated into a viable *in vitro* system for investigation and understanding of the processes underlying biliary epithelial cell (BEC) response to injury. Without such a reductionist approach, it would not be possible to prove / disprove experimental hypotheses or to test potential therapeutic interventions. The previous chapter also shows that primary human cells could be used to replicate the *in vivo* findings in human biopsy material, and therefore test the hypotheses arising from that work.

As a potential model system however, primary human cells do have a number of drawbacks. The cells are difficult to obtain, culture, and manipulate *in vitro*. They are inconsistent in their nature and behaviour and are subject to numerous uncontrollable variables - for example patient age, disease process in the organ of origin, drug exposure (e.g. platinum chemotherapy), or radiation. In addition, primary cells are only able to retain their characteristics for a limited number of passages, typically 5-6 in BEC (Bhogal, Hodson et al. , Leon, Kirby et al. 1995). This limits the number of cells that can be obtained from a single isolation. A normal yield from 30-40g of human liver is 1-2 million cells, which can only be expanded a limited number of times (Humphreys, Williams et al.). By contrast, an immortalised

cell line can in theory be passaged an unlimited number of times without losing its characteristics, although there are exceptions to this rule. For example the colonic cancer cell line Caco2 is limited to around 60 passages, after which its characteristic profile is lost.

Cells lines of human BEC are limited in number; many are cancer cell lines and therefore unsuitable for modelling benign disease. The options for a non-carcinoma human BEC line are very limited. Grubman (Grubman, Perrone et al. 1994) isolated a normal human cell line from a human liver resection and this method has been used within our group previously. This cell line would therefore be a candidate to replace primary BEC in modelling cellular injury *in vitro.*

4.1.2 Existing studies in vanishing bile duct syndromes

As mentioned previously, Yasuni Nakanuma's group have previously worked on vanishing bile duct syndromes (VBDS) using human sections, rodent models and rodent cell lines (Katayanagi, Kono et al. 1998, Sasaki, Ikeda et al. 2005, Sasaki, Ikeda et al. 2008). They have not, however, used a normal human BEC line. Chapter 3 shows that the p21 up-regulation noted by Nakanuma (Sasaki, Ikeda et al. 2006, Sasaki, Ikeda et al. 2010) was reproducible by another individual, using primary BEC. Based on the amount of available evidence, a logical progression of this work would be an attempt to replicate the findings in a human cell line. The cell line could then be validated against the findings demonstrated in chapter 3 as well as those of Nakanuma and others.

The senescence associated secretory phenotype (SASP) is particularly relevant to the model system described in chapter 3. Nakanuma et al (Sato, Harada et al. 2009, Sasaki, Miyakoshi et al. 2010, Harada, Chiba et al. 2011) have described relevant aspects in their work, but always in the context of pro-inflammatory factors (such as the chemokines monocyte chemoattractant protein, MCP-1 (CCL-2), or the cytokine Interleukin-6, IL-6), rather than pro-fibrotic factors that could drive an epithelial to mesenchymal transition (EMT). Given the oxidative stress-induced EMT observed in chapter 3, this may be an overlooked aspect of the SASP in VBDS and a potential area of experimental interest.

4.1.3 Oxidative stress

Oxidative stress is a feature of many disease states. It occurs when production of reactive oxygen species (ROS) outstrips the cell or tissue's ability to scavenge free radicals and is therefore dependent upon the number and type of ROS producers and the amount of scavengers (antioxidants) present (Arends, Slump et al. 2008, Sasaki, Ikeda et al. 2008, Gorowiec 2009, Rajawat, Hilioti et al. 2009). Specific to the current study, VBDS are immune-mediated diseases within which inflammatory processes such as the respiratory burst and increased metabolic activity generate increased amounts of ROS.

In the context of transplantation, ischaemia reperfusion injury (IRI) leads to mitochondrial-generated ROS in addition to that produced by the epithelial and endothelial cells (Pirenne, Gunson et al. 1997, Passos and Von Zglinicki 2006, Shaked, Ghobrial et al. 2009). In alcoholic liver disease (ALD), the toxic breakdown

products of ethanol induce ROS production (Holstege, Bedossa et al. 1994, Paradis, Scoazec et al. 1996, Raynard, Balian et al. 2002).

The prime source of free radicals during aerobic respiration and the subsequent senescence-mediated increased ROS production is the mitochondrion. More specifically, electron 'leakage' from mitochondria is capable of generating superoxide, which although short-lived is capable of generating further free radicals, and modification of molecules (such as lipid moieties) within the cell (Droge 2003, Kovacic and Pozos 2006, Aw 2012, Csiszar, Podlutsky et al. 2012, Zhou, Zong et al. 2012). In addition to the effects on lipids and proteins, ROS-mediated damage can lead directly to DNA damage, both within the mitochondria and the nucleus. By doing so, ROS may lead directly to cell cycle arrest, senescence, apoptosis or necrosis, depending on the nature and extent of damage to the DNA (Kovacic and Pozos 2006, Okamura and Himmelfarb 2009). Of course, inducing senescence further increases the amount of ROS generated (Passos, Saretzki et al. 2007).

Hydrogen peroxide (H_2O_2) persists for a much longer time period *in vivo* compared to superoxide (Passos and Von Zglinicki 2006) and has various functions, including as a signalling molecule. H_2O_2 can also be generated by the amine oxidase functions of adhesion molecules in inflammation (Weston and Adams).

4.1.4 Senescence

Cell senescence is defined as the irreversible loss of a cell's ability to divide and was classically described by Hayflick (Razin, Pfendt et al. 1977). The concept of

senescence has developed from the classical telomere-dependent replicative arrest to a more complicated phenomenon. It is now accepted that senescence can occur in the absence of telomere shortening, for example as the result of oncogene activation or due to cell damage and injury (Passos and von Zglinicki 2005, Passos, Saretzki et al. 2007). The markers for senescence are thus complicated to define and senescence may indeed be regarded as a reversible or an irreversible phenomenon (Lawless, Wang et al. 2010, Correia-Melo, Jurk et al. 2013). It is therefore most accurate to refer to predictors of senescence rather than to assign a definitive role to a certain marker / group of markers.

Cell senescence *in vivo* has been well described and is associated with specific morphological changes (Demetris, Adams et al. 2000, Lunz, Contrucci et al. 2001, Sebagh, Blakolmer et al. 2002, Demetris, Adeyi et al. 2006). Cells are noted to increase in size and to have a flatter morphology, with more variation in cell size and shape (Harada and Nakanuma 2006, Hubscher 2006). These features are readily discernible in cultured cells that are senescent.

4.1.5 Hepatocyte Growth Factor (HGF)

Hepatocyte Growth Factor (HGF) or scatter factor, as it is also known, is a well-known growth factor composed of an α chain, itself comprising an N-terminal domain and 4 kringle-like domains, and a β chain with a serine protease domain (Gherardi, Hartmann et al. 1997). During responses to liver injury, the stored form of HGF (the inactive precursor) is cleaved to form both the α and β chains, which are then linked by a disulphide bond. Endogenous HGF is a key mediator of regrowth and regeneration and has been shown to reverse fibrosis in rodent

models (Xia, Dai et al. 2006, Tojima, Kakizaki et al. 2011). HGF acts through the c-Met receptor, by inducing receptor phosphorylation which can then be used as a surrogate marker of activity (Hirono, Afford et al. 1995).

HGF is a large protein molecule and is therefore difficult to deliver and use *in vivo*. While much work has been performed investigating the potential of HGF to act in an anti-fibrotic and pro-regenerative capacity in animal models, it is not practical as a therapeutic agent as it would require administration by regular infusion, and delivery to specific organs is much more difficult. HGF activity is also increased upon the binding of glycosaminoglycans (GAGs), without which it has reduced signalling via c-Met (Youles, Holmes et al. 2008, Nakamura, Sakai et al. 2011, Ross, Gherardi et al. 2012).

1.1.1.1. Splice variants

Several biologically produced splice variants of HGF are described; the most significant being NK1 and NK2. These are composed of the N-terminal domain and either the first kringle domain (NK1) or first two kringle domains (NK2). These molecules both retain agonist activity towards c-Met and this binding is GAG dependent. An engineered form of NK1 has also been described (Ross, Gherardi et al. 2012) which contains the N-terminal and Kringle 1 domains and has a similar requirement for heparan sulphate proteoglycan binding to NK1, far more than full length HGF (HSPG, a specific GAG-containing molecule). It therefore has the potential to be developed as a therapeutic agent as it should be easier to deliver, and has a different specificity for GAG binding and possibly for sequestration into tissues.

4.1.6 Aims

Aims

- To assess the suitability of a cell line model of immortalised human BEC for the investigation of oxidative stress-induced senescence
- To further validate Nakanuma's oxidative stress modelling experiments
- To investigate the oxidative stress-mediated EMT observed in primary BEC and compare it to that in an immortalised BEC cell line
- To assess the ability of HGF and the engineered splice variant 1K1 to stimulate immortalised BEC

4.2 Specific Materials and Methods

4.2.1 Sircol Collagen assay

Media was harvested from T75 flasks of cells treated with H_2O_2 and stored at -80°C for subsequent analysis of collagen I-IV content by the "Sircol" collagen assay (Biocolor: # S1000) as indicated in the manufacturer's instructions. Sirius Red dye is known to bind to Gly-X-Y repeats (Ramshaw et al., 1998) present in the helixes of all acid soluble collagen subtypes (I-IV) This assay relies on the colourimetric detection of Sirius red bound to collagen in a concentration dependant manner. This is determined by references to a serially diluted standard curve prepared from 20μg/mL collagen I, diluted to a terminal concentration of 0.325μg/ml. Significance was then calculated using a one-way ANOVA.

4.2.2 Fluorescent in situ hybridisation

Fluorescent in situ hybridisation (FISH) was performed using commercially produced probes supplied by Creative Biolabs, NY, USA. The TGF-β2 probe used was produced using a proprietary sequence that was not divulged. The probes were used according to the manufacturer's instructions.

To minimise RNase activity, all solutions used were treated with DEPC and autoclaved. Formalin fixed paraffin embedded (FFPE) sections were de-waxed in Xylene for two periods of five minutes and rehydrated in ethanol solutions of 100%, 95% and 70% before rinsing in distilled water. Sections were microwaved at full power (850W) in 1mM EDTA solution for two periods of five minutes, before being allowed to cool for 10 minutes and then rinsed in running tap water. Two distilled water washes of five minutes were followed by pepsin digestion with 1mg/ml pepsin in 0.01M HCl at 37°C for 25 minutes. Sections were rinsed in distilled water before rehydrating in ethanol solutions of 70%, 95% and 100% before air drying.

Probes were diluted at 1:10 in Cytocell Hybridization Solution B (Labtech, East Sussex, UK) with 2.5μl added per section. Coverslips were applied and sealed with rubber cement. Once dry, the slides were placed in a HyBrite Hybridisation oven (Abbott Molecular, IL, USA) with a small amount of fluid as per the manufacturer's instructions. The programme used was for a 20 minute 80°C denaturation step followed by a 14 hour hybridisation step at 45°C. Once completed, rubber cement was removed with forceps and the sections were rinsed with 0.4% SSC buffer containing 0.3% NP40 at 72°C for two minutes and then again at room temperature. This was followed by two further washes in 2X SCC buffer, each for

two minutes. Sections were then mounted in Fluoromount containing DAPI (Sigma Aldrich) and imaged on a Leica TCS2 confocal microscope.

4.3 Results

4.3.1 Response of immortalised BEC to oxidative stress: senescence

In the first instance, immortalised BEC were grown in chamber slides until 90-95% confluent and then treated with two concentrations of H_2O_2 for two hours before removing the medium (see section 2.2 for constituents of medium), washing in PBS and adding fresh medium. The cells were then incubated for 24, 48, 72, 96 or 120 hours before fixation and staining. In order to be consistent with the work of Nakanuma (Sasaki, Ikeda et al. 2006, Sasaki, Ikeda et al. 2008, Sasaki, Ikeda et al. 2010) and the work described in Chapter 3, H_2O_2 was used at 200μM and all results in this chapter pertain to that concentration. The first antigen investigated was p21 and representative results are shown in Fig. 4.1 (the experiment was repeated more than 3 times with three to four technical replicates in each experiment). There was no evidence of p21 expression at baseline or at 24 hours post H_2O_2 exposure. The most marked up-regulation was at 48 hours post H_2O_2 exposure. There was still expression of p21 at 72 hours post H_2O_2 exposure, however when images of p21 immunofluorescence were viewed at higher power, it was evident that staining was cytoplasmic rather than nuclear. As only nuclear p21 is active (Erol), this was counted by hand using a single field from each of three replicates for

each time point. One-way ANOVA showed a statistically significant change in p21 expression ($p < 0.01$).

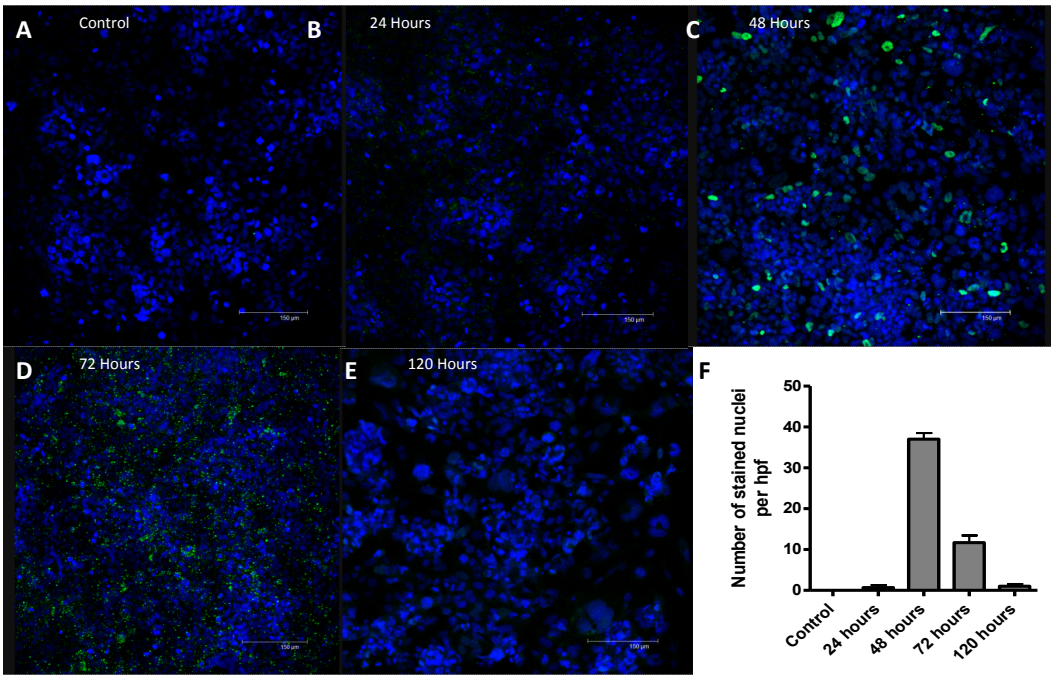

Figure 4.1 Confocal microscopy images (representative of more than 3 experiments with 3 technical replicates) of p21 expression in immortalised BEC. Nuclear positivity for p21 was counted per high power field (HPF) at each time point shown post exposure to H_2O_2. Cells were exposed to 200μM H_2O_2 for two hours, followed by washing in PBS and incubation in fresh medium for the indicated time. Little p21 expression was seen until 48 hours, when a notable population of $p21^+$ cells was observed (Panel C). As p21 was phosphorylated for translocation to the cytoplasm and breakdown, staining at 72 hours showed cytoplasmic p21 and very few positive nuclei (panel D). Nuclear counts are demonstrated in Panel F, with nuclei positive for p21 staining green. One-way ANOVA showed the change in p21 expression to be statistically significant ($p < 0.01$).

4.3.2 Do immortalised BEC respond to hydrogen peroxide with an EMT?

In chapter 3, primary BEC were shown to undergo a spontaneous EMT. Once it was established that an up-regulation of p21 occurs in response to oxidative stress in primary BEC, the next logical step was to identify whether immortalised BEC responded in a similar manner. Immortalised BEC were grown in chamber slides until 90-95% confluent and treated with 200μM H_2O_2 for two hours before removal of the medium, washing in PBS and addition of fresh medium (see section 2.2. for constituents of medium). This was followed by incubation for 24 -120 hours. Following incubation, cells were fixed, blocked and stained with antibodies (see section 2). Results are shown in Figures 4.2 and 4.4.

All experiments were repeated a minimum of three times with at least three technical replicates for each experiment; Figure 4.2 shows expression levels of S100A4, ZO-1 and αSMA in immortalised BEC following treatment with 200μM H_2O_2. There is a clear increase in the expression of the mesenchymal markers S100A4 and αSMA (S100A4 has a low baseline expression; and baseline expression is absent for αSMA. The epithelial marker ZO-1 showed high levels of expression at baseline, which rapidly fell away after H_2O_2 treatment. Of note, ZO-1 expression seemed to increase slightly at the 72-hour time point, and on closer examination it appeared that the staining is intracellular rather than of the cell membrane. This could indicate either breakdown or *de novo* production of ZO-1 within the cell.

Figure 4.3 shows densitometric analysis of the images from the S100A4, ZO-1 and αSMA staining following exposure to H_2O_2. All of the markers showed a statistically

significant change in expression (p = 0.0096, 0.0087 and 0.0068 respectively; values given by one-way ANOVA). Experiment reproducibility is demonstrated by the small error bars on the graphs, which represent the standard deviation (not the standard error). This experiment was repeated more than three times each with a minimum of three technical replicates, results are representative.

Figure 4.4 includes both the immunofluorescence and densitometry data for the expression of CK19 and E-Cadherin in immortalised BEC following exposure to H_2O_2. Cells were grown and treated as for the experiments in Figures 4.1 and 4.2. Time points of note in the assay were 48 and 72 hours after H_2O_2 exposure; these showed a clear drop in both of these epithelial markers. The drop in both CK19 and E-Cadherin expression was found to be statistically significant in a one-way ANOVA ($p < 0.0273$ and < 0.039 respectively). Most notable was the classical senescent morphology seen in Panel B where large, multi-nucleated flattened cells are clearly visible, and it is these cells that also seemed to be retaining CK19 expression.

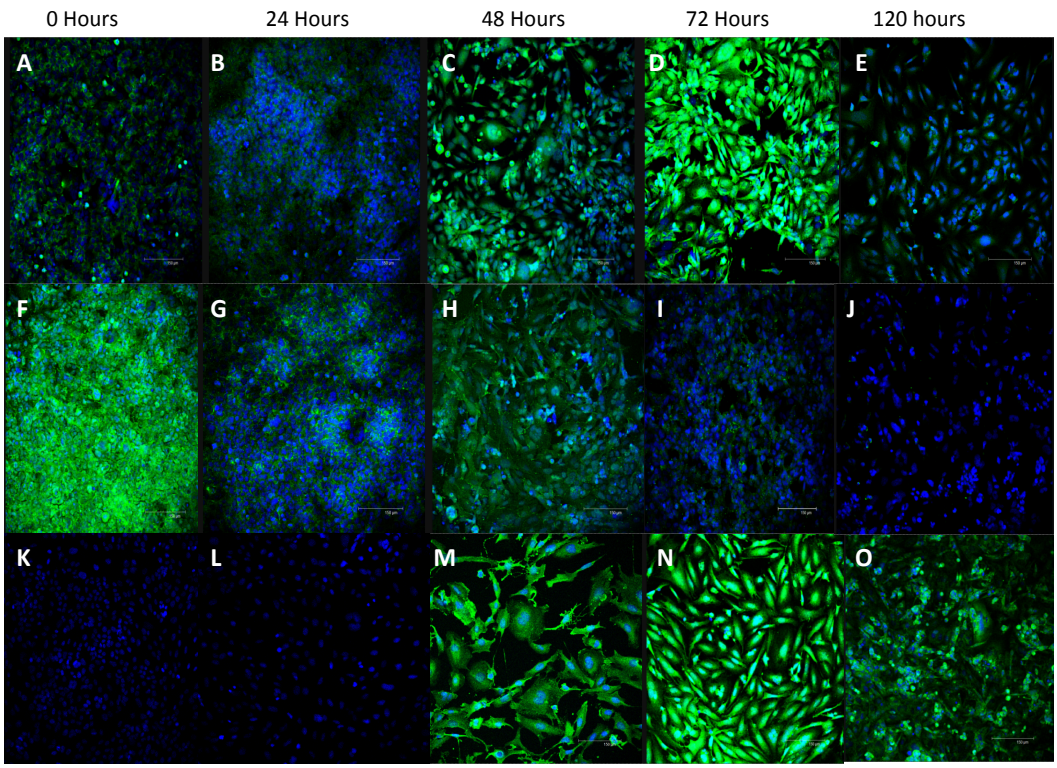

Figure 4.2: Confocal microscopy images of immortalised BEC exposed to H_2O_2 (200μM) for two hours, washed in PBS then incubated in fresh medium for the times indicated. The top row (Panels A-E) demonstrates S100A4 expression, which is present faintly at baseline before peaking at 72 hours before returning to baseline. The middle row (Panels F-J) shows ZO-1 expression which is high at baseline before falling rapidly and failing to recover by 120 hours. The bottom row (Panels K-O) shows αSMA expression which is entirely absent at baseline before peaking at 48-72 hours and regressing by 120 hours. Significant changes in cellular morphology are present and can be seen particularly in panels D, M and N. Images are representative of a minimum of three separate experiments with 3 technical replicates each.

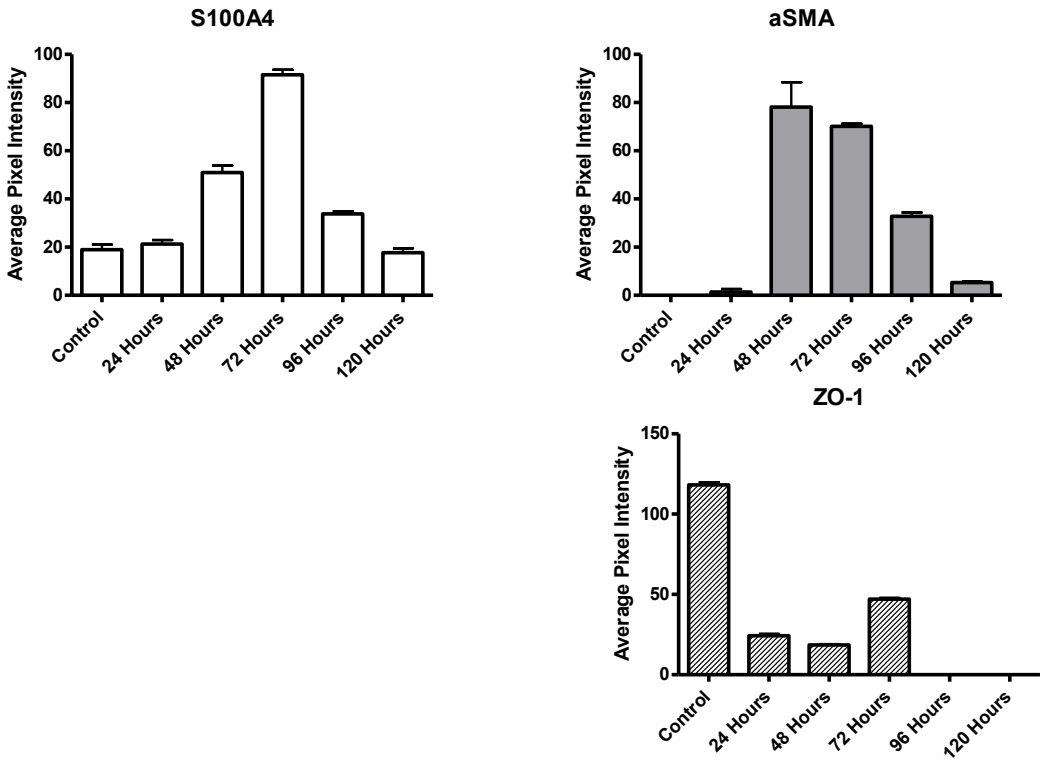

Figure 4.3: Densitometric analysis of confocal microscopy images of immortalised BEC exposed to H_2O_2. The average pixel intensity is displayed for triplicate measurements of each time point and antigen. One-way ANOVA test showed S100A4 expression to be significant ($p<0.0096$), likewise for αSMA ($p<0.0068$) and ZO-1 ($p< 0.0087$). Results are representative of three separate experiments each with a minimum of three technical replicates

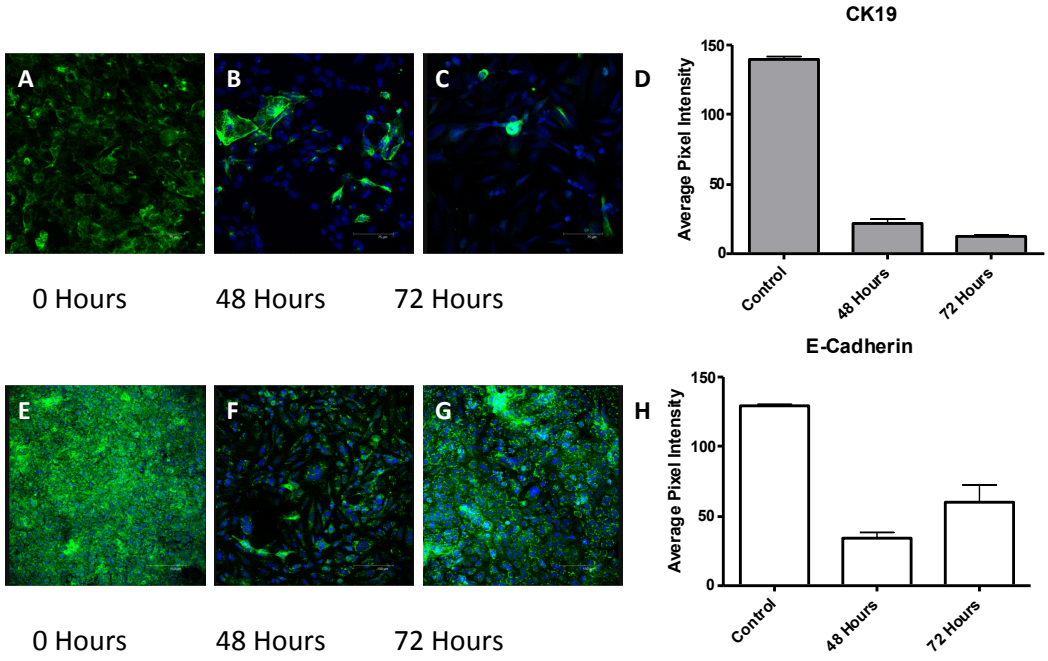

Figure 4.4: Expression of CK19 and E-Cadherin antigens by immortalised BEC. Confocal microscopy images are present for both antigens from baseline, 48 and 72 hours post H_2O_2 exposure, alongside densitometric analysis. Panels A-D show CK19 expression; a one-way ANOVA test showed CK19 expression to be significant ($p < 0.0273$). Panels E-H show E-Cadherin expression; a one-way ANOVA test showed E-Cadherin expression to be significant ($p < 0.039$). Figures are representative of a minimum of three experiments

4.3.3 Characterisation of the EMT observed in immortalised BEC

Once it had been established that immortalised BEC had the same phenotypic changes in response to oxidative stress as primary BEC, it was deemed important to further describe the phenotypic changes occurring within the observed EMT. While the change in epithelial and mesenchymal antigens had already been described in the immortalised BEC, the fundamental feature of myofibroblasts (namely the expression of extracellular matrix (ECM) components) had not. For this reason, immortalised BEC were grown and treated as in the previous experiments in this chapter, but stained for fibronectin, vimentin and collagen expression. Figure 4.5 shows the expression levels of vimentin (panels A-C) and fibronectin (Panels D-F). Densitometry data of these antigens is shown in panels I and H (respectively). A one-way ANOVA test showed fibronectin expression to be significant ($p<0.0241$); likewise for vimentin ($p< 0.0273$). For further verification of these results, a western blot for the presence of fibronectin on whole cell lysates of immortalised BEC was performed. Results are shown in panel G of Figure 4.5 and demonstrate a clear up-regulation of fibronectin expression following oxidative stress (indicated by an increase in the density and darkness of the bands).

A further western blot for vimentin was conducted on whole cell lysates of immortalised BEC, this was repeated more than three times and a representative result is shown in Figure 4.6. The blot appeared to show a change in the subtypes of vimentin being expressed, shown by the presence of different molecular weights in different proportions, at each time point. This could be due to non-specific binding, post-translational modification of the vimentin or another unidentified change. It is

clear however that there is a change in the vimentin expression but this does not readily relate to the changes observed on confocal microscopy.

Expression of collagen I is a fundamental step in organ fibrogenesis (Section 1.7) and may be the critical step in determining whether or not fibrosis will be resolved. The expression of collagen I by immortalised BEC was assessed by immunofluorescence at baseline, 48 and 72 hours after H_2O_2 exposure - results are shown in Figure 4.7. There was a substantial increase in collagen I expression between baseline and 72 hours. To corroborate this finding, the commercially available Sircol collagen assay kit was used (Figure 4.7). This also revealed a clear increase in the level of expression from baseline but little variation between time points (not significant, given by a one way ANOVA).

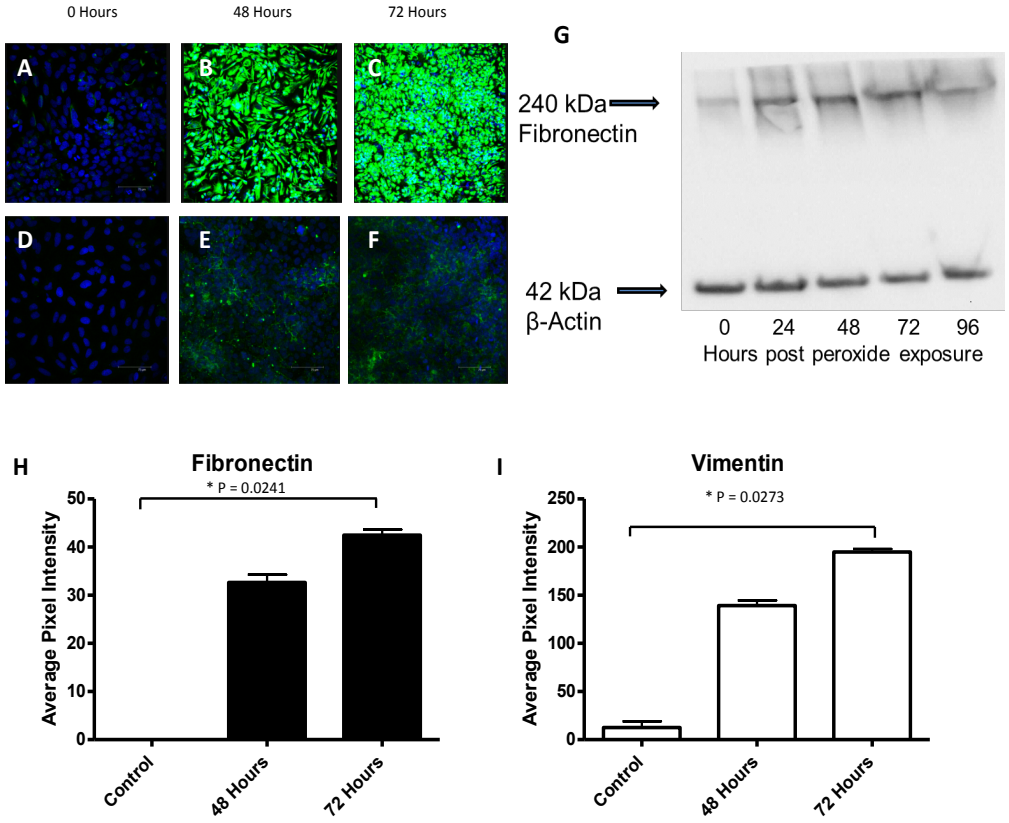

Figure 4.5: Expression of ECM components by immortalised BEC. Panels A-C show vimentin expression at baseline (A) versus 48 and 72 hours after H_2O_2 exposure (200μM for 2 hours). A one-way ANOVA showed that vimentin expression was statistically significant (p <0.0273). Panels D-F show fibronectin expression of BEC at baseline, 48 and 72 hours post H_2O_2 exposure. A representative Western blot for fibronectin expression was performed on whole cell lysates of immortalised BEC, and is shown in panel G. Densitometric analysis of the immunofluorescence data for fibronectin and vimentin is shown in panels H and I respectively. A one-way ANOVA showed that vimentin expression was statistically significant (p<0.0241). All data are representative of a minimum of three separate experiments.

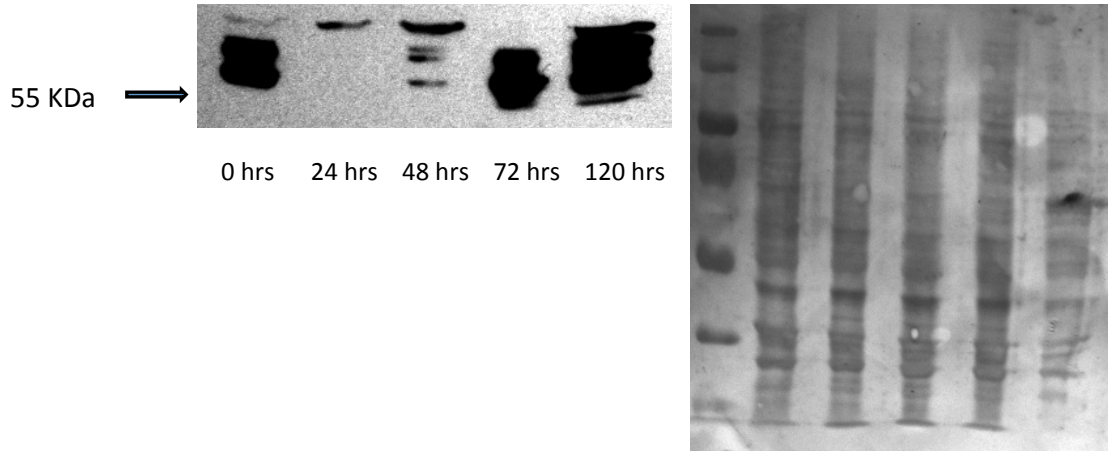

Figure. 4.6: A representative Western blot for vimentin expression on whole cell lysates of immortalised BEC exposed to H_2O_2. There is a clear shift in the molecular weight of bands observed. However there seemed to be no simple relationship between this and the vimentin expression observed by confocal microscopy.

A protein-loading control is shown on the right, this is an image of the entire membrane treated with copper solution, to show all protein present.

Collagen I expression

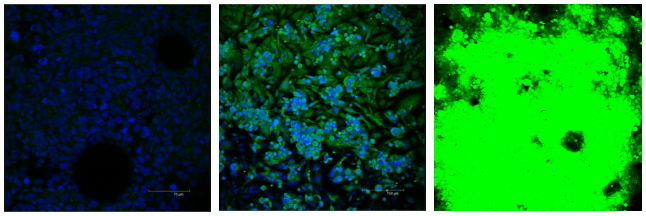

0 Hours 48 Hours 72 Hours

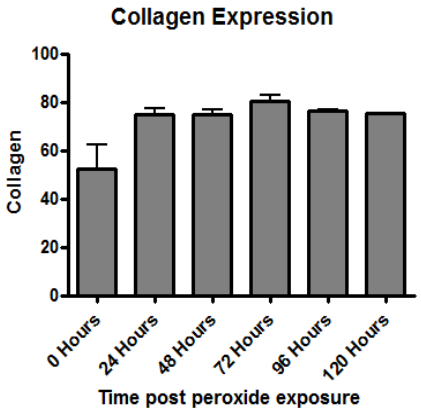

Figure: 4.7: Collagen I expression in H_2O_2 treated immortalised BEC. No evidence of collagen I expression was noted at baseline (Panel A) whereas expression was clearly up-regulated by 48 and 72 hours post H_2O_2 exposure (panels B and C). However colourimetric analysis by Sircol reagent assay (panel D) showed an increase in collagen I expression that was consistent in all treated groups, failing to reach statistical significance on a one-way ANOVA test. Figures are representative of at least three experiments.

4.3.4 Blockade of TGF-β signalling prevents oxidative stress-induced EMT

It was shown in chapter 3 (section 3.3.4) that both primary and immortalised BEC expressed increased amounts of TGF-β isoforms after exposure to H_2O_2. While this finding would be consistent with the observation of an EMT it does not conclusively prove that the EMT was driven by TGF-β or even that the mRNA was translated into protein. To ascertain whether the observed EMT was driven by TGF-β, the 72-hour incubation of immortalised BEC with 200μM H_2O_2 was re-run, with staining for αSMA, S100A4 and ZO-1. A further group was pre-treated by incubation with 1μM of SB-505124 for 1 hour before treatment with H_2O_2 and incubation for 72 hours. Results are shown in Figure 4.8. SB-505124 is a specific inhibitor of the ALK-5 TGF-β receptor type 1. Inhibition of this receptor prevents TGF-β from signalling via the canonical SMAD pathway and therefore prevents any of the downstream signalling that might be expected of a TGF-β mediated process.

There was a clear prevention of the previously observed EMT. Panels A-C (-SB-505124) show the expected changes in expression of the antigens in response to oxidative stress; panels D-F (+SB-505124) show retention of the expected epithelial morphology with prevention of the expression of the mesenchymal antigens S100A4 and αSMA.

Fig. 4.9 shows densitometric analysis of both H_2O_2 treated cells and cells treated with SB-505124 for one hour before incubation with H_2O_2. A two-way ANOVA test was performed on the results and showed that changes in marker expression were

significant ($p<0.0001$) with the significance attributable to the treatment difference between the groups (i.e. the absence or presence of SB-505124).

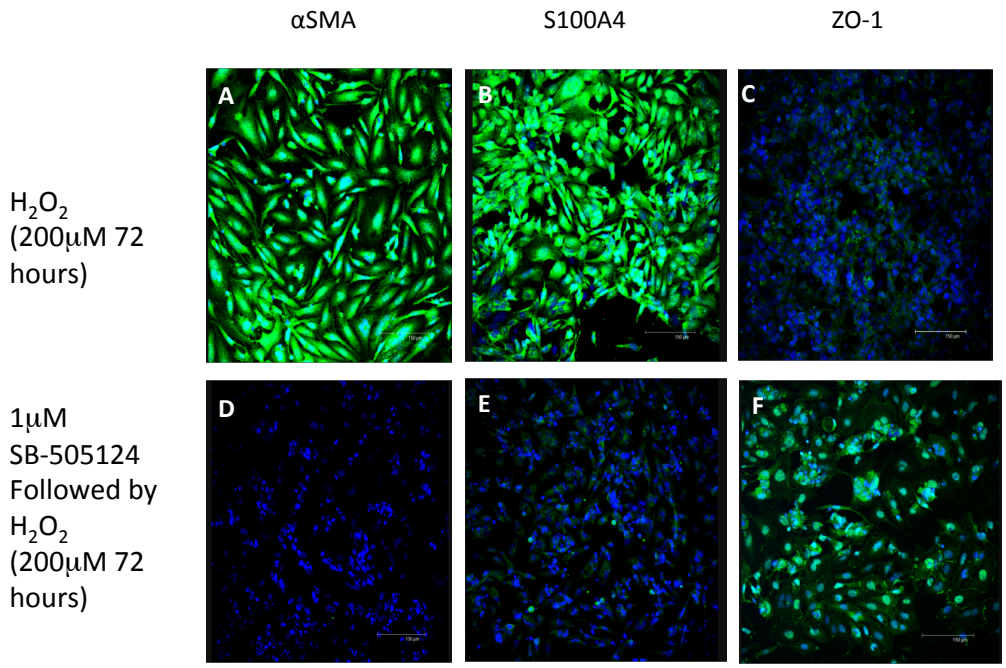

Figure 4.8:Blockade of TGF-β signalling blocks H_2O_2 induced EMT of immortalised BEC. Panels A-C show expression of αSMA, S100A4 and ZO-1 72 hours after exposure to H_2O_2. Panels D-F show αSMA, S100A4 and ZO-1 expression in BEC pre-treated with the ALK-5 inhibitor SB-505124 prior to H_2O_2 exposure followed by incubation for 72 hours. The observed EMT in immortalised BEC is clearly inhibited by inhibition of the TGF-β signalling pathway, preventing the expression of αSMA, retaining ZO-1 expression and reducing S100A4 expression levels to below baseline. Figures representative of three separate experiments.

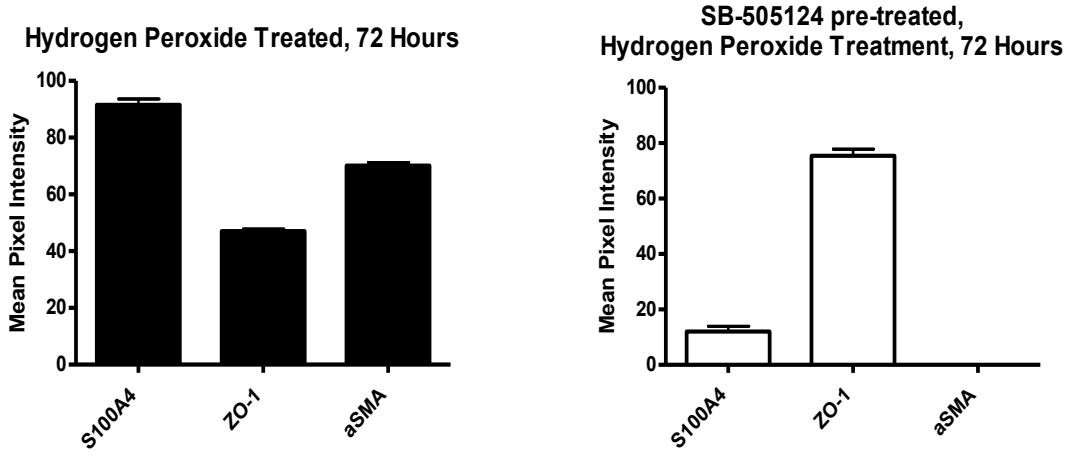

Figure 4.9: Densitometric analysis of immortalised BEC treated with H_2O_2 and incubated for 72 hours + / - the ALK-5 inhibitor SB505124. The cells pre-treated with SB-505124 show retention of ZO-1 and marked prevention of the up-regulation of S100A4 and αSMA seen in the H_2O_2 only treated group. A two-way ANOVA test showed the changes in marker expression to be statistically significant ($p < 0.0001$) with the significance attributable to the treatment difference between the groups (i.e. the absence or presence of SB-505124).

Results shown in Figures 4.8 and 4.9 clearly show that the presence / absence of TGF-β signalling is of fundamental importance in the production of an oxidative stress-induced EMT. Evidence from chapter 3 and from relevant literature (Passos, Nelson et al. 2010, Brain, Robertson et al. 2013) indicate that the molecule responsible for driving the oxidative stress/senescence dependent EMT forward may not be the classical candidate, namely TGF-β1. In order to identify the driver of the observed EMT, culture medium from three experiments (immortalised BEC treated with 200μM H_2O_2) was taken, treated with HCl (0.3M for 15 minutes with neutralisation by 0.3M NaCl) to remove latency associated peptide (LAP), and assayed for TGF-β1 and 2 using Enzyme Linked Immunosorbent Assay (ELISA) (R&D systems Quantikine ELISA kit). The results are shown in Fig. 4.10. In line with the previous real-time polymerase chain reaction (qPCR) results and with the putative pathway described by Passos (Passos, Nelson et al. 2010) the level of TGF-β1 did not rise, instead it fell at both 24 and 72 hours. However, the TGF-β2 level rose by almost four-fold, peaking at 96 hours.

To investigate further the effect of ALK-5 inhibition upon BEC exposed to H_2O_2, qPCR experiments were conducted on BEC mRNA, + / - SB-505124 at 6 and 24 hours. These experiments were conducted by Dr Kashif Ashgar, supervised by Dr John Brain. Results are shown in Figure 4.11. The baseline qPCR results for the H_2O_2 treated BEC are very similar to those shown in Fig. 3.14, indicating that this was a reproducible finding. The response at 6 hours in the presence of SB-505124 shows a reduction in p21 and TGF-β2 expression, with a small increase in TGF-β1. By 24 hours, both p21 and TGF-β1 expression had been suppressed and there was a huge

increase in TGF-β2 levels, to about 10 times the level seen at 24 hours in the absence of SB-505124. This would indicate the absence of a dampening signal from the TGF-β2 through ALK-5.

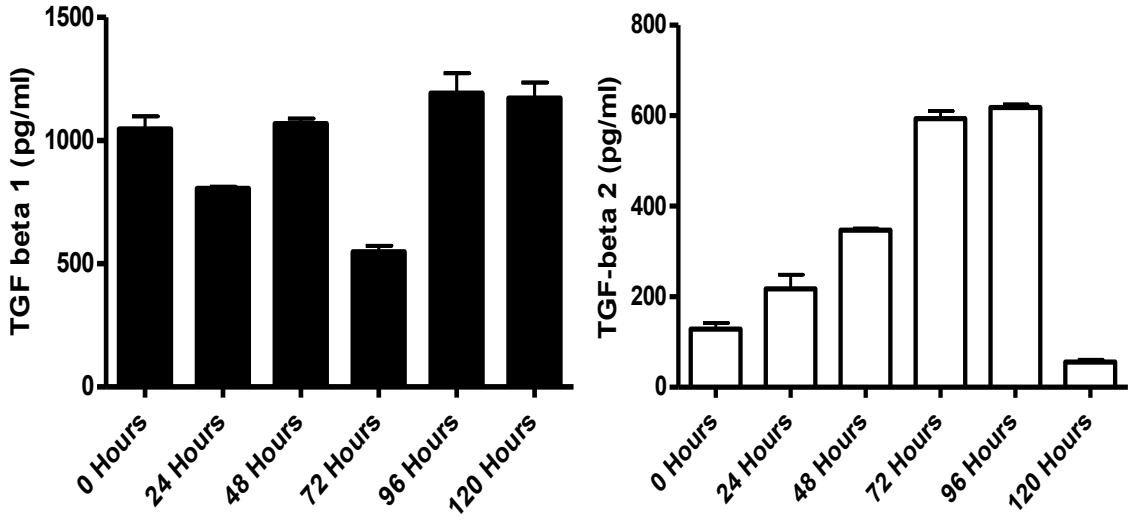

Figure 4.10: Results from ELISAs showing TGF-β1 and TGF-β2 levels in supernatant from H_2O_2 treated BEC. Supernatant was treated with HCl then neutralised to allow calculation of total TGF levels. Aside from a slight decrease at 72 hours, TGF-β1 levels were remarkably consistent. TGF-β2 levels were present at low levels from baseline but showed a four-fold increase from 72 hours. This increase was shown in a one-way ANOVA test to be significant ($p < 0.0058$) and was sustained until 96 hours before falling to levels below baseline. Results are representative of supernatant from three separate experiments and run in triplicate.

RQ-PCR

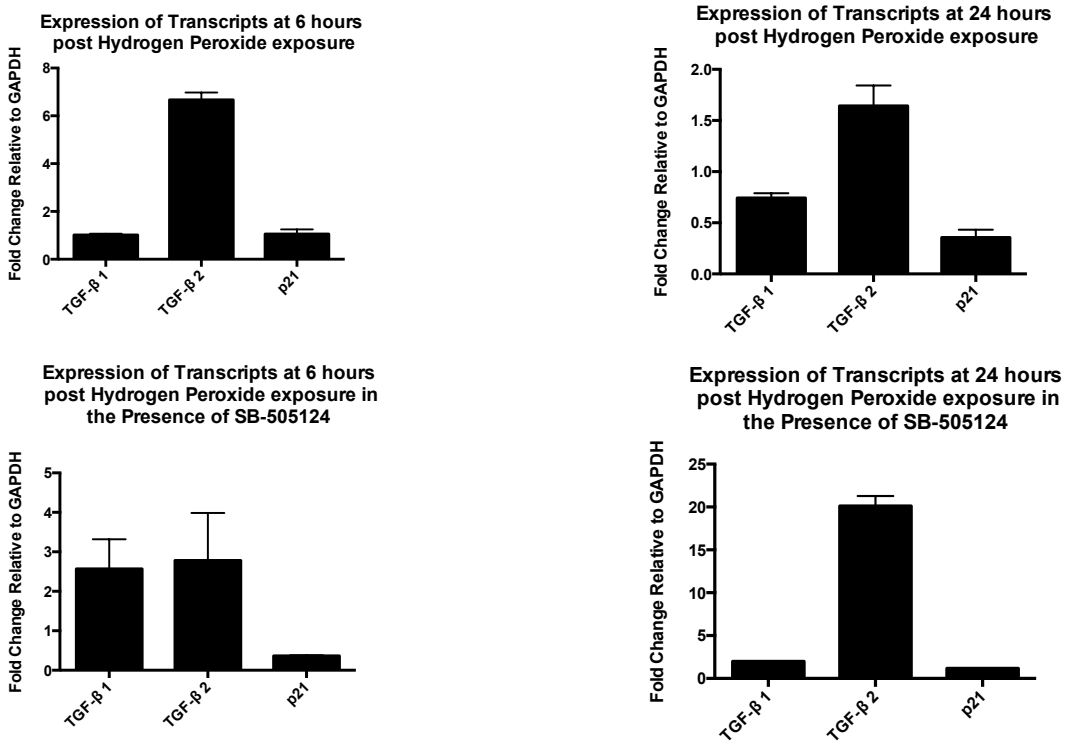

Figure 4.11: qPCR expression of mRNA obtained from H_2O_2 treated immortalised BEC + / - TGF-β receptor inhibitor (SB-505124). Cells were either treated with 200μM H_2O_2 for two hours then incubated for 6 / 24 hours (top row), or were pre-treated with SB-505124 at 1μM for one hour before being treated with H_2O_2 for two hours then incubated for 6 / 24 hours (bottom row). The profile of BEC that were not pre-treated with SB-505124 was found to be very similar to the profile shown in Fig. 3.14. In the presence of SB-505124, there is a reduction in p21 and TGF-β2 expression and a small increase in TGF-β1. By 24 hours both p21 and TGF-β1 levels are back to baseline, whereas TGF-β2 has increased dramatically. These data are grouped from three separate experiments each with three technical replicates.

4.3.5 Can HGF-related compounds activate c-Met in immortalised BEC?

It has been previously described that hepatocyte growth factor (HGF) can prevent a TGF-β1 induced EMT in BEC (Rygiel, Robertson et al. 2008). Having established that the oxidative stress/senescence-induced EMT observed in immortalised BEC was driven by TGF-β, it was deemed logical to consider which factors could potentially be utilised therapeutically, for retaining epithelial function in the presence of oxidative stress, for example in vanishing bile duct syndromes (VBDS). While it is not realistic to develop HGF itself therapeutically, this may be possible with its derivatives and splice variants as they are easier to produce, are potentially more stable and would be easier to administer. Testing such compounds *in vitro* prior to *in vivo* testing should identify their efficacy and potential for development in a logical manner.

Binding of HGF and many of its splice variants to the c-Met receptor is dependent upon proteoglycans (e.g. HSPG Section 1.10.6)(Ali, Hardy et al. 2003, Johnson, Proudfoot et al. 2005). In order to determine the potential for assessing HGF and the engineered HGF related compound 1K1 in the oxidative stress assay of immortalised BEC, both HGF and 1K1 were added at concentrations between 0 and 4.1nM to immortalised BEC in a R&D systems whole cell based ELISA for c-Met activity. Samples were incubated at 37˚C for 60 minutes before the reaction was stopped and developed. The ratio of phosphorylated to unphosphorylated c-Met was shown given by the two colours produced in the assay. Once the baseline reading from the plate was subtracted, the ratio for each group was calculated - this is shown in Figure 4.12. The optimum concentration of HGF stimulation of BEC

in this assay was 41μM and for 1K1 around 0.46nM (equal to approximately 10ng/ml in both cases). Interestingly, while the stimulation of BEC by HGF was clearly decreasing towards the lower concentrations in the assay; this was not clearly the case with 1K1. Therefore this assay was repeated at lower concentrations, shown in Figure 4.13.

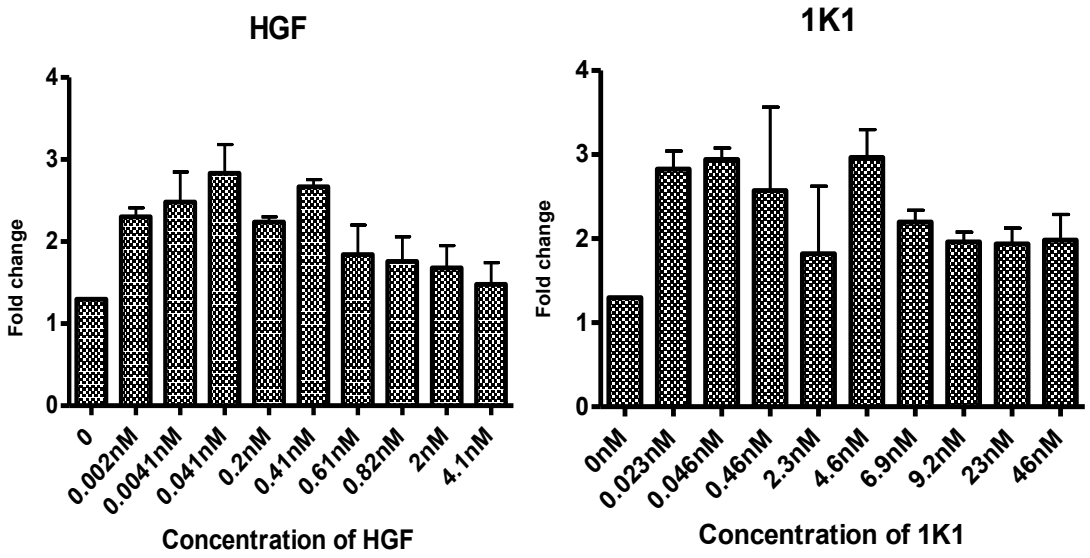

Figure 4.12: Whole Cell ELISA showing phosphorylated C-Met expression in immortalised BEC following exposure to either 1K1 or HGF. Both graphs show the fold change of phosphorylated c-Met relative to un-phosphorylated c-Met. BEC were seeded in a 96 well plate and incubated overnight at 37 ˚C in 5% CO_2. Three wells were then incubated with the concentrations of HGF or 1K1 shown above for 60 minutes before reactions were terminated and then developed according to the manufacturer's instructions. Data shown represents a representative experiment of three, all with three technical replicates.

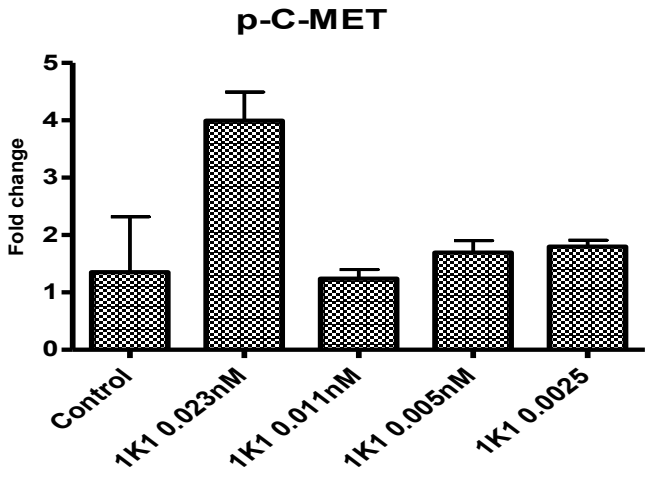

Figure 4.13 Whole cell ELISA showing phosphorylated C-Met expression in immortalised BEC following exposure to 1K1. The previous experiment (see Fig. 4.12) only demonstrated 1K1 activity at the lowest concentration tested (0.023nM). A further experiment was therefore conducted to determine the lowest concentration with 1K1 activity in immortalised BEC. As can be seen, there is activity at half (0.011nM) the previous concentration but lower concentrations elicit virtually no response. These data are 1 representative experiment of a total of three experiments.

4.3.6 Can HGF and its' derivatives alter signalling via the canonical TGF-β pathway

In order to further investigate the signalling characteristics of both HGF and the 1K1 derivative, further whole cell ELISA assays were performed on immortalised BEC. The known TGF-β canonical SMAD pathway was assessed using the readout from phosphorylated SMAD 2/3, as this is phosphorylated within minutes of TGF-β receptor activation. The MAP kinase family members, extracellular signal regulated kinase (ERK) 1 and 2, are known to be activated (by phosphorylation) downstream of HGF/c-Met activation and were therefore also chosen as an indicator of c-Met downstream signalling.

Conversion of the concentrations of HGF and 1K1 from section 4.3.5 revealed maximum activity of both compounds at around 10ng/ml and concentrations are shown in this format. It should be remembered that HGF is around 20 times larger than 1K1 (in terms of molecular weight) and therefore around 20 times more potent as an agonist. As well as the optimal concentration of 10ng/ml, a larger concentration (50ng/ml) was also chosen for both compounds and incubations of 30 and 60 minutes were performed. Results are shown in Fig. 4.14.

Activation of ERK was observed in the presence of both HGF and 1K1. No significant difference was found between the 30 and 60 minute time points. For both compounds, the anticipated difference between concentration of the compounds was seen – the strongest ERK activation was observed at 10ng/ml, with less activation seen at the higher strength (50ng/ml). HGF showed a higher total ERK

activation at each concentration, with around 30% more ERK phosphorylation evident. Both 1K1 and HGF caused a significant reduction in phosphorylation of SMAD2/3, with 1K1 causing a greater decrease.

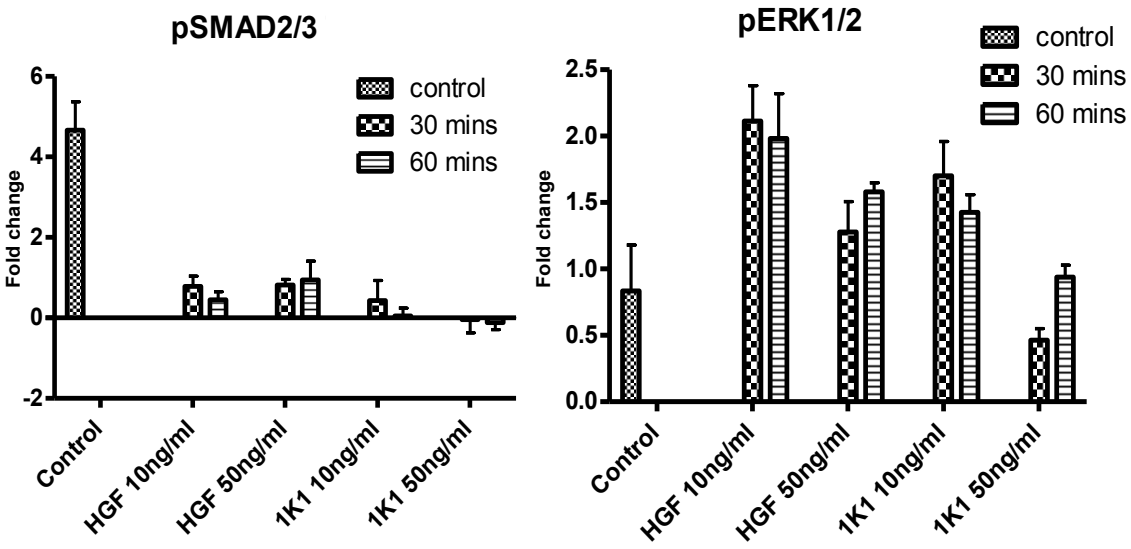

Figure 4.14: Whole cell ELISA showing phosphorylation of ERK1/2 and SMAD 2/3 following exposure of BEC to HGF or 1K1. For these assays immortalised BEC were plated out (96 well plates) and incubated overnight at 37 ˚C in 5% CO_2. Cells were then treated with either 10ng/ml or 50ng/ml of HGF/1K1 for either 30 or 60 minutes before reactions were terminated and the plate developed according to the manufacturer's instructions. Phosphorylation of SMAD 2/3 was shown to be rapidly down regulated by both 1K1 and HGF, this effect being more marked with 1K1. Phosphorylation of ERK 1/2 was shown to be up-regulated in response to both HGF and 1K1 with evidence of HGF having a slightly more pronounced effect. These data represent one of three experiments, conducted in triplicate

4.3.7 Fluorescence in situ hybridisation provides evidence of TGF-β2 in human ACR biopsies

Sections from patients with biopsy proven ACR in liver allografts were obtained and subjected to fluorescent in situ hybridisation (FISH) analysis using commercial probes against TGF-β2 (described in section 4.2.2). Results are shown in Fig. 4.15. The purpose of this was to further validate the emerging hypothesis that oxidative stress/senescence of BEC in VBDS could not only drive forward a pro-inflammatory immune response (Sasaki, Miyakoshi et al. 2010); but could also potentially drive fibrosis and act as an immune modulator via TGF-β2. Some low level staining of TGF-β2 is shown in Fig. 4.15, however this was variable in nature and was not seen in all biopsies. Arising from this observation, a student co-supervised by JGB investigated mRNA transcript loss during the process of formalin fixing and subsequent paraffin embedding, demonstrating a sequence dependent loss of TGF-β2 transcripts when isolated from FFPE tissue and analysed by qPCR. This would explain, at least in part, why mRNA specific for TGF-β2 is difficult to identify in FFPE tissue. This work was published recently (Thompson, Burt et al. 2013).

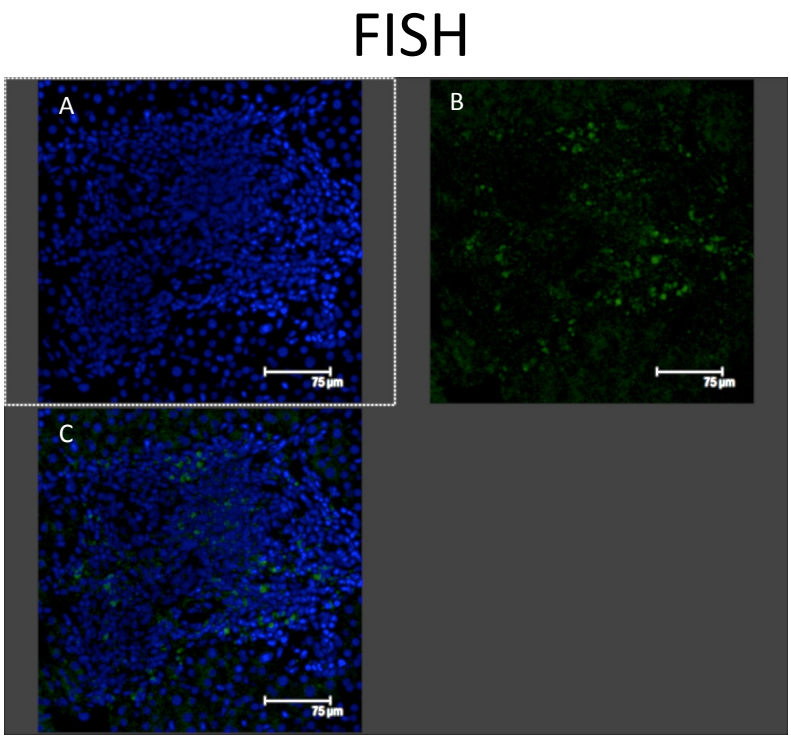

Figure 4.15: FISH of TGF-β2 in human acute cellular rejection (ACR) liver allograft biopsies. Commercial FISH probes for TGF-β2 mRNA were used on sections from human liver allografts with biopsy proven ACR. Panel A is the combined image of both the DAPI (blue nuclear stain) and FISH probes (green). Panel B is the separated green FISH channel and Panel C the separated blue DAPI channel. Staining was apparent and is visualised in green with the nuclear DAPI stain visible in blue. Staining is quite faint and must be viewed on the separate channel rather than the combined image. Evidence of positivity for TGF-β2 mRNA was seen within BEC and peri-portal hepatocytes. This experiment was conducted on sections from a total of 10 cases in 2 separate batches. The demonstrated data is representative.

4.4 Discussion

4.4.1 Aim 1: To assess the suitability of a cell line model of immortalised human BEC for the investigation of oxidative stress-induced senescence

This chapter aimed to appraise the use of a cell line model rather than primary cells for investigating oxidative stress mediated senescence in BEC. It was shown that immortalised BEC had a similar response to primary BEC when treated with H_2O_2. The most notable difference observed between primary and immortalised BEC was the kinetics of p21 up-regulation. In the primary cells, up-regulation was evident by 72 hours and rapidly fell back to baseline; this was consistent with the reports of Nakanuma (Sasaki, Ikeda et al. 2005, Sasaki, Ikeda et al. 2006). With the immortalised cells, there was a more rapid up-regulation at 48 hours but this was followed by a rapid down-regulation by 72 hours; this difference in kinetics may be explained by the effects of the immortalisation process.

The immortalised cell line of BEC used was produced in 1994 by Grubman et al (Grubman, Perrone et al. 1994). Cells were isolated from a section of normal liver and immortalised using the SV40 large T-cell antigen. This antigen interferes with cell cycle regulation by stabilising p53 levels as well as levels of retinoblastoma protein and the interaction between p300 and E2F1. This prevents up-regulation of p21 due to normal cell cycle progression, so that any p21 up-regulation observed is due to DNA damage (Ali and DeCaprio 2001). This has several advantages as an experimental model. It is easier to ascertain in the immortalised cells whether the p21 up-regulation is due to cell cycle changes or due to the effects of DNA damage.

It does however mean that the kinetics of the p21 up-regulation are not identical to that observed in primary cells. It has though been conclusively shown that the phenotypic changes of both primary and immortalised cells when exposed to 200μM H_2O_2 are very similar, if not identical. While this is close enough for a single insult model such as the one under test, further investigation would be required to ascertain whether the immortalised BEC could be used in a chronic disease model. With this in mind, the cell line used can be considered close enough to primary BEC to use as a substitute model.

4.4.2 Aim 2: To further validate Nakanuma's oxidative stress modelling experiments

Validation of the p21 up-regulation in primary cells seen by Nakanuma's group was described in chapter 3. p21 up-regulation observed in immortalised BEC was very similar to that seen in primary cells, with the response occurring over a shorter time period. The phenotypic changes observed in immortalised BEC were almost identical to those seen in primary cells. The response of both types of cell to the same dose of H_2O_2 was also comparable, in terms of both the quantity and quality of antigen expression change.

The work of Nakanuma et al (Sasaki, Ikeda et al. 2008) has focused upon the pro-inflammatory aspects of the SASP alongside the expression of senescence markers in BEC that were either in vivo as FFPE tissue blocks or cultured rodent cells. The validation carried out in this work has investigated the application of oxidative stress to human BEC with the associated increase in senescence markers. Rather than repeat the experiments of Nakanuma verbatim in human cells it was decided

to investigate other aspects of the SASP and their potential relevance to disease progression. Therefore the recapitulation of Nakanuma's work was completed in this context.

4.4.3 Aim 3: To investigate the oxidative stress-mediated EMT observed in primary BEC and compare it to that in an immortalised BEC cell line

As noted in section 3.3.3, primary BEC underwent an epithelial to mesenchymal transition (EMT) in response to oxidative stress. This was not entirely unexpected as oxidative stress has been described to induce EMT in several epithelial cell types (Cannito, Novo et al. , Rhyu, Yang et al. 2005). The change in markers was shown in section 3.3.3 and indicated a significant shift from epithelial cell expression of CK7, E-CAD, CK19 to a more mesenchymal panel of markers, such as αSMA, S100A4 and Vimentin.

The application of oxidative stress to immortalised BEC elicited a frank EMT. The expression of epithelial markers decreased over the same time course as seen in primary cells. In addition the expression of mesenchymal markers also followed the same kinetics as seen in primary cells. The expression of markers was much more consistent with the immortalised BEC, this may have been due to several factors. The cell population were originally derived from a single donor, which may explain some of the consistency. Not being grown on a collagen matrix is also likely to have made a significant difference, the consistency of the matrix applied to the cell can influence whether cells are protected or induced to undergo EMT (Cannito, Novo et al. , Thiery, Acloque et al. 2009).

Unequivocally the consistency of such a cell line in an experimental model is valuable. The results obtained matched the results obtained with primary cells but with fewer culture requirements. The immortalised BEC also allow a consistent platform for the assessment of modulation of any of the processes that may influence senescence and EMT, such as inhibiting TGF-b or Autophagy, which will be discussed in chapter 5.

4.4.4 Aim 4: To assess the ability of HGF and the engineered splice variant 1K1 to stimulate immortalised BEC

Having established that immortalised BEC react consistently under culture conditions to oxidative stress in a similar way to primary BEC, the next aim was to assess whether the HGF receptor c-Met was present on immortalised BEC and whether it operated in a functional way. It has been reported previously that treatment with HGF is able to prevent a TGF-β1 mediated EMT in biliary cells (Rygiel, Robertson et al. 2008). This is dependent upon both the presence of the c-Met receptor and the correct GAGs being present in the assay system. Previous use of HGF *in vitro* has revealed the need to add HSPG in order to facilitate HGF/c-Met binding (Ross, Gherardi et al. 2012). To assess whether the cell surface of immortalised BEC contained sufficient HSPG to allow HGF binding, a whole cell ELISA was used. Cells were treated in a 96 well plate with various concentrations of either HGF or the engineered 1K1 variant for 60 minutes. This assay revealed the ratio of phosphorylated c-Met to unphosphorylated in each well (see Fig. 4.13). There was a significant increase in phosphorylated c-Met between untreated and

treated cells, indicating that both HGF and 1K1 were able to activate c-Met in immortalised BEC without the addition of exogenous proteoglycan.

Ross (Ross, Gherardi et al. 2012) suggests that hepatocyte isolation removes HSPG from the cells surface (which is undoubtedly true). However, these molecules are turned over very quickly so much so that following overnight culture and then during any period of culture with HGF (for example during a proliferation assay) the cells will restore some level of normal cell surface HSPG expression. Wild-type HGF is inhibited by excess soluble heparin (seemingly in a similar way to the inhibition of chemokines) (Delehedde, Lyon et al. 2002). Work by Delehedde (Delehedde, Lyon et al. 2002) and Zioncheck (Zioncheck, Richardson et al. 1995, Schwall, Chang et al. 1996) suggests that HSPG do not modify HGF-receptor affinity but promote HGF oligomer formation.

1K1 is active at a low level in contact with normal cell surface HSPG, but this activity is greatly increased by soluble heparin. So we conclude that an excess of heavily sulphated heparin inhibits the activity of full length HGF. Although it can't be concluded that some level of cell-surface HSPG is required for normal activity, it is suspected this is the case. By contrast, 1K1 needs relatively more HSPG for full activity. This suggests that certain cells (such as hepatocellular carcinoma cells, which are deficient in these GAGs) will be more resistant to the mitogenic action of the 1K1 mutein than HGF. Clearly this is a confused area - we remain keen to explore this in more detail in future work, however it falls outside the remit of the current study.

The data in the current study suggest that HGF and any related compounds would be able to activate the c-Met receptor in immortalised BEC. The specific signalling pathways and effect of c-Met activation in relation to cellular processes such as EMT is developed in chapter 5.

5 Pharmacological manipulation of injured biliary epithelial cells

5.1 Introduction

Of the vanishing bile duct syndromes (VBDS), only one - primary biliary cirrhosis (PBC) - has any drugs available for treatment. The drug licensed for treatment of PBC is ursodeoxycholic acid (UDCA or 'Urso'); this is effective in some patients but entirely ineffective in around 30% (Pells, Mells et al. 2013). These patients, as well as those suffering from primary sclerosing cholangitis (PSC), chronic allograft rejection or GvHD have no therapeutic options and are treated with supportive care only. The progress of these patients is an inevitable slide into jaundice, decompensated liver failure and death, occurring over a protracted period and interspersed with intractable itching and debilitating fatigue, both of which are a significant cause of morbidity and often the worst aspect for patients, leading to withdrawal from the labour market. There is therefore a clear and present unmet clinical need in these diseases for drugs that have the potential to prevent duct loss and enhance its regeneration (Mells, Pells et al. 2013).

5.1.1 Autophagy

Autophagy is a ubiquitous cellular process that has been studied for over 40 years (Glick, Barth et al. 2010). Only relatively recently has the potential to manipulate and utilise autophagy and its pathways been pursued as a target for therapeutic intervention. There are three distinct types of autophagy; these are reviewed in

section 1.9). For the purposes of this work, only macroautophagy will be referred to.

Autophagy is a means of disposal for cellular organelles and debris, and is activated in times of cellular stress. Autophagy can reduce the energy requirements of the cell, by removing energy-consuming organelles, and in doing so, provide cells that are stressed or deprived of essential amino or fatty acids (Mehrpour, Esclatine et al. 2010). Autophagy can also dispose of misfolded proteins or those with toxic aggregates (Martinez-Vicente, Sovak et al. 2005). An essential early step in autophagy regulation is formation of the Vps34-containing class III PI3K complex, of which the mammalian homologue Atg14 is a fundamental component and acts as a Beclin-dependent Autophagy regulator (Simonsen and Tooze 2009). Once the autophagosomal membrane has begun to form, one of the key proteins in its extension is LC3B. This forms a pool with the other two LC3 proteins (A+B) and is incorporated into the autophagosome membrane by cleavage dependent on the Atg12, -5 and -16L complex, which is cleaved and then recycled from the membrane by Atg4.

In terms of regulators of autophagy that can act as surrogate markers, Atg14 offers an easily identifiable member of the initiation complex, and LC3B offers a clear visualisation of autophagosomal membrane formation. Both act as surrogate markers of the process.

5.1.2 αVβ6 Integrin

The specific structure and function of integrins has been discussed (section 1.6). In a series of experiments, Kraft (Kraft, Diefenbach et al. 1999) demonstrated the presence of an hitherto unexpected binding motif containing the consensus sequence DLXXL rather than the more conventional RGD binding motif identified in integrins (Humphries, McEwan et al. 2003). The DLXXL motif is known to bind to the latency-associated peptide (LAP) of both TGF-β1 and 3 at the RGD motif, but is unlikely to bind the LAP of TGF-β2 as it does not contain an RGD sequence. Kraft et al (Kraft, Diefenbach et al. 1999) also demonstrated that phage display sequences had the ability to inhibit the RGD specific binding between integrin and ligand at an IC50 of 20 - 50 mM, depending on the context. This very specific sequence (RTDLDSLRT) and a scramble control peptide (LDTRTRLSD) have been used previously to show specific inhibition of β6 integrin binding to LAP (Goodman, Holzemann et al. 2002)

It has been shown that αVβ6 integrin acts to induce a conformational change within LAP-1 and LAP-3 that allows the active form of TGF-β to interact with its receptors. The potential therefore exists for β6 integrin-dependent TGF-β activation to be inhibited by such a blocking peptide. Of note, there are other integrins that also have the same or similar activity on latent TGF-β and can be blocked with this peptide, specifically αVβ5 and αVβ8 (Neurohr, Nishimura et al. 2006), though the mechanisms of action of these integrins is markedly different.

5.1.3 HGF, GSK and 1K1

A fundamental part of this translational project was the establishment of an industrial partnership with GSK. Collaborative links were established with the Development and Regenerative medicine DPU at GSK. From some early data sharing discussions it became apparent that a developed therapeutic agent existed which had been withdrawn from further development in a specific area. This agent was 1K1, an engineered splice variant of hepatocyte growth factor (HGF).

As discussed in section 1.10, HGF has two biologically produced splice variants; NK1 and NK2. These comprise the N terminal and either the first or first two kringle domains of the full HGF protein. Both of these compounds are dependent upon heparan sulphate proteoglycans (HSPG) to allow binding to the c-Met receptor and have a relatively low activity when compared to HGF binding. Gherardi (Ross, Gherardi et al. 2012) had developed a variant of NK1 in which the protein was point mutated with reverse charge of Lysine 132 and Arginine 134, disrupting the HSPG low affinity binding domain of K1 and altering the electrostatic potential on the tertiary structure of 1K1 (Youles, Holmes et al. 2008, Ross, Gherardi et al. 2012).

The protein engineering steps leading to the production of 1K1 are outlined clearly by Ross (Ross, Gherardi et al. 2012) and are not further summarized here. The proteins in question were produced in yeast which was made possible by their size (being around a tenth of the size of the full length HGF molecule). Ross et al (Ross, Gherardi et al. 2012) also produced a mutated full length HGF that is not developed or discussed further here. It was demonstrated that 1K1 was monodispersible and stable in physiologically relevant buffers, thus avoiding the issues surrounding

aggregation and breakdown of HGF during storage. The relative activity in the model was assessed by DNA synthesis in response to HGF and mutant proteins when applied to isolated primary human hepatocytes. These assays revealed a potency of 1K1 that was around a hundredth that of full length HGF in the absence of heparin. When heparin was administered at a dose of 10μg/mL this altered so that the activity of 1K1 was around one fifth the potency of HGF (Ross, Gherardi et al. 2012).

5.1.4 HGF signalling

HGF signals via the c-Met receptor, inducing phosphorylation of this membrane-associated tyrosine kinase, leading to conformational change of the c-Met receptor, and leading to down-stream signalling activity. Phosphorylation of c-Met by 1K1 has been demonstrated by western blot previously (Ross, Gherardi et al. 2012). In the previous chapter phosphorylation of c-Met was shown by whole cell-based ELISA, confirming these results and also demonstrating that 1K1 was active at concentrations far below those previously described.

1K1 has also been used in a number of rodent models and has demonstrated efficacy in partial hepatectomy (rats) and CCl_4 administration (mice) (Ross, Gherardi et al. 2012).

It is known that downstream signaling following c-Met phosphorylation includes the activation of the RAS and PI3K pathways as well as STAT3, β catenin and NOTCH (Machide, Hashigasako et al. 2006), which are all signaling cascades fundamental to regulation of the balance between epithelial to mesenchymal transition (EMT) and

mesenchymal to epithelial transition (MET). It is therefore likely that HGF activates and transduces signals that interfere with the fundamental processes of EMT and autophagy, namely preventing EMT and potentially promoting reversal by MET.

5.1.5 Aims

The aims of this chapter are:

- To investigate autophagy and its manipulation using the previously described biliary epithelial cells (BEC) in vitro model of oxidative stress-induced EMT
- To investigate potential routes by which TGF-β could be activated in BEC undergoing oxidative stress-induced EMT
- To identify what role, if any, is played by immunosuppressive agents in contributing to BEC dysfunction
- To investigate the potential of 1K1 to prevent oxidative stress -induced EMT in our *in vitro* model

5.2 Materials and Methods

5.2.1 1K1

HGF and 1K1 (QRF) were supplied by GSK R&D, Stevenage UK. Both proteins were synthesised on site and shipped at -20 °C on dry ice in buffer containing 10% sorbitol, 20mM $NaPO_4$ and either 0.2 or 0.3M NaCl. Both proteins were diluted to a final concentration of 1μg/ml and stored at -80°C until required. The buffer containing the proteins was also supplied and was added to culture with immortalised BEC with no noticeable effect.

5.2.2 αVβ6 integrin blocking peptides

The αVβ6 integrin-blocking peptide (RTDLDSLRT) and scramble control (LDTRTRLSD) originally described by Kraft (Kraft, Diefenbach et al. 1999) were synthesized by Genscript Laboratories (NJ, USA). These were received lyophilized. Immediately prior to use the proteins were reconstituted in sterile PBS according to the manufacturer's instructions and used at a final concentration of 1μM as indicated in the literature (Kraft, Diefenbach et al. 1999).

5.2.3 Drugs and inhibitors

3, Methyl-adenine (3-MA), rapamycin and FK506 (Tacrolimus) were supplied by Sigma Aldrich (Cambridge, UK) and stored at -20° C until required. Working solutions were made up in diverse solvents for administration of 3-MA and these are covered in section 5.3.4. Rapamycin was received as a re-diluted solution requiring no further manipulation. FK506 was dissolved in analytical grade ethanol.

5.2.4 Non-Radioactive MTT/Formazan based proliferation assay

A non-radioactive assay was utilized to measure cell proliferation. This was the Promega CellTiter 96® Aqueous 'One Solution' Cell Proliferation Assay. This kit uses a tetrazolium compound related to MTS (a tetrazolium dye known as Owen's reagent formula 3-(4,5-dimethylthiazol-2-yl)-5-(3-carboxymethoxyphenyl)-2-(4-sulfophenyl)-2H-tetrazolium)) and a further agent as an electron-coupling reagent, known as phenazine ethosulphate (PES). In this system, the MTS (or related compound) is reduced by the cellular production of either NADPH or NADH, which is directly proportional to the mitochondrial activity of the cells (therefore cell

numbers can be inferred from the number of mitochondria). This reduction produces a formazan compound that is soluble and can be read by measuring absorbance at 490nm.

This kit was used in accordance with the manufacturer's instructions and was optimized for cell number and reaction time. It was found that the best results were obtained with 12,000 cells per well in a 96 well plate and by incubating with the 'One Solution' reagent for 90 minutes before reading.

5.3 Results

5.3.1 Detection of autophagy in immortalised biliary epithelial cells

LC3B and Atg14 were used as markers to determine whether or not autophagy was activated by hydrogen peroxide (H_2O_2)-induced oxidative stress of BEC. Figs. 5.1 and 5.2 demonstrate the expression of LC3B after treatment with 200μM H_2O_2. It had been hoped that discrete puncta of LC3B could be counted per field. Fig. 5.1 shows that this is not possible. The up-regulation of LC3B was so great that even at small antibody concentrations it was frequently necessary to reduce the voltage across the confocal photomultiplier tubes to avoid saturation. It is clear from Fig. 5.1 that background autophagy levels are present at baseline, as would be expected in a normally functioning cell population (Klionsky, Abdalla et al. 2012).

Fig. 5.2 shows results of a western blot demonstrating that the LC3B antibody was also able to pick up both forms of LC3B (section 1.9) and that both of these levels increased in response to oxidative stress. There was an increase in the 16 and 18 kDa subtypes at 24 and 48 hours post H_2O_2 exposure; this is seen on the second row of Fig. 5.2, on the very top row a shorter duration exposure shows a clearer picture of the increase in the 16-kDa sub-type which is related to the time course (Klionsky, Abdalla et al. 2012). The levels seen on the western blot would indicate that protein levels are returning to normal or near normal levels by 72 hours. This indicates that total LC3B levels can be used as an indicator of autophagy activity.

Figure 5.3 shows Atg14 levels post H_2O_2 exposure. Puncta are clearly visible at baseline, and there was an increase in Atg14 levels at both 48 and 72 hours post H_2O_2 exposure. Again the expression increases so markedly that individual puncta

were not discernible and only the total protein level could be assessed. These data back up the data shown in Figures 5.1 and 5.2 and indicate that Atg14 is also an acceptable surrogate marker of autophagy levels within individual cells.

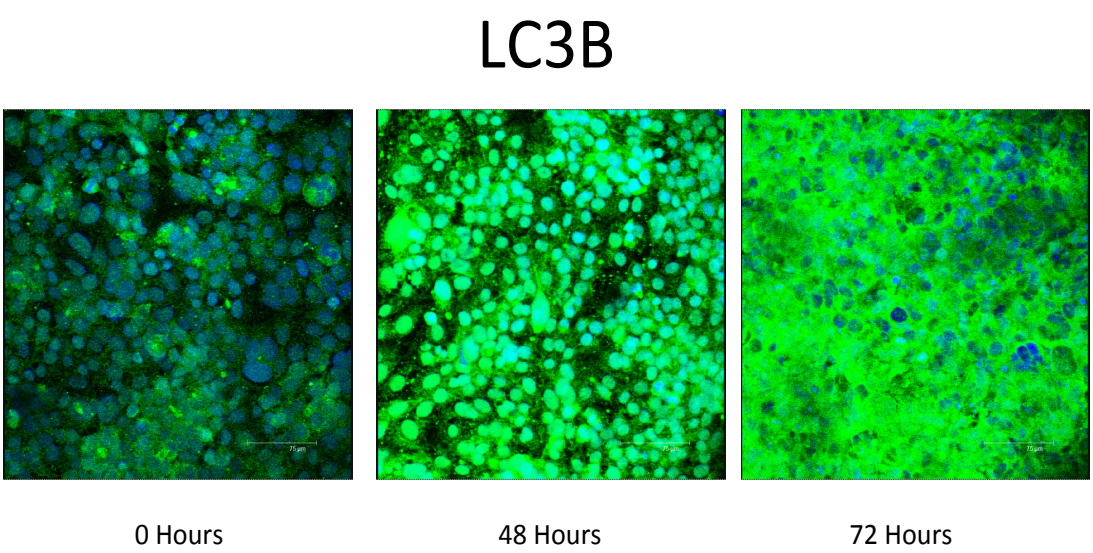

Figure 5.1: Detection of autophagosomal membranes following H_2O_2 exposure and autophagic vacuole formation in H_2O_2 treated immortalised BEC. LC3B is a specific protein cleaved during formation of the autophagosome membrane; its level correlates with the amount of autophagy occurring in the cell. To investigate whether cells exposed to H_2O_2 had increased levels of autophagy, confocal microscopy was performed. There was a clear increase in levels at 48 and 72 hours post H_2O_2 exposure. Figures are representative of more than three separate experiments.

LC3B protein expression post H_2O_2 exposure in BEC

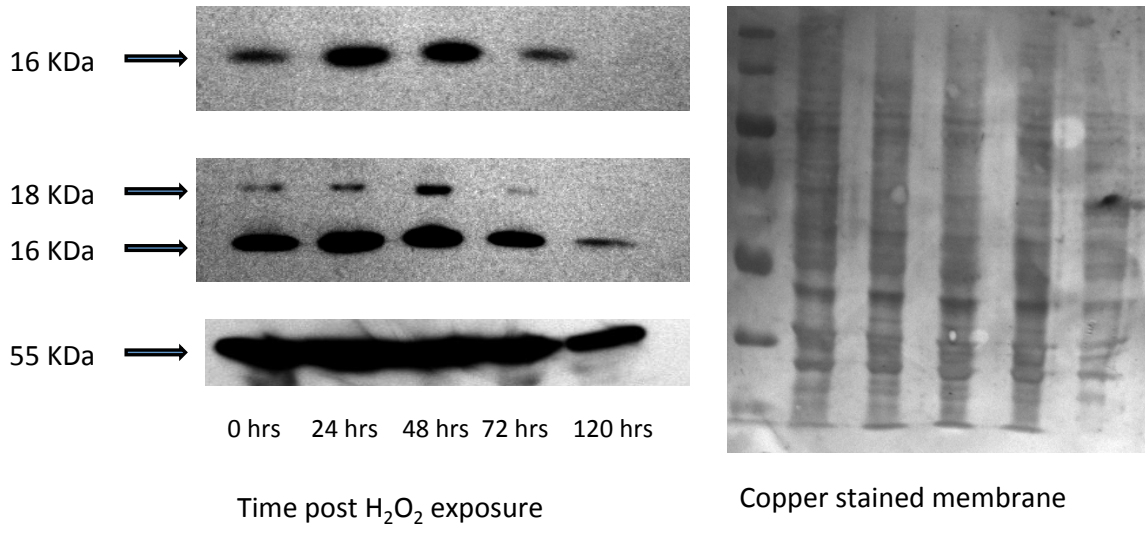

Figure 5.2: Validation of LC3B staining in BEC subjected to oxidative stress. LC3B exists in two forms, an 18-kDa form and a cleaved 16-kDa form that is associated with the autophagosomal membrane. Western blots for LC3B expression are shown, with an increase in the cleaved 16 kDa protein in the top panel, and further H_2O_2 exposure causing an increase in the uncleaved form at 18 kDa (second panel) that was most noticeable at 48 hours. Protein loading control (alpha tubulin) staining was present at 55 kDa, shown in the lowest panel on the left, and a total protein copper stained blot is present in the far right panel. These results are representative of three individual experiments.

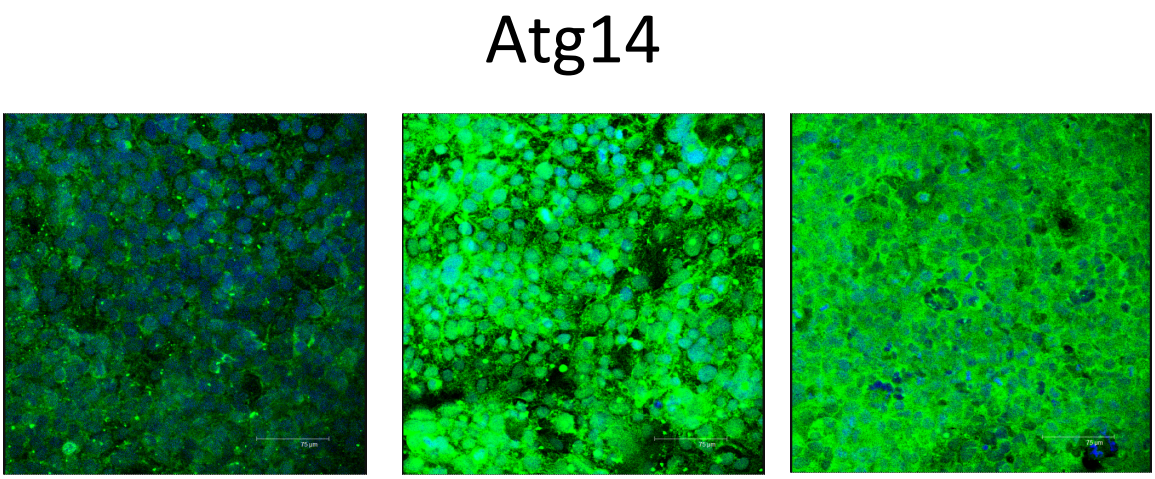

Figure 5.3: Substantial increase in autophagy associated with H_2O_2 induced EMT of immortalised BEC. Atg14 is a specific protein responsible for the formation of the autophagosome membrane and its level correlates with the amount of autophagy ongoing within the cell. To investigate whether cells exposed to H_2O_2 had increased levels of autophagy, Atg14 confocal microscopy was performed. There was a clear increase in Atg14 levels at 48 and 72 hours post H_2O_2 exposure. Results representative of a minimum of three separate experiments

5.3.2 β6 Integrin induction and blockade in oxidative stress-induced EMT in BEC

As shown in chapters 3 and 4, TGF-β and its regulation appear to play a key role in directing the oxidative stress-induced EMT observed in BEC after H_2O_2 exposure. One of the key regulators of TGF-β latency is the αVβ6 integrin. Expression of the β6 integrin is restricted to the αV chain, therefore αvβ6 integrin can be detected by antibodies specific for the β6 chain. Fig. 5.4 shows staining for β6 integrin in BEC following exposure to 200μM H_2O_2. There was a substantial increase in β6 integrin expression at 48 hours.

As noted previously, the emergence of new immunosuppressives seems to have altered the way that chronic rejection presents, with relative duct sparing as noted in patients treated with tacrolimus (Lunz, Contrucci et al. 2001). One, possibly pro-fibrotic, agent of potential interest is rapamycin (or Sirolimus), an immunosuppressive agent and a known inducer of autophagy via targeting of the mTOR pathway (section 1.9.4). In this study, BEC were treated with a single dose of 2 or 4μM rapamycin, rather than being treated with H_2O_2. Staining for β6 integrin after exposure to rapamycin for 48 hours was even more remarkable than that seen after H_2O_2 exposure.

Blocking peptides (sequences at section 5.2.2) were used in order to determine if the αVβ6 integrin was involved in the regulation of TGF-β in this system. After exposure to H_2O_2 200μM for two hours as previously, cells had either the blocking peptide or a scramble control added to their fresh medium (at final concentrations

of 1μM). After 48 and 72 hours cells were imaged; results are shown in Figures. 5.5 and 5.6 and show that the administration of blocking peptides appears to block the oxidative stress induced EMT in BEC. However the consistency of this staining was not robust. In several experiments there was either no appreciable effect of the blocking peptides or there was no discernible effect on the cells normal state. There did not appear to be maintenance of epithelial integrity as would be hoped if the blockade of αVβ6 integrin was the rate limiting step for TGF-b activation. The results obtained from αVβ6 integrin blockade could indicate a number of things and are discussed in section 5.4.

αVβ6 Integrin

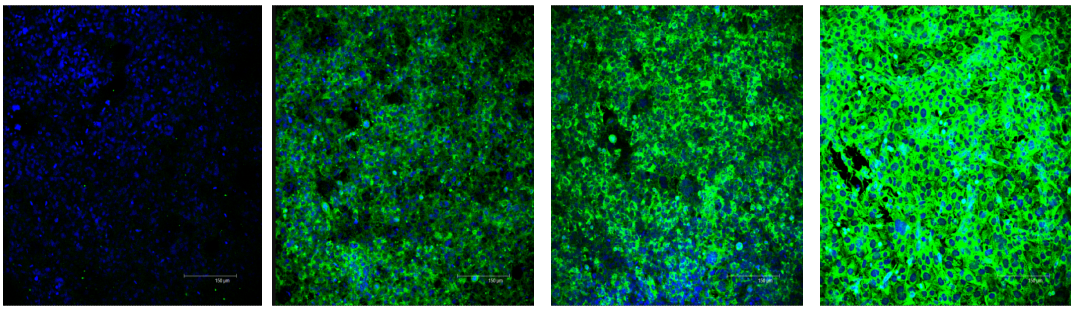

Figure 5.4: H_2O_2 and rapamycin induce BEC expression of β6 integrin. To identify the cause of TGFβ activation within BEC, staining for β6-containing integrins was performed. This showed a substantial up-regulation at 48 hours post H_2O_2 exposure, at levels very similar to those seen in BEC + 2μM rapamycin (28 hours). β6 integrin levels were less than those seen in BEC + 4μM rapamycin (at 48 hours). This provides an indication of the agent responsible for activation of latent TGF-β both in the H_2O_2 treated cells and in liver allograft patients receiving rapamycin as a renal sparing agent.

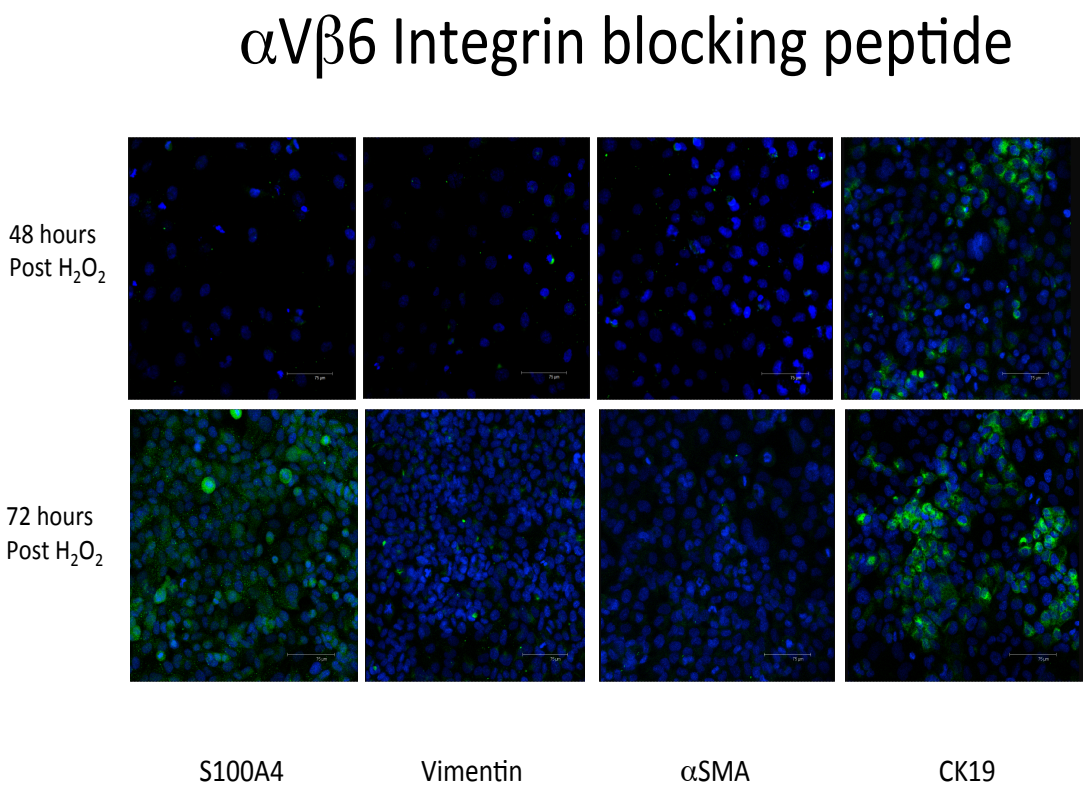

Figure 5.5: Blockade of β6 integrins inhibits H_2O_2 induced EMT of immortalised BEC. To prove that β6 containing integrins were responsible for the activation of latent TGF-β in the H_2O_2 treated BEC model, BEC were exposed to H_2O_2 as before but then either a scramble control peptide or a peptide with β6 blocking properties was added to the medium. As can be seen by the relative lack of staining, addition of the blocking peptide appeared to reduce the expression of the EMT associated antigens S100A4, Vimentin and αSMA. However, CK19 expression is lower than would be expected in an untreated BEC population and S100A4 expression is raised at 72 hours.

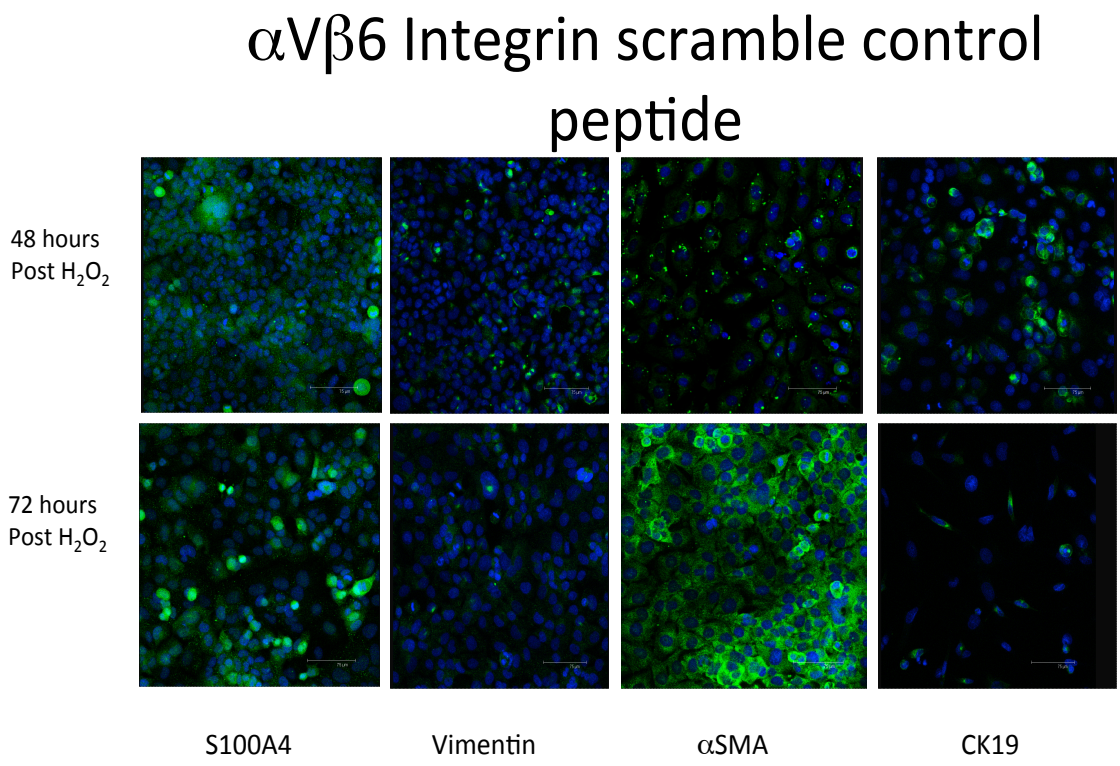

Figure 5.6 A scrambled peptide has no effect on H_2O_2 induced EMT of immortalised BEC. To prove that β6-containing integrins were responsible for the activation of latent TGF-β in the H_2O_2 treated BEC model, BEC were exposed to H_2O_2 as before but then either a scrambled control peptide or a peptide with β6 blocking properties was added to the medium. As shown above, addition of the scramble peptide appeared to have no effect on the expression of αSMA at 72 hours. There was however a great degree of variability in the staining, with Vimentin showing no staining at all, indicating it was inhibited. CK19 staining is lower than would be expected for an untreated population of BEC.

5.3.3 Effect of immunosuppressive agents on biliary epithelial cell phenotype

The availability of new immunosuppressive agents appears to have altered the prevalence and presentation of disease in liver allografts. Ductopenic rejection is now rarely seen, but in its place are new and emerging conditions such as chronic rejection in the absence of ductopenia (defined as predominantly centrilobular necroinflammation with or without fibrosis or portal changes with preservation of intralobular bile ducts), and chronic antibody-mediated rejection. It appears that there has been no investigation into the effects of the agents tacrolimus and rapamycin on BEC, the focus being largely upon the effects of immunosuppression on the immune system. For this reason, the current study investigated the effect of rapamycin on BEC. As demonstrated earlier in this chapter, rapamycin has the ability to induce β6 integrin on BEC, suggesting that it has a pro-fibrotic effect through its action on latent TGF-β. A time course experiment was conducted to corroborate this observation (Figure 5.7). The expected induction of autophagy was seen, as well as a marked increase in S100A4 expression. This apparent induction of EMT was followed up with longer-term experiments (Figure 5.8).

Next, rapamycin was added to BEC cultures as a single dose (2μM / 4μM), but the cells were incubated for 48 or 72 hours prior to staining. Results of this staining are shown in Fig. 5.8 where there is a visible shift towards a mesenchymal phenotype, which seems to bear no relation to p21 expression. Figure 5.8 shows a decrease in the epithelial antigen CK19, whereas the antigens αSMA, S100A4 and vimentin are all increased.

Rapamycin is used infrequently as an immunosuppressive agent in liver transplantation and finds use in a small number of units, usually as a third or later line agent (Wiesner and Fung). Its use here owed primarily to its ability to induce autophagy through the mTOR pathway. One primary immunosuppressive agent used in liver transplantation is FK506, or tacrolimus. As a counterpoint to the changes seen following rapamycin treatment, 5ng/l FK506 was administered to immortalised BEC in a time course experiment (see Figure 5.9). No induction of β6 integrin was observed in the presence of FK506. Furthermore, the level of autophagy induction observed was substantially lower than that seen with rapamycin. No phenotypic changes were observed after the addition of FK506 (data not shown).

The antifungal amphotericin B is occasionally administered to transplant recipients and is frequently used in tissue culture laboratories. Figure 5.10 depicts the marked EMT changes that this agent can induce. All culture experiments in this thesis were conducted in the absence of antifungals.

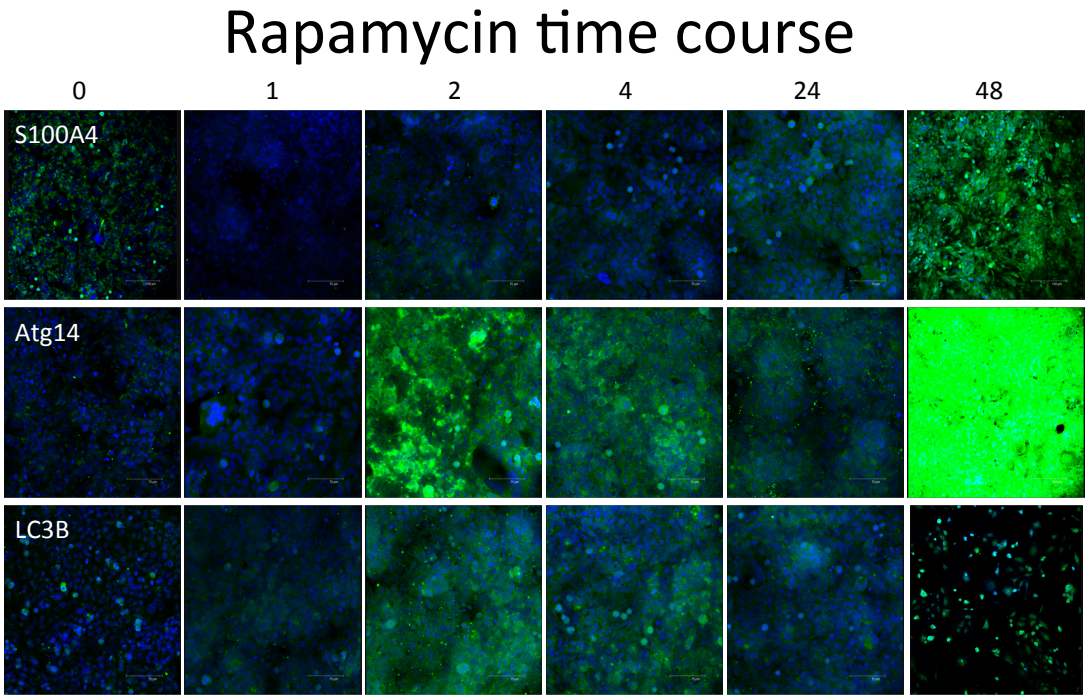

Figure 5.7: Rapamycin-induced expression of autophagy-associated antigens and EMT in immortalised BEC. To quantify the changes seen in the BEC due to rapamycin exposure, 2μM of Rapamycin was added to immortalised BEC and the effects observed at 1, 2, 4 12, 24 and 48 hours, with comparison to baseline. The ability of rapamycin to induce autophagy is a key interest and Atg14 and LC3B are key markers that demonstrate autophagy induction. There was an early peak at two hours in the Atg14 staining, with a small decline up to 24 hours, followed by a large increase in Atg14 expression at 48 hours. LC3B also seemed to follow this pattern. There was a decrease from baseline in S100A4 expression, before a steady increase to the 48 hour time point. Images are representative of 3 separate experiments.

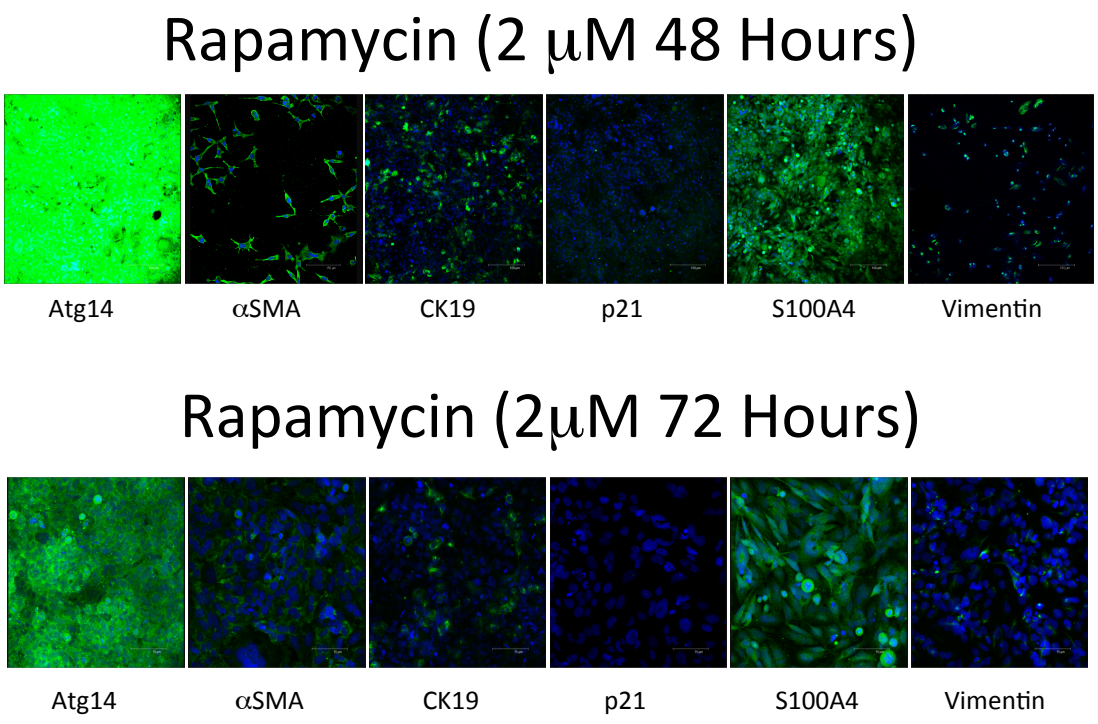

Figure 5.8: Expression of epithelial and mesenchymal antigens in immortalised BEC following exposure to rapamycin. Rapamycin is an immunosuppressive agent that is associated with increased fibrosis in human liver allograft recipients, and is a known inducer of autophagy via the mTOR pathway. To investigate the effects of rapamycin in culture it was added to immortalised BEC at 2 and 4μM for 48 – 72 hours (results are shown for 2μM). While there was a preservation of CK19 expression, there was also induction of antigens associated with EMT, including αSMA and S100A4. There was no change in the levels of p21 expression, indicating that the effect of rapamycin is independent of the effects seen in H_2O_2 treated BEC. Therefore, rapamycin appears to induce an EMT in BEC.

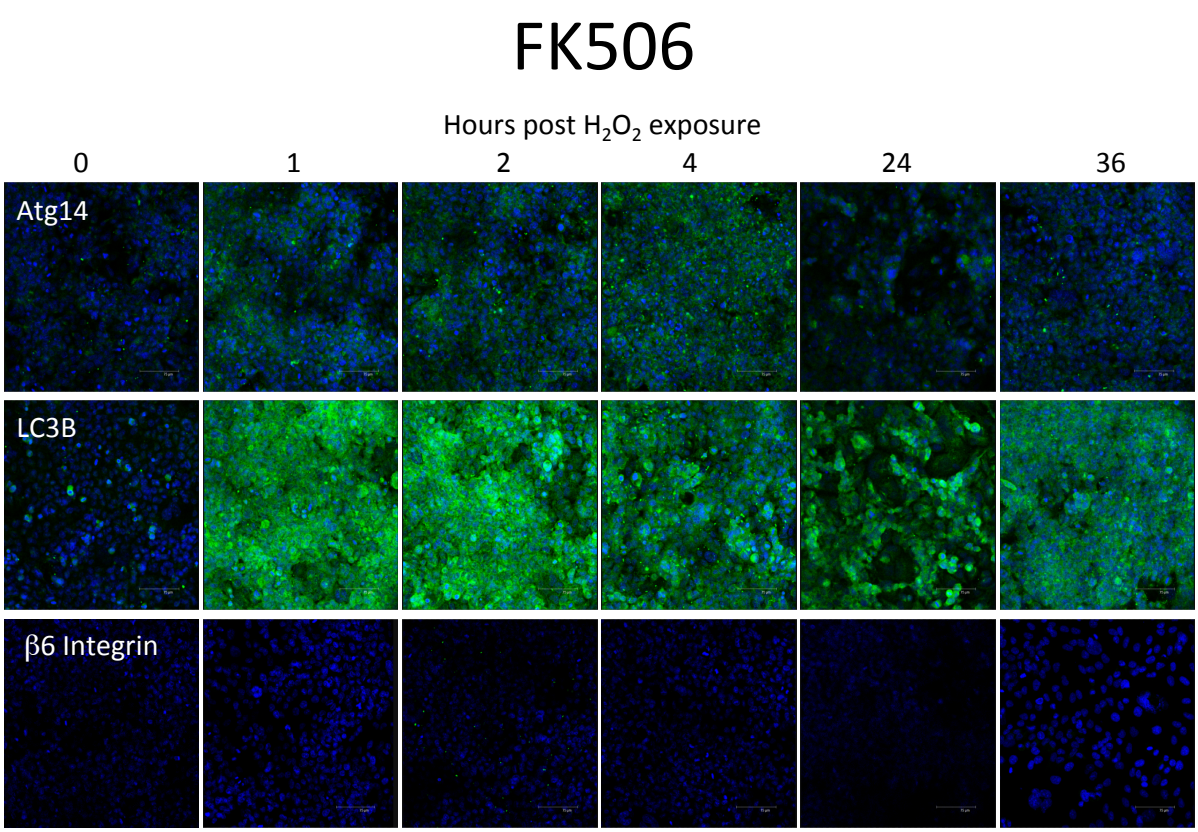

Figure 5.9: FK506 does not induce β6 integrin expression in immortalised BEC. BEC expression of Atg14, LC3B and β6 Integrin was assessed following exposure to 2μM FK506 for 1, 2, 4, 24 or 36 hours. There was a clear increase in Atg14 from virtually no expression at baseline, to a consistent amount that exhibited no obvious change between 1 and 24 hours. This pattern was also seen in LC3B expression, which was much more easily observed, due to higher expression levels. There was no evidence of β6 integrin expression at any point following FK506 treatment. Figure representative of three separate experiments.

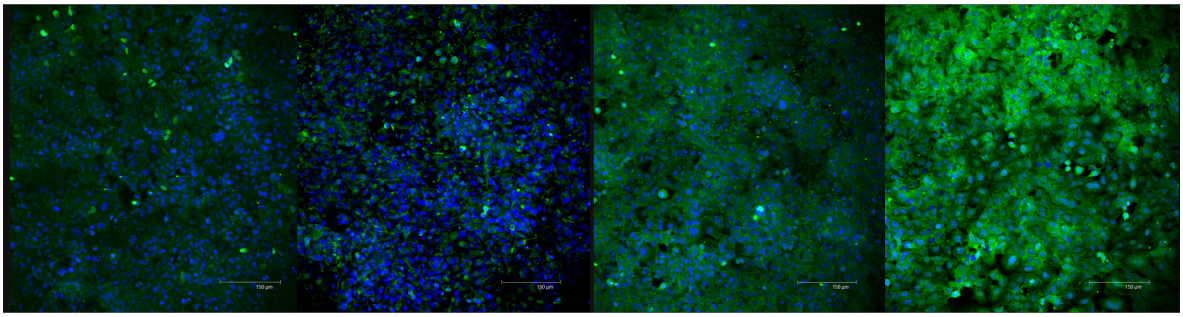

P21 **vimentin** **Atg14** **LC3B**

Effect of Amphotericin B on Culture

5 μg/ml for 72 hours

Figure 5.10: The antifungal Amphotericin B induces senescence and EMT-like changes in immortalised BEC.

5.3.4 Inhibition of Autophagy and it's effect on oxidative stress-induced EMT in biliary epithelial cells

It has been observed by Nakanuma et al (Sasaki, Miyakoshi et al.) that inhibition of autophagy may prevent senescence in rodent BEC. 3-MethylAdenine (3-MA) is a frequently used specific inhibitor of autophagy that inhibits the Class III PI3K complex (Section 1.9). Manufacturers' instructions vary as to how 3-MA should be handled. In order to clarify this issue several dissolution experiments were conducted. The solvent recommended by Sigma-Aldrich was Dimethylformamide (DMF); the 3-MA was dissolved at 13mg/mL and added to BEC at a final concentration of 5mM. Interestingly the addition of 3-MA appeared to induce an EMT, and certainly a reduction in CK19, as shown in Figure 5.11. Inhibition of autophagy was somewhat delayed, with initial levels remaining quite high. 3-MA prevents autophagosomal membrane extension (one of the later stages of autophagy (Klionsky, Codogno et al. 2010)), so it is perhaps not surprising that the autophagy levels remained high.

DMSO was used as an alternative solvent, as recommended by Invivogen. From the onset there were problems with solution (as predicted by Sigma-Aldrich). However, when DMSO was incubated at 37˚C, the solubility (of 3-MA) improved drastically. If the solution of 3-MA in DMSO was allowed to cool, a precipitate was observed. It was possible to keep the 3-MA in DMSO at 37˚C and add this to the cultured cells; results are shown in Figure 5.12. The reduction in autophagy was substantially greater than with DMF, and CK19 expression was retained.

Nakanuma (Sasaki, Miyakoshi et al.) demonstrated that by inhibiting autophagy, p21 up-regulation in rodent BEC following exposure to H_2O_2 was prevented. Therefore 3-MA was added to BEC immediately after H_2O_2 exposure. No evidence of p21 expression was observed (data not shown). It was expected that if p21 expression was prevented, then the EMT related to this would not occur. Figure 5.13 demonstrates that while autophagy levels were reduced they were not abolished. Vimentin expression was prevented (as demonstrated against the inset image); CK19 expression also decreased. It is unclear why this partial response occurred, but this was a consistent finding in three separate experiments. However the experiments themselves were quite inconsistent, on several occasions the cells seemed unable to stick to the culture surface, coming loose in cell rafts, rather than as individual cells. This would indicate that cell-to-cell adhesion was retained, but cell to surface adhesion was not. Viability stains would be required to see if this was merely due to cell death, however these were not performed.

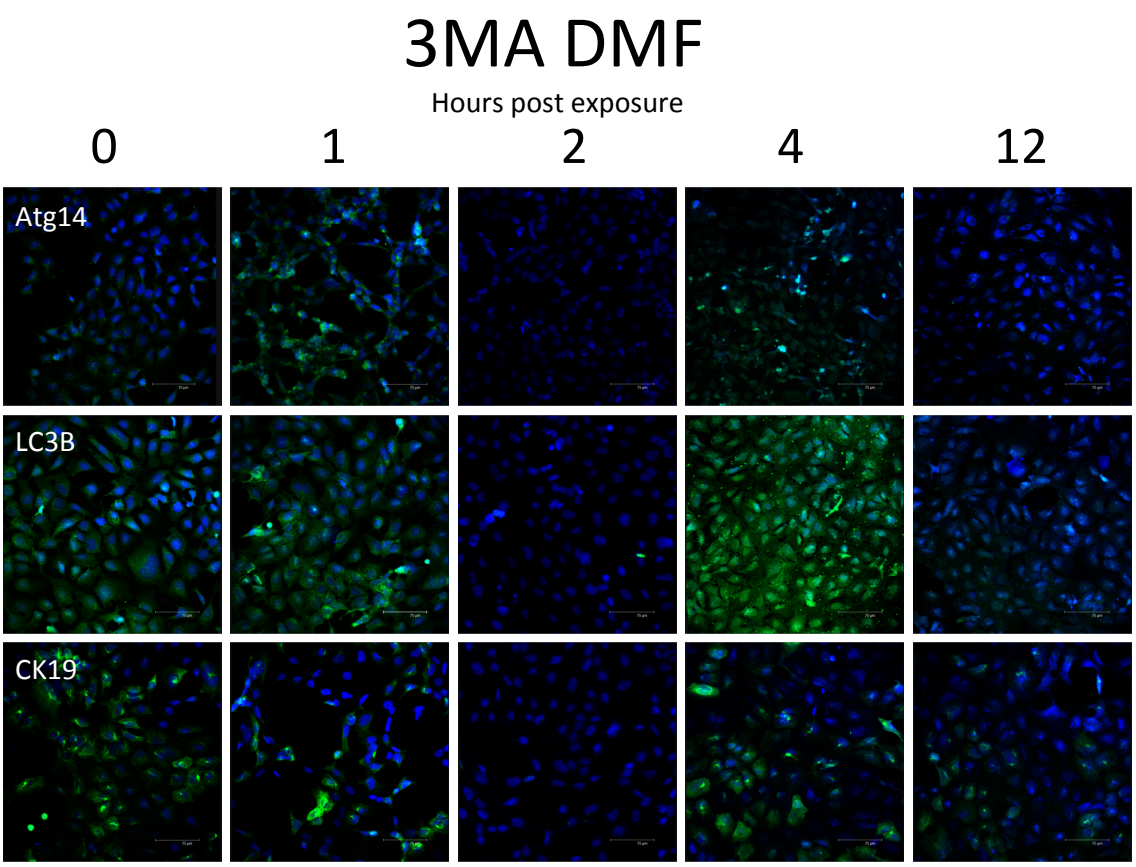

Figure 5.11: Effect of 3-MA in DMF on autophagy in unstimulated immortalised BEC. The recommended solvent for 3-MA is DMF as this requires no heating. 3-MA was added to DMF at a concentration of 13mg/ml and added to BEC at a final concentration of 5mM with incubation for 1, 2, 4, 12 and 24 hours. The top row shows Atg14 staining and the middle row LC3B; there is a delay in the onset of autophagy inhibition to levels of around zero at four hours, with a rapid up-regulation observed by 12 hours. The bottom row shows a fall in the expression of CK19 mirrors the fall in the markers of autophagy Atg14 and LC3B. Images representative of 3 separate experiments.

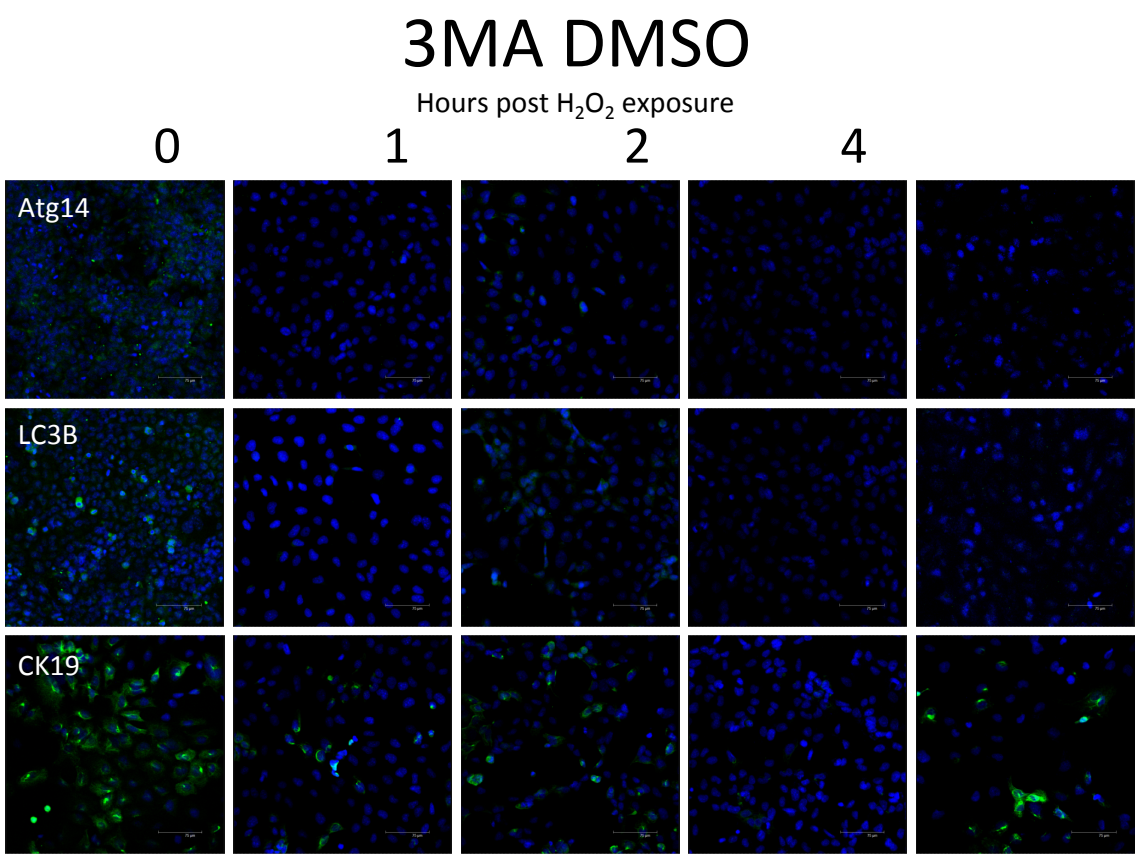

Figure 5.12: Effect of the autophagy inhibitor 3-MA dissolved in DMSO at 37˚C on BEC. 3-MA is a specific Class III PI3 kinase inhibitor that is routinely used to inhibit autophagy at 5mM (Klionsky, Abdalla et al. 2012). To assess the effect of 3MA on unstimulated BEC, DMSO was heated to 37 ˚C and 3MA added to a concentration of 14mg/ml. This was added to BEC to a final concentration of 5mM with incubation for 1, 2, 4, 12 or 24 hours. The top row shows Atg14 staining and the middle row shows LC3B staining. There was a notable effect on autophagy with a reduction to levels near zero by one hour, which was maintained past 12 hours. The bottom row shows CK19 staining. It is clear that the inhibition of autophagy has an effect on BEC expression of CK19; whether or not this has any other effects on protein expression requires further investigation.

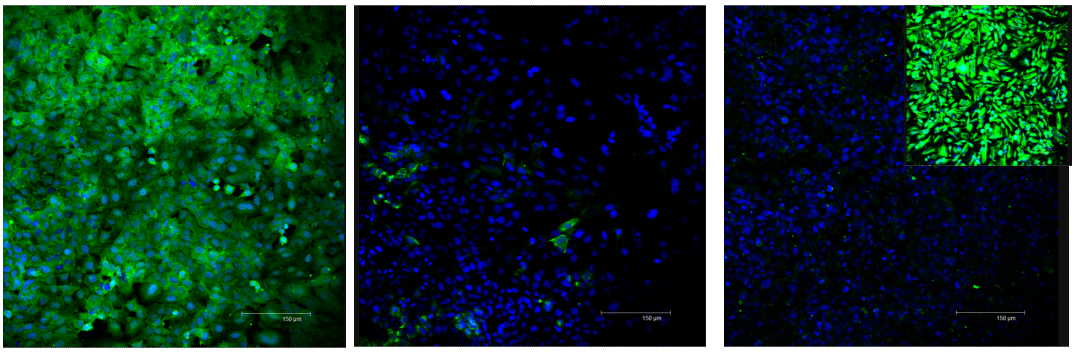

LC3B CK19 Vimentin

3-MA at 5mM post 200mM H_2O_2 (48 hours)

Figure 5.13: Effect of 3-MA on BEC treated with H_2O_2. BEC were treated with H_2O_2 (200μM for 2 hours), washed and then incubated with fresh medium containing 5mM 3-MA. It appeared that 3MA did not prevent an increase in autophagy levels or a decrease in CK19 expression, but did reduce vimentin expression. There is an inset image from a non 3-MA treated H_2O_2 exposed culture stained for Vimentin, this shows quite clearly the difference in 3-MA treatment.

5.3.5 Effects of 1K1 and HGF on intracellular signalling in biliary epithelial cells following oxidative stress

The results described in chapter 4 show that HGF and 1K1 are able to induce phosphorylation of the c-Met receptor. The functional effects of this are investigated here. Firstly, proliferation of immortalised BEC following administration of 1K1 was assessed (Figure 5.14). This gave a characteristic curve that was reproduced for various incubation periods of the MTT-based reagent ('One Solution'). There was an initial proliferative response to small doses of either 1K1 or HGF, followed by a decrease and then a subsequent peak. The peak response in proliferation appeared to be at around 10 ng/ml for both 1K1 and HGF.

The potential for 1K1 to affect c-Met, ERK and SMAD2/3 phosphorylation following H_2O_2 exposure was also investigated using ELISA assays (as shown in chapter 4). Immortalised BEC were grown in 96-well plates before treatment with 200 μM H_2O_2 for two hours, washing and then incubation in fresh medium containing either no additive or 1K1 at 10 or 50 ng/ml, HGF at 10 or 50 ng/ml or both 1K1 and HGF at 10ng/ml each. After incubation for either 48 or 72 hours, reactions were terminated and developed (results are shown in Figures 5.15, 5.16 and 5.17). Control groups comprised confluent cells that were untreated with H_2O_2 and either assayed directly or treated with 1K1, HGF or both for 60 mins to give a baseline reading. (as per the original assays). This gave a reflection of the variation in c-Met, ERK and SMAD2/3 phosphorylation following H_2O_2 exposure, relative to baseline activation in the assay.

Figure 5.15 shows c-Met phosphorylation in BEC after H_2O_2 treatment and addition of HGF or 1K1. c-Met phosphorylation appeared to decrease in the treated groups, although this may have been an artefact. In the untreated groups, there was an increase in c-Met phosphorylation over time and a small increase was seen in the 72 versus 48 hours groups. A two way ANOVA was used in order to determine if the changes observed were due to the treatments (and if so, which treatment). This was significant ($p < 0.0092$), though this was not due to either treatment / duration of treatment, making interpretation of this result difficult. What was clear however was that any influence on c-Met phosphorylation (and therefore activity) due to HGF or 1K1 was abolished by 72 hours following the dose.

The effect of 1K1 and HGF on SMAD2/3 and ERK phosphorylation in BEC treated with 200 μM H_2O_2 for two hours is shown in Figures 5.16 and 5.17. SMAD activity (Figure 5.16) appeared to be suppressed at 48 and 72 hours, with 1K1 appearing to have a longer lasting effect on SMAD suppression - indicated by lower levels at 72 hours and a lower baseline level of activity versus the unstimulated / HGF treated groups. A two-way ANOVA revealed that both the changes in treatment and the duration of exposure caused significant changes in SMAD2/3 phosphorylation ($p < 0.02$). This indicates that while there was a variation in SMAD phosphorylation over time, there was also a significant effect due to the 1K1 or HGF at time points of 48 and/or 72 hours. This suggests that the effect on TGF-β dependent SMAD signalling was longer lasting.

ERK activity (Figure 5.27) was higher at baseline in the HGF and 1K1 treated groups than at baseline, however there was also a difference between HGF- and 1K1-

dependent ERK activity. HGF seemed to be more potent than 1K1 in terms of ERK activation at all time points. The 50ng/ml 1K1 group had a similar ERK activation as the 10ng/ml. At both 48 and 72 hours, HGF appeared to be a stronger, and more persistent, activator of ERK. A two-way ANOVA revealed that the duration of exposure, rather than the treatment itself, caused a significant change ($p < 0.002$) in ERK activity.

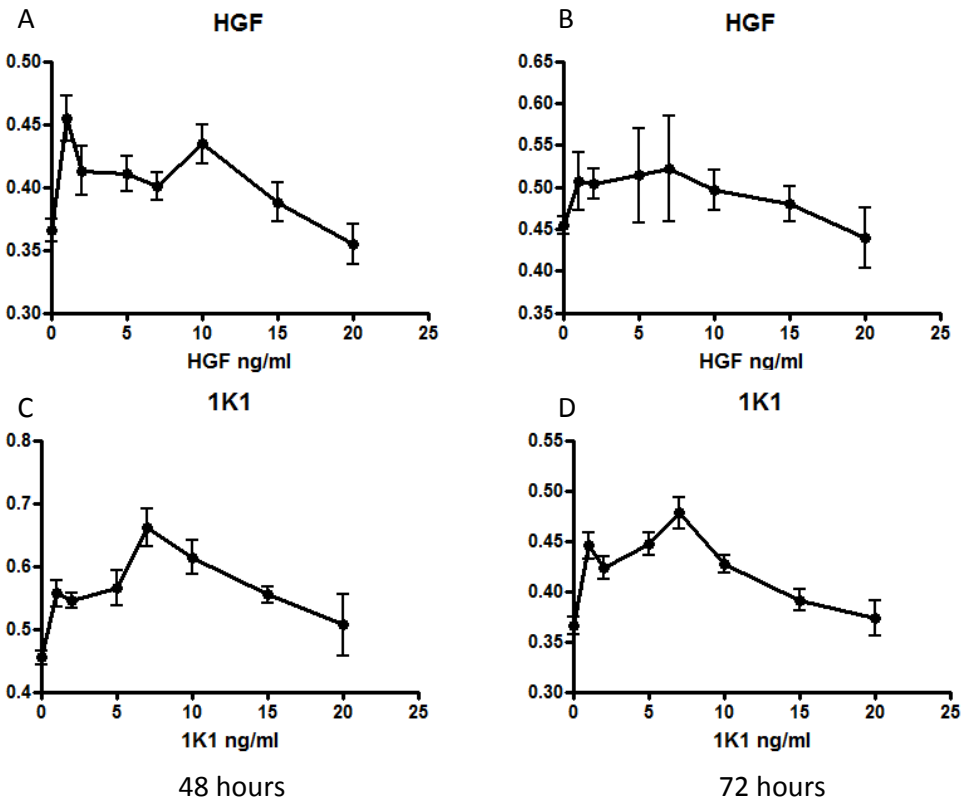

Figure 5.14: The proliferative response of immortalised BEC to HGF and 1K1. An assay based around MTT/formazan was utilised with 12,000 cells per well in a 96-well plate. Either HGF or 1K1 were added at concentrations of 0, 1, 2, 5, 7, 10, 15 or 20 ng/ml, with incubation for 48 (panels A + C) or 72 (panels B + D) hours at 37 ˚C. Plates were then read at 490nm. HGF showed a maximal proliferation at between 7 and 10 ng/ml, 1K1 gave a clear maximal proliferation at 7 ng/ml.

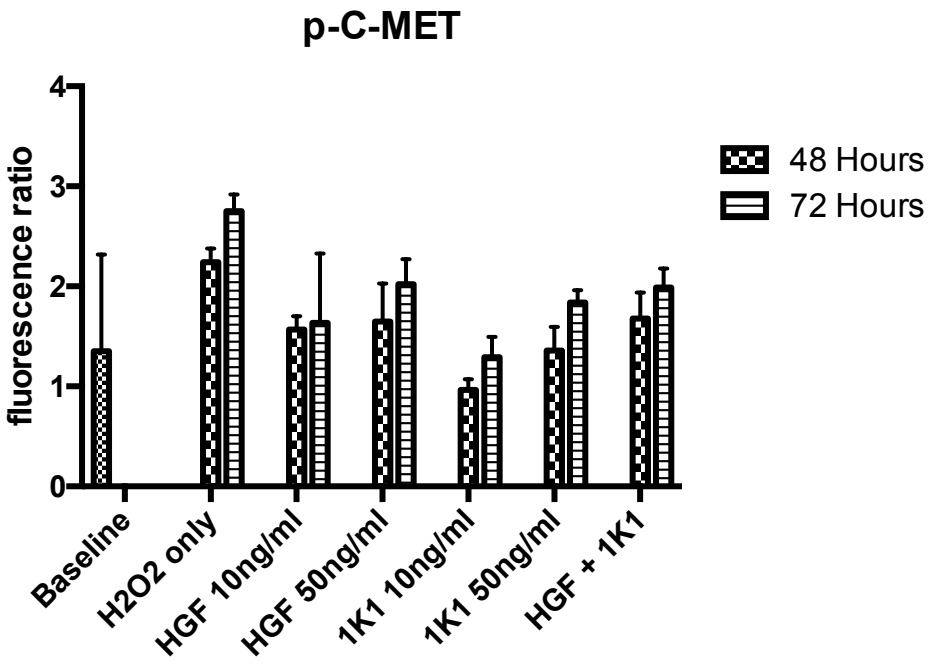

Figure 5.15: C-Met phosphorylation of BEC after H_2O_2 treatment and addition of HGF or 1K1, Baseline results for c-Met phosphorylation for confluent but untreated (neither H_2O_2, 1K1 or HGF) cells are shown for comparison. BEC were grown in T75 flasks until confluent and treated with 200µM H_2O_2 for two hours. Cells were incubated for 48 or 72 hours in fresh medium with either no additive (H_2O_2 Only), 1K1 or HGF at 10 or 50 ng/ml or both at 10ng each per ml. There was one treatment only. There was an up-regulation in c-Met phosphorylation at 48 and 72 hours relative to baseline cells. Treatment with both 1K1 and HGF lead to a relative reduction in c-Met phosphorylation at 48 and 72 hours. It is not clear whether this was a true reflection of decreased phosphorylation or whether the cells have been stimulated to produce more unphosphorylated protein.

Two way ANOVA showed an overall change in levels of c-Met phosphorylation that was significant ($p < 0.0092$) but no variation due to either the treatment itself or the duration of treatment.

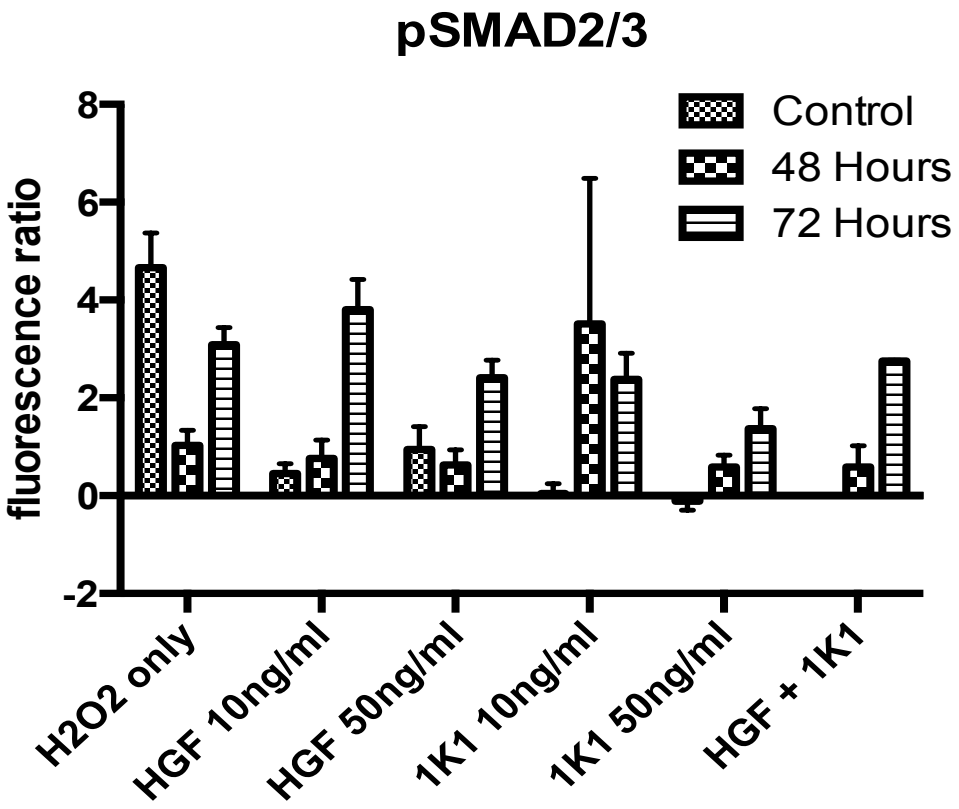

Figure 5.16 Phosphorylation of SMAD2/3 following H_2O_2 treatment of BEC + / - 1K1 or HGF. BEC were grown in T75 flasks until confluent and then assayed. The first three columns of the graph show cells that were either confluent and not treated (control group of H2O2 only cells) or treated with 200µM H_2O_2 for two hours with incubation for 48 or 72 hours in fresh medium with either no additive (H2O2 only, 48 and 72 hours respectively). The control groups in the remaining columns were confluent cells, not treated with H_2O_2 but treated with the additive noted on the x axis (1K1, HGF or both) for 60 mins. Remaining groups were treated with 200µM H_2O_2 for two hours with incubation for 48 or 72 hours in fresh medium with the additive labelled on the x axis. These are labelled as 48 or 72 hours. There was one treatment with additive only and this occurred immediately after H_2O_2 exposure. In cells treated with H_2O_2 alone, there was a down regulation of pSMAD2/3 at 48 and 72 hours, with a more marked effect at 48 hours. Levels of pSMAD2/3 were similar for control samples and HGF treated cells at all time points. 1K1 treated cells showed a possible increase at 48hours at the 10ng/ml dose. These results could indicate that any treatment effect of drug had occurred, and that phosphorylation levels had returned to normal. A two way

ANOVA showed that the combination of treatment and duration of treatment caused a significant change in SMAD2/3 phosphorylation (p <0.02 - 0.037), as well as the factors individually.

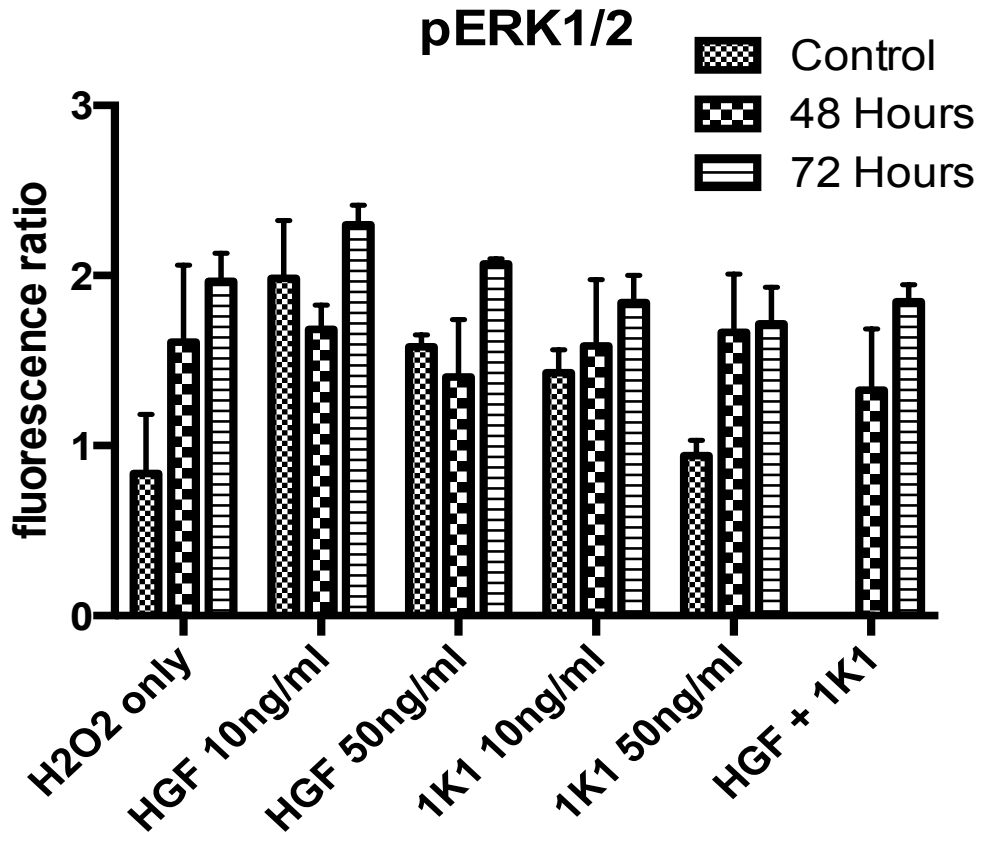

Figure 5.17 Phosphorylation of ERK 1/2 following H_2O_2 treatment of BEC + / - 1K1 or HGF. BEC were grown in T75 flasks until confluent and then assayed. The first set of columns show cells that were either confluent and not treated (control group of H2O2 only cells) or treated with 200µM H_2O_2 for two hours with incubation for 48 or 72 hours in fresh medium with either no additive (H2O2 only, 48 and 72 hours respectively). The control groups in the remaining columns were confluent cells, not treated with H_2O_2 but treated with the additive noted on the x axis (1K1, HGF or both) for 60 mins. Remaining groups were treated with 200µM H_2O_2 for two hours with incubation for 48 or 72 hours in fresh medium with the additive labelled on the x axis. These are

labelled as 48 or 72 hours (post H_2O_2 treatment). There was an increase in ERK phosphorylation (pERK) from control to 48 and 72 hours with little effect seen in the presence of 1K1 or HGF at either time point. Two way ANOVA showed a significant difference due to time point ($p < 0.002$), but not overall and not due to treatment.

5.3.6 Effect of 1K1 and HGF upon the biliary epithelial cell EMT phenotype induced by oxidative stress

The experiments on 1K1 and HGF downstream signalling and the proliferation assays indicated that both 1K1 and HGF were active in immortalised BEC. Therefore the next logical experiment therefore was to investigate the effect that 1K1 and HGF had upon the EMT phenotype in BEC exposed to H_2O_2. To do so, BEC were treated with 200μM H_2O_2 for two hours as previously; cells were then washed and new medium was added (no treatment, + / - 1K1 or HGF at 10ng/ml). This was the only treatment point; drugs were not re-administered. Incubation was for 48 or 72 hours with staining by immunofluorescence. Results are shown in Figures 5.17-5.26.

In terms of epithelial antigens, only CK19 was investigated (Figure 5.18), as this had proved to be a reliable indicator during previous experiments and is used clinically as a marker to define BEC. 48 hours after H_2O_2 treatment, cells treated with 1K1 or HGF had retained much stronger CK19 staining than the H_2O_2 treated cells. The BEC also retained cobblestone morphology. At 72 hours it appeared that HGF-treated cells had a stronger CK19 expression than those treated with 1K1, as they also seem to be increased in number, however morphological assessment is extremely subjective and should be used with caution. It was decided not to quantify the immunofluorescence data as before (using image J), this was due to the fact that the numerical results reflected changes that were apparent to the naked eye and served only to produce a numerical value that meant very little. If a change was not obvious using the naked eye, then previous results would dictate that the numbers

and subsequent statistics derived from them, would be equivocal too. For these reasons it was decided that further quantification would not be used.

The mesenchymal antigens fibronectin (Figure 5.19), vimentin (Figure 5.20), S100A4 (Figure 5.22) and αSMA (Fig. 5.26) were assessed following H_2O_2 exposure, + / - 1K1 or HGF (10ng/ml). Almost universally, expression of these antigens was abolished by either 1K1 or HGF. The most notable observations were that vimentin expression (Figure 5.20) appeared to have an increased expression at 72 hours after HGF administration, as did αSMA (which also showed a slight increase with 1K1 at 48 hours).

pSMAD2/3 expression (Figure 5.21) was assessed following H_2O_2 exposure, + / - 1K1 or HGF (10ng/ml) and showed an up-regulation at 72 hours, although this was less evident (though still present) at 48 hours. When 1K1 and HGF were added, this expression was completely abolished, aside for a slight expression at 48 hours following treatment with 1K1, and this was only seen in a few cells.

Autophagy levels were also assessed as they had been previously, by the assessment of Atg14 (Figure 5.24) and LC3B (Figure 5.25) levels. Following H_2O_2 exposure, these levels were dramatically increased. Atg14 levels were decreased by both 1K1 and HGF treatment, with 1K1 treated cells exhibiting more obvious puncta at both 48 and 72 hours. LC3B levels were reduced by both 1K1 and HGF at 48 hours but were massively increased by HGF at 72 hours, while they were reduced further by 1K1 at 72 hours.

In order to identify the underlying mechanism(s) for the changes observed in mesenchymal antigens and markers of autophagy, β6 Integrin (Figure 5.23) and p21 (Figure 5.27) were stained for. αVβ6 Integrin expression was not observed in any of the treated groups compared to the H_2O_2 only treated groups, at 48 and 72 hours. The expression of p21 was dramatically reduced by both 1K1 and HGF, but was still observed in both groups.

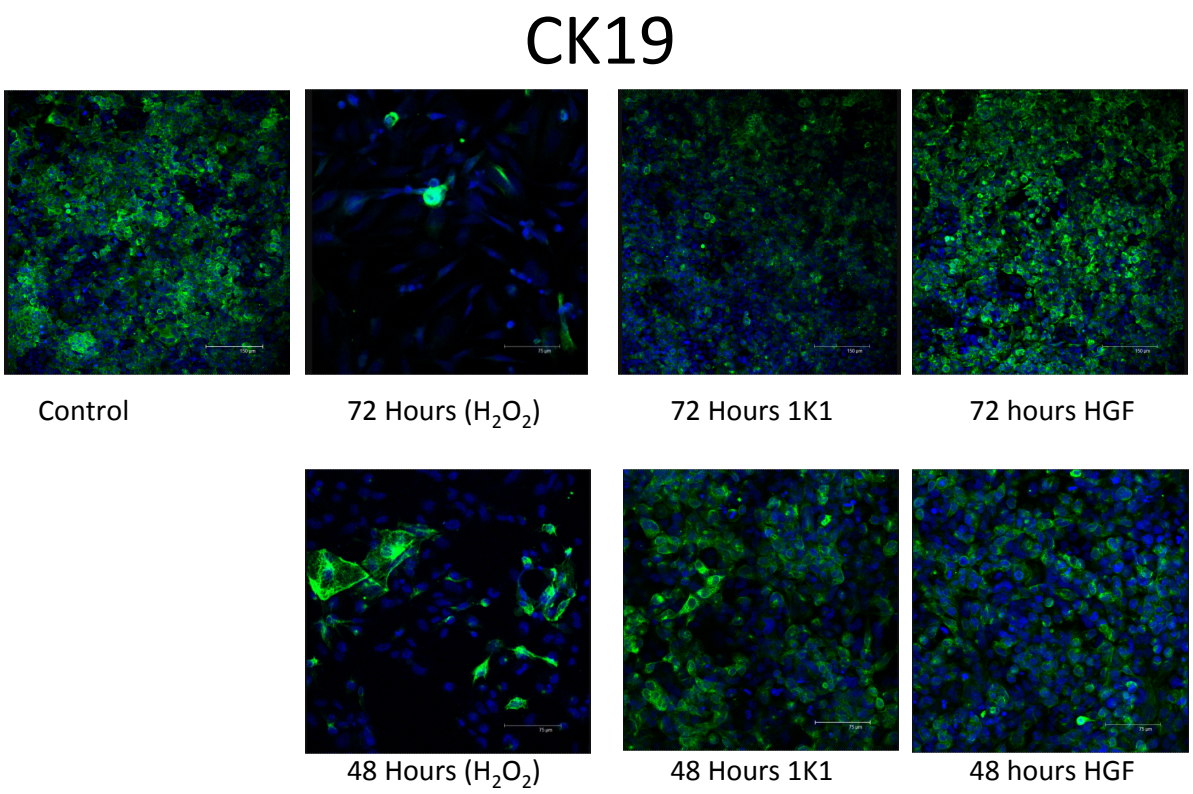

Figure 5.18: Expression of CK19 in immortalised BEC following H_2O_2 treatment + / - 1K1 or HGF at 10ng/ml. As shown previously, oxidative stress-induced EMT lead to the loss of CK19 expression in BEC at 48 and 72 hours after the insult by H_2O_2. Addition of either 1K1 or HGF prevented this loss; there was some variability in this with HGF seeming to have a slightly greater effect upon retention of CK19. Figures representative of three separate experiments

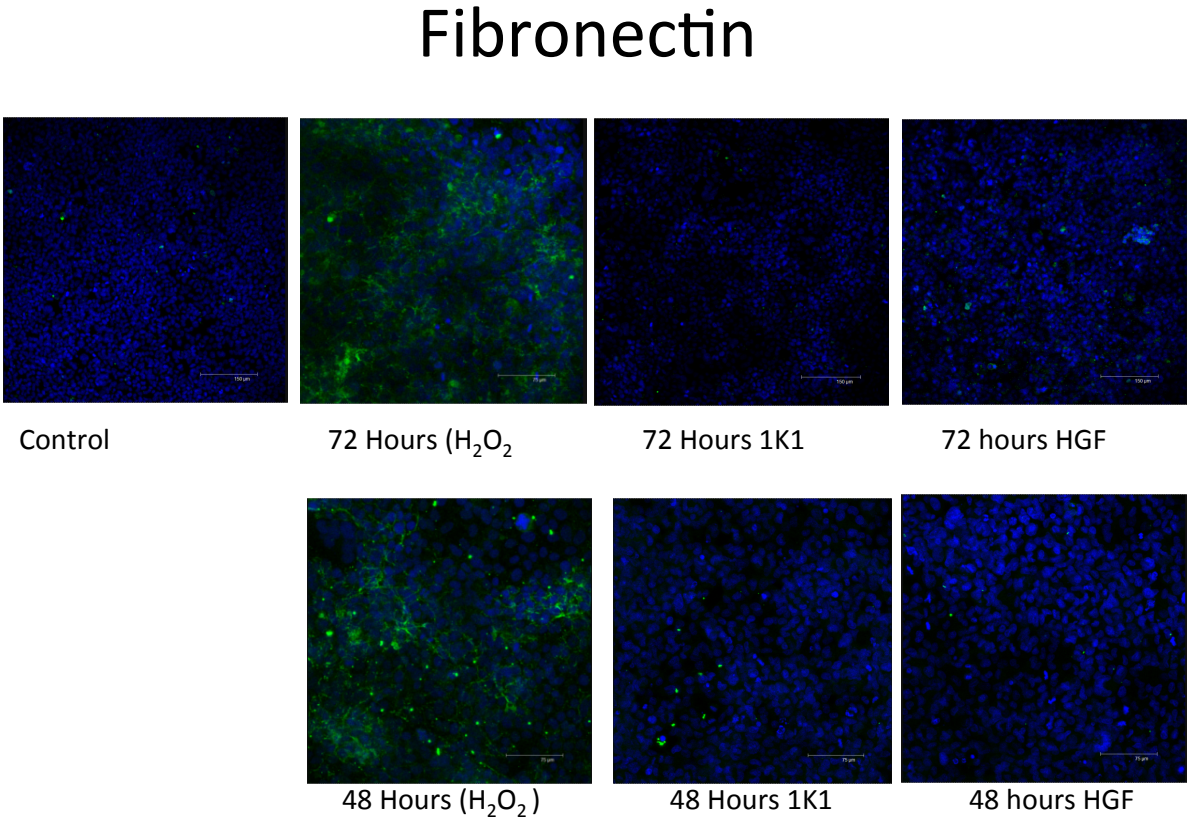

Figure 5.19: Expression of fibronectin in immortalised BEC following H_2O_2 treatment + / - 1K1 or HGF at 10ng/ml. Fibronectin expression is a feature of the defined EMT in reaction to oxidative stress. Addition of either 1K1 or HGF entirely prevented the expression of fibronectin following H_2O_2 exposure. Figure representative of three separate experiments.

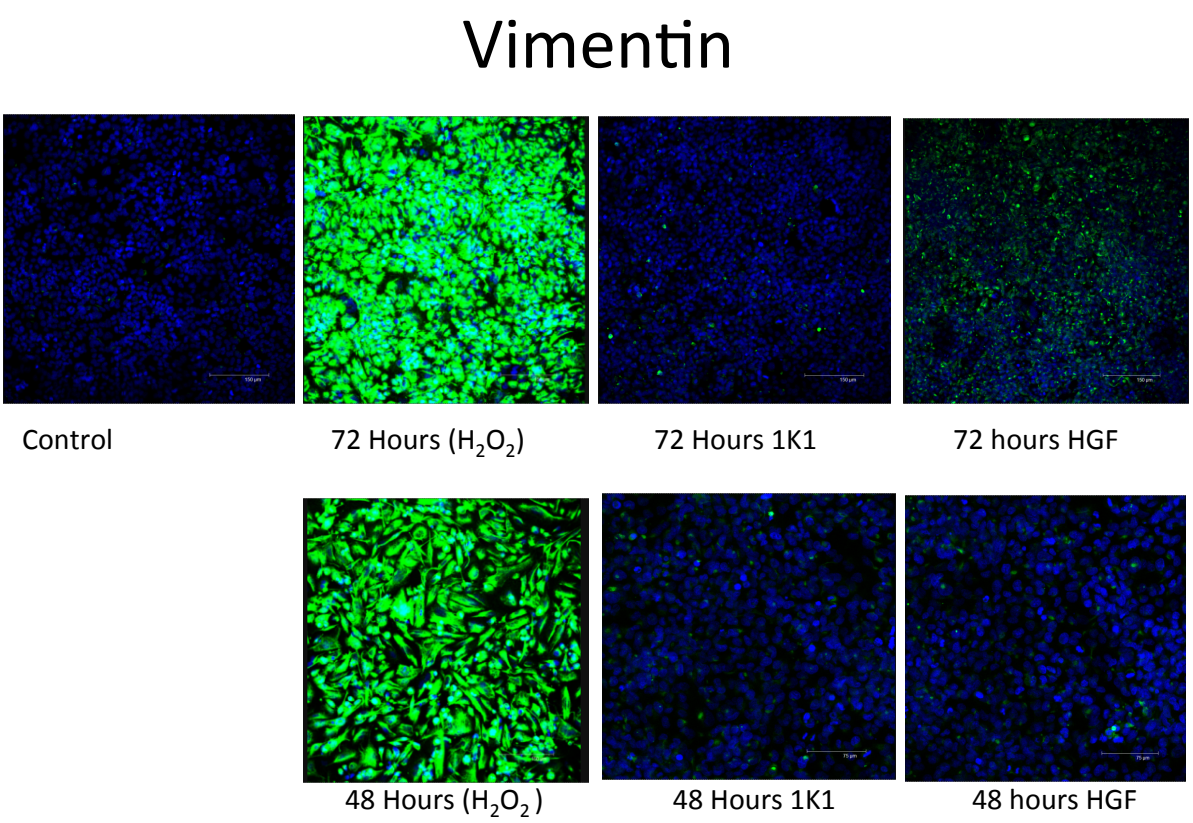

Figure 5.20: Expression of vimentin in immortalised BEC following H_2O_2 treatment + / - 1K1 or HGF at 10ng/ml. Strong expression of vimentin was seen following the insult with H_2O_2. This was entirely abrogated by the presence of 1K1. There is a smaller, but nevertheless notable, effect in the presence of HGF, seen in the reduced level of vimentin expression at 72 hours. Figure representative of three separate experiments.

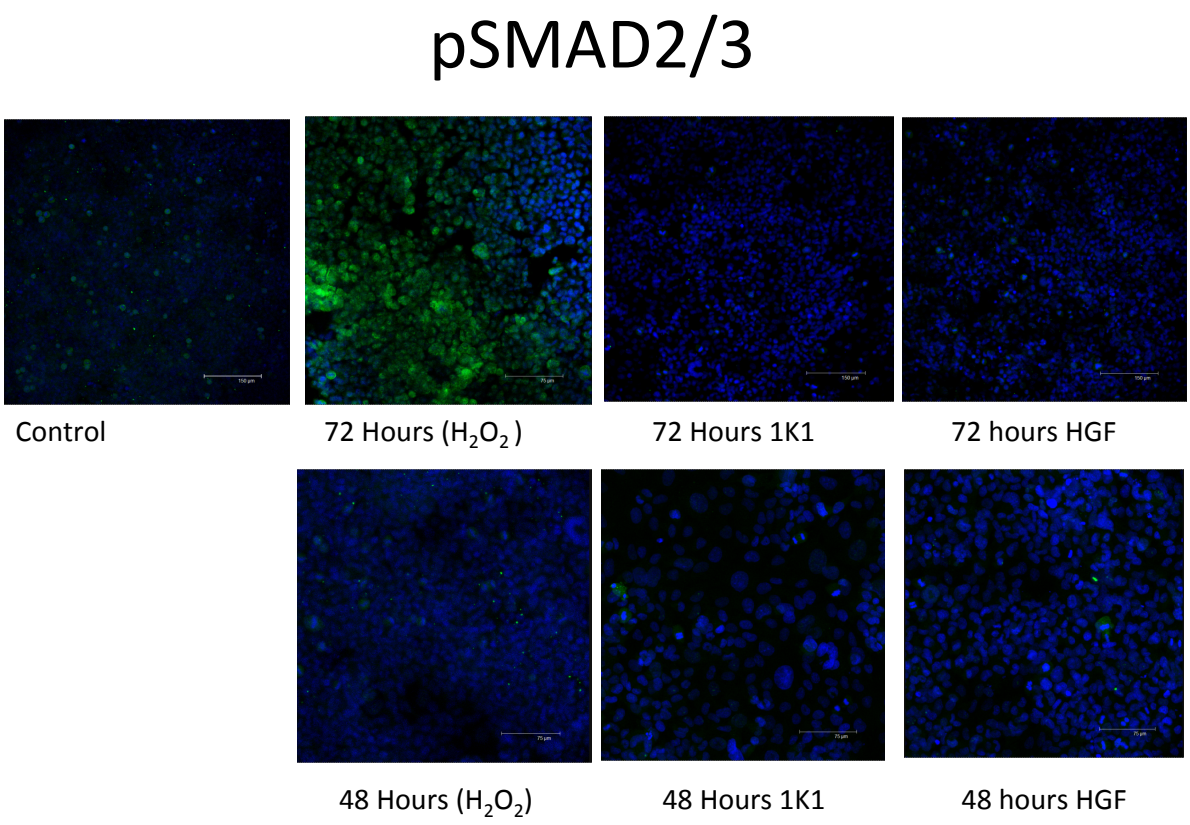

Figure 5.21: Expression of pSMAD2/3 in immortalised BEC following H_2O_2 treatment + / - 1K1 or HGF at 10ng/ml. pSMAD2/3 expression was substantially up-regulated at 72 hours; this effect was entirely prevented by the addition of either HGF or 1K1. Figure representative of at least three separate experiments.

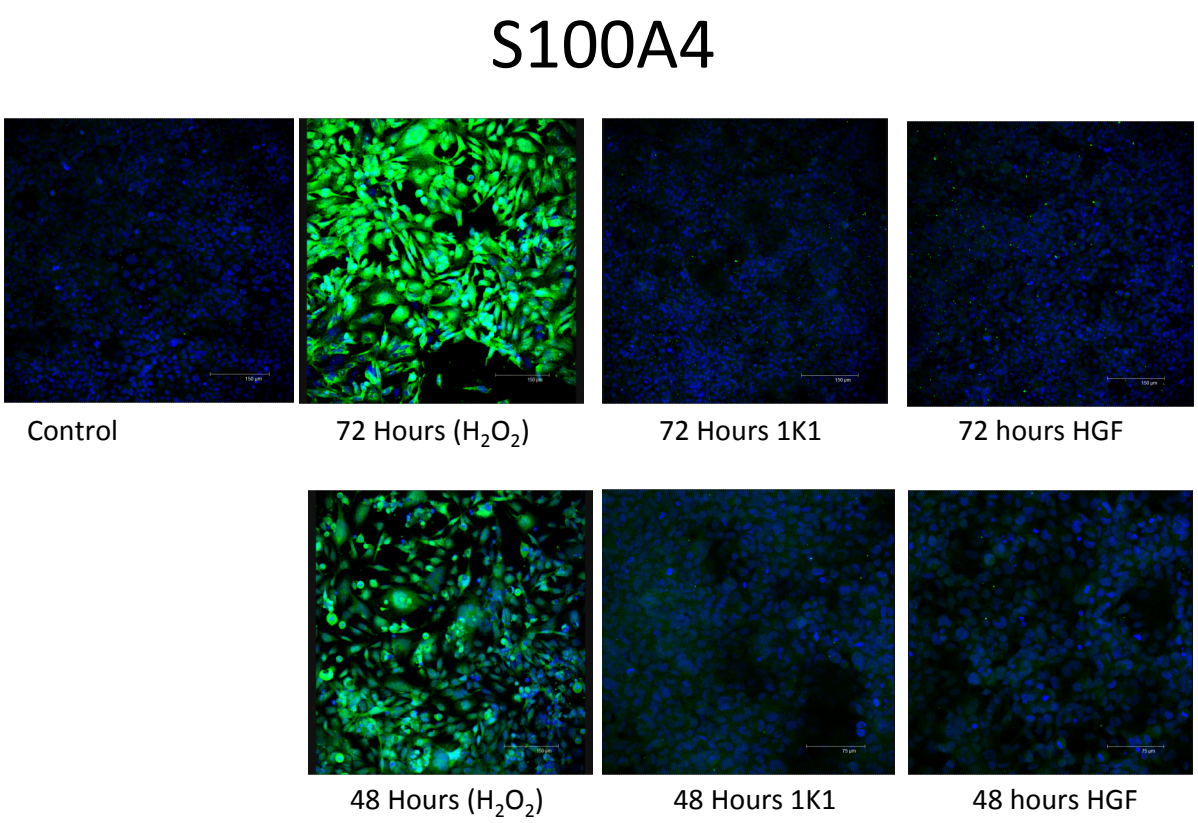

Figure 5.22: Expression of S100A4 in immortalised BEC following H_2O_2 treatment + / - 1K1 or HGF at 10ng/ml. S100A4 is one of the fundamental proteins to the EMT process and was strongly up-regulated following H_2O_2 exposure. Again, this antigen was completely prevented from expression in the presence of either HGF or 1K1. Figure representative of three separate experiments.

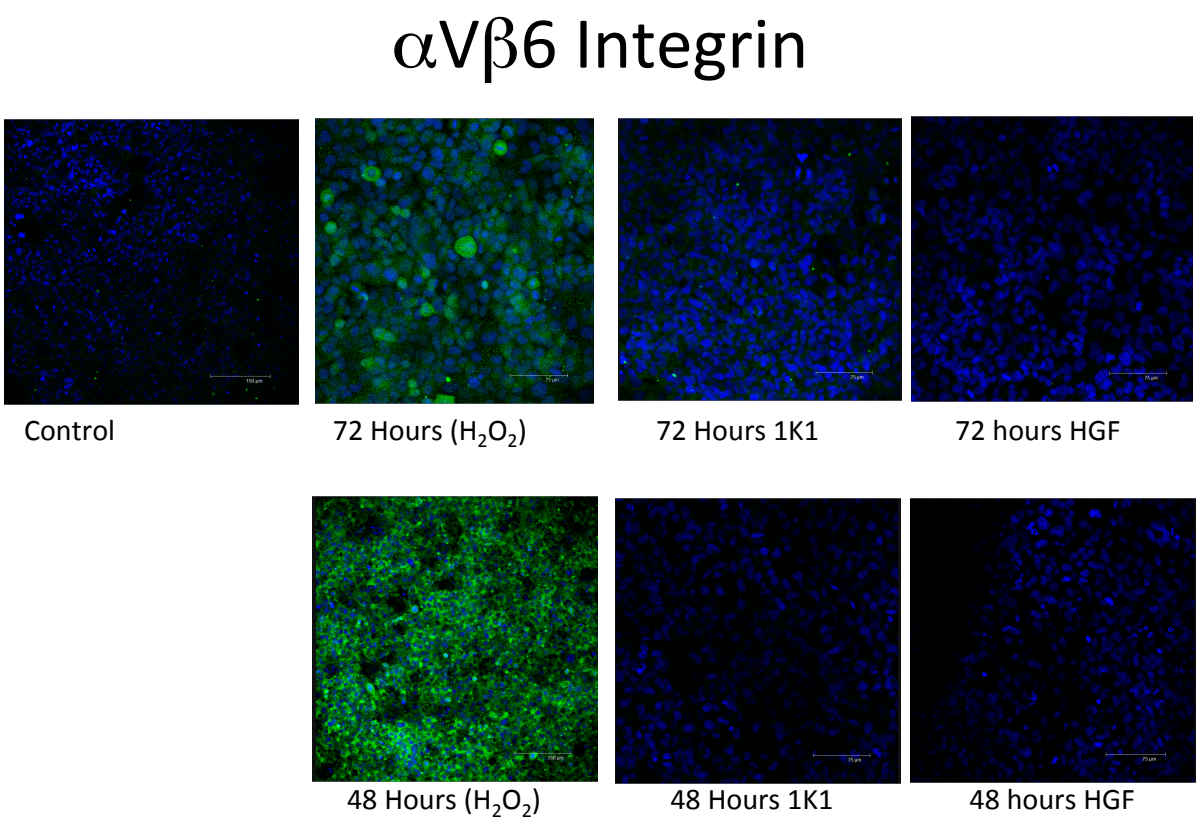

Figure 5.23: Expression of β6 integrin in immortalised BEC following H_2O_2 treatment + / - 1K1 or HGF at 10ng/ml. Strong β6 integrin expression was seen following H_2O_2 exposure. There is no evidence of any β6 expression following the addition of either HGF or 1K1. Figure representative of three separate experiments.

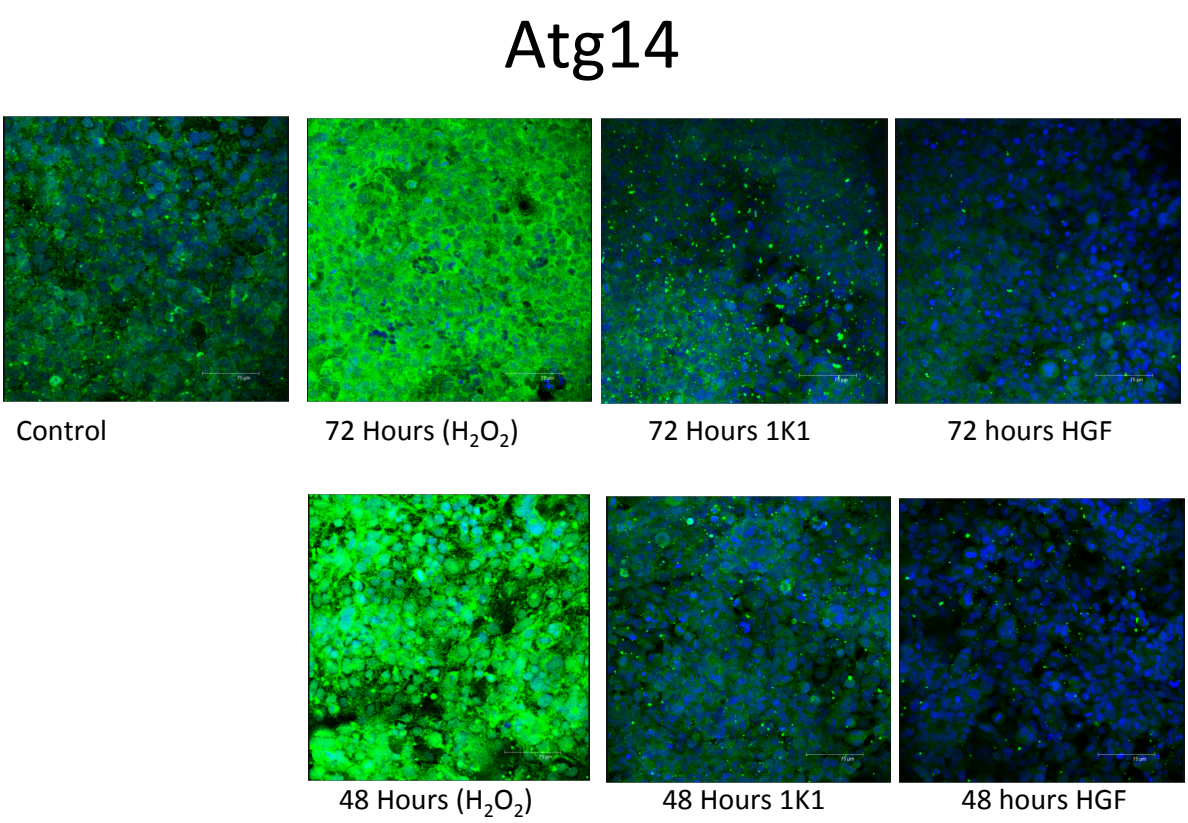

Figure 5.24: Expression of Atg14 in immortalised BEC following H_2O_2 treatment + / - 1K1 or HGF at 10ng/ml. Atg14 expression was up-regulated to a large extent following oxidative stress at both 48 and 72 hours. While neither HGF nor 1K1 reduced these levels to zero, they both seemed to cause a reduction in levels to baseline or below baseline. There appeared to be slightly more Atg14 expressed in the 1K1 treated groups relative to those receiving HGF. Figure representative of three separate experiments.

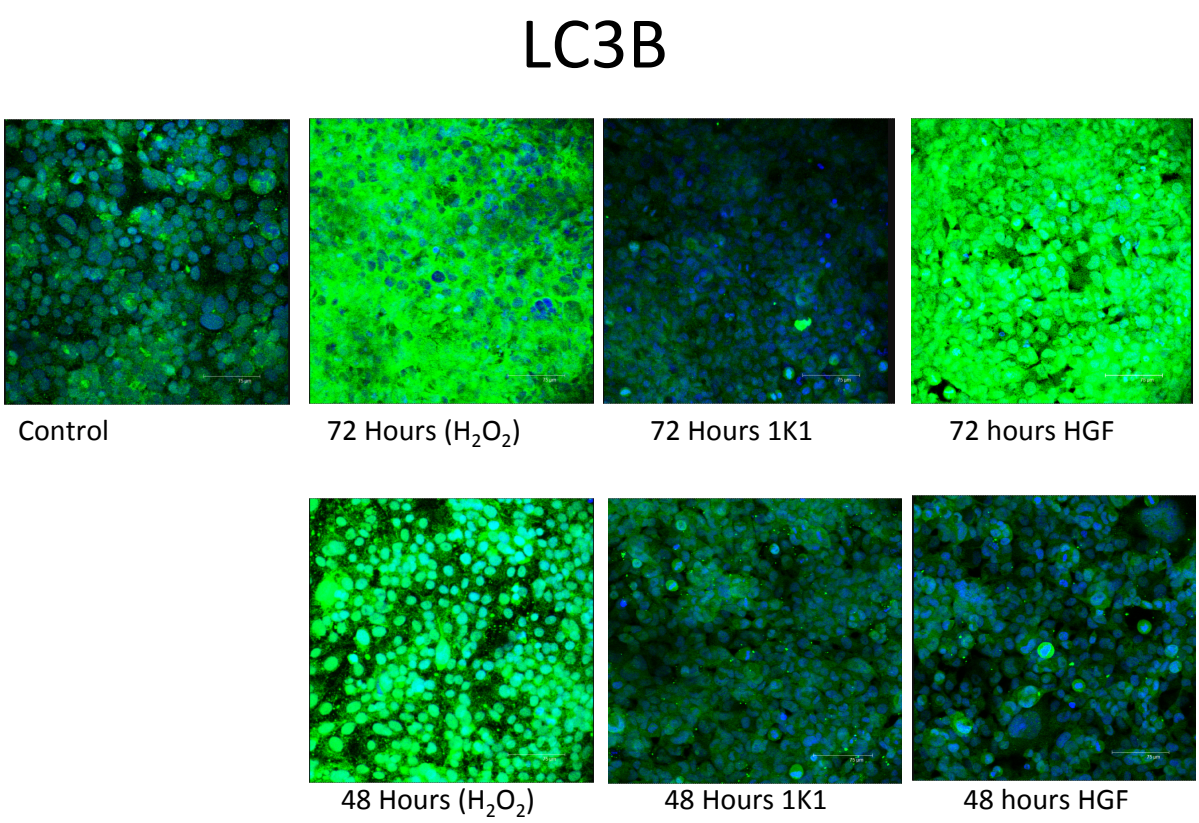

Figure 5.25: Expression of LC3B in immortalised BEC following H_2O_2 treatment + / - 1K1 or HGF at 10ng/ml. LC3B expression increased by a large amount following oxidative stress. The addition of HGF reduced the level seen at 48 hours, but not at 72 hours. Addition of 1K1 reduced the expression of LC3B in a sustained manner. Figure representative of three separate experiments.

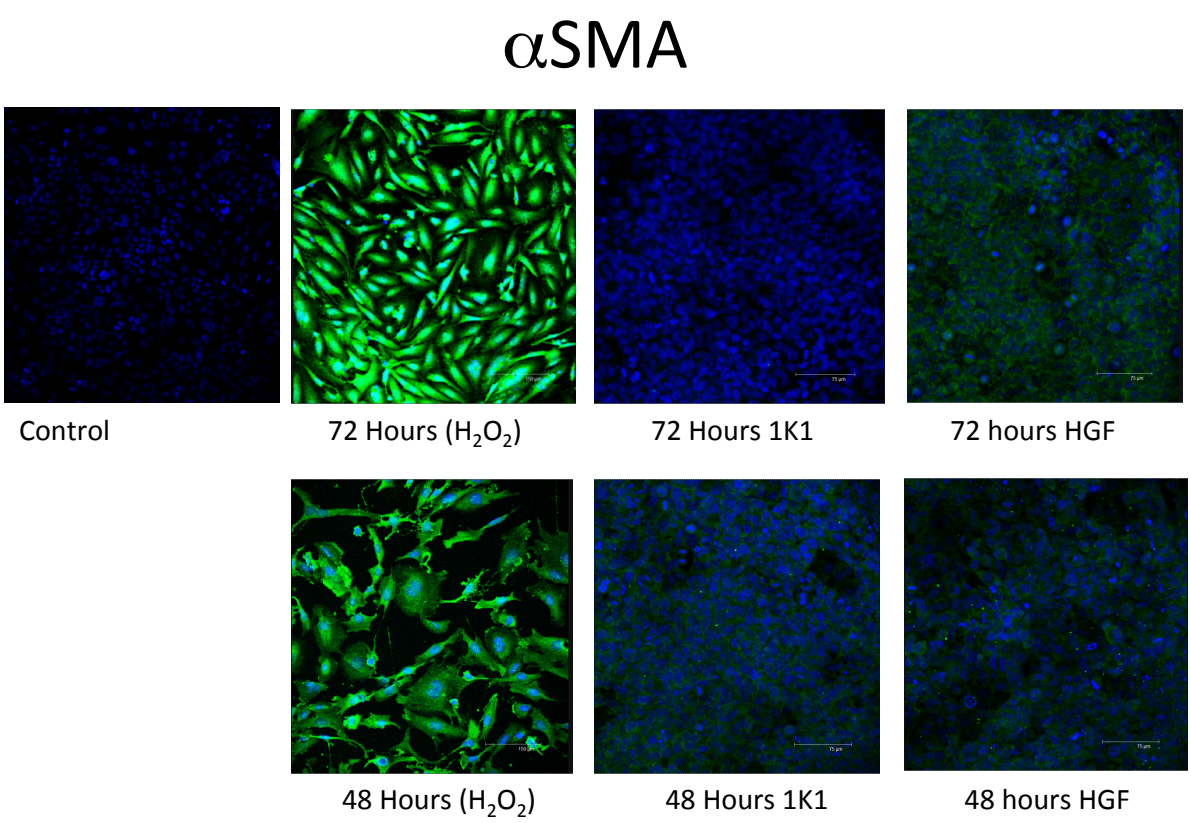

Figure 5.26: Expression of αSMA in immortalised BEC following H_2O_2 treatment + / - 1K1 or HGF at 10ng/ml. αSMA is often used as a marker for myofibroblasts or activated hepatic stellate cells (HSC). It was notably increased in BEC following oxidative stress. Addition of 1K1 prevented this expression, whereas the expression of αSMA at 72 hours was only partially prevented by HGF. Figure representative of three separate experiments.

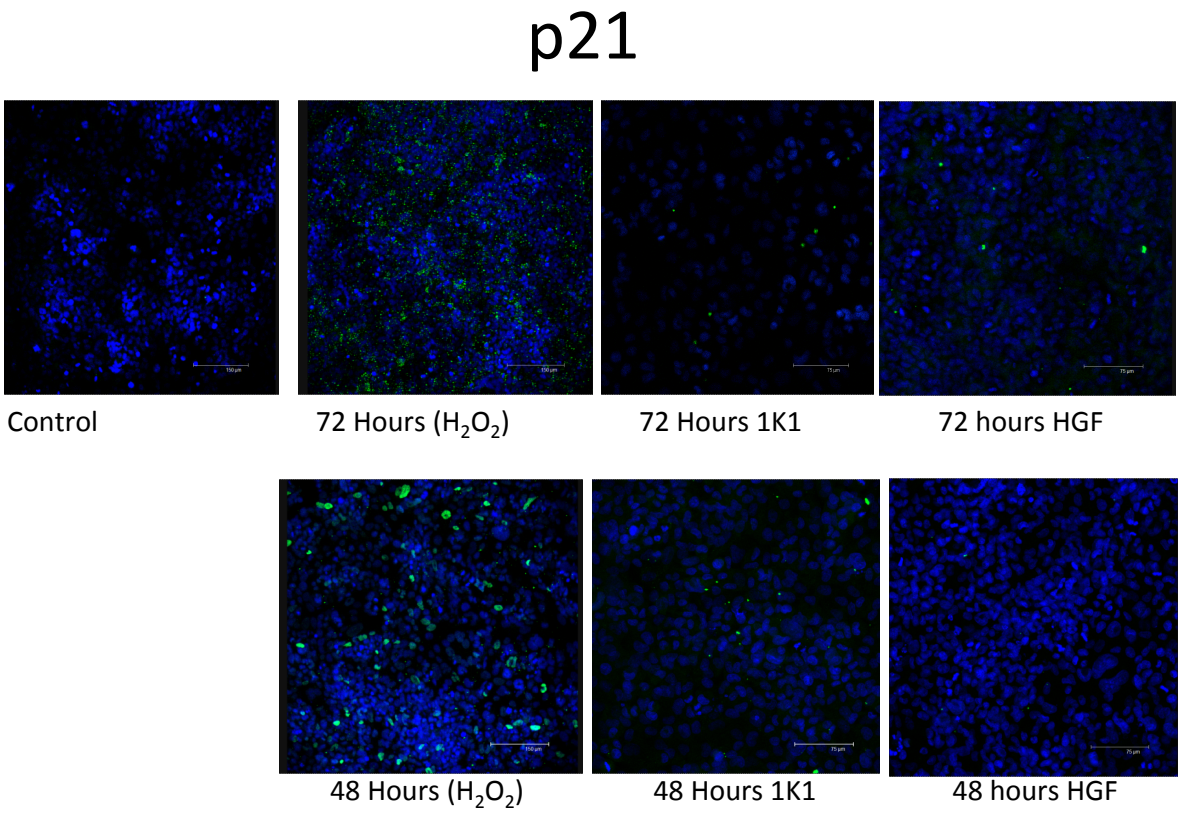

Figure 5.27: Expression of p21 in immortalised BEC following H_2O_2 treatment + / - 1K1 or HGF at 10ng/ml. Both HGF and 1K1 prevented any up-regulation of p21 following H_2O_2 injury, with only occasional cells staining positive for p21. Figure representative of three separate experiments.

5.4 Discussion

5.4.1 To investigate autophagy and its manipulation within the previously described biliary epithelial cells (BEC) in vitro model of oxidative stress-induced EMT

As previous research had identified a link between autophagy and p21 activity in rodent BEC (Sasaki, Miyakoshi et al.), assays to investigate autophagy levels were conducted in line with the literature. This made it possible to show altered levels of autophagy, and to manipulate autophagy with inhibitors and pharmaceutical compounds. In the current study, use of the most widely used autophagy inhibitor, 3-MA (Barth, Glick et al. 2010) yielded interesting results. The choice of solvent was clearly important in working with 3-MA, with DMF causing an apparent loss of epithelial characteristics that was not observed when 3-MA was dissolved in DMSO. As noted in section 1.9; the use of two indicators of the autophagy cycle showed different responses, with Atg14 showing early autophagy changes and LC3B late changes associated with extension of the autophagosome membrane.

The application of 3-MA to H_2O_2 treated cells was not as helpful as expected given that it is the inhibitor of choice for autophagy assays *in vitro*. The presence of 3-MA gave a reduction is LC3B levels, and vimentin expression was prevented. However, reduction in CK19 was not prevented and numerous other experiments remained incomplete as the cells sloughed off the chamber slides following 3-MA application. It is unclear whether this was due to effects on adhesion, toxicity or was unrelated to the 3-MA exposure. It was clear however that autophagy inhibition on it's own is

not the panacea for treatment that some might believe (Sasaki, Miyakoshi et al.), as epithelial function was still lost when autophagy was inhibited.

Previously a FACS experiment had been utilised comparing ROS with autophagy and apoptosis/necrosis specific dyes (Bhogal, Weston et al. 2012) and is described in section 2.5. Several attempts were made to use this assay in the immortalised BEC model here in order to provide an alternative readout for autophagy as well as to investigate intracellular ROS production, identifying whether mitochondrial ROS could be identified in senescent cells as has been previously described (Passos and von Zglinicki 2005, Passos, Saretzki et al. 2007, Passos, Nelson et al. 2010). The initial data from this experiment were not encouraging and are displayed in section 5.5. Numerous attempts were made to resolve the issues experienced with the spectral overlap and lack of good controls, none of these became sufficiently robust enough in the time available to present the work here. It is envisaged that this assay will be further optimised for the conditions available and is discussed in chapter 6.

5.4.2 To investigate potential routes by which TGF-β could be activated in BEC undergoing oxidative stress-induced EMT

The observation of αVβ6 integrin induction due to H_2O_2 exposure as well as by immunosuppressive agents also suggested that this integrin played a significant role in the regulation of TGF-β in this system. A strategy that has been used successfully is αVβ6 integrin blockade, using a specific peptide. This was first discovered by Kraft et al (Kraft, Diefenbach et al. 1999). When this peptide was applied to the BEC H_2O_2

model, the results were variable, both between experiments and antigens. αSMA was occasionally seen to be up-regulated in peptide-treated groups, as was S100A4. Ck19 expression levels were also variable. It may be that, due to the close nature of the contact between integrins and latent TGF-β, peptide penetrance was variable; and that this was affected by the cell density. The images given by these experiments are representative of a series of observations, but it would be inappropriate to state that the reproducibility was anything other than poor in these experiments.

At the onset of the experiments it was believed that a likely candidate for an oxidative stress induced EMT would be TGF-β1. Inhibition of the RGD motif on the LAP of TGF-β1 would therefore be a reasonable method of inhibiting this phenomenon. As we have seen in this assay system, TGF-β1 levels remain constant whereas TGF-β2 levels are dramatically increased. This would imply some role for TGF-β2 that has not been previously described. The activation and up regulation of αVβ6 integrin would, however imply that LAP containing RGD would be preferentially active in this system, precluding TGF-β2. What is not certain is how TGF-β2 is activated, while the LAP of TGF-β2 lacks an RGD motif this does not mean that there are not other binding sites that act in the same manner to RGD.

Work from Dean Sheppard's laboratory has investigated differential activation of TGF-β subtypes by specific integrins during wound healing. This indicates that there may be specific integrins that regulate TGF-β in ways that are context dependent (Neurohr, Nishimura et al. 2006, Katsumoto, Violette et al. 2011). Blocking αVβ6 integrin alone would work if this is the only integrin involved in this regulation and

if TGF-β2 is not the main candidate responsible. When these factors are considered it is reasonable to conclude that the inconsistent nature of the αVβ6 integrin blocking experiments hints at a more complex regulation of TGF-β within the BEC assay and potentially at a degree of redundancy in TGF-β activity. Investigation of these aspects of BEC biology would require a separate study.

5.4.3 To identify what role, if any, is played by immunosuppressive agents in contributing to BEC dysfunction

Two immunosuppressive agents were investigated for their effects upon BEC. While most liver units use Tacrolimus/FK506 with mycophenolate mofetil (MMF) being used as a second line agent, some use rapamycin (Sirolimus) more frequently (Wiesner and Fung , Neuberger, Mamelok et al. 2009, Shaked, Ghobrial et al. 2009). By using autophagy readouts as well as EMT markers it was shown that the presence of FK506 conferred a lower level of autophagy induction onto H_2O_2 treated immortalised BEC, and did not induce an EMT or any β6 integrin expression. Conversely, the effect of rapamycin on BEC was to up-regulate autophagy (also a known feature of rapamycin, owing to its inhibition of mTOR).

The up-regulation of β6 integrin in response to rapamycin added a further level of complexity to this work. αVβ6 integrin is a known activator of TGF-β {Sullivan, 2011 #316}{Chen, 2013 #321}, and this implies that rapamycin has the ability to induce activation of latent TGF-β found in the ECM - thereby increasing the degree of fibrosis. This is in stark contrast to publications by many commentators who advocate the anti-fibrotic effects of rapamycin (Dunkelberg, Trotter et al. 2003,

Fung and Marcos 2003, Trotter 2003, Fung, Wu et al. 2009, McKenna and Trotter 2012). It was shown in this study that rapamycin alone could induce EMT in BEC, independent of p21 up-regulation. This implies that another signalling pathway or pathways were responsible for these changes, possibly related to the autophagy induction that was observed in these cells.

These data may hint at the long described duct sparing effects that are known in patients treated with tacrolimus (Lunz, Contrucci et al. 2001). In order to further investigate this phenomenon a further study of the in vitro effects of the agents would be required with corroboration from human biopsy material. Simply adding these compounds to the existing oxidative stress induced EMT is unlikely to yield a meaningful result.

5.4.4 To investigate the potential of 1K1 to prevent oxidative stress-induced EMT in our *in vitro* model

It was shown in chapter 4 that HGF and 1K1 had evidence of activity in immortalised BEC without the need for administration of HSPG. HGF has been shown to prevent TGF-β1-induced EMT in BEC; more specifically it has been shown to work in the cell line used here. It was therefore expected that the prevention of EMT observed with HGF would occur in this model. It was also hoped that 1K1 would show a similar efficacy in this regard; this was also demonstrated. The signalling pathway data for these two molecules is interesting, as HGF appears to induce proliferation of BEC (and the activation of the proliferative MAPK, ERK) to a greater degree than 1K1. In addition, the suppression of TGF-β signalling pathways via SMAD2/3 appears to be more effective in the presence of 1K1. Combined with

the autophagy data (1K1 being a much less potent inducer of autophagy) and the variability in antigen expression, a case could be made that HGF and 1K1 utilise related, but different, signalling pathways.

It is not clear exactly which pathways these could be. Interestingly a phosphor-specific ELISA of Akt conducted along the same lines as the SMAD2/3 and ERK 1/2 ELISA failed to show any up regulation in response to oxidative stress, 1K1 or HGF. Due to the paucity of time available it was not possible to further investigate this, it is quite possible that the assay simply did not work or there was a technical issues with the plate reader. However, Akt is a known key downstream target of c-Met (Nakamura, Sakai et al. 2011) and a lack of response would be surprising, although there are reports of c-Met activation leading to potentiation of the EGFR pathway independently of Akt (Dulak, Gubish et al. 2011).

HGF has been assessed as a potential therapeutic agent in liver disease many times. It has known positive effects in hepatectomies and in regeneration of the liver generally (Burr, Toole et al. 1998, Xia, Dai et al. 2006, Arends, Slump et al. 2008). There is however the theoretical risk of potentiation of carcinogenesis and angiogenesis (Ding, Merkulova-Rainon et al. 2003, Leroy, Deheuninck et al. 2006, Mangold, Wu et al. 2011, Shang, Deguchi et al. 2011), which would not be ideal. This study has shown that engineered forms of HGF may have the therapeutic potential of HGF but in more stable forms, with lower activation of autophagy and with a lower proliferative capacity. Whether these molecules can offer a convincing therapeutic option requires further study into the targeting, sequestration,

breakdown and pro-carcinogenic effects; This falls outside the scope of the current study.

5.5 Appendix

The data in this appendix relate to the 4-colour FACS assay originally described by Bhogal (Bhogal, Weston et al. 2012). Several attempts were made to optimise this assay for the BEC oxidative stress model. Sadly it was not possible to optimise an apoptosis control, which severely limited the data that could be obtained. The following graphs (figures S1-S3) demonstrate the gating strategy and single stain data for the DCF, MDC and 7-AAD stains that were used (section 2.5). It is intended that these experiments will be repeated but using an alternative necrosis/apoptosis stain. It is also envisaged that the current assay could be used in a confocal microscope providing further data regarding the subcellular location of these processes and their interrelation.

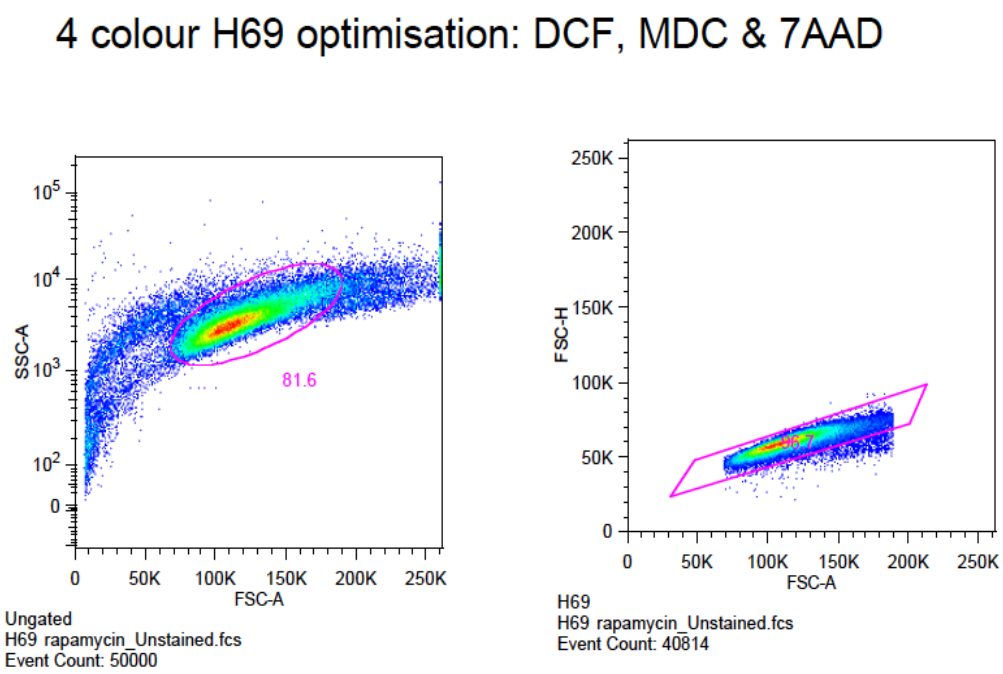

Figure S1: FACS plots showing unstained immortalised BEC plotted forward versus side scatter. The initial gating strategy is shown, encompassing over 80% of events.

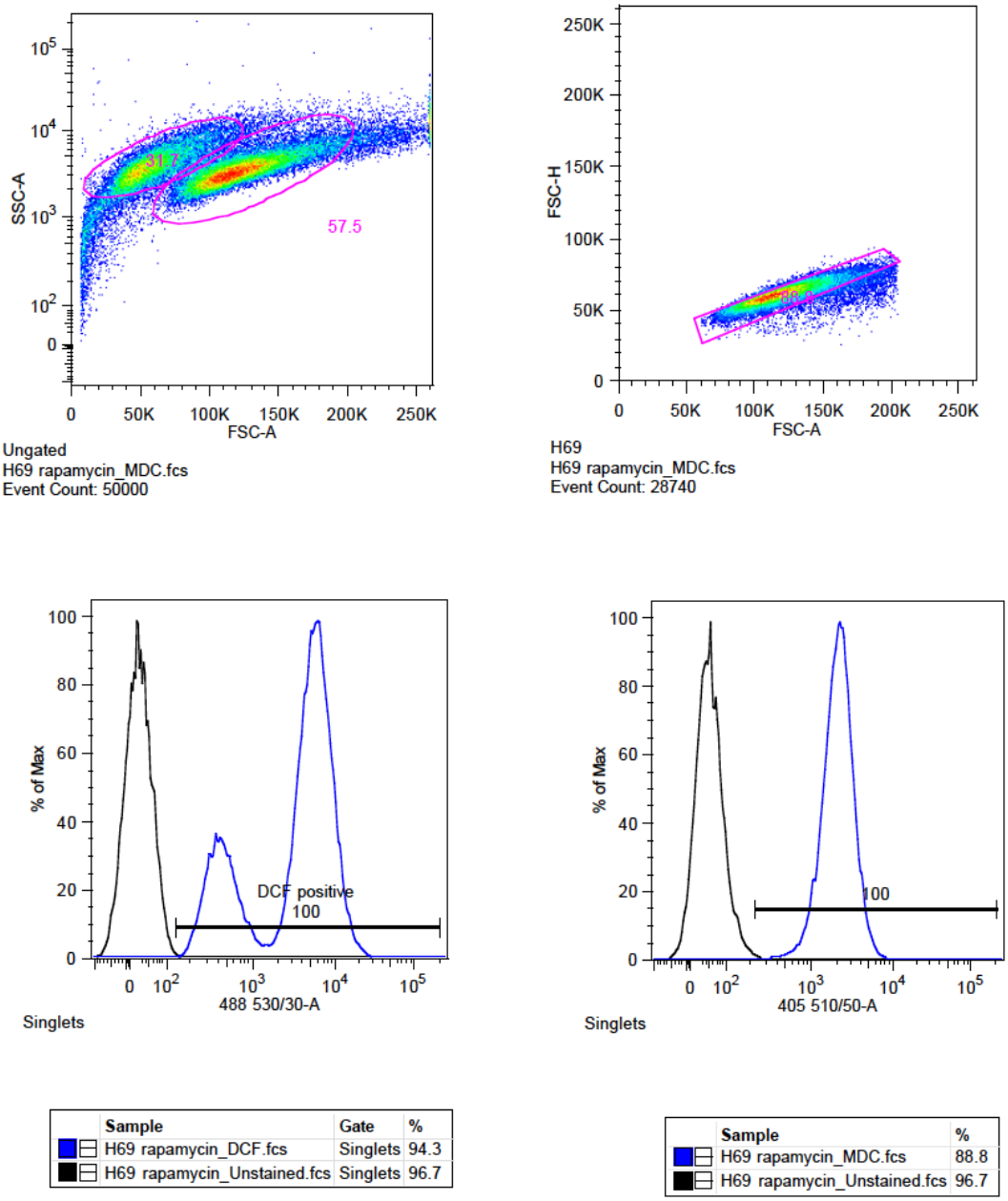

Figure S2: FACS plots showing immortalised BEC post 48 hours of H_2O_2 exposure. The previously applied gating strategy now accounts for less than 60% of events and there is a shift towards a bimodal population. Clear staining controls are shown for 2,7 DCF (ROS dye) and MDC (Autophagy dye).

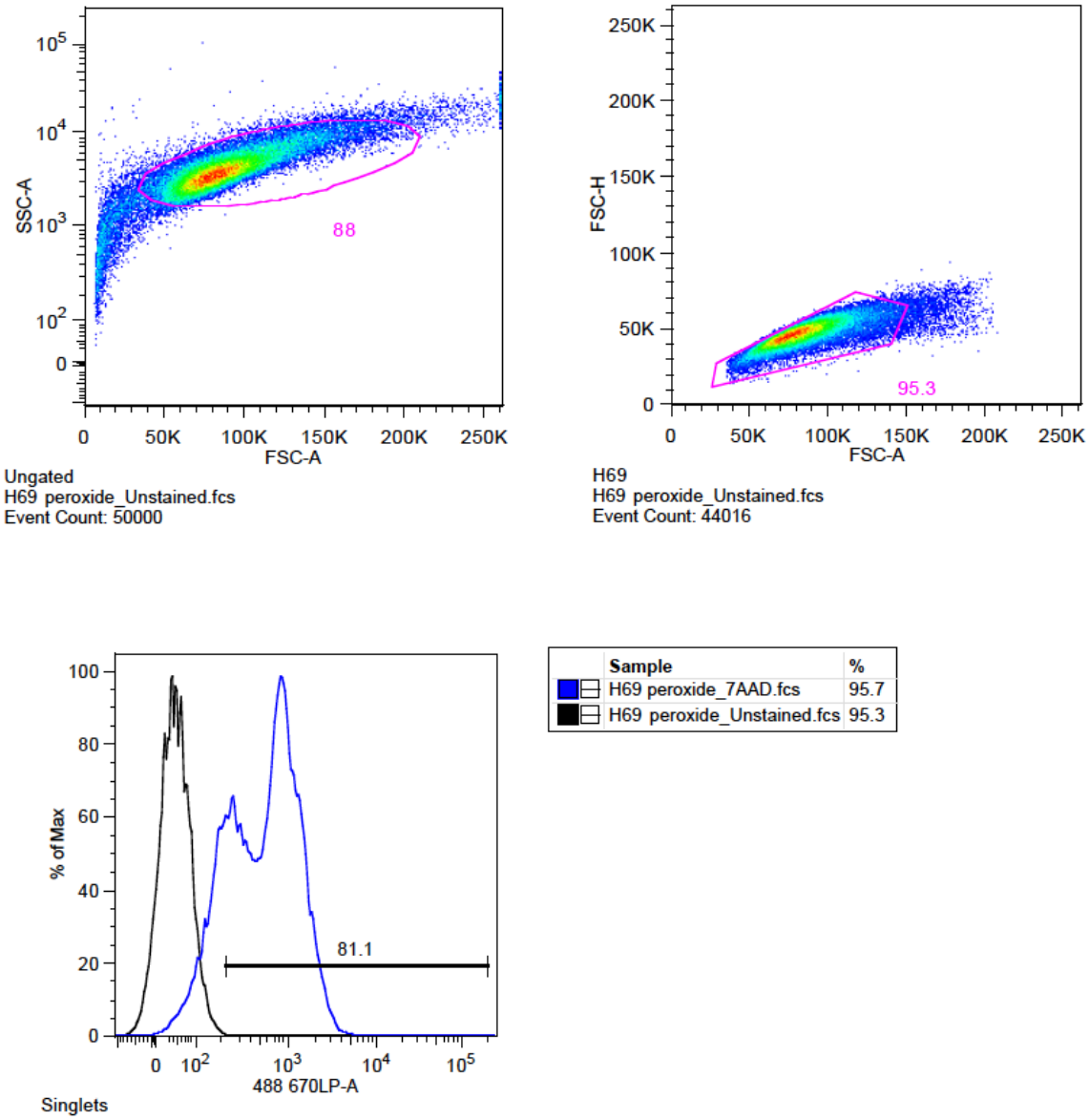

Figure S3: FACS plots showing the gating strategy and staining for the viability stain 7-AAD. There was some overlap but clear populations could be defined. The staining for Annexin V showed no positivity with any of the apoptosis induction agents used.

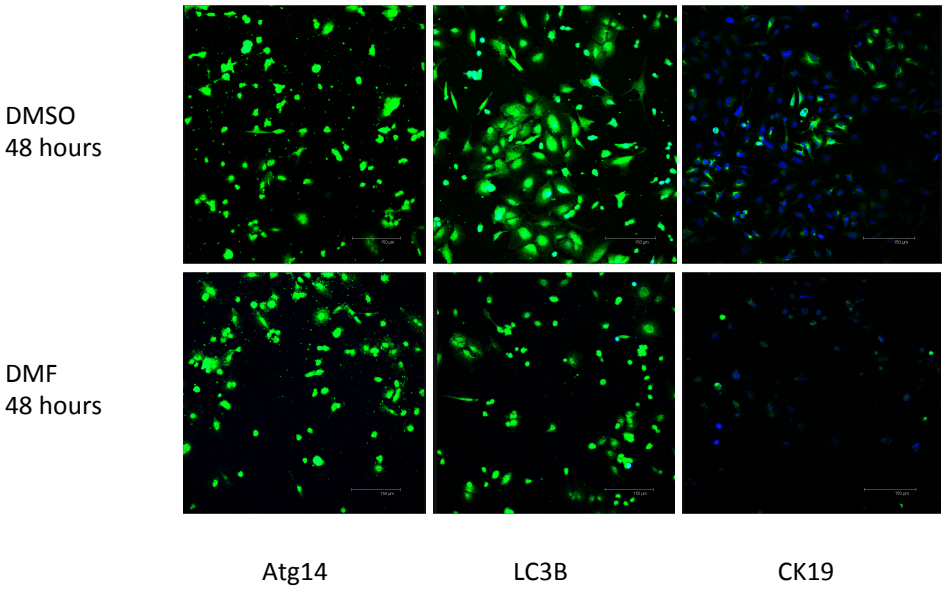

Figure S4; Effect of solvents on BEC autophagy. Immortalised BEC were treated with the same concentration and volume of solvent as used in inhibitor experiments (10µl). BEC were then incubated for 48 hours at 37°C and 5% CO_2. The effect of both solvents on autophagy was similar, a slight increase over baseline. However DMF repeatedly showed a reduction in epithelial characteristics, shown here as a loss of CK19.

6 Discussion

The work in the previous five chapters has shown evidence for the role of senescence in human vanishing bile duct diseases, that senescence has a number of potential effects on BEC that may lead to promotion of disease and fibrosis and that these process can be pharmacologically modified. Inevitably in research, questions arise or are left unanswered; this study is no different. This study was also challenging for a number of reasons unrelated to the conduct of the lab work.

The objectives laid out at the beginning of the fellowship specified a translational project and an industrial partner. What exactly constitutes translational research is a matter of debate. The interpretation of translational research applied here was laboratory-based research that should show a demonstrable patient benefit within 5 years of the conclusion of the study. This inevitably constrains the projects that can be undertaken. Furthermore establishing an industrial partner places further limits on the research areas that can be considered. However, it was clear early on from discussions with the industrial partner that there were significant areas of overlap and potential mutual benefit.

In order to fulfil the initial criteria outlined in the fellowship it was necessary to develop a cell injury assay that would provide reproducible results and that had capacity to test a large number of parameters at once. The BEC assay that had been used in the PhD was developed and refined during the masters project. Once the objectives were clearly defined between the supervisory team and industrial partner several changes were put in place to further optimise the assay, namely the

use of 8-chamber slides rather than 4-chamber (to increase capacity) and the use of ImageJ rather than Volocity software for analysis. Ultimately densitometry analysis was not used for the entire project as it was felt to add little value. The changes that were seen were either present unequivocally or were equivocal and further numerical analysis merely underlined this rather than adding an objective assessment.

6.1 Human biopsy study

Prior to the current study, investigation into senescent BEC had been conducted in some VBDS, most notably PBC but also chronic ductopenic rejection and showed a relationship between increasing numbers of senescent cells with increasing grade of disease (Sasaki, Ikeda et al. 2008, Sasaki, Ikeda et al. 2010). There is a non-concordance between the association of acute rejection and chronic rejection in liver allografts. While there is a clear association between severity and number of episodes of acute rejection and the subsequent development of chronic ductopenic rejection, it is not universally accepted that acute and chronic ductopenic rejection are due to the same phenomenon (Prof. A D Burt, personal communication). Establishing whether there was evidence of senescence in acute rejection of liver allografts would provide more information as to whether acute and chronic rejection are linked by senescence of BEC.

The first experiment (section 3.3.1) was to identify senescence and EMT markers in human liver allograft biopsies and to correlate these with acute rejection grade. This showed unequivocally that there was an association between acute rejection

grade and early senescence of BEC and between grade of acute rejection and BEC EMT.

Knowing that senescent cells are persistent in tissues for up to 10 years (Aravinthan, Scarpini et al. 2013) it is tempting to draw the conclusion that senescent BEC are responsible for the association between acute and chronic rejection. If this is the case it would mean that a human model system could be used to elucidate the time line and association between injury and senescent cell numbers and their effect. With most human diseases we do not know the association between the onset or initiation of injury and the development of the cellular and tissue response that are seen, for example, at biopsy. With allograft recipients we do know when the injury occurred, how long the ischaemic times of the graft were and what drugs the patient has received. This makes transplant recipients ideal candidates for the study of disease processes. However, the results presented were observational only and required validation in an *in vitro* system.

6.2 Establishing and validating a cell line model

Nakanuma's group had already established an *in vitro* model system using rodent BEC that recapitulated the senescence findings observed *in vivo* (Sasaki, Miyakoshi et al. 2010, Sasaki, Miyakoshi et al. 2012). A further aim of this study was to repeat these experiments using human cells and to ascertain the utility of the H_2O_2 induced senescence model worked for human cells. The model was validated using primary human BEC, which gave good results. However, the p21 staining was not the most consistent with there being some problems of antibody trapping in the rat-tail collagen substratum. The p21 staining of primary BEC did serve to reinforce

the findings of Nakanuma's group. However, the next step in this process was to evaluate immortalised BEC in the same model. This worked much more reproducibly, with the immortalised cells giving similar results to those described by Nakanuma (Sasaki, Ikeda et al. 2008). This was most likely due to the lack of inter-donor variability with the cell line in contrast to the primary cells.

Following on from the observation that senescence and rejection grade were associated with markers of BEC EMT, *in vitro* experiments were designed to assess markers of EMT. Oxidative stress-induced EMT was observed clearly using both primary and immortalised cells. Once this was characterised and defined it could then be used for evaluation of potential therapeutics. Characterisation included establishing what was driving the EMT in this system. EMT *in vitro* can be induced by a number of agents; the most classical and well described is TGF-β (Iwano, Plieth et al. 2002, Kalluri and Neilson 2003, Lee, Dedhar et al. 2006). To ascertain if TGF-β was the agent responsible in the oxidative stress model, a pharmacological inhibitor of the TGF-βR was used. This showed clearly and for the first time, that the oxidative stress induced EMT was TGF-β dependent. To my knowledge this was also the first time that TGF-β has been implicated as part of the SASP.

Putting together the data that had been accrued thus far suggested the model system outlined in Figure 6.1. Stressed BEC undergo either death (as necrosis or apoptosis) or opt for a survival niche, such as senescence, with the promotion of the SASP and fibrosis/promoting EMT of other BEC, or via autophagic "slimming down" of the cells. Autophagy had been highlighted as a potential means of manipulating senescent cells by Nakanuma (Sasaki, Miyakoshi et al. 2010, Sasaki,

Miyakoshi et al. 2012) and is an established cellular phenomenon supported by a great deal of freely available data.

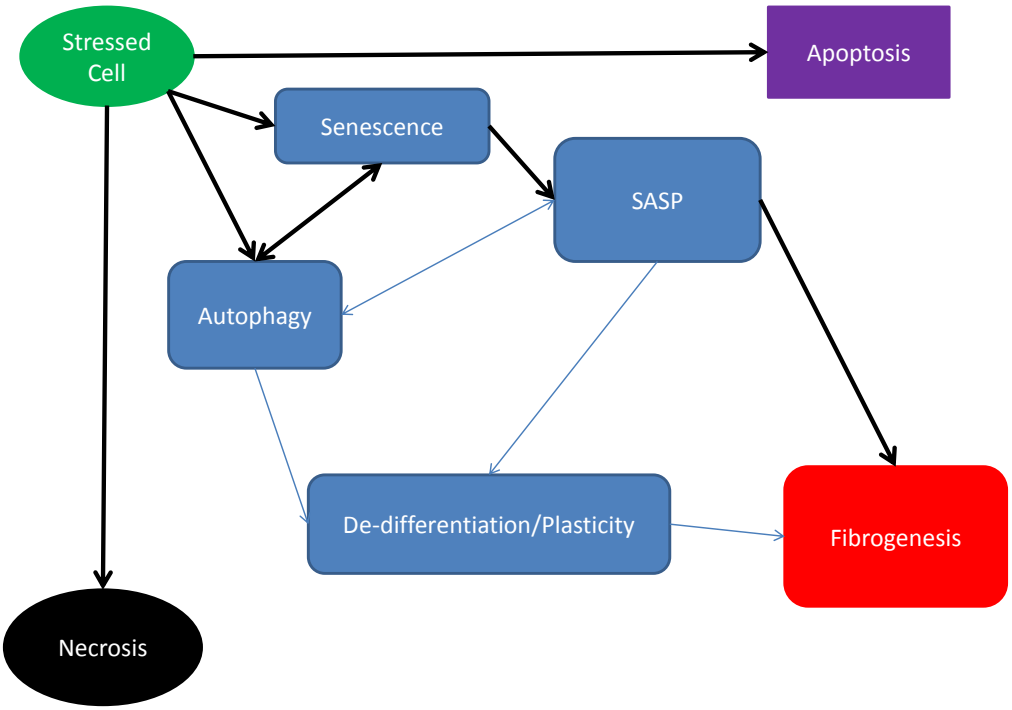

Figure 6.1: Summary of potential stress responses by biliary epithelial cells. Those cells not undergoing apoptosis or necrosis have the potential to activate autophagy and/or become senescent. These processes, and the balance between them, appears able to define the secretory phenotype of the cells and may therefore impact on fibrosis. Bold lines show areas that are established areas of research, whereas the thinner arrows are more speculative or tenuous areas of research.

6.3 Therapeutic modulation of BEC injury

Prior to the investigation of therapeutic agents with the industrial partner it was decided to investigate potential routes of manipulating the in vitro BEC assay. As autophagy had been highlighted by the group of Nakanuma as a potential method of manipulating senescent BEC, blockade (by 3-MA) and stimulation (with the

immunosuppressive agent sirolimus/rapamycin) of autophagy were investigated in the current study, alongside blockade of integrin αVβ6. This integrin had been investigated previously in wound healing and is known to activate TGF-β family members (Giacomini, Travis et al. 2012) (section 1.6.3). Indeed a recent study in rodents showed that pharmacological blockade of αVβ6 integrin was able to prevent ischaemic biliary fibrosis (Chen, Zhang et al. 2013).

Using synthesised peptides several attempts were made to block αVβ6 integrin activity in the *in vitro* assay. This had varying degrees of success. It is unclear if this was due to redundancy in the methods of activating TGF-β, or whether there was an issue with penetrance of the peptide into the autocrine system of confluent cells that prevented the action. Of note, the predominant secreted TGF-β in this system was TGF-β2, which is not activated by the αVβ6 integrin (Neurohr, Nishimura et al. 2006).

There are other integrins that may activate TGF-β family members, though it is believed that this is entirely dependent upon binding RGD sequences in the LAP (section 1.5). The αVβ8 integrin deserves a mention here however, as this activates TGF-β in an entirely different manner. Rather than a traction effect upon the LAP of latent TGF-β, αVβ8 integrin presents TGF-β to cell membrane associated proteases that elaborate soluble TGF-β (Jenkins 2008). While the αVβ8 integrin works in an RGD sequence dependent manner it does highlight alternative methods of TGF-β activation. Monoclonal antibodies specific for several integrins are available and could be tried in this model system (Neurohr, Nishimura et al. 2006). However it is

felt that the most likely candidates for activity in this assay are TGF-β2 and TGF-β3. The molecule Thrombospondin-1 (TSP-1) is also a candidate for the activation of latent TGF-β, acting in an RGD independent manner, via LSKL sequences found in LAP (Willet, Pichitsiri et al. 2013). As TGF-β2 may be the key driver in this model, the role of TSP-1 and the analogous molecule neuropillin-1 (NRP-1) should also be assessed. It should be stated that αVβ8 integrin has a pivotal role in dendritic cell function in the gut. Mice with inactivated αVβ8 function develop colitis (Worthington, Fenton et al. 2012) this may be relevant to the establishment of transplant tolerance.

Two MRes students supervised by JGB during this project undertook further work investigating TGF-β3, showing an increase in TGF-β3 as part of the SASP in BEC (Thompson, Burt et al. 2013). The activation of the TGF-β subtypes requires further investigation as this was not part of either masters project.

Sirolimus became a drug of interest in this assay because of its controversial role as an immunosuppressive agent (Fung and Marcos 2003, Wu, Wen et al. 2006, Saemann, Haidinger et al. 2009) and because it potentiates autophagy. Nakanuma et al (Sasaki, Miyakoshi et al. 2010, Sasaki, Miyakoshi et al. 2012) had shown that inhibition of autophagy prevented the up regulation of senescence markers and the associated SASP. 3-MA used in this context had significant effects upon the cells. The solvents used to dissolve 3-MA themselves had effects upon autophagy, which were largely abrogated by the 3-MA. However, treatment of the immortalised BEC with 3-MA often lead to rafts of cells detaching from the chamber slides, it is not clear whether these cells were viable or whether they had died as a result of

necrosis or apoptosis. It is likely however that 3-MA interfered with the adhesion of the cells in some way. From the surviving cells it was shown that inhibition of autophagy had some merit as a modulator of the oxidative stress-induced EMT.

It follows, therefore, that if blockade of autophagy could have an effect upon senescence and SASP, so could potentiation in the current study this was mediated by sirolimus.

Sirolimus has been both vilified and praised as an agent in allograft recipients (Dunkelberg, Trotter et al. 2003, Fung and Marcos 2003, Trotter 2003). Some have stated that sirolimus has anti-fibrotic properties (Wu, Wen et al. 2006, Damiao, Bertocchi et al. 2007) and are keen that it is returned to clinical practice and used more widely (McKenna and Trotter 2012). However, there are those who suggest that sirolimus is not an appropriate agent for use in allograft recipients due to safety concerns (McKenna, Trotter et al. 2013). From the observations made by Nakanuma (Sasaki, Miyakoshi et al. 2010), it would seem likely that if sirolimus potentiates autophagy it will have negative, pro-senescent, effects.

Sirolimus has been shown to have an effect on wound healing, prolonging the time it takes for surgical wounds to heal (Schaffer, Schier et al. 2007, Hulbert, Delahunty et al. 2013). This has been postulated to be due to a differential effect upon $\alpha V\beta 6$ and $\alpha V\beta 8$ integrins. It has been shown by Dean Sheppard's group that during *in vitro* scratch assays $\alpha V\beta 8$ integrin appears to be the key regulator of TGF-β mediated wound healing, whereas $\alpha V\beta 6$ integrin has almost no effect (Neurohr, Nishimura et al. 2006). In the current study sirolimus produced clear up regulation

of the αVβ6 integrin as well as inducing autophagy in BEC. Indeed, the current study showed that sirolimus on its own was sufficient to induce EMT in immortalised BEC, something that has, to my knowledge, never before been reported. Due to time pressure it was not possible to follow this up as thoroughly as would be liked. However, when viewed in the context of the literature, these data are congruous.

In clinical practice it is always the goal of clinicians to wean patients from immunosuppressive agents. This makes sense, as immunosuppressives have many potential adverse reactions and sequelae, such as predisposing patients to skin cancer and opportunistic infections. Weaning rates in liver recipients have been, at best, 20% (Levitsky, Mathew et al. 2013). In order to enhance this there have been attempts to change immunosuppressive protocols that will favour weaning. One such protocol relies very heavily upon sirolimus, with the explanation that sirolimus increases the number of measurable T reg (Defined as $CD4^+$ $CD25^{hi}$ $FOXP3^+$) and tolerogenic dendritic cells (Tol DC) (Levitsky, Mathew et al. 2013). This change in the immune landscape clearly has the potential to favour tolerance induction. However, the generation of stable FOXP3 expressing T cells is dependent upon activeTGFβ (as well as functioning dendritic cells, which are inhibited by tacrolimus) This has further sequelae, such as being pro-fibrogenic.

Furthermore, in the only published study investigating allograft recipients classed as functionally tolerant, protocol biopsies demonstrated significant amounts of sub-clinical fibrosis (Yoshitomi, Koshiba et al. 2009). This not only implies a role for TGF-β but also suggests that functional tolerance is not true tolerance, as there is on

going allograft injury. The liver's capacity for regeneration and significant physiological reserve often means that patients with liver disease present late. The study by Yoshitomi et al (Yoshitomi, Koshiba et al. 2009) would imply that this is also the case with liver allografts; as fibrosis is not a feature of normal ageing. Data presented in this study also reinforces the established phenomenon of duct sparing by tacrolimus. This study showed no evidence of EMT as a result of tacrolimus exposure and there was no evidence of αVβ6 integrin expression as a result of tacrolimus exposure. The ideas and concepts postulated here are shown diagrammatically in Figure 6.2

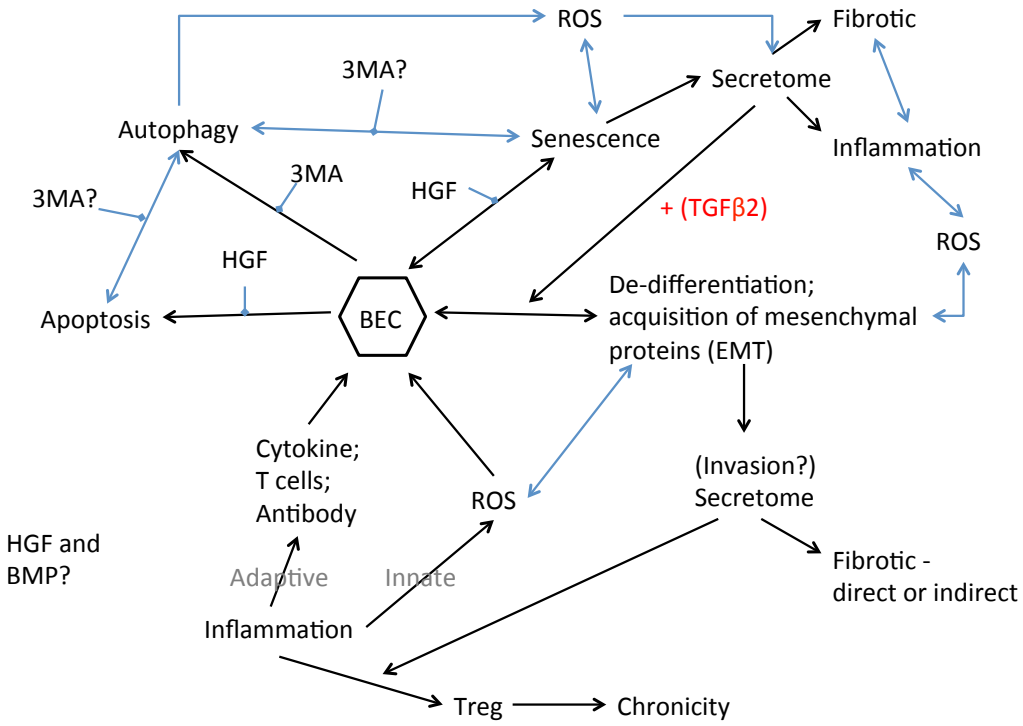

Figure 6.2; A refined version of the model postulated by the work in the current study and detailed in figure 6.1. As shown above, there are numerous branch points in the postulated life cycle of injured BEC, any or all of which may occur in a specific disease state. Identifying when

they occur and what modulation is effective at what time points during injury will determine the effective treatment, a biliary version of personalised medicine.

6.4 Future research

Data from in vitro experiments may explain the apparent dichotomy between the pro- and anti-fibrotic effects of sirolimus. In favour of the data supporting the fibrotic debate, Song (Song, Wang et al. 2006) demonstrated that mTOR mediates Akt-induced suppression of Smad3. Therefore if mTOR is inhibited (such as via sirolimus) it is possible to potentiate Smad dependent TGF-β signalling. However the group of Derynck (Lamouille and Derynck 2011) have shown that TGF-β also drives mTOR complex 2 which phosphorylates Akt. If the mTOR Complex 2 (mTORC2) key regulator rictor is inhibited there is no mTORC2 activity and cells are unable to complete a TGF-β mediated EMT (Lamouille and Derynck 2011). This paper also showed that down regulation of rictor down regulates Snail by 40%, again in favour of a sirolimus mediated anti-fibrotic effect. These changes appear to be a late stage effect in EMT, as rictor inhibition did not change epithelial characteristics of the cells under test, but prevented the latter stages of EMT (Lamouille and Derynck 2011, Lamouille, Connolly et al. 2012).

Confusingly, Liu (Liu 2006) postulates that there is mTOR dependent upregulation of Snail, which is then inhibited by sirolimus. However this paper also shows that sirolimus FKBP12 binding prevents cell cycle progression beyond G1, which is associated with an increase in p21. This latter observation would fit with the data of Nakanuma et al (Sasaki, Miyakoshi et al. 2010) in that autophagy inhibition prevented the up regulation of p21 and induction of senescence in rodent BEC, if

the G1 arrest seen by Liu et al is autophagy mediated, rather than due to other effects of sirolimus. These data are all further complicated by the fact that mTORC2 activity is only down regulated by high doses of sirolimus, likely higher than those given to humans but not than those given to rodents. This dose dependent effect of sirolimus could very well be the explaining factor behind the discrepancy between the rodent and human data. There are assays available to investigate mTORC2 activity (Lamouille and Derynck 2011, Lamouille, Connolly et al. 2012); coupling these with an escalating dose of sirolimus to both human and rodent BEC should provide an answer as to whether there is a dose dependent effect on mTORC2. It may be difficult to determine how this observation applies to a clinical setting as, to the best of my knowledge, there is no data available on the correlation between serum and biliary levels of sirolimus in humans.

HGF has had a long-standing role in experimental models of recovery from injury and of preventing EMT (Arends, Slump et al. 2008, Inagaki, Higashi et al. 2008, Kwiecinski, Noetel et al. 2011, Tojima, Kakizaki et al. 2011). As a therapeutic agent HGF is not ideal as it is difficult to synthesise (due to its size) and deliver, and has problems with precipitation and with failure to monodisperse in solution (Ross, Gherardi et al. 2012). Small peptide or small molecule mimetics of HGF therefore have potential as therapeutic agents as they are easier to synthesise and monodisperse much more easily (Ross, Gherardi et al. 2012). The current study evaluated the use of HGF in the established *in vitro* assay. HGF has been shown previously to block TGF-β mediated EMT in immortalised BEC (Xia, Dai et al. 2006). It was not surprising to see that HGF blocked the oxidative stress induced EMT in

the assay. This therefore acted as the benchmark for assessment of the engineered HGF derivative 1K1. *In vitro*, 1K1 had similar effects to HGF upon the morphology of BEC. 1K1 is therefore able to prevent an oxidative stress induced EMT in BEC.

There were clear differences between 1K1 and HGF in signalling pathway data and autophagy data, which was interesting as these were the most obvious differences between HGF and 1K1. 1K1 seemed to induce autophagy at a much lower level than HGF. This would imply that it had a lower metabolic effect upon the cells, something that seems to be born out by the proliferation data. 1K1 and HGF were used at equivalent mass doses, rather than at molar mass levels, so the molar equivalence of 1K1 was around 20 times higher than with HGF. One large piece of missing data is that of a phospho- specific cell based ELISA for Akt, as this is a known downstream activator of HGF and may have effects on TGF-β downstream signalling. The ELISA was attempted but gave surprising results. The level seen in some wells was below the baseline (though this was also seen in some of the other assays), but there was no appreciable signalling via the Akt pathway at any point in the samples tested. This is likely a spurious result as the other signalling data obtained would imply that there were Akt mediated effects seen in the cells. 1K1 had a more profound effect upon Smad2/3 suppression, something that was likely mediated by Akt. 1K1 also appeared to have a suppressive effect upon ERK 1/2 expression at higher doses. It was clear from the data that the effect of either HGF or 1K1 was mediated immediately after the injury. Further experiments are required to further delineate the downstream signalling pathways that are activated in this assay and also by HGF and 1K1 as the data so far imply that HGF

and 1K1 may be signalling by different but complementary pathways. It would also be interesting to see at what point an HGF/1K1 mediated rescue of the BEC phenotype was possible, as this is likely to be an important factor in the administration of agents to patients.

The apparent interplay between the cMet and TGF-β signalling pathways may be explained by considering some of the receptor associated molecules. Protein phosphatase 2A (PP2A) may even provide a link between cMet and TGF-βR ((Jin Jung, Hyun Kim et al. 2013) PP2A is a calcineurin-like protein (calcineurin is PP3) that has a negative regulatory role on cytokine expression. PP2A is also implicated in age-related inflammation as it becomes inactive during ageing (due to the effects of ROS), leading to increased NF-κB signalling. Caloric restriction has been shown to prolong life and caloric restriction relates to reduced ROS production in ageing mice. A study by Jung et al also demonstrated that PP2A knock down induced p38, ERK and JNK activation via NF-κB (Jin Jung, Hyun Kim et al. 2013). This could also be a target of HGF/CMet that acts to inhibit TGF-β and, if so, is it the non-canonical pathway that is important in this situation (section 1.5)?

Regulation of PP1 and PP2A is not clearly defined but seems to be dependent on de-phosphorylation (and therefore activated) downstream of CDK inhibitors, such as p21. If this is the case PP2A could act as a negative regulator of the SASP. Hashigasako (Hashigasako, Machide et al. 2004) showed that oxidative stress, produced with H_2O_2, down regulates the response of cMet to HGF. H_2O_2 induces Ser985 phosphorylation of the cMet receptor, dependent upon PKC. PP2A is constitutively associated with cMet and de-phosphorylates the ser985 residue,

though it cannot do this in the presence of ROS. Hypoxic conditions allow PP2A specific de-phosphorylation of Smad 3 but not Smad 2 (Heikkinen, Nummela et al. 2010). This specifically inhibits the activity of p15 (stops activation). PP2A also negatively regulates HDACs and has been shown to prevent TGF-β induced αSMA expression (Guo, Shan et al. 2009). PP2A is therefore the natural candidate for further investigation.

What would I do differently?

While setting up and optimising the immunofluorescence assays used extensively in this project the decision to use FITC as the conjugate on secondary antibodies, with the aim of making all images reproducible and consistent was a mistake. Unbeknown to the author at the time FITC suffers from a number of artefacts, such as bleaching after contact with light sources and lacking long term stability in storage, that make it less suitable for reproducible experiments than say, Alexa Fluor 488 or TRITC. However once the initial experiments and optimisation had been performed, justifying a change of reagent became difficult, especially as one of the key factors in the assay was the rapid throughput and reproducible readout. Another alternative would have been to use immunohistochemistry techniques, these would have also been more stable than FITC but would also have had the benefit of being themselves more permanent. This would mean that further validation could have been carried out by third parties.

The isolation of primary cells was a significant hurdle in this project. Local tissue supply was not possible which limited the supply of primary cells. More primary cell

focused work would have been desirable in order to ascertain if the responses observed were influenced by the disease suffered by the donors of the tissue. This would also be another logical step in explaining some of the apparently incongruous data.

Work arising from this project

Two MRes students had projects that arose, in whole or in part, from the work in this thesis. This included a publication (Thompson, Burt et al. 2013) for investigating the ability of cDNA to be accurately obtained from FFPE tissue and also of validating the oxidative stress EMT model in renal tubular epithelium.

UK-PBC: This project made a significant contribution to the MRC stratified medicine bid made by UK-PBC. This was led by Professor DEJ Jones and successfully funded at £5.8million. Many of the points noted above will be further investigated as part of this multicentre initiative. These include, further investigation of signalling in the BEC model, isolation and testing the paradigms above in cohorts of patients who are stratified by their drug response to identify morphological and response related changes in tandem with further data from a targeted GWAS in the same patients.

There are options being pursued to carry out further development work with GSK on 1K1 and also a further potential collaboration with Intercept pharmaceuticals. In collaboration with Professor Neil Sheerin it is planned to look at the senescence paradigm in renal disease.

Bibliography

"<Chirgadze HGF work.pdf>."
(1997). "Banff schema for grading liver allograft rejection: an international consensus document." Hepatology **25**(3): 658-663.
Afzali, B., R. I. Lechler and M. P. Hernandez-Fuentes (2007). "Allorecognition and the alloresponse: clinical implications." Tissue Antigens **69**(6): 545-556.
Ai, K. X., L. Y. Lu, X. Y. Huang, W. Chen and H. Z. Zhang (2008). "Prognostic significance of S100A4 and vascular endothelial growth factor expression in pancreatic cancer." World J Gastroenterol **14**(12): 1931-1935.
Aichinger, G. and R. I. Lechler (1995). "Endogenous pathway of class II presentation." Biochem Soc Trans **23**(3): 657-660.
Ali, J. M., E. M. Bolton, J. A. Bradley and G. J. Pettigrew (2013). "Allorecognition Pathways in Transplant Rejection and Tolerance." Transplantation.
Ali, S., L. A. Hardy and J. A. Kirby (2003). "Transplant immunobiology: a crucial role for heparan sulfate glycosaminoglycans?" Transplantation **75**(11): 1773-1782.
Ali, S. H. and J. A. DeCaprio (2001). "Cellular transformation by SV40 large T antigen: interaction with host proteins." Semin Cancer Biol **11**(1): 15-23.
Aravinthan, A., C. Scarpini, P. Tachtatzis, S. Verma, S. Penrhyn-Lowe, R. Harvey, S. E. Davies, M. Allison, N. Coleman and G. Alexander (2013). "Hepatocyte senescence predicts progression in non-alcohol-related fatty liver disease." J Hepatol **58**(3): 549-556.
Arends, B., E. Slump, B. Spee, J. Rothuizen and L. C. Penning (2008). "Hepatocyte growth factor improves viability after H2O2-induced toxicity in bile duct epithelial cells." Comp Biochem Physiol C Toxicol Pharmacol **147**(3): 324-330.
Arnhold, J. (2004). "Properties, functions, and secretion of human myeloperoxidase." Biochemistry (Mosc) **69**(1): 4-9.
Arnhold, J., P. G. Furtmuller and C. Obinger (2003). "Redox properties of myeloperoxidase." Redox Rep **8**(4): 179-186.
Asawa, S., T. Saito, A. Satoh, K. Ohtake, T. Tsuchiya, H. Okada, E. G. Neilson and M. Gotoh (2007). "Participation of bone marrow cells in biliary fibrosis after bile duct ligation." J Gastroenterol Hepatol **22**(11): 2001-2008.
Askari, J. A., P. A. Buckley, A. P. Mould and M. J. Humphries (2009). "Linking integrin conformation to function." J Cell Sci **122**(Pt 2): 165-170.
Askari, J. A., C. J. Tynan, S. E. Webb, M. L. Martin-Fernandez, C. Ballestrem and M. J. Humphries (2010). "Focal adhesions are sites of integrin extension." J Cell Biol **188**(6): 891-903.
Aw, T. Y. (2012). "Tissue oxidative stress revisited: significance of ROS and redox signaling." Semin Cell Dev Biol **23**(7): 721.
Bahr, A. and A. B. Wilson (2012). "The evolution of MHC diversity: evidence of intralocus gene conversion and recombination in a single-locus system." Gene **497**(1): 52-57.
Barth, S., D. Glick and K. F. Macleod (2010). "Autophagy: assays and artifacts." J Pathol.
Beaussier, M., D. Wendum, E. Schiffer, S. Dumont, C. Rey, A. Lienhart and C. Housset (2007). "Prominent contribution of portal mesenchymal cells to liver fibrosis in ischemic and obstructive cholestatic injuries." Lab Invest **87**(3): 292-303.
Bedossa, P. and V. Paradis (2003). "Liver extracellular matrix in health and disease." J Pathol **200**(4): 504-515.
Bedossa, P. and T. Poynard (1996). "An algorithm for the grading of activity in chronic hepatitis C. The METAVIR Cooperative Study Group." Hepatology **24**(2): 289-293.

Bellamy, C. O., A. M. DiMartini, K. Ruppert, A. Jain, F. Dodson, M. Torbenson, T. E. Starzl, J. J. Fung and A. J. Demetris (2001). "Liver transplantation for alcoholic cirrhosis: long term follow-up and impact of disease recurrence." Transplantation **72**(4): 619-626.

Bellamy, C. O., M. M. Herriot, D. J. Harrison and A. J. Bathgate (2007). "C4d immunopositivity is uncommon in ABO-compatible liver allografts, but correlates partially with lymphocytotoxic antibody status." Histopathology **50**(6): 739-749.

Bendorf, A., P. J. Kelly, I. H. Kerridge, G. W. McCaughan, B. Myerson, C. Stewart and B. A. Pussell (2013). "An international comparison of the effect of policy shifts to organ donation following cardiocirculatory death (DCD) on donation rates after brain death (DBD) and transplantation rates." PLoS One **8**(5): e62010.

Berzigotti, A., E. Reverter, A. Garcia-Criado, J. G. Abraldes, F. Cerini, J. C. Garcia-Pagan and J. Bosch (2013). "Reliability of the estimation of total hepatic blood flow by Doppler ultrasound in patients with cirrhotic portal hypertension." J Hepatol.

Bhogal, R. H. and S. C. Afford (2011). "Anti-oxidants do not prevent bile acid-induced cell death in rat hepatocytes." Liver Int **31**(2): 273-274; author reply 274-275.

Bhogal, R. H., S. M. Curbishley, C. J. Weston, D. H. Adams and S. C. Afford (2010). "Reactive oxygen species mediate human hepatocyte injury during hypoxia/reoxygenation." Liver Transpl **16**(11): 1303-1313.

Bhogal, R. H., J. Hodson, D. C. Bartlett, C. J. Weston, S. M. Curbishley, E. Haughton, K. T. Williams, G. M. Reynolds, P. N. Newsome, D. H. Adams and S. C. Afford "Isolation of primary human hepatocytes from normal and diseased liver tissue: a one hundred liver experience." PLoS One **6**(3): e18222.

Bhogal, R. H., J. Hodson, D. C. Bartlett, C. J. Weston, S. M. Curbishley, E. Haughton, K. T. Williams, G. M. Reynolds, P. N. Newsome, D. H. Adams and S. C. Afford (2011). "Isolation of primary human hepatocytes from normal and diseased liver tissue: a one hundred liver experience." PLoS One **6**(3): e18222.

Bhogal, R. H., C. J. Weston, S. M. Curbishley, D. H. Adams and S. C. Afford (2012). "Autophagy: a cyto-protective mechanism which prevents primary human hepatocyte apoptosis during oxidative stress." Autophagy **8**(4): 545-558.

Billing, H., T. Giese, C. Sommerer, M. Zeier, R. Feneberg, S. Meuer and B. Tonshoff (2010). "Pharmacodynamic monitoring of cyclosporine A by NFAT-regulated gene expression and the relationship with infectious complications in pediatric renal transplant recipients." Pediatr Transplant **14**(7): 844-851.

Billingham, R. E., L. Brent and P. B. Medawar (1955). "Acquired tolerance of skin homografts." Ann N Y Acad Sci **59**(3): 409-416.

Bird, T. G., W. Y. Lu, L. Boulter, S. Gordon-Keylock, R. A. Ridgway, M. J. Williams, J. Taube, J. A. Thomas, D. Wojtacha, A. Gambardella, O. J. Sansom, J. P. Iredale and S. J. Forbes (2013). "Bone marrow injection stimulates hepatic ductular reactions in the absence of injury via macrophage-mediated TWEAK signaling." Proc Natl Acad Sci U S A **110**(16): 6542-6547.

Bradley, J. A., G. J. Pettigrew and C. J. Watson (2013). "Time to death after withdrawal of treatment in donation after circulatory death (DCD) donors." Curr Opin Organ Transplant **18**(2): 133-139.

Brain, J. G., H. Robertson, E. Thompson, E. H. Humphreys, A. Gardner, T. A. Booth, D. E. Jones, S. C. Afford, T. von Zglinicki, A. D. Burt and J. A. Kirby (2013). "Biliary epithelial senescence and plasticity in acute cellular rejection." Am J Transplant **13**(7): 1688-1702.

Brain, J. G., A. J. Rostron, J. H. Dark and J. A. Kirby (2008). "Activation and modulation of cardiac poly-adenosine diphosphate ribose polymerase activity in a rat model of brain death." Transplantation **85**(9): 1348-1350.

Bridgen, D. T., C. L. Gilchrist, W. J. Richardson, R. E. Isaacs, C. R. Brown, K. L. Yang, J. Chen and L. A. Setton (2013). "Integrin-mediated interactions with extracellular matrix proteins for nucleus pulposus cells of the human intervertebral disc." J Orthop Res.

Bridgewater, R. E., J. C. Norman and P. T. Caswell (2012). "Integrin trafficking at a glance." J Cell Sci **125**(Pt 16): 3695-3701.
Brown, R. S., Jr. (2008). "Live donors in liver transplantation." Gastroenterology **134**(6): 1802-1813.
Brunt, E. M., C. G. Janney, A. M. Di Bisceglie, B. A. Neuschwander-Tetri and B. R. Bacon (1999). "Nonalcoholic steatohepatitis: a proposal for grading and staging the histological lesions." Am J Gastroenterol **94**(9): 2467-2474.
Buechter, K. J., R. Zeppa and G. Gomez (1990). "The use of segmental anatomy for an operative classification of liver injuries." Ann Surg **211**(6): 669-673; discussion 673-665.
Burr, A. W., K. Toole, C. Chapman, J. E. Hines and A. D. Burt (1998). "Anti-hepatocyte growth factor antibody inhibits hepatocyte proliferation during liver regeneration." J Pathol **185**(3): 298-302.
Burra, P., M. Senzolo, R. Adam, V. Delvart, V. Karam, G. Germani and J. Neuberger "Liver transplantation for alcoholic liver disease in Europe: a study from the ELTR (European Liver Transplant Registry)." Am J Transplant **10**(1): 138-148.
Burt, A. D. (2011). MacSweens Pathology of the Liver, Churchill Livingstone.
Calne, R. Y. (1984). "Gordon Murray Lecture. Organ transplantation and cyclosporin A." Can J Surg **27**(1): 10-13.
Calne, R. Y. (1984). "Organ transplantation with special emphasis on Cyclosporin A." Jpn J Surg **14**(6): 435-443.
Campbell, I. D. and M. J. Humphries (2011). "Integrin structure, activation, and interactions." Cold Spring Harb Perspect Biol **3**(3).
Cannito, S., E. Novo, L. V. di Bonzo, C. Busletta, S. Colombatto and M. Parola "Epithelial-mesenchymal transition: from molecular mechanisms, redox regulation to implications in human health and disease." Antioxid Redox Signal **12**(12): 1383-1430.
Cao, S., G. B. Walker, X. Wang, J. Z. Cui and J. A. Matsubara (2013). "Altered cytokine profiles of human retinal pigment epithelium: oxidant injury and replicative senescence." Mol Vis **19**: 718-728.
Cao, Y., A. Szabolcs, S. K. Dutta, U. Yaqoob, K. Jagavelu, L. Wang, E. B. Leof, R. A. Urrutia, V. H. Shah and D. Mukhopadhyay (2011). "Neuropilin-1 mediates divergent R-Smad signaling and the myofibroblast phenotype." J Biol Chem **285**(41): 31840-31848.
Carbone, M., S. Bufton, A. Monaco, L. Griffiths, D. E. Jones and J. M. Neuberger (2013). "The effect of liver transplantation on fatigue in patients with primary biliary cirrhosis: A prospective study." J Hepatol **59**(3): 490-494.
Carbone, M., G. F. Mells, G. Pells, M. F. Dawwas, J. L. Newton, M. A. Heneghan, J. M. Neuberger, D. B. Day, S. J. Ducker, U. P. Consortium, R. N. Sandford, G. J. Alexander and D. E. Jones (2013). "Sex and age are determinants of the clinical phenotype of primary biliary cirrhosis and response to ursodeoxycholic acid." Gastroenterology **144**(3): 560-569 e567; quiz e513-564.
Cassiman, D., L. Libbrecht, V. Desmet, C. Denef and T. Roskams (2002). "Hepatic stellate cell/myofibroblast subpopulations in fibrotic human and rat livers." J Hepatol **36**(2): 200-209.
Chan, E. Y., S. Kir and S. A. Tooze (2007). "siRNA screening of the kinome identifies ULK1 as a multidomain modulator of autophagy." J Biol Chem **282**(35): 25464-25474.
Chang, H. L., K. Qu, C. Liu, Y. Lv, L. Yu, X. M. Liu, B. Wang, Z. Wang, M. Tian and L. Wang (2013). "Liver Transplantation Using DCD Donors: The Current Strategy to Expand the Organ Donor Pool in China." Am J Transplant **13**(7): 1939-1940.
Chapple, I. L. and J. B. Matthews (2007). "The role of reactive oxygen and antioxidant species in periodontal tissue destruction." Periodontol 2000 **43**: 160-232.

Chen, G., L. Zhang, L. Chen, H. Wang, Y. Zhang and P. Bie (2013). "Role of integrin alphavbeta6 in the pathogenesis of ischemia-related biliary fibrosis after liver transplantation." Transplantation **95**(9): 1092-1099.
Chen, J., V. Repunte-Canonigo, T. Kawamura, C. Lefebvre, W. Shin, L. L. Howell, S. E. Hemby, B. K. Harvey, A. Califano, M. Morales, G. F. Koob and P. P. Sanna (2013). "Hypothalamic proteoglycan syndecan-3 is a novel cocaine addiction resilience factor." Nat Commun **4**: 1955.
Chiba, M., M. Sasaki, S. Kitamura, H. Ikeda, Y. Sato and Y. Nakanuma (2011). "Participation of bile ductular cells in the pathological progression of non-alcoholic fatty liver disease." J Clin Pathol.
Chirgadze, D. Y., J. Hepple, R. A. Byrd, R. Sowdhamini, T. L. Blundell and E. Gherardi (1998). "Insights into the structure of hepatocyte growth factor/scatter factor (HGF/SF) and implications for receptor activation." FEBS Lett **430**(1-2): 126-129.
Chu, A. S., R. Diaz, J. J. Hui, K. Yanger, Y. Zong, G. Alpini, B. Z. Stanger and R. G. Wells (2011). "Lineage tracing demonstrates no evidence of cholangiocyte epithelial-to-mesenchymal transition in murine models of hepatic fibrosis." Hepatology **53**(5): 1685-1695.
Collins, R. W., H. A. Stephens and R. W. Vaughan (2003). "Molecular typing of the MHC class I chain-related gene locus." Methods Mol Biol **210**: 305-321.
Cooke, M. S., M. D. Evans, M. Dizdaroglu and J. Lunec (2003). "Oxidative DNA damage: mechanisms, mutation, and disease." FASEB J **17**(10): 1195-1214.
Cooper, M. H., S. H. Gregory, A. W. Thomson, J. J. Fung, T. E. Starzl and E. J. Wing (1991). "Evaluation of the influence of FK 506, rapamycin, and cyclosporine on processing and presentation of particulate antigen by macrophages: assessment of a drug "carry-over" effect." Transplant Proc **23**(6): 2957-2958.
Coppe, J. P., P. Y. Desprez, A. Krtolica and J. Campisi (2011). "The senescence-associated secretory phenotype: the dark side of tumor suppression." Annu Rev Pathol **5**: 99-118.
Coppe, J. P., C. K. Patil, F. Rodier, A. Krtolica, C. M. Beausejour, S. Parrinello, J. G. Hodgson, K. Chin, P. Y. Desprez and J. Campisi (2011). "A human-like senescence-associated secretory phenotype is conserved in mouse cells dependent on physiological oxygen." PLoS One **5**(2): e9188.
Correale, J., M. Arias and W. Gilmore (1998). "Steroid hormone regulation of cytokine secretion by proteolipid protein-specific CD4+ T cell clones isolated from multiple sclerosis patients and normal control subjects." J Immunol **161**(7): 3365-3374.
Correia-Melo, C., D. Jurk and J. F. Passos (2013). "Robust multiparametric assessment of cellular senescence." Methods Mol Biol **965**: 409-419.
Csiszar, A., A. Podlutsky, N. Podlutskaya, W. E. Sonntag, S. Z. Merlin, E. E. Philipp, K. Doyle, A. Davila, F. A. Recchia, P. Ballabh, J. T. Pinto and Z. Ungvari (2012). "Testing the oxidative stress hypothesis of aging in primate fibroblasts: is there a correlation between species longevity and cellular ROS production?" J Gerontol A Biol Sci Med Sci **67**(8): 841-852.
Da Gama, L. M., F. L. Ribeiro-Gomes, U. Guimaraes, Jr. and A. C. Arnholdt (2004). "Reduction in adhesiveness to extracellular matrix components, modulation of adhesion molecules and in vivo migration of murine macrophages infected with Toxoplasma gondii." Microbes Infect **6**(14): 1287-1296.
Damiao, M. J., A. P. Bertocchi, R. M. Monteiro, G. M. Goncalves, M. A. Cenedeze, C. Q. Feitoza, G. D. Marques, G. Giannocco, M. Mazzali, V. P. Teixeira, M. A. Dos Reis, A. Pacheco-Silva and N. O. Camara (2007). "The effects of rapamycin in the progression of renal fibrosis." Transplant Proc **39**(2): 457-459.
Dannewitz, B., E. M. Kruck, H. J. Staehle, P. Eickholz, T. Giese, S. Meuer, V. Kaever, M. Zeier and C. Sommerer (2011). "Cyclosporine-induced gingival overgrowth correlates with NFAT-regulated gene expression: a pilot study." J Clin Periodontol **38**(11): 984-991.

Delehedde, M., M. Lyon, R. Vidyasagar, T. J. McDonnell and D. G. Fernig (2002). "Hepatocyte growth factor/scatter factor binds to small heparin-derived oligosaccharides and stimulates the proliferation of human HaCaT keratinocytes." J Biol Chem **277**(14): 12456-12462.

Demetris, A., D. Adams, C. Bellamy, K. Blakolmer, A. Clouston, A. P. Dhillon, J. Fung, A. Gouw, B. Gustafsson, H. Haga, D. Harrison, J. Hart, S. Hubscher, R. Jaffe, U. Khettry, C. Lassman, K. Lewin, O. Martinez, Y. Nakazawa, D. Neil, O. Pappo, M. Parizhskaya, P. Randhawa, S. Rasoul-Rockenschaub, F. Reinholt, M. Reynes, M. Robert, A. Tsamandas, I. Wanless, R. Wiesner, A. Wernerson, F. Wrba, J. Wyatt and H. Yamabe (2000). "Update of the International Banff Schema for Liver Allograft Rejection: working recommendations for the histopathologic staging and reporting of chronic rejection. An International Panel." Hepatology **31**(3): 792-799.

Demetris, A. J., O. Adeyi, C. O. Bellamy, A. Clouston, F. Charlotte, A. Czaja, I. Daskal, M. S. El-Monayeri, P. Fontes, J. Fung, B. Gridelli, M. Guido, H. Haga, J. Hart, E. Honsova, S. Hubscher, T. Itoh, N. Jhala, P. Jungmann, U. Khettry, C. Lassman, S. Ligato, J. G. Lunz, 3rd, A. Marcos, M. I. Minervini, J. Molne, M. Nalesnik, I. Nasser, D. Neil, E. Ochoa, O. Pappo, P. Randhawa, F. P. Reinholt, P. Ruiz, M. Sebagh, M. Spada, A. Sonzogni, A. C. Tsamandas, A. Wernerson, T. Wu and F. Yilmaz (2006). "Liver biopsy interpretation for causes of late liver allograft dysfunction." Hepatology **44**(2): 489-501.

Demetris, A. J., K. Ruppert, I. Dvorchik, A. Jain, M. Minervini, M. A. Nalesnik, P. Randhawa, T. Wu, A. Zeevi, K. Abu-Elmagd, B. Eghtesad, P. Fontes, T. Cacciarelli, W. Marsh, D. Geller and J. J. Fung (2002). "Real-time monitoring of acute liver-allograft rejection using the Banff schema." Transplantation **74**(9): 1290-1296.

Diaz, R., J. W. Kim, J. J. Hui, Z. Li, G. P. Swain, K. S. Fong, K. Csiszar, P. A. Russo, E. B. Rand, E. E. Furth and R. G. Wells (2008). "Evidence for the epithelial to mesenchymal transition in biliary atresia fibrosis." Hum Pathol **39**(1): 102-115.

Ding, S., T. Merkulova-Rainon, Z. C. Han and G. Tobelem (2003). "HGF receptor up-regulation contributes to the angiogenic phenotype of human endothelial cells and promotes angiogenesis in vitro." Blood **101**(12): 4816-4822.

Direkze, N. C., S. J. Forbes, M. Brittan, T. Hunt, R. Jeffery, S. L. Preston, R. Poulsom, K. Hodivala-Dilke, M. R. Alison and N. A. Wright (2003). "Multiple organ engraftment by bone-marrow-derived myofibroblasts and fibroblasts in bone-marrow-transplanted mice." Stem Cells **21**(5): 514-520.

Doignon, I., B. Julien, V. Serriere-Lanneau, I. Garcin, G. Alonso, A. Nicou, F. Monnet, M. Gigou, L. Humbert, D. Rainteau, D. Azoulay, D. Castaing, M. C. Gillon, D. Samuel, J. C. Duclos-Vallee and T. Tordjmann (2011). "Immediate neuroendocrine signaling after partial hepatectomy through acute portal hyperpressure and cholestasis." J Hepatol **54**(3): 481-488.

Dooley, S., J. Hamzavi, L. Ciuclan, P. Godoy, I. Ilkavets, S. Ehnert, E. Ueberham, R. Gebhardt, S. Kanzler, A. Geier, K. Breitkopf, H. Weng and P. R. Mertens (2008). "Hepatocyte-specific Smad7 expression attenuates TGF-beta-mediated fibrogenesis and protects against liver damage." Gastroenterology **135**(2): 642-659.

Droge, W. (2003). "Oxidative stress and aging." Adv Exp Med Biol **543**: 191-200.

Drugge, R. J. and R. E. Handschumacher (1988). "Cyclosporine--mechanism of action." Transplant Proc **20**(2 Suppl 2): 301-309.

Duarte, R. F., H. Greinix, B. Rabin, S. A. Mitchell, G. Basak, D. Wolff, J. A. Madrigal, S. Z. Pavletic and S. J. Lee (2013). "Uptake and use of recommendations for the diagnosis, severity scoring and management of chronic GVHD: an international survey of the EBMT-NCI Chronic GVHD Task Force." Bone Marrow Transplant.

Dukhanina, E. A., T. I. Lukyanova, E. A. Romanova, A. S. Dukhanin and L. P. Sashchenko (2008). "Comparative analysis of secretion of S100A4 metastatic marker by immune and tumor cells." Bull Exp Biol Med **145**(1): 78-80.
Dulak, A. M., C. T. Gubish, L. P. Stabile, C. Henry and J. M. Siegfried (2011). "HGF-independent potentiation of EGFR action by c-Met." Oncogene **30**(33): 3625-3635.
Dunkelberg, J. C., J. F. Trotter, M. Wachs, T. Bak, M. Kugelmas, T. Steinberg, G. T. Everson and I. Kam (2003). "Sirolimus as primary immunosuppression in liver transplantation is not associated with hepatic artery or wound complications." Liver Transpl **9**(5): 463-468.
Erol, A. "Deciphering the intricate regulatory mechanisms for the cellular choice between cell repair, apoptosis or senescence in response to damaging signals." Cell Signal **23**(7): 1076-1081.
Evan, G. I. and F. d'Adda di Fagagna (2009). "Cellular senescence: hot or what?" Curr Opin Genet Dev **19**(1): 25-31.
Fallowfield, J. A., T. J. Kendall and J. P. Iredale (2006). "Reversal of fibrosis: no longer a pipe dream?" Clin Liver Dis **10**(3): 481-497, viii.
Feng, S., U. D. Ekong, S. J. Lobritto, A. J. Demetris, J. P. Roberts, P. Rosenthal, E. M. Alonso, M. C. Philogene, D. Ikle, K. M. Poole, N. D. Bridges, L. A. Turka and N. K. Tchao (2012). "Complete immunosuppression withdrawal and subsequent allograft function among pediatric recipients of parental living donor liver transplants." JAMA **307**(3): 283-293.
Flanders, K. C. (2004). "Smad3 as a mediator of the fibrotic response." Int J Exp Pathol **85**(2): 47-64.
Fleig, S. V., S. S. Choi, L. Yang, Y. Jung, A. Omenetti, H. M. VanDongen, J. Huang, J. K. Sicklick and A. M. Diehl (2007). "Hepatic accumulation of Hedgehog-reactive progenitors increases with severity of fatty liver damage in mice." Lab Invest **87**(12): 1227-1239.
Forbes, S. J., F. P. Russo, V. Rey, P. Burra, M. Rugge, N. A. Wright and M. R. Alison (2004). "A significant proportion of myofibroblasts are of bone marrow origin in human liver fibrosis." Gastroenterology **126**(4): 955-963.
Friedman, S. L. (2008). "Hepatic fibrosis -- overview." Toxicology **254**(3): 120-129.
Friedman, S. L. (2008). "Hepatic stellate cells: protean, multifunctional, and enigmatic cells of the liver." Physiol Rev **88**(1): 125-172.
Friedman, S. L. (2008). "Mechanisms of hepatic fibrogenesis." Gastroenterology **134**(6): 1655-1669.
Friedman, S. L., F. J. Roll, J. Boyles and D. M. Bissell (1985). "Hepatic lipocytes: the principal collagen-producing cells of normal rat liver." Proc Natl Acad Sci U S A **82**(24): 8681-8685.
Fung, A. S., L. Wu and I. F. Tannock (2009). "Concurrent and sequential administration of chemotherapy and the Mammalian target of rapamycin inhibitor temsirolimus in human cancer cells and xenografts." Clin Cancer Res **15**(17): 5389-5395.
Fung, J. and A. Marcos (2003). "Rapamycin: friend, foe, or misunderstood?" Liver Transpl **9**(5): 469-472.
Furtmuller, P. G., J. Arnhold, W. Jantschko, H. Pichler and C. Obinger (2003). "Redox properties of the couples compound I/compound II and compound II/native enzyme of human myeloperoxidase." Biochem Biophys Res Commun **301**(2): 551-557.
Gadaleta, R. M., S. W. van Mil, B. Oldenburg, P. D. Siersema, L. W. Klomp and K. J. van Erpecum (2010). "Bile acids and their nuclear receptor FXR: Relevance for hepatobiliary and gastrointestinal disease." Biochim Biophys Acta **1801**(7): 683-692.
Geiger, B. and K. M. Yamada (2011). "Molecular architecture and function of matrix adhesions." Cold Spring Harb Perspect Biol **3**(5).
Gherardi, E., G. Hartmann, J. Hepple, D. Chirgadze, N. Srinivasan and T. Blundell (1997). "Domain structure of hepatocyte growth factor/scatter factor (HGF/SF)." Ciba Found Symp **212**: 84-93; discussion 93-104.

Giacomini, M. M., M. A. Travis, M. Kudo and D. Sheppard (2012). "Epithelial cells utilize cortical actin/myosin to activate latent TGF-beta through integrin alpha(v)beta(6)-dependent physical force." Exp Cell Res **318**(6): 716-722.
Glick, D., S. Barth and K. F. Macleod (2010). "Autophagy: cellular and molecular mechanisms." J Pathol **221**(1): 3-12.
Gohda, E., H. Tsubouchi, H. Nakayama, S. Hirono, O. Sakiyama, K. Takahashi, H. Miyazaki, S. Hashimoto and Y. Daikuhara (1988). "Purification and partial characterization of hepatocyte growth factor from plasma of a patient with fulminant hepatic failure." J Clin Invest **81**(2): 414-419.
Goodman, S. L., G. Holzemann, G. A. Sulyok and H. Kessler (2002). "Nanomolar small molecule inhibitors for alphav(beta)6, alphav(beta)5, and alphav(beta)3 integrins." J Med Chem **45**(5): 1045-1051.
Gorowiec, M. R. (2009). The Role of Oxidative Stress in Lung Epithelial Cells Undergoing Epithelial-to-Mesenchymal Transition (EMT). Doctor of Philosophy PhD, Newcastle University.
Grubman, S. A., R. D. Perrone, D. W. Lee, S. L. Murray, L. C. Rogers, L. I. Wolkoff, A. E. Mulberg, V. Cherington and D. M. Jefferson (1994). "Regulation of intracellular pH by immortalized human intrahepatic biliary epithelial cell lines." Am J Physiol **266**(6 Pt 1): G1060-1070.
Grzelakowska-Sztabert, B. and M. Dudkowska (2011). "Paradoxical action of growth factors: antiproliferative and proapoptotic signaling by HGF/c-MET." Growth Factors **29**(4): 105-118.
Guo, W., B. Shan, R. C. Klingsberg, X. Qin and J. A. Lasky (2009). "Abrogation of TGF-beta1-induced fibroblast-myofibroblast differentiation by histone deacetylase inhibition." Am J Physiol Lung Cell Mol Physiol **297**(5): L864-870.
Guyot, C., S. Lepreux, C. Combe, E. Doudnikoff, P. Bioulac-Sage, C. Balabaud and A. Desmouliere (2006). "Hepatic fibrosis and cirrhosis: the (myo)fibroblastic cell subpopulations involved." Int J Biochem Cell Biol **38**(2): 135-151.
Hanks, B. A., A. Holtzhausen, K. S. Evans, R. Jamieson, P. Gimpel, O. M. Campbell, M. Hector-Greene, L. Sun, A. Tewari, A. George, M. Starr, A. Nixon, C. Augustine, G. Beasley, D. S. Tyler, T. Osada, M. A. Morse, L. Ling, H. K. Lyerly and G. C. Blobe (2013). "Type III TGF-beta receptor downregulation generates an immunotolerant tumor microenvironment." J Clin Invest **123**(9): 3925-3940.
Hara, T., A. Takamura, C. Kishi, S. Iemura, T. Natsume, J. L. Guan and N. Mizushima (2008). "FIP200, a ULK-interacting protein, is required for autophagosome formation in mammalian cells." J Cell Biol **181**(3): 497-510.
Harada, K., M. Chiba, A. Okamura, M. Hsu, Y. Sato, S. Igarashi, X. S. Ren, H. Ikeda, H. Ohta, S. Kasashima, A. Kawashima and Y. Nakanuma (2011). "Monocyte chemoattractant protein-1 derived from biliary innate immunity contributes to hepatic fibrogenesis." J Clin Pathol **64**(8): 660-665.
Harada, K. and Y. Nakanuma (2006). "Molecular mechanisms of cholangiopathy in primary biliary cirrhosis." Med Mol Morphol **39**(2): 55-61.
Harada, K. and Y. Nakanuma (2010). "Biliary innate immunity in the pathogenesis of biliary diseases." Inflamm Allergy Drug Targets **9**(2): 83-90.
Harrison, R. G. (1911). "On the Stereotropism of Embryonic Cells." Science **34**(870): 279-281.
Hartsock, A. and W. J. Nelson (2008). "Adherens and tight junctions: structure, function and connections to the actin cytoskeleton." Biochim Biophys Acta **1778**(3): 660-669.
Hashigasako, A., M. Machide, T. Nakamura, K. Matsumoto and T. Nakamura (2004). "Bi-directional regulation of Ser-985 phosphorylation of c-met via protein kinase C and protein

phosphatase 2A involves c-Met activation and cellular responsiveness to hepatocyte growth factor." J Biol Chem **279**(25): 26445-26452.
Hashiguchi, T., T. Kobayashi, D. Fongmoon, A. K. Shetty, S. Mizumoto, N. Miyamoto, T. Nakamura, S. Yamada and K. Sugahara (2011). "Demonstration of the hepatocyte growth factor signaling pathway in the in vitro neuritogenic activity of chondroitin sulfate from ray fish cartilage." Biochim Biophys Acta **1810**(4): 406-413.
Hayflick, L. and P. S. Moorhead (1961). "The serial cultivation of human diploid cell strains." Exp Cell Res **25**: 585-621.
Heikkinen, P. T., M. Nummela, S. K. Leivonen, J. Westermarck, C. S. Hill, V. M. Kahari and P. M. Jaakkola (2010). "Hypoxia-activated Smad3-specific dephosphorylation by PP2A." J Biol Chem **285**(6): 3740-3749.
Heinen, C. A., S. Reuss, G. L. Amidon and P. Langguth (2013). "Ion Pairing with Bile Salts Modulates Intestinal Permeability and Contributes to Food-Drug Interaction of BCS Class III Compound Trospium Chloride." Mol Pharm.
Hemandas, A. K., M. Salto-Tellez, S. H. Maricar, A. F. Leong and C. K. Leow (2006). "Metastasis-associated protein S100A4--a potential prognostic marker for colorectal cancer." J Surg Oncol **93**(6): 498-503.
Henderson, N. C. and J. P. Iredale (2007). "Liver fibrosis: cellular mechanisms of progression and resolution." Clin Sci (Lond) **112**(5): 265-280.
Henderson, N. C. and D. Sheppard (2013). "Integrin-mediated regulation of TGFbeta in fibrosis." Biochim Biophys Acta **1832**(7): 891-896.
Herskowitz, A., F. Tamura, K. Ueda, D. A. Neumann, M. Slepian, N. R. Rose, W. E. Beschorner, W. A. Baumgartner, B. R. Reitz, K. W. Sell and et al. (1989). "Induction of donor major histocompatibility complex antigens in coronary arterial vessels: mechanism of arterial vasculitis in rat allografts treated with cyclosporine." J Heart Transplant **8**(1): 11-19.
Hewitt, G., D. Jurk, F. D. Marques, C. Correia-Melo, T. Hardy, A. Gackowska, R. Anderson, M. Taschuk, J. Mann and J. F. Passos (2012). "Telomeres are favoured targets of a persistent DNA damage response in ageing and stress-induced senescence." Nat Commun **3**: 708.
Hirono, S., S. Afford and A. J. Strain (1995). "Expression of hepatocyte growth factor receptor (c-met) mRNA in primary cultures of human hepatocytes." Clin Mol Pathol **48**(4): M205-209.
Hoerter, J. A., J. Brzostek, M. N. Artyomov, S. M. Abel, J. Casas, V. Rybakin, J. Ampudia, C. Lotz, J. M. Connolly, A. K. Chakraborty, K. G. Gould and N. R. Gascoigne (2013). "Coreceptor affinity for MHC defines peptide specificity requirements for TCR interaction with coagonist peptide-MHC." J Exp Med **210**(9): 1807-1821.
Hoffmann, M., J. Rychlewski, M. Chrzanowska and T. Hermann (2001). "Mechanism of activation of an immunosuppressive drug: azathioprine. Quantum chemical study on the reaction of azathioprine with cysteine." J Am Chem Soc **123**(26): 6404-6409.
Hofmann, A. F. (2009). "Chronic diarrhea caused by idiopathic bile acid malabsorption: an explanation at last." Expert Rev Gastroenterol Hepatol **3**(5): 461-464.
Hohenester, S., R. P. Oude-Elferink and U. Beuers (2009). "Primary biliary cirrhosis." Semin Immunopathol **31**(3): 283-307.
Holstege, A., P. Bedossa, T. Poynard, M. Kollinger, J. C. Chaput, K. Houglum and M. Chojkier (1994). "Acetaldehyde-modified epitopes in liver biopsy specimens of alcoholic and nonalcoholic patients: localization and association with progression of liver fibrosis." Hepatology **19**(2): 367-374.
Horoldt, B. S., M. Burattin, B. K. Gunson, S. R. Bramhall, P. Nightingale, S. G. Hubscher and J. M. Neuberger (2006). "Does the Banff rejection activity index predict outcome in patients with early acute cellular rejection following liver transplantation?" Liver Transpl **12**(7): 1144-1151.

Hosper, N. A., P. P. van den Berg, S. de Rond, E. R. Popa, M. J. Wilmer, R. Masereeuw and R. A. Bank (2013). "Epithelial-to-mesenchymal transition in fibrosis: Collagen type I expression is highly upregulated after EMT, but does not contribute to collagen deposition." Exp Cell Res.

http://www.britannica.co.uk. (2013). "The Encyclopedia Britannica." Retrieved 4th July 2013, 2013.

Hubscher, S. a. C., A. (2011). Transplantation Pathology. MacSween's Pathology of the Liver. A. Burt.

Hubscher, S. G. (2006). "Transplantation pathology." Semin Diagn Pathol **23**(3-4): 170-181.

Hubscher, S. G. (2012). "Antibody-mediated rejection in the liver allograft." Curr Opin Organ Transplant **17**(3): 280-286.

Hulbert, A. L., A. J. Delahunty, A. Rajab, R. C. Forbes and H. A. Winters (2013). "The utilization of sirolimus and the impact on wound-healing complications in obese kidney transplant recipients." Clin Transplant **27**(4): E521-527.

Humphreys, B. D., S. L. Lin, A. Kobayashi, T. E. Hudson, B. T. Nowlin, J. V. Bonventre, M. T. Valerius, A. P. McMahon and J. S. Duffield (2010). "Fate tracing reveals the pericyte and not epithelial origin of myofibroblasts in kidney fibrosis." Am J Pathol **176**(1): 85-97.

Humphreys, E. H., K. T. Williams, D. H. Adams and S. C. Afford "Primary and malignant cholangiocytes undergo CD40 mediated Fas dependent apoptosis, but are insensitive to direct activation with exogenous Fas ligand." PLoS One **5**(11): e14037.

Humphries, J. D., A. Byron and M. J. Humphries (2006). "Integrin ligands at a glance." J Cell Sci **119**(Pt 19): 3901-3903.

Humphries, M. J. (2000). "Integrin structure." Biochem Soc Trans **28**(4): 311-339.

Humphries, M. J. (2004). "Monoclonal antibodies as probes of integrin priming and activation." Biochem Soc Trans **32**(Pt3): 407-411.

Humphries, M. J., P. A. McEwan, S. J. Barton, P. A. Buckley, J. Bella and A. P. Mould (2003). "Integrin structure: heady advances in ligand binding, but activation still makes the knees wobble." Trends Biochem Sci **28**(6): 313-320.

Hyytiainen, M., C. Penttinen and J. Keski-Oja (2004). "Latent TGF-beta binding proteins: extracellular matrix association and roles in TGF-beta activation." Crit Rev Clin Lab Sci **41**(3): 233-264.

Ijzer, J., B. A. Schotanus, S. Vander Borght, T. A. Roskams, R. Kisjes, L. C. Penning, J. Rothuizen and T. S. van den Ingh (2010). "Characterisation of the hepatic progenitor cell compartment in normal liver and in hepatitis: an immunohistochemical comparison between dog and man." Vet J **184**(3): 308-314.

Ikeda, H., M. Sasaki, Y. Sato, K. Harada, Y. Zen, T. Mitsui and Y. Nakanuma (2009). "Large cell change of hepatocytes in chronic viral hepatitis represents a senescent-related lesion." Hum Pathol **40**(12): 1774-1782.

Inagaki, Y., K. Higashi, M. Kushida, Y. Y. Hong, S. Nakao, R. Higashiyama, T. Moro, J. Itoh, T. Mikami, T. Kimura, G. Shiota, I. Kuwabara and I. Okazaki (2008). "Hepatocyte growth factor suppresses profibrogenic signal transduction via nuclear export of Smad3 with galectin-7." Gastroenterology **134**(4): 1180-1190.

Iredale, J. P., A. Thompson and N. C. Henderson (2013). "Extracellular matrix degradation in liver fibrosis: Biochemistry and regulation." Biochim Biophys Acta **1832**(7): 876-883.

Isenberg, B. C. and J. Y. Wong (2006). "Building structure into engineered tissues." Materials Today **9**(12): 54-60.

Ishak, K., A. Baptista, L. Bianchi, F. Callea, J. De Groote, F. Gudat, H. Denk, V. Desmet, G. Korb, R. N. MacSween and et al. (1995). "Histological grading and staging of chronic hepatitis." J Hepatol **22**(6): 696-699.

Ishikawa, A., M. Sasaki, Y. Sato, S. Ohira, M. F. Chen, S. F. Huang, K. Oda, Y. Nimura and Y. Nakanuma (2004). "Frequent p16ink4a inactivation is an early and frequent event of

intraductal papillary neoplasm of the liver arising in hepatolithiasis." Hum Pathol **35**(12): 1505-1514.
Iwano, M., D. Plieth, T. M. Danoff, C. Xue, H. Okada and E. G. Neilson (2002). "Evidence that fibroblasts derive from epithelium during tissue fibrosis." J Clin Invest **110**(3): 341-350.
Jenkins, G. (2008). "The role of proteases in transforming growth factor-beta activation." Int J Biochem Cell Biol **40**(6-7): 1068-1078.
Jiang, S., R. I. Lechler, X. S. He and J. F. Huang (2006). "Regulatory T cells and transplantation tolerance." Hum Immunol **67**(10): 765-776.
Jin Jung, K., D. Hyun Kim, E. Kyeong Lee, C. Woo Song, B. Pal Yu and H. Young Chung (2013). "Oxidative stress induces inactivation of protein phosphatase 2A, promoting proinflammatory NF-kappaB in aged rat kidney." Free Radic Biol Med **61C**: 206-217.
Jin, Y., S. A. Birlea, P. R. Fain, K. Gowan, S. L. Riccardi, P. J. Holland, D. C. Bennett, D. M. Herbstman, M. R. Wallace, W. T. McCormack, E. H. Kemp, D. J. Gawkrodger, A. P. Weetman, M. Picardo, G. Leone, A. Taieb, T. Jouary, K. Ezzedine, N. van Geel, J. Lambert, A. Overbeck and R. A. Spritz (2011). "Genome-wide analysis identifies a quantitative trait locus in the MHC class II region associated with generalized vitiligo age of onset." J Invest Dermatol **131**(6): 1308-1312.
Johnson, Z., A. E. Proudfoot and T. M. Handel (2005). "Interaction of chemokines and glycosaminoglycans: a new twist in the regulation of chemokine function with opportunities for therapeutic intervention." Cytokine Growth Factor Rev **16**(6): 625-636.
Jones, D. E. (2008). "Pathogenesis of primary biliary cirrhosis." Clin Liver Dis **12**(2): 305-321; viii.
Jules- Elysee, K. M., S. E. Wilfred, S. G. Memtsoudis, D. H. Kim, J. T. YaDeau, M. K. Urban, M. L. Lichardi, A. S. McLawhorn and T. P. Sculco (2012). "Steroid modulation of cytokine release and desmosine levels in bilateral total knee replacement: a prospective, double-blind, randomized controlled trial." J Bone Joint Surg Am **94**(23): 2120-2127.
Kalluri, R. and E. G. Neilson (2003). "Epithelial-mesenchymal transition and its implications for fibrosis." J Clin Invest **112**(12): 1776-1784.
Kaminska, B., K. Gaweda-Walerych and M. Zawadzka (2004). "Molecular mechanisms of neuroprotective action of immunosuppressants--facts and hypotheses." J Cell Mol Med **8**(1): 45-58.
Katayanagi, K., N. Kono and Y. Nakanuma (1998). "Isolation, culture and characterization of biliary epithelial cells from different anatomical levels of the intrahepatic and extrahepatic biliary tree from a mouse." Liver **18**(2): 90-98.
Katsumoto, T. R., S. M. Violette and D. Sheppard (2011). "Blocking TGFbeta via Inhibition of the alphavbeta6 Integrin: A Possible Therapy for Systemic Sclerosis Interstitial Lung Disease." Int J Rheumatol **2011**: 208219.
Kelly, D. M., H. Shiba, S. Nakagawa, S. Irefin, B. Eghtesad, C. Quintini, F. Aucejo, K. Hashimoto, J. J. Fung and C. Miller (2011). "Hepatic blood flow plays an important role in ischemia-reperfusion injury." Liver Transpl **17**(12): 1448-1456.
Kent, G., S. Gay, T. Inouye, R. Bahu, O. T. Minick and H. Popper (1976). "Vitamin A-containing lipocytes and formation of type III collagen in liver injury." Proc Natl Acad Sci U S A **73**(10): 3719-3722.
Khalil, N. (1999). "TGF-beta: from latent to active." Microbes Infect **1**(15): 1255-1263.
Khanna, A. K. (2000). "Mechanism of the combination immunosuppressive effects of rapamycin with either cyclosporine or tacrolimus." Transplantation **70**(4): 690-694.
Kiani-Esfahani, A., S. Bahrami, M. Tavalaee, M. R. Deemeh, A. A. Mahjour and M. H. Nasr-Esfahani (2013). "Cytosolic and mitochondrial ROS: which one is associated with poor chromatin remodeling?" Syst Biol Reprod Med.
Kim, K. K., M. C. Kugler, P. J. Wolters, L. Robillard, M. G. Galvez, A. N. Brumwell, D. Sheppard and H. A. Chapman (2006). "Alveolar epithelial cell mesenchymal transition

develops in vivo during pulmonary fibrosis and is regulated by the extracellular matrix." Proc Natl Acad Sci U S A **103**(35): 13180-13185.
Kinnman, N., C. Francoz, V. Barbu, D. Wendum, C. Rey, R. Hultcrantz, R. Poupon and C. Housset (2003). "The myofibroblastic conversion of peribiliary fibrogenic cells distinct from hepatic stellate cells is stimulated by platelet-derived growth factor during liver fibrogenesis." Lab Invest **83**(2): 163-173.
Kirby, J. A., H. Robertson, H. L. Marshall, K. A. Rygiel, M. Hudson, D. E. Jones and A. D. Burt (2008). "Epithelial to mesenchymal transition in primary sclerosing cholangitis." Liver Int **28**(8): 1176-1177.
Kleiner, D. E., E. M. Brunt, M. Van Natta, C. Behling, M. J. Contos, O. W. Cummings, L. D. Ferrell, Y. C. Liu, M. S. Torbenson, A. Unalp-Arida, M. Yeh, A. J. McCullough, A. J. Sanyal and N. Nonalcoholic Steatohepatitis Clinical Research (2005). "Design and validation of a histological scoring system for nonalcoholic fatty liver disease." Hepatology **41**(6): 1313-1321.
Klionsky, D. J., F. C. Abdalla, H. Abeliovich, R. T. Abraham, A. Acevedo-Arozena, K. Adeli, L. Agholme, M. Agnello, P. Agostinis, J. A. Aguirre-Ghiso, H. J. Ahn, O. Ait-Mohamed, S. Ait-Si-Ali, T. Akematsu, S. Akira, H. M. Al-Younes, M. A. Al-Zeer, M. L. Albert, R. L. Albin, J. Alegre-Abarrategui, M. F. Aleo, M. Alirezaei, A. Almasan, M. Almonte-Becerril, A. Amano, R. Amaravadi, S. Amarnath, A. O. Amer, N. Andrieu-Abadie, V. Anantharam, D. K. Ann, S. Anoopkumar-Dukie, H. Aoki, N. Apostolova, G. Arancia, J. P. Aris, K. Asanuma, N. Y. Asare, H. Ashida, V. Askanas, D. S. Askew, P. Auberger, M. Baba, S. K. Backues, E. H. Baehrecke, B. A. Bahr, X. Y. Bai, Y. Bailly, R. Baiocchi, G. Baldini, W. Balduini, A. Ballabio, B. A. Bamber, E. T. Bampton, G. Banhegyi, C. R. Bartholomew, D. C. Bassham, R. C. Bast, Jr., H. Batoko, B. H. Bay, I. Beau, D. M. Bechet, T. J. Begley, C. Behl, C. Behrends, S. Bekri, B. Bellaire, L. J. Bendall, L. Benetti, L. Berliocchi, H. Bernardi, F. Bernassola, S. Besteiro, I. Bhatia-Kissova, X. Bi, M. Biard-Piechaczyk, J. S. Blum, L. H. Boise, P. Bonaldo, D. L. Boone, B. C. Bornhauser, K. R. Bortoluci, I. Bossis, F. Bost, J. P. Bourquin, P. Boya, M. Boyer-Guittaut, P. V. Bozhkov, N. R. Brady, C. Brancolini, A. Brech, J. E. Brenman, A. Brennand, E. H. Bresnick, P. Brest, D. Bridges, M. L. Bristol, P. S. Brookes, E. J. Brown, J. H. Brumell, N. Brunetti-Pierri, U. T. Brunk, D. E. Bulman, S. J. Bultman, G. Bultynck, L. F. Burbulla, W. Bursch, J. P. Butchar, W. Buzgariu, S. P. Bydlowski, K. Cadwell, M. Cahova, D. Cai, J. Cai, Q. Cai, B. Calabretta, J. Calvo-Garrido, N. Camougrand, M. Campanella, J. Campos-Salinas, E. Candi, L. Cao, A. B. Caplan, S. R. Carding, S. M. Cardoso, J. S. Carew, C. R. Carlin, V. Carmignac, L. A. Carneiro, S. Carra, R. A. Caruso, G. Casari, C. Casas, R. Castino, E. Cebollero, F. Cecconi, J. Celli, H. Chaachouay, H. J. Chae, C. Y. Chai, D. C. Chan, E. Y. Chan, R. C. Chang, C. M. Che, C. C. Chen, G. C. Chen, G. Q. Chen, M. Chen, Q. Chen, S. S. Chen, W. Chen, X. Chen, X. Chen, X. Chen, Y. G. Chen, Y. Chen, Y. Chen, Y. J. Chen, Z. Chen, A. Cheng, C. H. Cheng, Y. Cheng, H. Cheong, J. H. Cheong, S. Cherry, R. Chess-Williams, Z. H. Cheung, E. Chevet, H. L. Chiang, R. Chiarelli, T. Chiba, L. S. Chin, S. H. Chiou, F. V. Chisari, C. H. Cho, D. H. Cho, A. M. Choi, D. Choi, K. S. Choi, M. E. Choi, S. Chouaib, D. Choubey, V. Choubey, C. T. Chu, T. H. Chuang, S. H. Chueh, T. Chun, Y. J. Chwae, M. L. Chye, R. Ciarcia, M. R. Ciriolo, M. J. Clague, R. S. Clark, P. G. Clarke, R. Clarke, P. Codogno, H. A. Coller, M. I. Colombo, S. Comincini, M. Condello, F. Condorelli, M. R. Cookson, G. H. Coombs, I. Coppens, R. Corbalan, P. Cossart, P. Costelli, S. Costes, A. Coto-Montes, E. Couve, F. P. Coxon, J. M. Cregg, J. L. Crespo, M. J. Cronje, A. M. Cuervo, J. J. Cullen, M. J. Czaja, M. D'Amelio, A. Darfeuille-Michaud, L. M. Davids, F. E. Davies, M. De Felici, J. F. de Groot, C. A. de Haan, L. De Martino, A. De Milito, V. De Tata, J. Debnath, A. Degterev, B. Dehay, L. M. Delbridge, F. Demarchi, Y. Z. Deng, J. Dengjel, P. Dent, D. Denton, V. Deretic, S. D. Desai, R. J. Devenish, M. Di Gioacchino, G. Di Paolo, C. Di Pietro, G. Diaz-Araya, I. Diaz-Laviada, M. T. Diaz-Meco, J. Diaz-Nido, I. Dikic, S. P. Dinesh-Kumar, W. X. Ding, C. W. Distelhorst, A. Diwan, M. Djavaheri-Mergny, S. Dokudovskaya, Z. Dong, F. C. Dorsey, V. Dosenko, J. J. Dowling, S. Doxsey, M. Dreux, M. E. Drew, Q. Duan, M. A. Duchosal, K.

Duff, I. Dugail, M. Durbeej, M. Duszenko, C. L. Edelstein, A. L. Edinger, G. Egea, L. Eichinger, N. T. Eissa, S. Ekmekcioglu, W. S. El-Deiry, Z. Elazar, M. Elgendy, L. M. Ellerby, K. E. Eng, A. M. Engelbrecht, S. Engelender, J. Erenpreisa, R. Escalante, A. Esclatine, E. L. Eskelinen, L. Espert, V. Espina, H. Fan, J. Fan, Q. W. Fan, Z. Fan, S. Fang, Y. Fang, M. Fanto, A. Fanzani, T. Farkas, J. C. Farre, M. Faure, M. Fechheimer, C. G. Feng, J. Feng, Q. Feng, Y. Feng, L. Fesus, R. Feuer, M. E. Figueiredo-Pereira, G. M. Fimia, D. C. Fingar, S. Finkbeiner, T. Finkel, K. D. Finley, F. Fiorito, E. A. Fisher, P. B. Fisher, M. Flajolet, M. L. Florez-McClure, S. Florio, E. A. Fon, F. Fornai, F. Fortunato, R. Fotedar, D. H. Fowler, H. S. Fox, R. Franco, L. B. Frankel, M. Fransen, J. M. Fuentes, J. Fueyo, J. Fujii, K. Fujisaki, E. Fujita, M. Fukuda, R. H. Furukawa, M. Gaestel, P. Gailly, M. Gajewska, B. Galliot, V. Galy, S. Ganesh, B. Ganetzky, I. G. Ganley, F. B. Gao, G. F. Gao, J. Gao, L. Garcia, G. Garcia-Manero, M. Garcia-Marcos, M. Garmyn, A. L. Gartel, E. Gatti, M. Gautel, T. R. Gawriluk, M. E. Gegg, J. Geng, M. Germain, J. E. Gestwicki, D. A. Gewirtz, S. Ghavami, P. Ghosh, A. M. Giammarioli, A. N. Giatromanolaki, S. B. Gibson, R. W. Gilkerson, M. L. Ginger, H. N. Ginsberg, J. Golab, M. S. Goligorsky, P. Golstein, C. Gomez-Manzano, E. Goncu, C. Gongora, C. D. Gonzalez, R. Gonzalez, C. Gonzalez-Estevez, R. A. Gonzalez-Polo, E. Gonzalez-Rey, N. V. Gorbunov, S. Gorski, S. Goruppi, R. A. Gottlieb, D. Gozuacik, G. E. Granato, G. D. Grant, K. N. Green, A. Gregorc, F. Gros, C. Grose, T. W. Grunt, P. Gual, J. L. Guan, K. L. Guan, S. M. Guichard, A. S. Gukovskaya, I. Gukovsky, J. Gunst, A. B. Gustafsson, A. J. Halayko, A. N. Hale, S. K. Halonen, M. Hamasaki, F. Han, T. Han, M. K. Hancock, M. Hansen, H. Harada, M. Harada, S. E. Hardt, J. W. Harper, A. L. Harris, J. Harris, S. D. Harris, M. Hashimoto, J. A. Haspel, S. Hayashi, L. A. Hazelhurst, C. He, Y. W. He, M. J. Hebert, K. A. Heidenreich, M. H. Helfrich, G. V. Helgason, E. P. Henske, B. Herman, P. K. Herman, C. Hetz, S. Hilfiker, J. A. Hill, L. J. Hocking, P. Hofman, T. G. Hofmann, J. Hohfeld, T. L. Holyoake, M. H. Hong, D. A. Hood, G. S. Hotamisligil, E. J. Houwerzijl, M. Hoyer-Hansen, B. Hu, C. A. Hu, H. M. Hu, Y. Hua, C. Huang, J. Huang, S. Huang, W. P. Huang, T. B. Huber, W. K. Huh, T. H. Hung, T. R. Hupp, G. M. Hur, J. B. Hurley, S. N. Hussain, P. J. Hussey, J. J. Hwang, S. Hwang, A. Ichihara, S. Ilkhanizadeh, K. Inoki, T. Into, V. Iovane, J. L. Iovanna, N. Y. Ip, Y. Isaka, H. Ishida, C. Isidoro, K. Isobe, A. Iwasaki, M. Izquierdo, Y. Izumi, P. M. Jaakkola, M. Jaattela, G. R. Jackson, W. T. Jackson, B. Janji, M. Jendrach, J. H. Jeon, E. B. Jeung, H. Jiang, H. Jiang, J. X. Jiang, M. Jiang, Q. Jiang, X. Jiang, X. Jiang, A. Jimenez, M. Jin, S. Jin, C. O. Joe, T. Johansen, D. E. Johnson, G. V. Johnson, N. L. Jones, B. Joseph, S. K. Joseph, A. M. Joubert, G. Juhasz, L. Juillerat-Jeanneret, C. H. Jung, Y. K. Jung, K. Kaarniranta, A. Kaasik, T. Kabuta, M. Kadowaki, K. Kagedal, Y. Kamada, V. O. Kaminskyy, H. H. Kampinga, H. Kanamori, C. Kang, K. B. Kang, K. I. Kang, R. Kang, Y. A. Kang, T. Kanki, T. D. Kanneganti, H. Kanno, A. G. Kanthasamy, A. Kanthasamy, V. Karantza, G. P. Kaushal, S. Kaushik, Y. Kawazoe, P. Y. Ke, J. H. Kehrl, A. Kelekar, C. Kerkhoff, D. H. Kessel, H. Khalil, J. A. Kiel, A. A. Kiger, A. Kihara, D. R. Kim, D. H. Kim, D. H. Kim, E. K. Kim, H. R. Kim, J. S. Kim, J. H. Kim, J. C. Kim, J. K. Kim, P. K. Kim, S. W. Kim, Y. S. Kim, Y. Kim, A. Kimchi, A. C. Kimmelman, J. S. King, T. J. Kinsella, V. Kirkin, L. A. Kirshenbaum, K. Kitamoto, K. Kitazato, L. Klein, W. T. Klimecki, J. Klucken, E. Knecht, B. C. Ko, J. C. Koch, H. Koga, J. Y. Koh, Y. H. Koh, M. Koike, M. Komatsu, E. Kominami, H. J. Kong, W. J. Kong, V. I. Korolchuk, Y. Kotake, M. I. Koukourakis, J. B. Kouri Flores, A. L. Kovacs, C. Kraft, D. Krainc, H. Kramer, C. Kretz-Remy, A. M. Krichevsky, G. Kroemer, R. Kruger, O. Krut, N. T. Ktistakis, C. Y. Kuan, R. Kucharczyk, A. Kumar, R. Kumar, S. Kumar, M. Kundu, H. J. Kung, T. Kurz, H. J. Kwon, A. R. La Spada, F. Lafont, T. Lamark, J. Landry, J. D. Lane, P. Lapaquette, J. F. Laporte, L. Laszlo, S. Lavandero, J. N. Lavoie, R. Layfield, P. A. Lazo, W. Le, L. Le Cam, D. J. Ledbetter, A. J. Lee, B. W. Lee, G. M. Lee, J. Lee, J. H. Lee, M. Lee, M. S. Lee, S. H. Lee, C. Leeuwenburgh, P. Legembre, R. Legouis, M. Lehmann, H. Y. Lei, Q. Y. Lei, D. A. Leib, J. Leiro, J. J. Lemasters, A. Lemoine, M. S. Lesniak, D. Lev, V. V. Levenson, B. Levine, E. Levy, F. Li, J. L. Li, L. Li, S. Li, W. Li, X. J. Li, Y. B. Li, Y. P. Li, C. Liang, Q. Liang, Y. F. Liao, P. P. Liberski, A. Lieberman, H. J. Lim, K. L. Lim, K. Lim, C. F. Lin, F. C. Lin, J. Lin, J. D. Lin, K. Lin, W. W. Lin, W. C. Lin, Y. L. Lin, R. Linden, P. Lingor, J. Lippincott-

Schwartz, M. P. Lisanti, P. B. Liton, B. Liu, C. F. Liu, K. Liu, L. Liu, Q. A. Liu, W. Liu, Y. C. Liu, Y. Liu, R. A. Lockshin, C. N. Lok, S. Lonial, B. Loos, G. Lopez-Berestein, C. Lopez-Otin, L. Lossi, M. T. Lotze, P. Low, B. Lu, B. Lu, B. Lu, Z. Lu, F. Luciano, N. W. Lukacs, A. H. Lund, M. A. Lynch-Day, Y. Ma, F. Macian, J. P. MacKeigan, K. F. Macleod, F. Madeo, L. Maiuri, M. C. Maiuri, D. Malagoli, M. C. Malicdan, W. Malorni, N. Man, E. M. Mandelkow, S. Manon, I. Manov, K. Mao, X. Mao, Z. Mao, P. Marambaud, D. Marazziti, Y. L. Marcel, K. Marchbank, P. Marchetti, S. J. Marciniak, M. Marcondes, M. Mardi, G. Marfe, G. Marino, M. Markaki, M. R. Marten, S. J. Martin, C. Martinand-Mari, W. Martinet, M. Martinez-Vicente, M. Masini, P. Matarrese, S. Matsuo, R. Matteoni, A. Mayer, N. M. Mazure, D. J. McConkey, M. J. McConnell, C. McDermott, C. McDonald, G. M. McInerney, S. L. McKenna, B. McLaughlin, P. J. McLean, C. R. McMaster, G. A. McQuibban, A. J. Meijer, M. H. Meisler, A. Melendez, T. J. Melia, G. Melino, M. A. Mena, J. A. Menendez, R. F. Menna-Barreto, M. B. Menon, F. M. Menzies, C. A. Mercer, A. Merighi, D. E. Merry, S. Meschini, C. G. Meyer, T. F. Meyer, C. Y. Miao, J. Y. Miao, P. A. Michels, C. Michiels, D. Mijaljica, A. Milojkovic, S. Minucci, C. Miracco, C. K. Miranti, I. Mitroulis, K. Miyazawa, N. Mizushima, B. Mograbi, S. Mohseni, X. Molero, B. Mollereau, F. Mollinedo, T. Momoi, I. Monastyrska, M. M. Monick, M. J. Monteiro, M. N. Moore, R. Mora, K. Moreau, P. I. Moreira, Y. Moriyasu, J. Moscat, S. Mostowy, J. C. Mottram, T. Motyl, C. E. Moussa, S. Muller, S. Muller, K. Munger, C. Munz, L. O. Murphy, M. E. Murphy, A. Musaro, I. Mysorekar, E. Nagata, K. Nagata, A. Nahimana, U. Nair, T. Nakagawa, K. Nakahira, H. Nakano, H. Nakatogawa, M. Nanjundan, N. I. Naqvi, D. P. Narendra, M. Narita, M. Navarro, S. T. Nawrocki, T. Y. Nazarko, A. Nemchenko, M. G. Netea, T. P. Neufeld, P. A. Ney, I. P. Nezis, H. P. Nguyen, D. Nie, I. Nishino, C. Nislow, R. A. Nixon, T. Noda, A. A. Noegel, A. Nogalska, S. Noguchi, L. Notterpek, I. Novak, T. Nozaki, N. Nukina, T. Nurnberger, B. Nyfeler, K. Obara, T. D. Oberley, S. Oddo, M. Ogawa, T. Ohashi, K. Okamoto, N. L. Oleinick, F. J. Oliver, L. J. Olsen, S. Olsson, O. Opota, T. F. Osborne, G. K. Ostrander, K. Otsu, J. H. Ou, M. Ouimet, M. Overholtzer, B. Ozpolat, P. Paganetti, U. Pagnini, N. Pallet, G. E. Palmer, C. Palumbo, T. Pan, T. Panaretakis, U. B. Pandey, Z. Papackova, I. Papassideri, I. Paris, J. Park, O. K. Park, J. B. Parys, K. R. Parzych, S. Patschan, C. Patterson, S. Pattingre, J. M. Pawelek, J. Peng, D. H. Perlmutter, I. Perrotta, G. Perry, S. Pervaiz, M. Peter, G. J. Peters, M. Petersen, G. Petrovski, J. M. Phang, M. Piacentini, P. Pierre, V. Pierrefite-Carle, G. Pierron, R. Pinkas-Kramarski, A. Piras, N. Piri, L. C. Platanias, S. Poggeler, M. Poirot, A. Poletti, C. Pous, M. Pozuelo-Rubio, M. Praetorius-Ibba, A. Prasad, M. Prescott, M. Priault, N. Produit-Zengaffinen, A. Progulske-Fox, T. Proikas-Cezanne, S. Przedborski, K. Przyklenk, R. Puertollano, J. Puyal, S. B. Qian, L. Qin, Z. H. Qin, S. E. Quaggin, N. Raben, H. Rabinowich, S. W. Rabkin, I. Rahman, A. Rami, G. Ramm, G. Randall, F. Randow, V. A. Rao, J. C. Rathmell, B. Ravikumar, S. K. Ray, B. H. Reed, J. C. Reed, F. Reggiori, A. Regnier-Vigouroux, A. S. Reichert, J. J. Reiners, Jr., R. J. Reiter, J. Ren, J. L. Revuelta, C. J. Rhodes, K. Ritis, E. Rizzo, J. Robbins, M. Roberge, H. Roca, M. C. Roccheri, S. Rocchi, H. P. Rodemann, S. Rodriguez de Cordoba, B. Rohrer, I. B. Roninson, K. Rosen, M. M. Rost-Roszkowska, M. Rouis, K. M. Rouschop, F. Rovetta, B. P. Rubin, D. C. Rubinsztein, K. Ruckdeschel, E. B. Rucker, 3rd, A. Rudich, E. Rudolf, N. Ruiz-Opazo, R. Russo, T. E. Rusten, K. M. Ryan, S. W. Ryter, D. M. Sabatini, J. Sadoshima, T. Saha, T. Saitoh, H. Sakagami, Y. Sakai, G. H. Salekdeh, P. Salomoni, P. M. Salvaterra, G. Salvesen, R. Salvioli, A. M. Sanchez, J. A. Sanchez-Alcazar, R. Sanchez-Prieto, M. Sandri, U. Sankar, P. Sansanwal, L. Santambrogio, S. Saran, S. Sarkar, M. Sarwal, C. Sasakawa, A. Sasnauskiene, M. Sass, K. Sato, M. Sato, A. H. Schapira, M. Scharl, H. M. Schatzl, W. Scheper, S. Schiaffino, C. Schneider, M. E. Schneider, R. Schneider-Stock, P. V. Schoenlein, D. F. Schorderet, C. Schuller, G. K. Schwartz, L. Scorrano, L. Sealy, P. O. Seglen, J. Segura-Aguilar, I. Seiliez, O. Seleverstov, C. Sell, J. B. Seo, D. Separovic, V. Setaluri, T. Setoguchi, C. Settembre, J. J. Shacka, M. Shanmugam, I. M. Shapiro, E. Shaulian, R. J. Shaw, J. H. Shelhamer, H. M. Shen, W. C. Shen, Z. H. Sheng, Y. Shi, K. Shibuya, Y. Shidoji, J. J. Shieh, C. M. Shih, Y. Shimada, S. Shimizu, T. Shintani, O. S.

Shirihai, G. C. Shore, A. A. Sibirny, S. B. Sidhu, B. Sikorska, E. C. Silva-Zacarin, A. Simmons, A. K. Simon, H. U. Simon, C. Simone, A. Simonsen, D. A. Sinclair, R. Singh, D. Sinha, F. A. Sinicrope, A. Sirko, P. M. Siu, E. Sivridis, V. Skop, V. P. Skulachev, R. S. Slack, S. S. Smaili, D. R. Smith, M. S. Soengas, T. Soldati, X. Song, A. K. Sood, T. W. Soong, F. Sotgia, S. A. Spector, C. D. Spies, W. Springer, S. M. Srinivasula, L. Stefanis, J. S. Steffan, R. Stendel, H. Stenmark, A. Stephanou, S. T. Stern, C. Sternberg, B. Stork, P. Stralfors, C. S. Subauste, X. Sui, D. Sulzer, J. Sun, S. Y. Sun, Z. J. Sun, J. J. Sung, K. Suzuki, T. Suzuki, M. S. Swanson, C. Swanton, S. T. Sweeney, L. K. Sy, G. Szabadkai, I. Tabas, H. Taegtmeyer, M. Tafani, K. Takacs-Vellai, Y. Takano, K. Takegawa, G. Takemura, F. Takeshita, N. J. Talbot, K. S. Tan, K. Tanaka, K. Tanaka, D. Tang, D. Tang, I. Tanida, B. A. Tannous, N. Tavernarakis, G. S. Taylor, G. A. Taylor, J. P. Taylor, L. S. Terada, A. Terman, G. Tettamanti, K. Thevissen, C. B. Thompson, A. Thorburn, M. Thumm, F. Tian, Y. Tian, G. Tocchini-Valentini, A. M. Tolkovsky, Y. Tomino, L. Tonges, S. A. Tooze, C. Tournier, J. Tower, R. Towns, V. Trajkovic, L. H. Travassos, T. F. Tsai, M. P. Tschan, T. Tsubata, A. Tsung, B. Turk, L. S. Turner, S. C. Tyagi, Y. Uchiyama, T. Ueno, M. Umekawa, R. Umemiya-Shirafuji, V. K. Unni, M. I. Vaccaro, E. M. Valente, G. Van den Berghe, I. J. van der Klei, W. van Doorn, L. F. van Dyk, M. van Egmond, L. A. van Grunsven, P. Vandenabeele, W. P. Vandenberghe, I. Vanhorebeek, E. C. Vaquero, G. Velasco, T. Vellai, J. M. Vicencio, R. D. Vierstra, M. Vila, C. Vindis, G. Viola, M. T. Viscomi, O. V. Voitsekhovskaja, C. von Haefen, M. Votruba, K. Wada, R. Wade-Martins, C. L. Walker, C. M. Walsh, J. Walter, X. B. Wan, A. Wang, C. Wang, D. Wang, F. Wang, F. Wang, G. Wang, H. Wang, H. G. Wang, H. D. Wang, J. Wang, K. Wang, M. Wang, R. C. Wang, X. Wang, X. Wang, Y. J. Wang, Y. Wang, Z. Wang, Z. C. Wang, Z. Wang, D. G. Wansink, D. M. Ward, H. Watada, S. L. Waters, P. Webster, L. Wei, C. C. Weihl, W. A. Weiss, S. M. Welford, L. P. Wen, C. A. Whitehouse, J. L. Whitton, A. J. Whitworth, T. Wileman, J. W. Wiley, S. Wilkinson, D. Willbold, R. L. Williams, P. R. Williamson, B. G. Wouters, C. Wu, D. C. Wu, W. K. Wu, A. Wyttenbach, R. J. Xavier, Z. Xi, P. Xia, G. Xiao, Z. Xie, Z. Xie, D. Z. Xu, J. Xu, L. Xu, X. Xu, A. Yamamoto, A. Yamamoto, S. Yamashina, M. Yamashita, X. Yan, M. Yanagida, D. S. Yang, E. Yang, J. M. Yang, S. Y. Yang, W. Yang, W. Y. Yang, Z. Yang, M. C. Yao, T. P. Yao, B. Yeganeh, W. L. Yen, J. J. Yin, X. M. Yin, O. J. Yoo, G. Yoon, S. Y. Yoon, T. Yorimitsu, Y. Yoshikawa, T. Yoshimori, K. Yoshimoto, H. J. You, R. J. Youle, A. Younes, L. Yu, L. Yu, S. W. Yu, W. H. Yu, Z. M. Yuan, Z. Yue, C. H. Yun, M. Yuzaki, O. Zabirnyk, E. Silva-Zacarin, D. Zacks, E. Zacksenhaus, N. Zaffaroni, Z. Zakeri, H. J. Zeh, 3rd, S. O. Zeitlin, H. Zhang, H. L. Zhang, J. Zhang, J. P. Zhang, L. Zhang, L. Zhang, M. Y. Zhang, X. D. Zhang, M. Zhao, Y. F. Zhao, Y. Zhao, Z. J. Zhao, X. Zheng, B. Zhivotovsky, Q. Zhong, C. Z. Zhou, C. Zhu, W. G. Zhu, X. F. Zhu, X. Zhu, Y. Zhu, T. Zoladek, W. X. Zong, A. Zorzano, J. Zschocke and B. Zuckerbraun (2012). "Guidelines for the use and interpretation of assays for monitoring autophagy." Autophagy **8**(4): 445-544.

Klionsky, D. J., P. Codogno, A. M. Cuervo, V. Deretic, Z. Elazar, J. Fueyo-Margareto, D. A. Gewirtz, G. Kroemer, B. Levine, N. Mizushima, D. C. Rubinsztein, M. Thumm and S. A. Tooze (2010). "A comprehensive glossary of autophagy-related molecules and processes." Autophagy **6**(4): 438-448.

Klionsky, D. J. and S. D. Emr (2000). "Autophagy as a regulated pathway of cellular degradation." Science **290**(5497): 1717-1721.

Komatsu, M., Q. J. Wang, G. R. Holstein, V. L. Friedrich, Jr., J. Iwata, E. Kominami, B. T. Chait, K. Tanaka and Z. Yue (2007). "Essential role for autophagy protein Atg7 in the maintenance of axonal homeostasis and the prevention of axonal degeneration." Proc Natl Acad Sci U S A **104**(36): 14489-14494.

Kong, F., Z. Li, W. M. Parks, D. W. Dumbauld, A. J. Garcia, A. P. Mould, M. J. Humphries and C. Zhu (2013). "Cyclic mechanical reinforcement of integrin-ligand interactions." Mol Cell **49**(6): 1060-1068.

Konkel, J. E. and W. Chen (2011). "Balancing acts: the role of TGF-beta in the mucosal immune system." Trends Mol Med **17**(11): 668-676.

Kovacic, P. and R. S. Pozos (2006). "Cell signaling (mechanism and reproductive toxicity): redox chains, radicals, electrons, relays, conduit, electrochemistry, and other medical implications." Birth Defects Res C Embryo Today **78**(4): 333-344.
Kraft, S., B. Diefenbach, R. Mehta, A. Jonczyk, G. A. Luckenbach and S. L. Goodman (1999). "Definition of an unexpected ligand recognition motif for alphav beta6 integrin." J Biol Chem **274**(4): 1979-1985.
Ksiazek, K., J. F. Passos, S. Olijslagers and T. von Zglinicki (2008). "Mitochondrial dysfunction is a possible cause of accelerated senescence of mesothelial cells exposed to high glucose." Biochem Biophys Res Commun **366**(3): 793-799.
Kwiecinski, M., A. Noetel, N. Elfimova, J. Trebicka, S. Schievenbusch, I. Strack, L. Molnar, M. von Brandenstein, U. Tox, R. Nischt, O. Coutelle, H. P. Dienes and M. Odenthal (2011). "Hepatocyte growth factor (HGF) inhibits collagen I and IV synthesis in hepatic stellate cells by miRNA-29 induction." PLoS One **6**(9): e24568.
Lakkis, F. G. and R. I. Lechler (2013). "Origin and biology of the allogeneic response." Cold Spring Harb Perspect Med **3**(8).
Lamouille, S., E. Connolly, J. W. Smyth, R. J. Akhurst and R. Derynck (2012). "TGF-beta-induced activation of mTOR complex 2 drives epithelial-mesenchymal transition and cell invasion." J Cell Sci **125**(Pt 5): 1259-1273.
Lamouille, S. and R. Derynck (2011). "Emergence of the phosphoinositide 3-kinase-Akt-mammalian target of rapamycin axis in transforming growth factor-beta-induced epithelial-mesenchymal transition." Cells Tissues Organs **193**(1-2): 8-22.
Lawless, C., D. Jurk, C. S. Gillespie, D. Shanley, G. Saretzki, T. von Zglinicki and J. F. Passos (2012). "A stochastic step model of replicative senescence explains ROS production rate in ageing cell populations." PLoS One **7**(2): e32117.
Lawless, C., C. Wang, D. Jurk, A. Merz, T. Zglinicki and J. F. Passos (2010). "Quantitative assessment of markers for cell senescence." Exp Gerontol **45**(10): 772-778.
Lawrence, D. A. (1996). "Transforming growth factor-beta: a general review." Eur Cytokine Netw **7**(3): 363-374.
Lebleu, V. S., G. Taduri, J. O'Connell, Y. Teng, V. G. Cooke, C. Woda, H. Sugimoto and R. Kalluri (2013). "Origin and function of myofibroblasts in kidney fibrosis." Nat Med **19**(8): 1047-1053.
Lechler, R. I., G. Lombardi, J. R. Batchelor, N. Reinsmoen and F. H. Bach (1990). "The molecular basis of alloreactivity." Immunol Today **11**(3): 83-88.
Lee, J., A. Belanger, J. T. Doucette, C. Stanca, S. Friedman and N. Bach (2007). "Transplantation trends in primary biliary cirrhosis." Clin Gastroenterol Hepatol **5**(11): 1313-1315.
Lee, J. M., S. Dedhar, R. Kalluri and E. W. Thompson (2006). "The epithelial-mesenchymal transition: new insights in signaling, development, and disease." J Cell Biol **172**(7): 973-981.
Lee, Y. J., H. Y. Jeong, Y. B. Kim, Y. J. Lee, S. Y. Won, J. H. Shim, M. K. Cho, H. S. Nam and S. H. Lee (2012). "Reactive oxygen species and PI3K/Akt signaling play key roles in the induction of Nrf2-driven heme oxygenase-1 expression in sulforaphane-treated human mesothelioma MSTO-211H cells." Food Chem Toxicol **50**(2): 116-123.
Legoux, F., L. Gautreau, L. Hesnard, A. Leger, M. Moyon, M. C. Devilder, M. Bonneville and X. Saulquin (2013). "Characterization of the human CD4 T-cell repertoire specific for MHC Class I-restricted antigens." Eur J Immunol.
Leon, M. P., J. A. Kirby, P. Gibbs, A. D. Burt and M. F. Bassendine (1995). "Immunogenicity of biliary epithelial cells: study of the expression of B7 molecules." J Hepatol **22**(5): 591-595.
Leroy, C., J. Deheuninck, S. Reveneau, B. Foveau, Z. Ji, C. Villenet, S. Quief, D. Tulasne, J. P. Kerckaert and V. Fafeur (2006). "HGF/SF regulates expression of apoptotic genes in MCF-10A human mammary epithelial cells." Ann N Y Acad Sci **1090**: 188-202.

Lerut, J., J. Mathys, C. Verbaandert, S. Talpe, O. Ciccarelli, J. Lemaire, E. Bonaccorsi-Riani, V. Vanthuyne, N. Hetsch, F. Roggen, C. D. Reyck, P. Goffette, D. Latinne, G. Orlando, J. Rahier, C. Sempoux, P. Wallemacq, P. F. Laterre and P. Gianello (2008). "Tacrolimus monotherapy in liver transplantation: one-year results of a prospective, randomized, double-blind, placebo-controlled study." Ann Surg **248**(6): 956-967.

Leventhal, J., M. Abecassis, J. Miller, L. Gallon, D. Tollerud, M. J. Elliott, L. D. Bozulic, C. Houston, N. Sustento-Reodica and S. T. Ildstad (2013). "Tolerance induction in HLA disparate living donor kidney transplantation by donor stem cell infusion: durable chimerism predicts outcome." Transplantation **95**(1): 169-176.

Levitsky, J., J. M. Mathew, M. Abecassis, A. Tambur, J. Leventhal, D. Chandrasekaran, N. Herrera, P. Al-Saden, L. Gallon, A. Abdul-Nabi, G. Y. Yang, S. M. Kurian, D. R. Salomon and J. Miller (2013). "Systemic immunoregulatory and proteogenomic effects of tacrolimus to sirolimus conversion in liver transplant recipients." Hepatology **57**(1): 239-248.

Li, F. and M. Zhou (2013). "Conditional expression of the dominant-negative TGF-beta receptor type II elicits lingual epithelial hyperplasia in transgenic mice." Dev Dyn **242**(5): 444-455.

Li, T., L. Longobardi, T. J. Myers, J. D. Temple, R. L. Chandler, H. Ozkan, C. Contaldo and A. Spagnoli (2013). "Joint TGF-beta type II receptor-expressing cells: ontogeny and characterization as joint progenitors." Stem Cells Dev **22**(9): 1342-1359.

Libbrecht, L., D. Cassiman, V. Desmet and T. Roskams (2002). "The correlation between portal myofibroblasts and development of intrahepatic bile ducts and arterial branches in human liver." Liver **22**(3): 252-258.

Lietha, D., D. Y. Chirgadze, B. Mulloy, T. L. Blundell and E. Gherardi (2001). "Crystal structures of NK1-heparin complexes reveal the basis for NK1 activity and enable engineering of potent agonists of the MET receptor." EMBO J **20**(20): 5543-5555.

Lindstedt, S., J. Hlebowicz, B. Koul, P. Wierup, J. Sjogren, R. Gustafsson, S. Steen and R. Ingemansson (2011). "Comparative outcome of double lung transplantation using conventional donor lungs and non-acceptable donor lungs reconditioned ex vivo." Interact Cardiovasc Thorac Surg **12**(2): 162-165.

Liu, Y. (2006). "Rapamycin and chronic kidney disease: beyond the inhibition of inflammation." Kidney Int **69**(11): 1925-1927.

Liu, Y., Q. F. Shi, Y. C. Ye, S. Tashiro, S. Onodera and T. Ikejima (2012). "Activated O2(*-) and H2O2 mediated cell survival in SU11274-treated non-small-cell lung cancer A549 cells via c-Met-PI3K-Akt and c-Met-Grb2/SOS-Ras-p38 pathways." J Pharmacol Sci **119**(2): 150-159.

Lo, I. J., J. H. Lefkowitch, N. Feirt, B. Alkofer, C. Kin, B. Samstein, J. V. Guarrera and J. F. Renz (2008). "Utility of liver allograft biopsy obtained at procurement." Liver Transpl **14**(5): 639-646.

Lokker, N. A., L. G. Presta and P. J. Godowski (1994). "Mutational analysis and molecular modeling of the N-terminal kringle-containing domain of hepatocyte growth factor identifies amino acid side chains important for interaction with the c-Met receptor." Protein Eng **7**(7): 895-903.

Lu, C. Y. (1996). "Ischemia, injury, and renal allograft rejection." Curr Opin Nephrol Hypertens **5**(2): 107-110.

Lunec, J., K. Holloway, M. Cooke and M. Evans (2003). "Redox-regulation of DNA repair." Biofactors **17**(1-4): 315-324.

Lunz, J. G., 3rd, S. Contrucci, K. Ruppert, N. Murase, J. J. Fung, T. E. Starzl and A. J. Demetris (2001). "Replicative senescence of biliary epithelial cells precedes bile duct loss in chronic liver allograft rejection: increased expression of p21(WAF1/Cip1) as a disease marker and the influence of immunosuppressive drugs." Am J Pathol **158**(4): 1379-1390.

Machide, M., A. Hashigasako, K. Matsumoto and T. Nakamura (2006). "Contact inhibition of hepatocyte growth regulated by functional association of the c-Met/hepatocyte growth factor receptor and LAR protein-tyrosine phosphatase." J Biol Chem **281**(13): 8765-8772.
MacSween, R. N. and A. D. Burt (1986). "Histologic spectrum of alcoholic liver disease." Semin Liver Dis **6**(3): 221-232.
Mallat, A. and S. Lotersztajn (2013). "Reversion of hepatic stellate cell to a quiescent phenotype: From myth to reality?" Journal of Hepatology **59**(2): 383-386.
Mandai, S., E. Kanda, Y. Arai, S. Hirasawa, T. Hirai, S. Aki, N. Inaba, M. Aoyagi, H. Tanaka, T. Ikeda, T. Tamura and S. Sasaki (2013). "Anti-centromere antibody is an independent risk factor for chronic kidney disease in patients with primary biliary cirrhosis." Clin Exp Nephrol **17**(3): 405-410.
Mangold, S., S. K. Wu, S. J. Norwood, B. M. Collins, N. A. Hamilton, P. Thorn and A. S. Yap (2011). "Hepatocyte growth factor acutely perturbs actin filament anchorage at the epithelial zonula adherens." Curr Biol **21**(6): 503-507.
Marchioro, T. L., W. R. Waddell and T. E. Starzl (1963). "Use of Extracorporeal Cadaver Perfusion for Preparation of Organ Homografts." Surg Forum **14**: 174-176.
Martinez-Vicente, M., G. Sovak and A. M. Cuervo (2005). "Protein degradation and aging." Exp Gerontol **40**(8-9): 622-633.
Massague, J. (1990). "The transforming growth factor-beta family." Annu Rev Cell Biol **6**: 597-641.
Masszi, A., P. Speight, E. Charbonney, M. Lodyga, H. Nakano, K. Szaszi and A. Kapus (2011). "Fate-determining mechanisms in epithelial-myofibroblast transition: major inhibitory role for Smad3." J Cell Biol **188**(3): 383-399.
Matsuda, R., T. Koide, C. Tokoro, T. Yamamoto, T. Godai, T. Morohashi, Y. Fujita, D. Takahashi, I. Kawana, S. Suzuki and S. Umemura (2009). "Quantitive cytokine mRNA expression profiles in the colonic mucosa of patients with steroid naive ulcerative colitis during active and quiescent disease." Inflamm Bowel Dis **15**(3): 328-334.
Matsumura, A., T. Kubota, H. Taiyoh, H. Fujiwara, K. Okamoto, D. Ichikawa, A. Shiozaki, S. Komatsu, M. Nakanishi, Y. Kuriu, Y. Murayama, H. Ikoma, T. Ochiai, Y. Kokuba, T. Nakamura, K. Matsumoto and E. Otsuji (2013). "HGF regulates VEGF expression via the c-Met receptor downstream pathways, PI3K/Akt, MAPK and STAT3, in CT26 murine cells." Int J Oncol **42**(2): 535-542.
McCrudden, R. and J. P. Iredale (2000). "Liver fibrosis, the hepatic stellate cell and tissue inhibitors of metalloproteinases." Histol Histopathol **15**(4): 1159-1168.
McKenna, G. J. and J. F. Trotter (2012). "Sirolimus--it doesn't deserve its bad Rap(a)." J Hepatol **56**(1): 285-287.
McKenna, G. J., J. F. Trotter, E. Klintmalm, R. Ruiz, N. Onaca, G. Testa, G. Saracino, M. F. Levy, R. M. Goldstein and G. B. Klintmalm (2013). "Sirolimus and cardiovascular disease risk in liver transplantation." Transplantation **95**(1): 215-221.
Medawar, P. B. (1956). "The immunology of transplantation." Harvey Lect(Series 52): 144-176.
Mehrpour, M., A. Esclatine, I. Beau and P. Codogno (2010). "Overview of macroautophagy regulation in mammalian cells." Cell Res **20**(7): 748-762.
Meindl-Beinker, N. M. and S. Dooley (2008). "Transforming growth factor-beta and hepatocyte transdifferentiation in liver fibrogenesis." J Gastroenterol Hepatol **23 Suppl 1**: S122-127.
Mells, G. F., G. Pells, J. L. Newton, A. J. Bathgate, A. K. Burroughs, M. A. Heneghan, J. M. Neuberger, D. B. Day, S. J. Ducker, R. N. Sandford, G. J. Alexander, D. E. Jones and U.-P. Consortium (2013). "Impact of primary biliary cirrhosis on perceived quality of life: The UK-PBC national study." Hepatology **58**(1): 273-283.

Mengel, M., B. Sis, M. Haas, R. B. Colvin, P. F. Halloran, L. C. Racusen, K. Solez, L. Cendales, A. J. Demetris, C. B. Drachenberg, C. F. Farver, E. R. Rodriguez, W. D. Wallace, D. Glotz and B. M. R. W. Comm (2012). "Banff 2011 Meeting Report: New Concepts in Antibody-Mediated Rejection." American Journal of Transplantation **12**(3): 563-570.

Michalak, S., M. C. Rousselet, P. Bedossa, C. Pilette, D. Chappard, F. Oberti, Y. Gallois and P. Cales (2003). "Respective roles of porto-septal fibrosis and centrilobular fibrosis in alcoholic liver disease." J Pathol **201**(1): 55-62.

Mishra, M., V. Chandavarkar, V. V. Naik and A. D. Kale (2013). "An immunohistochemical study of basement membrane heparan sulfate proteoglycan (perlecan) in oral epithelial dysplasia and squamous cell carcinoma." J Oral Maxillofac Pathol **17**(1): 31-35.

Miyagawa-Hayashino, A., A. Yoshizawa, Y. Uchida, H. Egawa, K. Yurugi, S. Masuda, S. Minamiguchi, T. Maekawa, S. Uemoto and H. Haga (2012). "Progressive graft fibrosis and donor-specific human leukocyte antigen antibodies in pediatric late liver allografts." Liver Transpl **18**(11): 1333-1342.

Miyazaki, M., Y. Fujikawa, C. Takita and H. Tsumura (2007). "Tacrolimus and cyclosporine A inhibit human osteoclast formation via targeting the calcineurin-dependent NFAT pathway and an activation pathway for c-Jun or MITF in rheumatoid arthritis." Clin Rheumatol **26**(2): 231-239.

Modica, S., R. M. Gadaleta and A. Moschetta (2010). "Deciphering the nuclear bile acid receptor FXR paradigm." Nucl Recept Signal **8**: e005.

Mohamed, M. A., A. D. Burt, H. Robertson, J. A. Kirby and D. Talbot (2001). "TGF-beta expression in protocol transplant liver biopsies: a comparative study between cyclosporine-A (CyA) and tacrolimus (FK 506) immunosuppression." Transplant Proc **33**(1-2): 1378-1380.

Molinari, M., K. Berman, G. Meeberg, J. A. Shapiro, D. Bigam, J. F. Trotter and N. Kneteman (2010). "Multicentric outcome analysis of sirolimus-based immunosuppression in 252 liver transplant recipients." Transpl Int **23**(2): 155-168.

Moon, R. T., B. Bowerman, M. Boutros and N. Perrimon (2002). "The promise and perils of Wnt signaling through beta-catenin." Science **296**(5573): 1644-1646.

Mould, A. P. and M. J. Humphries (2004). "Regulation of integrin function through conformational complexity: not simply a knee-jerk reaction?" Curr Opin Cell Biol **16**(5): 544-551.

Mould, A. P., E. J. Koper, A. Byron, G. Zahn and M. J. Humphries (2009). "Mapping the ligand-binding pocket of integrin alpha5beta1 using a gain-of-function approach." Biochem J **424**(2): 179-189.

Mould, A. P., E. J. Symonds, P. A. Buckley, J. G. Grossmann, P. A. McEwan, S. J. Barton, J. A. Askari, S. E. Craig, J. Bella and M. J. Humphries (2003). "Structure of an integrin-ligand complex deduced from solution x-ray scattering and site-directed mutagenesis." J Biol Chem **278**(41): 39993-39999.

Mracek, T., E. Holzerova, Z. Drahota, N. Kovarova, M. Vrbacky, P. Jesina and J. Houstek (2013). "ROS generation and multiple forms of mammalian mitochondrial glycerol-3-phosphate dehydrogenase." Biochim Biophys Acta.

Mueller, X. M. (2004). "Drug immunosuppression therapy for adult heart transplantation. Part 1: immune response to allograft and mechanism of action of immunosuppressants." Ann Thorac Surg **77**(1): 354-362.

Munger, J. S. and D. Sheppard (2011). "Cross talk among TGF-beta signaling pathways, integrins, and the extracellular matrix." Cold Spring Harb Perspect Biol **3**(11): a005017.

Murphy-Ullrich, J. E. and M. Poczatek (2000). "Activation of latent TGF-beta by thrombospondin-1: mechanisms and physiology." Cytokine Growth Factor Rev **11**(1-2): 59-69.

Mutze, S., U. Hebling, W. Stremmel, J. Wang, J. Arnhold, K. Pantopoulos and S. Mueller (2003). "Myeloperoxidase-derived hypochlorous acid antagonizes the oxidative stress-mediated activation of iron regulatory protein 1." J Biol Chem **278**(42): 40542-40549.
Nagatsuma, K., H. Hano, K. Murakami, D. Shindo, Y. Matsumoto, J. Mitobe, K. Tanaka, M. Saito, H. Maehashi, M. Owada, M. Ikegami, A. Tsubota, T. Ohkusa, Y. Aizawa, I. Takagi, H. Tajiri and T. Matsuura (2013). "Hepatic stellate cells that coexpress LRAT and CRBP-1 partially contribute to portal fibrogenesis in patients with human viral hepatitis." Liver Int.
Nakamura, T., T. Nishizawa, M. Hagiya, T. Seki, M. Shimonishi, A. Sugimura, K. Tashiro and S. Shimizu (1989). "Molecular cloning and expression of human hepatocyte growth factor." Nature **342**(6248): 440-443.
Nakamura, T., K. Sakai, T. Nakamura and K. Matsumoto (2011). "Hepatocyte growth factor twenty years on: Much more than a growth factor." J Gastroenterol Hepatol **26 Suppl 1**: 188-202.
Nakanuma, Y. and K. Harada (2011). "The role of the pathologist in diagnosing and grading biliary diseases." Clin Res Hepatol Gastroenterol **35**(5): 347-352.
Neil, D. A. and S. G. Hubscher (2010). "Current views on rejection pathology in liver transplantation." Transpl Int **23**(10): 971-983.
Neuberger, J. (1997). "Primary biliary cirrhosis." Lancet **350**(9081): 875-879.
Neuberger, J. (1997). "Transplantation for primary biliary cirrhosis." Semin Liver Dis **17**(2): 137-146.
Neuberger, J. M., R. D. Mamelok, P. Neuhaus, J. Pirenne, D. Samuel, H. Isoniemi, L. Rostaing, A. Rimola, S. Marshall and A. D. Mayer (2009). "Delayed introduction of reduced-dose tacrolimus, and renal function in liver transplantation: the 'ReSpECT' study." Am J Transplant **9**(2): 327-336.
Neurohr, C., S. L. Nishimura and D. Sheppard (2006). "Activation of transforming growth factor-beta by the integrin alphavbeta8 delays epithelial wound closure." Am J Respir Cell Mol Biol **35**(2): 252-259.
Nitta, T., J. S. Kim, D. Mohuczy and K. E. Behrns (2008). "Murine cirrhosis induces hepatocyte epithelial mesenchymal transition and alterations in survival signaling pathways." Hepatology **48**(3): 909-919.
Novakova, Z., S. Hubackova, M. Kosar, L. Janderova-Rossmeislova, J. Dobrovolna, P. Vasicova, M. Vancurova, Z. Horejsi, P. Hozak, J. Bartek and Z. Hodny (2010). "Cytokine expression and signaling in drug-induced cellular senescence." Oncogene **29**(2): 273-284.
Oetting, W. S., P. A. Jacobson and A. K. Israni (2013). "Transplant rejection and risk: in search of the genetic dark matter." J Gastrointestin Liver Dis **22**(2): 125-126.
Okamura, D. M. and J. Himmelfarb (2009). "Tipping the redox balance of oxidative stress in fibrogenic pathways in chronic kidney disease." Pediatr Nephrol **24**(12): 2309-2319.
Omenetti, A., L. Yang, Y. X. Li, S. J. McCall, Y. Jung, J. K. Sicklick, J. Huang, S. Choi, A. Suzuki and A. M. Diehl (2007). "Hedgehog-mediated mesenchymal-epithelial interactions modulate hepatic response to bile duct ligation." Lab Invest **87**(5): 499-514.
Ong, W. Y., A. M. Jenner, N. Pan, C. N. Ong and B. Halliwell (2009). "Elevated oxidative stress, iron accumulation around microvessels and increased 4-hydroxynonenal immunostaining in zone 1 of the liver acinus in hypercholesterolemic rabbits." Free Radic Res **43**(3): 241-249.
Orr, A. L., D. Ashok, M. R. Sarantos, T. Shi, R. E. Hughes and M. D. Brand (2013). "Inhibitors of ROS production by the ubiquinone-binding site of mitochondrial complex I identified by chemical screening." Free Radic Biol Med.
Paiva, C. N. and M. T. Bozza (2013). "Are ROS always detrimental to pathogens?" Antioxid Redox Signal.

Palmer, J. M., M. Doshi, J. A. Kirby, S. J. Yeaman, M. F. Bassendine and D. E. Jones (2000). "Secretory autoantibodies in primary biliary cirrhosis (PBC)." Clin Exp Immunol **122**(3): 423-428.
Palmer, J. M., J. A. Kirby and D. E. Jones (2002). "The immunology of primary biliary cirrhosis: the end of the beginning?" Clin Exp Immunol **129**(2): 191-197.
Panasenko, O. M., H. Spalteholz, J. Schiller and J. Arnhold (2003). "Myeloperoxidase-induced formation of chlorohydrins and lysophospholipids from unsaturated phosphatidylcholines." Free Radic Biol Med **34**(5): 553-562.
Papassavas, A. C., M. C. Barnardo, M. Bunce and K. I. Welsh (2002). "Is there MHC Class II restriction of the response to MHC Class I in transplant patients?" Transplantation **73**(4): 642-651.
Paradis, V., J. Y. Scoazec, M. Kollinger, A. Holstege, A. Moreau, G. Feldmann and P. Bedossa (1996). "Cellular and subcellular localization of acetaldehyde-protein adducts in liver biopsies from alcoholic patients." J Histochem Cytochem **44**(9): 1051-1057.
Parkman, R. (2013). "A 2-hit model for chronic GVHD." Blood **122**(5): 623-624.
Parola, M., F. Marra and M. Pinzani (2008). "Myofibroblast - like cells and liver fibrogenesis: Emerging concepts in a rapidly moving scenario." Mol Aspects Med **29**(1-2): 58-66.
Passos, J. F., G. Nelson, C. Wang, T. Richter, C. Simillion, C. J. Proctor, S. Miwa, S. Olijslagers, J. Hallinan, A. Wipat, G. Saretzki, K. L. Rudolph, T. B. Kirkwood and T. von Zglinicki (2010). "Feedback between p21 and reactive oxygen production is necessary for cell senescence." Mol Syst Biol **6**: 347.
Passos, J. F., G. Saretzki, S. Ahmed, G. Nelson, T. Richter, H. Peters, I. Wappler, M. J. Birket, G. Harold, K. Schaeuble, M. A. Birch-Machin, T. B. Kirkwood and T. von Zglinicki (2007). "Mitochondrial dysfunction accounts for the stochastic heterogeneity in telomere-dependent senescence." PLoS Biol **5**(5): e110.
Passos, J. F. and T. von Zglinicki (2005). "Mitochondria, telomeres and cell senescence." Exp Gerontol **40**(6): 466-472.
Passos, J. F. and T. Von Zglinicki (2006). "Oxygen free radicals in cell senescence: are they signal transducers?" Free Radic Res **40**(12): 1277-1283.
Passos, J. F. and T. von Zglinicki (2007). "Methods for cell sorting of young and senescent cells." Methods Mol Biol **371**: 33-44.
Passos, J. F., T. von Zglinicki and T. B. Kirkwood (2007). "Mitochondria and ageing: winning and losing in the numbers game." Bioessays **29**(9): 908-917.
Passos, J. F., T. von Zglinicki and G. Saretzki (2006). "Mitochondrial dysfunction and cell senescence: cause or consequence?" Rejuvenation Res **9**(1): 64-68.
Patsenker, E., Y. Popov, F. Stickel, A. Jonczyk, S. L. Goodman and D. Schuppan (2008). "Inhibition of integrin alphavbeta6 on cholangiocytes blocks transforming growth factor-beta activation and retards biliary fibrosis progression." Gastroenterology **135**(2): 660-670.
Patsenker, E., Y. Popov, F. Stickel, V. Schneider, M. Ledermann, H. Sagesser, G. Niedobitek, S. L. Goodman and D. Schuppan (2009). "Pharmacological inhibition of integrin alphavbeta3 aggravates experimental liver fibrosis and suppresses hepatic angiogenesis." Hepatology **50**(5): 1501-1511.
Patsenker, E., V. Schneider, M. Ledermann, H. Saegesser, C. Dorn, C. Hellerbrand and F. Stickel (2011). "Potent antifibrotic activity of mTOR inhibitors sirolimus and everolimus but not of cyclosporine A and tacrolimus in experimental liver fibrosis." J Hepatol **55**(2): 388-398.
Pells, G., G. F. Mells, M. Carbone, J. L. Newton, A. J. Bathgate, A. K. Burroughs, M. A. Heneghan, J. M. Neuberger, D. B. Day, S. J. Ducker, U.-P. Consortium, R. N. Sandford, G. J. Alexander and D. E. Jones (2013). "The impact of liver transplantation on the phenotype of primary biliary cirrhosis patients in the UK-PBC cohort." J Hepatol **59**(1): 67-73.

Pidala, J., M. Sarwal, S. Roedder and S. J. Lee (2013). "Biologic markers of chronic GVHD." Bone Marrow Transplant.

Pirenne, J., B. Gunson, H. Khaleef, S. Hubscher, S. Afford, P. McMaster and D. Adams (1997). "Influence of ischemia-reperfusion injury on rejection after liver transplantation." Transplant Proc **29**(1-2): 366-367.

Polakis, P. (2000). "Wnt signaling and cancer." Genes Dev **14**(15): 1837-1851.

Rajawat, Y. S., Z. Hilioti and I. Bossis (2009). "Aging: central role for autophagy and the lysosomal degradative system." Ageing Res Rev **8**(3): 199-213.

Ramachandran, P. and J. P. Iredale (2009). "Reversibility of liver fibrosis." Ann Hepatol **8**(4): 283-291.

Rao, V., S. Haywood, M. Abecassis and J. Levitsky (2013). "A non-induction renal sparing approach after liver transplantation: high dose mycophenolate mofetil with delayed, low-dose tacrolimus." Transplant Proc **45**(1): 320-322.

Rappaport, A. M. (1958). "The structural and functional unit in the human liver (liver acinus)." Anat Rec **130**(4): 673-689.

Rautou, P. E., A. Mansouri, D. Lebrec, F. Durand, D. Valla and R. Moreau (2011). "Autophagy in liver diseases." J Hepatol **53**(6): 1123-1134.

Raynard, B., A. Balian, D. Fallik, F. Capron, P. Bedossa, J. C. Chaput and S. Naveau (2002). "Risk factors of fibrosis in alcohol-induced liver disease." Hepatology **35**(3): 635-638.

Razin, S., E. A. Pfendt, T. Matsumura and L. Hayflick (1977). "Comparison by autoradiography of macromolecular biosynthesis in "young" and "old" human diploid fibroblast cultures. A brief note." Mech Ageing Dev **6**(5): 379-384.

Reya, T. and H. Clevers (2005). "Wnt signalling in stem cells and cancer." Nature **434**(7035): 843-850.

Rhyu, D. Y., Y. Yang, H. Ha, G. T. Lee, J. S. Song, S. T. Uh and H. B. Lee (2005). "Role of reactive oxygen species in TGF-beta1-induced mitogen-activated protein kinase activation and epithelial-mesenchymal transition in renal tubular epithelial cells." J Am Soc Nephrol **16**(3): 667-675.

Ribeiro, S. M., M. Poczatek, S. Schultz-Cherry, M. Villain and J. E. Murphy-Ullrich (1999). "The activation sequence of thrombospondin-1 interacts with the latency-associated peptide to regulate activation of latent transforming growth factor-beta." J Biol Chem **274**(19): 13586-13593.

Rizzo, G., B. Renga, A. Mencarelli, R. Pellicciari and S. Fiorucci (2005). "Role of FXR in regulating bile acid homeostasis and relevance for human diseases." Curr Drug Targets Immune Endocr Metabol Disord **5**(3): 289-303.

Robertson, H., S. Ali, B. J. McDonnell, A. D. Burt and J. A. Kirby (2004). "Chronic renal allograft dysfunction: the role of T cell-mediated tubular epithelial to mesenchymal cell transition." J Am Soc Nephrol **15**(2): 390-397.

Robertson, H., J. A. Kirby, W. W. Yip, D. E. Jones and A. D. Burt (2007). "Biliary epithelial-mesenchymal transition in posttransplantation recurrence of primary biliary cirrhosis." Hepatology **45**(4): 977-981.

Rodier, F., J. P. Coppe, C. K. Patil, W. A. Hoeijmakers, D. P. Munoz, S. R. Raza, A. Freund, E. Campeau, A. R. Davalos and J. Campisi (2009). "Persistent DNA damage signalling triggers senescence-associated inflammatory cytokine secretion." Nat Cell Biol **11**(8): 973-979.

Roskams, T., A. Katoonizadeh and M. Komuta (2010). "Hepatic progenitor cells: an update." Clin Liver Dis **14**(4): 705-718.

Ross, J., E. Gherardi, N. Mallorqui-Fernandez, M. Bocci, A. Sobkowicz, M. Rees, A. Rowe, S. Ellmerich, I. Massie, J. Soeda, C. Selden and H. Hodgson (2012). "Protein engineered variants of hepatocyte growth factor/scatter factor promote proliferation of primary human hepatocytes and in rodent liver." Gastroenterology **142**(4): 897-906.

Rostron, A., V. Carter, M. Mutunga, G. Cavanagh, C. O'Suilleabhain, A. Burt, B. Jaques, D. Talbot and D. Manas (2005). "A case of acute humoral rejection in liver transplantation: successful treatment with plasmapheresis and mycophenolate mofetil." Transpl Int **18**(11): 1298-1301.

Rostron, A. J., V. S. Avlonitis, D. M. Cork, D. S. Grenade, J. A. Kirby and J. H. Dark (2008). "Hemodynamic resuscitation with arginine vasopressin reduces lung injury after brain death in the transplant donor." Transplantation **85**(4): 597-606.

Rupp, C., A. Mummelthei, P. Sauer, K. H. Weiss, P. Schirmacher, A. Stiehl, W. Stremmel and D. N. Gotthardt (2013). "Non-IBD immunological diseases are a risk factor for reduced survival in PSC." Liver Int **33**(1): 86-93.

Rygiel, K. A. (2009). Epithelial to mesenchymal transition : a possible route to liver fibrogenesis PhD., Newcastle University.

Rygiel, K. A., H. Robertson, H. L. Marshall, M. Pekalski, L. Zhao, T. A. Booth, D. E. Jones, A. D. Burt and J. A. Kirby (2008). "Epithelial-mesenchymal transition contributes to portal tract fibrogenesis during human chronic liver disease." Lab Invest **88**(2): 112-123.

Rygiel, K. A., H. Robertson, J. D. P. Willet, J. G. Brain, A. D. Burt, D. E. J. Jones and J. A. Kirby (2010). "T Cell-Mediated Biliary Epithelial-to-Mesenchymal Transition in Liver Allograft Rejection." LIVER TRANSPLANTATION.

Saemann, M. D., M. Haidinger, M. Hecking, W. H. Horl and T. Weichhart (2009). "The multifunctional role of mTOR in innate immunity: implications for transplant immunity." Am J Transplant **9**(12): 2655-2661.

Safinia, N., J. Leech, M. Hernandez-Fuentes, R. Lechler and G. Lombardi (2013). "Promoting transplantation tolerance; adoptive regulatory T cell therapy." Clin Exp Immunol **172**(2): 158-168.

Sagoo, P., G. Lombardi and R. I. Lechler (2012). "Relevance of regulatory T cell promotion of donor-specific tolerance in solid organ transplantation." Front Immunol **3**: 184.

Sagoo, P., K. Ratnasothy, Y. Tsang, L. D. Barber, A. Noble, R. I. Lechler and G. Lombardi (2012). "Alloantigen-specific regulatory T cells prevent experimental chronic graft-versus-host disease by simultaneous control of allo- and autoreactivity." Eur J Immunol **42**(12): 3322-3333.

Saleem, M., M. H. Kweon, J. J. Johnson, V. M. Adhami, I. Elcheva, N. Khan, B. Bin Hafeez, K. M. Bhat, S. Sarfaraz, S. Reagan-Shaw, V. S. Spiegelman, V. Setaluri and H. Mukhtar (2006). "S100A4 accelerates tumorigenesis and invasion of human prostate cancer through the transcriptional regulation of matrix metalloproteinase 9." Proc Natl Acad Sci U S A **103**(40): 14825-14830.

Sasaki, M., A. A. Ansari, Y. Nakanuma, R. L. Coppel, E. B. Keeffe and M. E. Gershwin (2000). "The immunopathology of primary biliary cirrhosis: thoughts for the millennium." Arch Immunol Ther Exp (Warsz) **48**(1): 1-10.

Sasaki, M., H. Ikeda, H. Haga, T. Manabe and Y. Nakanuma (2005). "Frequent cellular senescence in small bile ducts in primary biliary cirrhosis: a possible role in bile duct loss." J Pathol **205**(4): 451-459.

Sasaki, M., H. Ikeda and Y. Nakanuma (2008). "Activation of ATM signaling pathway is involved in oxidative stress-induced expression of mito-inhibitory p21WAF1/Cip1 in chronic non-suppurative destructive cholangitis in primary biliary cirrhosis: an immunohistochemical study." J Autoimmun **31**(1): 73-78.

Sasaki, M., H. Ikeda, Y. Sato and Y. Nakanuma (2006). "Decreased expression of Bmi1 is closely associated with cellular senescence in small bile ducts in primary biliary cirrhosis." Am J Pathol **169**(3): 831-845.

Sasaki, M., H. Ikeda, Y. Sato and Y. Nakanuma (2008). "Proinflammatory cytokine-induced cellular senescence of biliary epithelial cells is mediated via oxidative stress and activation of ATM pathway: a culture study." Free Radic Res **42**(7): 625-632.

Sasaki, M., H. Ikeda, J. Yamaguchi, M. Miyakoshi, Y. Sato and Y. Nakanuma (2010). "Bile ductular cells undergoing cellular senescence increase in chronic liver diseases along with fibrous progression." Am J Clin Pathol **133**(2): 212-223.
Sasaki, M., H. Ikeda, J. Yamaguchi, S. Nakada and Y. Nakanuma (2008). "Telomere shortening in the damaged small bile ducts in primary biliary cirrhosis reflects ongoing cellular senescence." Hepatology **48**(1): 186-195.
Sasaki, M., M. Miyakoshi, Y. Sato and Y. Nakanuma "Autophagy mediates the process of cellular senescence characterizing bile duct damages in primary biliary cirrhosis." Lab Invest **90**(6): 835-843.
Sasaki, M., M. Miyakoshi, Y. Sato and Y. Nakanuma (2010). "Autophagy mediates the process of cellular senescence characterizing bile duct damages in primary biliary cirrhosis." Lab Invest.
Sasaki, M., M. Miyakoshi, Y. Sato and Y. Nakanuma (2010). "Modulation of the microenvironment by senescent biliary epithelial cells may be involved in the pathogenesis of primary biliary cirrhosis." J Hepatol **53**(2): 318-325.
Sasaki, M., M. Miyakoshi, Y. Sato and Y. Nakanuma (2012). "Autophagy may precede cellular senescence of bile ductular cells in ductular reaction in primary biliary cirrhosis." Dig Dis Sci **57**(3): 660-666.
Sasaki, M., M. Miyakoshi, Y. Sato and Y. Nakanuma (2012). "A possible involvement of p62/sequestosome-1 in the process of biliary epithelial autophagy and senescence in primary biliary cirrhosis." Liver Int **32**(3): 487-499.
Sasaki, M., M. Miyakoshi, Y. Sato and Y. Nakanuma (2013). "Increased expression of mitochondrial proteins associated with autophagy in biliary epithelial lesions in primary biliary cirrhosis." Liver Int **33**(2): 312-320.
Sato, Y., K. Harada, H. Ikeda, T. Fijii, M. Sasaki, Y. Zen and Y. Nakanuma (2009). "Hepatic stellate cells are activated around central scars of focal nodular hyperplasia of the liver--a potential mechanism of central scar formation." Hum Pathol **40**(2): 181-188.
Schaffer, M., R. Schier, M. Napirei, S. Michalski, T. Traska and R. Viebahn (2007). "Sirolimus impairs wound healing." Langenbecks Arch Surg **392**(3): 297-303.
Schneeberger, H., S. Aydemir, W. D. Illner and W. Land (1997). "Nonspecific primary ischemia/reperfusion injury in combination with secondary specific acute rejection-mediated injury of human kidney allografts contributes mainly to development of chronic transplant failure." Transplant Proc **29**(1-2): 948-949.
Scholten, D., C. H. Osterreicher, A. Scholten, K. Iwaisako, G. Gu, D. A. Brenner and T. Kisseleva (2011). "Genetic labeling does not detect epithelial-to-mesenchymal transition of cholangiocytes in liver fibrosis in mice." Gastroenterology **139**(3): 987-998.
Schwall, R. H., L. Y. Chang, P. J. Godowski, D. W. Kahn, K. J. Hillan, K. D. Bauer and T. F. Zioncheck (1996). "Heparin induces dimerization and confers proliferative activity onto the hepatocyte growth factor antagonists NK1 and NK2." J Cell Biol **133**(3): 709-718.
Sebagh, M., K. Blakolmer, B. Falissard, B. Roche, J. F. Emile, H. Bismuth, D. Samuel and M. Reynes (2002). "Accuracy of bile duct changes for the diagnosis of chronic liver allograft rejection: reliability of the 1999 Banff schema." Hepatology **35**(1): 117-125.
Serrick, C., A. Giaid, A. Reis and H. Shennib (1997). "Prolonged ischemia is associated with more pronounced rejection in the lung allograft." Ann Thorac Surg **63**(1): 202-208.
Shaked, A., R. M. Ghobrial, R. M. Merion, T. H. Shearon, J. C. Emond, J. H. Fair, R. A. Fisher, L. M. Kulik, T. L. Pruett and N. A. Terrault (2009). "Incidence and severity of acute cellular rejection in recipients undergoing adult living donor or deceased donor liver transplantation." Am J Transplant **9**(2): 301-308.
Shang, J., K. Deguchi, Y. Ohta, N. Liu, X. Zhang, F. Tian, T. Yamashita, Y. Ikeda, T. Matsuura, H. Funakoshi, T. Nakamura and K. Abe (2011). "Strong neurogenesis, angiogenesis,

synaptogenesis, and antifibrosis of hepatocyte growth factor in rats brain after transient middle cerebral artery occlusion." J Neurosci Res **89**(1): 86-95.
Shegogue, D. and M. Trojanowska (2004). "Mammalian target of rapamycin positively regulates collagen type I production via a phosphatidylinositol 3-kinase-independent pathway." J Biol Chem **279**(22): 23166-23175.
Sherbet, G. V. (2009). "Metastasis promoter S100A4 is a potentially valuable molecular target for cancer therapy." Cancer Lett **280**(1): 15-30.
Shetty, S., C. J. Weston, Y. H. Oo, N. Westerlund, Z. Stamataki, J. Youster, S. G. Hubscher, M. Salmi, S. Jalkanen, P. F. Lalor and D. H. Adams (2011). "Common lymphatic endothelial and vascular endothelial receptor-1 mediates the transmigration of regulatory T cells across human hepatic sinusoidal endothelium." J Immunol **186**(7): 4147-4155.
Shibata, M., K. Yoshimura, H. Tamura, T. Ueno, T. Nishimura, T. Inoue, M. Sasaki, M. Koike, H. Arai, E. Kominami and Y. Uchiyama (2010). "LC3, a microtubule-associated protein1A/B light chain3, is involved in cytoplasmic lipid droplet formation." Biochem Biophys Res Commun **393**(2): 274-279.
Shih, M. C., S. H. Tseng, Y. S. Weng, I. M. Chu and C. H. Liu (2013). "A microfluidic device mimicking acinar concentration gradients across the liver acinus." Biomed Microdevices.
Shimada, Y. and D. J. Klionsky (2012). "Autophagy contributes to lysosomal storage disorders." Autophagy **8**(5): 715-716.
Sicklick, J. K., S. S. Choi, M. Bustamante, S. J. McCall, E. H. Perez, J. Huang, Y. X. Li, M. Rojkind and A. M. Diehl (2006). "Evidence for epithelial-mesenchymal transitions in adult liver cells." Am J Physiol Gastrointest Liver Physiol **291**(4): G575-583.
Simonsen, A. and S. A. Tooze (2009). "Coordination of membrane events during autophagy by multiple class III PI3-kinase complexes." J Cell Biol **186**(6): 773-782.
Snyder, R. A., D. R. Moore and D. E. Moore (2013). "More donors or more delayed graft function? A cost-effectiveness analysis of DCD kidney transplantation." Clin Transplant **27**(2): 289-296.
Song, K., H. Wang, T. L. Krebs and D. Danielpour (2006). "Novel roles of Akt and mTOR in suppressing TGF-beta/ALK5-mediated Smad3 activation." EMBO J **25**(1): 58-69.
Spee, B., G. Carpino, B. A. Schotanus, A. Katoonizadeh, S. Vander Borght, E. Gaudio and T. Roskams (2010). "Characterisation of the liver progenitor cell niche in liver diseases: potential involvement of Wnt and Notch signalling." Gut **59**(2): 247-257.
Starzl, T. E., T. L. Marchioro, K. N. Vonkaulla, G. Hermann, R. S. Brittain and W. R. Waddell (1963). "Homotransplantation of the Liver in Humans." Surg Gynecol Obstet **117**: 659-676.
Starzl, T. E., T. L. Marchioro and W. R. Waddell (1963). "The Reversal of Rejection in Human Renal Homografts with Subsequent Development of Homograft Tolerance." Surg Gynecol Obstet **117**: 385-395.
Steen, S., R. Ingemansson, L. Eriksson, L. Pierre, L. Algotsson, P. Wierup, Q. Liao, A. Eyjolfsson, R. Gustafsson and T. Sjoberg (2007). "First human transplantation of a nonacceptable donor lung after reconditioning ex vivo." Ann Thorac Surg **83**(6): 2191-2194.
Steen, S., T. Sjoberg, L. Pierre, Q. Liao, L. Eriksson and L. Algotsson (2001). "Transplantation of lungs from a non-heart-beating donor." Lancet **357**(9259): 825-829.
Suchin, E. J., P. B. Langmuir, E. Palmer, M. H. Sayegh, A. D. Wells and L. A. Turka (2001). "Quantifying the frequency of alloreactive T cells in vivo: new answers to an old question." J Immunol **166**(2): 973-981.
Sullivan, B. P., K. M. Kassel, S. Manley, A. K. Baker and J. P. Luyendyk (2011). "Regulation of transforming growth factor-beta1-dependent integrin beta6 expression by p38 mitogen-activated protein kinase in bile duct epithelial cells." J Pharmacol Exp Ther **337**(2): 471-478.
Tanaka, A., K. Harada, H. Ebinuma, A. Komori, J. Yokokawa, K. Yoshizawa, M. Abe, Y. Miyake, K. Kikuchi, H. Ohira, M. Zeniya, K. Yamamoto, H. Ishibashi, M. Onji, Y. Nakanuma, H. Tsubouchi and H. Takikawa (2011). "Primary biliary cirrhosis - Autoimmune hepatitis

overlap syndrome: A rationale for corticosteroids use based on a nation-wide retrospective study in Japan." Hepatol Res **41**(9): 877-886.
Taura, K., K. Miura, K. Iwaisako, C. H. Osterreicher, Y. Kodama, M. Penz-Osterreicher and D. A. Brenner (2010). "Hepatocytes do not undergo epithelial-mesenchymal transition in liver fibrosis in mice." Hepatology **51**(3): 1027-1036.
Tay, S. S., B. Lu, F. Sierro, V. Benseler, C. M. McGuffog, G. A. Bishop, P. J. Cowan, G. W. McCaughan, K. M. Dwyer, D. G. Bowen and P. Bertolino (2013). "Differential migration of passenger leukocytes and rapid deletion of naive alloreactive CD8 T cells after mouse liver transplantation." Liver Transpl.
Telci, D., Z. Wang, X. Li, E. A. Verderio, M. J. Humphries, M. Baccarini, H. Basaga and M. Griffin (2008). "Fibronectin-tissue transglutaminase matrix rescues RGD-impaired cell adhesion through syndecan-4 and beta1 integrin co-signaling." J Biol Chem **283**(30): 20937-20947.
Teng, Y., M. Zeisberg and R. Kalluri (2007). "Transcriptional regulation of epithelial-mesenchymal transition." J Clin Invest **117**(2): 304-306.
Thiery, J. P., H. Acloque, R. Y. Huang and M. A. Nieto (2009). "Epithelial-mesenchymal transitions in development and disease." Cell **139**(5): 871-890.
Thirthagiri, E., C. M. Robinson, S. Huntley, M. Davies, L. F. Yap, S. S. Prime and I. C. Paterson (2007). "Spindle assembly checkpoint and centrosome abnormalities in oral cancer." Cancer Lett **258**(2): 276-285.
Thompson, E., A. D. Burt, C. E. Barker, J. A. Kirby and J. G. Brain (2013). "Development of a robust protocol for gene expression analysis using formalin-fixed, paraffin-embedded liver transplant biopsy specimens." J Clin Pathol.
Tocci, M. J. and N. H. Sigal (1992). "Recent advances in the mechanism of action of cyclosporine and FK506." Curr Opin Nephrol Hypertens **1**(2): 236-242.
Tojima, H., S. Kakizaki, T. Kosone, N. Horiguchi, Y. Yamazaki, K. Sato, H. Takagi and M. Mori (2011). "Hepatocyte growth factor overexpression ameliorates liver inflammation and fibrosis in a mouse model of nonalcoholic steatohepatitis." Hepatol Int.
Tooze, S. A., H. B. Jefferies, E. Kalie, A. Longatti, F. E. McAlpine, N. C. McKnight, A. Orsi, H. E. Polson, M. Razi, D. J. Robinson and J. L. Webber (2010). "Trafficking and signaling in mammalian autophagy." IUBMB Life **62**(7): 503-508.
Tripathi, G., T. Jafar, K. Mandal, A. A. Mahdi, S. Awasthi, R. K. Sharma, A. Kumar, S. Gulati and S. Agrawal (2008). "Does cytokine gene polymorphism affect steroid responses in idiopathic nephrotic syndrome?" Indian J Med Sci **62**(10): 383-391.
Trotter, J. F. (2003). "Sirolimus in liver transplantation." Transplant Proc **35**(3 Suppl): 193S-200S.
Trotter, J. F., M. Wachs, T. Bak, T. Trouillot, N. Stolpman, G. T. Everson and I. Kam (2001). "Liver transplantation using sirolimus and minimal corticosteroids (3-day taper)." Liver Transpl **7**(4): 343-351.
Turanyi, E., K. Dezso, J. Csomor, Z. Schaff, S. Paku and P. Nagy (2010). "Immunohistochemical classification of ductular reactions in human liver." Histopathology **57**(4): 607-614.
Uchiyama, H., H. Kayashima, R. Matono, K. Shirabe, T. Yoshizumi, T. Ikegami, Y. Soejima, T. Matsuura, T. Taguchi and Y. Maehara (2012). "Relevance of HLA compatibility in living donor liver transplantation: the double-edged sword associated with the patient outcome." Clin Transplant **26**(5): E522-529.
Valdramidou, D., M. J. Humphries and A. P. Mould (2008). "Distinct roles of beta1 metal ion-dependent adhesion site (MIDAS), adjacent to MIDAS (ADMIDAS), and ligand-associated metal-binding site (LIMBS) cation-binding sites in ligand recognition by integrin alpha2beta1." J Biol Chem **283**(47): 32704-32714.

van de Berg, P. J., S. L. Yong, S. D. Koch, N. Lardy, K. A. van Donselaar-van der Pant, S. Florquin, F. J. Bemelman, R. A. van Lier and I. J. ten Berge (2012). "Characteristics of alloreactive T cells measured before renal transplantation." Clin Exp Immunol **168**(2): 241-250.

van den Heuvel, M. C., K. P. de Jong, M. L. van der Horst, S. Poppema, M. J. Slooff and A. S. Gouw (2004). "Impaired regeneration of biliary cells in human chronic liver allograft rejection. Special emphasis on the role of the finest branches of the biliary tree." Liver Transpl **10**(1): 28-35.

Vicencio, J. M., L. Galluzzi, N. Tajeddine, C. Ortiz, A. Criollo, E. Tasdemir, E. Morselli, A. Ben Younes, M. C. Maiuri, S. Lavandero and G. Kroemer (2008). "Senescence, apoptosis or autophagy? When a damaged cell must decide its path--a mini-review." Gerontology **54**(2): 92-99.

Villalobos, M. D. G., R. Giles, I. Carreon, S. Vidrio and V. C. de Sanchez (2013). "Characterization of the hepatic stellate cell populations in carbon tetrachloride liver rat through Golgi-Cox Method." Faseb Journal **27**.

Wang, C. M., S. N. Tsai, T. W. Yew, Y. W. Kwan and S. M. Ngai (2010). "Identification of histone methylation multiplicities patterns in the brain of senescence-accelerated prone mouse 8." Biogerontology **11**(1): 87-102.

Wang, S. C., L. Tang Ch, H. L. Piao, R. Zhu, C. Sun, Y. Tao, Q. Fu, D. J. Li and M. R. Du (2013). "Cyclosporine A promotes in vitro migration of human first-trimester trophoblasts via MAPK/ERK1/2-mediated NF-kappaB and Ca2+/calcineurin/NFAT signaling." Placenta **34**(4): 374-380.

Ward, C., I. A. Forrest, D. M. Murphy, G. E. Johnson, H. Robertson, T. E. Cawston, A. J. Fisher, J. H. Dark, J. L. Lordan, J. A. Kirby and P. A. Corris (2005). "Phenotype of airway epithelial cells suggests epithelial to mesenchymal cell transition in clinically stable lung transplant recipients." Thorax **60**(10): 865-871.

Watson, P. M., M. J. Humphries, J. Relton, N. J. Rothwell, A. Verkhratsky and R. M. Gibson (2007). "Integrin-binding RGD peptides induce rapid intracellular calcium increases and MAPK signaling in cortical neurons." Mol Cell Neurosci **34**(2): 147-154.

Wells, T. N., C. A. Power, J. P. Shaw and A. E. Proudfoot (2006). "Chemokine blockers--therapeutics in the making?" Trends Pharmacol Sci **27**(1): 41-47.

Weston, C. J. and D. H. Adams "Hepatic consequences of vascular adhesion protein-1 expression." J Neural Transm **118**(7): 1055-1064.

Wiesner, R. H. and J. J. Fung "Present state of immunosuppressive therapy in liver transplant recipients." Liver Transpl **17 Suppl 3**: S1-9.

Willet, J. D., W. Pichitsiri, S. E. Jenkinson, J. G. Brain, K. Wood, A. A. Alhasan, J. Spielhofer, H. Robertson, S. Ali and J. A. Kirby (2013). "Kidney transplantation: analysis of the expression and T cell-mediated activation of latent TGF-beta." J Leukoc Biol **93**(4): 471-478.

Williams, C. H., T. Kajander, T. Hyypia, T. Jackson, D. Sheppard and G. Stanway (2004). "Integrin alpha v beta 6 is an RGD-dependent receptor for coxsackievirus A9." J Virol **78**(13): 6967-6973.

Wolfenson, H., I. Lavelin and B. Geiger (2013). "Dynamic regulation of the structure and functions of integrin adhesions." Dev Cell **24**(5): 447-458.

Worthington, J. J., T. M. Fenton, B. I. Czajkowska, J. E. Klementowicz and M. A. Travis (2012). "Regulation of TGFbeta in the immune system: an emerging role for integrins and dendritic cells." Immunobiology **217**(12): 1259-1265.

Wu, M. J., M. C. Wen, Y. T. Chiu, Y. Y. Chiou, K. H. Shu and M. J. Tang (2006). "Rapamycin attenuates unilateral ureteral obstruction-induced renal fibrosis." Kidney Int **69**(11): 2029-2036.

http://www.UKTransplant.org.uk. (2010). Retrieved 07/07/2010, 2010, from http://www.uktransplant.org.uk.

Xia, J. L., C. Dai, G. K. Michalopoulos and Y. Liu (2006). "Hepatocyte growth factor attenuates liver fibrosis induced by bile duct ligation." Am J Pathol **168**(5): 1500-1512.
Xu, M. Y., J. Porte, A. J. Knox, P. H. Weinreb, T. M. Maher, S. M. Violette, R. J. McAnulty, D. Sheppard and G. Jenkins (2009). "Lysophosphatidic acid induces alphavbeta6 integrin-mediated TGF-beta activation via the LPA2 receptor and the small G protein G alpha(q)." Am J Pathol **174**(4): 1264-1279.
Xu-Dubois, Y. C., E. Baugey, J. Peltier, M. Colombat, N. Ouali, C. Jouanneau, E. Rondeau and A. Hertig (2013). "Epithelial phenotypic changes are associated with a tubular active fibrogenic process in human renal grafts." Human Pathology **44**(7): 1251-1261.
Yang, Z. and D. J. Klionsky (2011). "Eaten alive: a history of macroautophagy." Nat Cell Biol **12**(9): 814-822.
Yeaman, S. J., J. A. Kirby and D. E. Jones (2000). "Autoreactive responses to pyruvate dehydrogenase complex in the pathogenesis of primary biliary cirrhosis." Immunol Rev **174**: 238-249.
Yip, W. W. and A. D. Burt (2006). "Alcoholic liver disease." Semin Diagn Pathol **23**(3-4): 149-160.
Yorimitsu, T. and D. J. Klionsky (2005). "Autophagy: molecular machinery for self-eating." Cell Death Differ **12 Suppl 2**: 1542-1552.
Yoshitomi, M., T. Koshiba, H. Haga, Y. Li, X. Zhao, D. Cheng, A. Miyagawa, H. Sakashita, T. Tsuruyama, H. Ohe, M. Ueda, S. Okamoto, H. Egawa, K. Wood, S. Sakaguchi, T. Manabe, K. Tanaka and S. Uemoto (2009). "Requirement of protocol biopsy before and after complete cessation of immunosuppression after liver transplantation." Transplantation **87**(4): 606-614.
Youles, M., O. Holmes, M. V. Petoukhov, M. A. Nessen, S. Stivala, D. I. Svergun and E. Gherardi (2008). "Engineering the NK1 fragment of hepatocyte growth factor/scatter factor as a MET receptor antagonist." J Mol Biol **377**(3): 616-622.
Zeisberg, E. M., S. Potenta, L. Xie, M. Zeisberg and R. Kalluri (2007). "Discovery of endothelial to mesenchymal transition as a source for carcinoma-associated fibroblasts." Cancer Res **67**(21): 10123-10128.
Zeisberg, M. and J. S. Duffield (2010). "Resolved: EMT produces fibroblasts in the kidney." J Am Soc Nephrol **21**(8): 1247-1253.
Zeisberg, M. and E. G. Neilson (2011). "Mechanisms of tubulointerstitial fibrosis." J Am Soc Nephrol **21**(11): 1819-1834.
Zeisberg, M., C. Yang, M. Martino, M. B. Duncan, F. Rieder, H. Tanjore and R. Kalluri (2007). "Fibroblasts derive from hepatocytes in liver fibrosis via epithelial to mesenchymal transition." J Biol Chem **282**(32): 23337-23347.
Zhang, Y. E. (2009). "Non-Smad pathways in TGF-beta signaling." Cell Res **19**(1): 128-139.
Zhou, R., L. Han, G. Li and T. Tong (2009). "Senescence delay and repression of p16INK4a by Lsh via recruitment of histone deacetylases in human diploid fibroblasts." Nucleic Acids Res **37**(15): 5183-5196.
Zhou, T., R. Zong, Z. Zhang, C. Zhu, F. Pan, X. Xiao, Z. Liu, H. He, J. X. Ma, Z. Liu and Y. Zhou (2012). "SERPINA3K protects against oxidative stress via modulating ROS generation/degradation and KEAP1-NRF2 pathway in the corneal epithelium." Invest Ophthalmol Vis Sci **53**(8): 5033-5043.
Zioncheck, T. F., L. Richardson, J. Liu, L. Chang, K. L. King, G. L. Bennett, P. Fugedi, S. M. Chamow, R. H. Schwall and R. J. Stack (1995). "Sulfated oligosaccharides promote hepatocyte growth factor association and govern its mitogenic activity." J Biol Chem **270**(28): 16871-16878.
Zode, G. S., A. Sethi, A. M. Brun-Zinkernagel, I. F. Chang, A. F. Clark and R. J. Wordinger (2011). "Transforming growth factor-beta2 increases extracellular matrix proteins in optic nerve head cells via activation of the Smad signaling pathway." Mol Vis **17**: 1745-1758.

7 Publications

Publications arising from this work are stated and appended below:

- Thompson E, Burt AD, Barker CE, Kirby JA, **Brain JG.** Development of a robust protocol for gene expression analysis using formalin-fixed, paraffin-embedded liver transplant biopsy specimens. *J Clin Pathol*. 2013 Jun 11

- **Brain JG**, Robertson H, Thompson E, Humphreys EH, Gardner A, Booth TA, Jones DE, Afford SC, von Zglinicki T, Burt AD, Kirby JA. Biliary epithelial senescence and plasticity in acute cellular rejection. *Am J Transplant*. 2013 Jul;13(7):1688-702